Understanding and Overcoming Barriers to Oral Immunization with Biomaterials and Applied Immunology

Hannah E. Frizzell

A dissertation

submitted in partial fulfillment of the

requirements for the degree of

Doctor of Philosophy

University of Washington

2019

Reading Committee:

Kim A. Woodrow, Chair

Daniel M. Ratner

Deborah H. Fuller

Program Authorized to Offer Degree:

Bioengineering

University of Washington

Abstract

Understanding and Overcoming Barriers to Oral Immunization

with Biomaterials and Applied Immunology

Hannah E. Frizzell

Chair of the Supervisory Committee:

Kim A. Woodrow, Associate Professor

Bioengineering

Immunization is an incredibly powerful intervention to provide protection from infectious diseases. The application of engineered materials for parenteral vaccination has illuminated pathways to increase vaccine uptake, traffic vaccines to lymphoid organs, and strategically activate cells, which may allow for the tailoring of specific immune responses and their magnitude. The importance of immunization at mucosal sites to generate protective immunity at the locations where pathogens most commonly invade the body is well-recognized. However, the majority of clinically licensed vaccines are not administered mucosally. Oral vaccines have the potential to reduce cost, improve compliance, and induce immunity at mucosal surfaces that are the first line of defense against infection. The gastrointestinal tract is highly evolved to efficiently digest and absorb nutrients without eliciting aberrant inflammation. Thus, these functions also limit the efficacy of

immunization by the oral route. Specifically, these barriers include digestion of antigens and immunogenic epitopes by gastric and intestinal proteases, limited epithelial absorption of macromolecules, and the immunotolerant nature of the gut. While mechanisms responsible for the development of immunity or tolerance to ingested antigens are being illuminated, the application of materials with precise physiochemical properties may accelerate our understanding of immunity within the gastrointestinal tract. Insight into these immunological mechanisms can inform the design of next-generation oral vaccines.

Here, we develop and evaluate a nanofiber vaccine platform to define and overcome immunological barriers associated with oral immunization. First, a drug delivery platform using emulsion electrospinning is developed for the oral delivery of protein therapeutics. We evaluate this platform for retention of protein bioactivity, pH-responsive protein release, and therapeutic shelf life. Next, we explore the use of adjuvants as a strategy to improve uptake of orally delivered vaccines through epithelial cell activation and recruitment of antigen presenting cells to the epithelium. *In vivo* immunization studies identify adjuvants capable of eliciting systemic and mucosal immune responses when delivered orally and also establish the initial differences in mechanism of action. Finally, the role of gastrointestinal digestion on immune responses to oral vaccines is investigated through the application of biomaterials carriers to provide selective protection of vaccines in certain gastrointestinal environments. We find that the susceptibility of immunogenic epitopes of a model protein antigen to be cleaved by gastrointestinal enzymes prevents the activation of epitope-specific T cell responses. The combination of protection from such cleavage through encapsulation in nanofibers and use of a potent mucosal adjuvant achieved expansion of epitope specific $CD8^+$ T cells in the local intestinal tissue compared to digestion protection or adjuvant use alone. Overall, this project provides insight into the immunology of oral vaccines and develops a biomaterial-based strategy to elicit immune responses through the protection of immunogenic epitopes from digestion and co-delivery of specific mucosal adjuvants.

TABLE OF CONTENTS

List of Figures vi
List of Tables ix
Chapter 1. Summary and Specific Aims 13
1.1 Significance and Motivation 13
1.2 Specific Aims 15
1.2.1 Aim 1. Develop electrospun fibers for oral delivery of protein therapeutics. 15
1.2.2 Aim 2. Evaluate ability of adjuvants to stimulate innate and adaptive immune responses when used in an oral vaccine 16
1.2.3 Aim 3. Determine innate and adaptive immune responses to fiber-protected oral vaccines co-delivered with mucosal adjuvants. 16
1.3 Summary 17
1.4 References 18
Chapter 2. Introduction 20
2.1 Background 20
2.1.1 Mucosal vaccines 20
2.1.2 Organization of the mucosal immune system 23
2.1.3 Defenses of the gastrointestinal tract 30
2.1.4 Application of advanced materials to study intestinal immunology 35
2.1.5 Applied immunology 68
2.2 Conclusions 69
2.3 References 70
Chapter 3. Electrospun Fibers for Oral Delivery of Protein Biotherapeutics 86
3.1 Abstract 86
3.2 Introduction 87
3.3 Materials and Methods 91

3.3.1 Materials 91
3.3.2 Emulsion Electrospinning 91
3.3.3 Characterization of Protein-Loaded Electrospun Fibers 92
3.3.4 Quantification of Bioactivity of Proteins Released from Emulsion Electrospun Fibers 94
3.3.5 Bioactivity in Simulated Gastric Fluid 95
3.3.6 Characterization of Lyophilized Electrospun Fibers 95
3.3.7 Blend Electrospinning 96
3.3.8 Antigen Functionality Assay 97
3.3.9 In Vitro Mucoadhesion Tests 97
3.3.10 Fiber Micronization and In Vivo Retention in Gastrointestinal Tract 98
3.3.11 Statistical Analysis 99
3.4 Results and Discussion 99
3.4.1 Characterization of Protein-Loaded Eudragit L100 Emulsion Electrospun Fibers 99
3.4.2 pH-Controlled Protein Release of Electrospun Eudragit L100 Fibers 103
3.4.3 Bioactivity Retention of Proteins Electrospun in Eudragit L100 Fibers by Emulsion Electrospinning 106
3.4.4 Bioactivity of Proteins Encapsulated in Eudragit L100 Fibers in Simulated Gastric Fluid 111
3.4.5 Evaluation and Extension of Protein-Loaded Fiber Shelf Life 113
3.4.6 Functionality of Antigens Encapsulated in Eudragit L100 Fibers 120
3.4.7 In Vitro Mucoadhesion 125
3.4.8 In Vivo Retention in Gastrointestinal Tract 129
3.5 Conclusions 131
3.6 Acknowledgements 132
3.7 References 133

Chapter 4. Mucosal Adjuvants to Enhance Immune Responses to Oral Vaccines 140
4.1 Abstract 140
4.2 Introduction 141
4.3 Materials and Methods 143
4.3.1 Materials 143
4.3.2 Adjuvant treatment of epithelial cells in vitro 144
4.3.3 Antigen uptake by epithelial and dendritic cells in vitro 145
4.3.4 In vivo studies 145
4.3.5 Statistics 150
4.4 Results and Discussion 150
4.4.1 Adjuvants induce epithelial cells to secrete DC-recruiting chemokines 150
4.4.2 DC migration towards chemokines and epithelial cell supernatants 153
4.4.3 Oral delivery of adjuvants expands intestinal antigen presenting cell population 154
4.4.4 Adjuvants modulate antigen uptake by DCs and epithelial cells in vitro 160
4.4.5 Protein localization and uptake 163
4.4.6 Induction of adaptive immune responses by oral adjuvants 169
4.5 Conclusions 173
4.6 Acknowledgements 174
4.7 References 175

Chapter 5. Biomaterial Formulation of Antigens to Study the Effect of Gastrointestinal Digestion on Immune Responses 179
5.1 Abstract 179
5.2 Introduction 180
5.3 Materials and Methods 183
5.3.1 Animals 183
5.3.2 Cell lines and bone marrow-derived dendritic cell derivation 183

5.3.3 In vitro antigen digestion 183
5.3.4 Polyacrylamide gel electrophoresis 184
5.3.5 Dendritic cell maturation 184
5.3.6 $CD8^+$ T cell activation 185
5.3.7 $CD4^+$ T cell activation 185
5.3.8 Nanoparticle synthesis 186
5.3.9 Electrospinning, nanofiber characterization, and nanofiber micronization 187
5.3.10 HRP activity assay 188
5.3.11 Release studies in simulated gastrointestinal fluids 188
5.3.12 Oral immunization 188
5.3.13 Organ processing and staining for flow cytometry 189
5.3.14 Statistical analysis 190
5.4 Results and Discussion 190
5.4.1 Gastrointestinal digestion of OVA reduces DC maturation 190
5.4.2 Ability of dendritic cells to activate T cells is influenced by antigen digestion in vitro 193
5.4.3 Differential ability of polymeric delivery platforms to protect OVA from gastrointestinal digestion 196
5.4.4 Formulation of OVA in nanofibers preserves ability to activate T cells after gastric digestion 201
5.4.5 Enhanced activation of intestinal $CD8^+$ T cell responses by an oral vaccine through epitope protection in nanofibers in combination with the mucosal adjuvant PEI 204
5.5 Conclusions 209
5.6 References 210
Chapter 6. Conclusions 214
6.1 Summary and Future Directions 214

6.2 List of Publications and Presentations 217

Appendix A: Chapter 4 Supplementary Information 219

Appendix B: Chapter 5 Supplementary Information 224

Appendix C: Dendritic Cell-Based Vaccine Programming 229

Vita 252

LIST OF FIGURES

Figure 2.1. Organization of the gut-associated lymphoid tissue. 28
Figure 2.2. Physiochemical and immunological barriers of oral vaccines. 30
Figure 2.3. Mechanisms of intestinal vaccine absorption and vaccine delivery systems used to modulate uptake. 45
Figure 2.4. Physiological and immunological differences along the gastrointestinal tract. 55
Figure 3.1. Scanning electron microscopy characterization of emulsion electrospun fiber morphology 101
Figure 3.2. Core/shell architecture of emulsion electrospun fibers. 102
Figure 3.3. pH-controlled release of proteins from Eudragit L100 nanofibers. 105
Figure 3.4. Bioactivity of proteins released from Eudragit L100 nanofibers prepared from emulsions with lower aqueous phase percentages. 108
Figure 3.5. Inclusion of hydrophilic polymer poly(vinyl alcohol) can enhance bioactivity retention from high aqueous phase emulsion formulations electrospun at high flow rates. 109
Figure 3.6. Bioactivity of HRP after incubation in simulated gastric fluid for 1 hour in soluble or emulsion electrospun Eudragit L100 fiber formulation. 112
Figure 3.7. Stability of proteins is enhanced or maintained by formulation into electrospun fibers. 114
Figure 3.8. Lyophilization of protein-loaded fibers can reduce water content and significantly extend protein bioactivity retention during storage. 116
Figure 3.9. Fiber lyophilization preserves protein bioactivity after 4 weeks of room temperature storage. 117

Figure 3.10. Bioactivity of lyophilized AP, AP-loaded PVA electrospun nanofibers, and lyophilized AP-loaded PVA electrospun nanofibers stored at 40 °C. 119
Figure 3.11. Ovalbumin encapsulated in emulsion electrospun fibers is functional and can activate antigen-specific $CD8^+$ T cells 122
Figure 3.12. Activation of B3Z T cell is not driven by the presence of fibers during treatment of DCs with antigen. 125
Figure 3.13. Eudragit L100 fibers exhibit mucoadhesive properties in vitro..... 128
Figure 3.14. Retention of BSA delivered in A) soluble form or B) loaded in micronized Eudragit L100 fibers in the mouse gastrointestinal tract after oral administration. 130
Figure 4.1. Production of the chemokine CCL20 by Caco-2 cells 152
Figure 4.2. The effect of the mucosal adjuvant CT on the antigen presenting cell population..... 155
Figure 4.3. Kinetics of antigen presenting cell recruitment in the small intestinal intraepithelial layer and lamina propria after oral adjuvant administration. 157
Figure 4.4. Effect of oral adjuvant administration on immune cell populations in the mesenteric lymph nodes..... 159
Figure 4.5. Co-delivery of PEI with protein antigen enhances uptake in DCs and epithelial cells in vitro 161
Figure 4.6. PEI complexation with protein antigens can enhance uptake 163
Figure 4.7. Protein localization in small intestine epithelial villi following oral delivery 164
Figure 4.8. Percentage of $FITC^+$ cells in the small intestine 4 hours after oral administration 165
Figure 4.9. Activation of antigen-specific $CD4^+$ T cells ex vivo by mucosal DCs 167
Figure 4.10. Systemic antibody responses to oral vaccines with different adjuvants 169

Figure 4.11. Intestinal antibody responses to oral vaccines with different adjuvants 170
Figure 4.12. Cellular immune responses to oral vaccines with different adjuvants..... 172
Figure 5.1. Gastric-digested OVA loses ability to mature dendritic cells. 192
Figure 5.2. Gastrointestinal digestion of OVA affects $CD4^+$ T cell polarization but not proliferation. 194
Figure 5.3. Gastrointestinal-digested OVA loses ability to be cross-presented to $CD8^+$ T cells in vitro. 195
Figure 5.4. OVA-loaded PLGA NPs lose ability to activate $CD8^+$ T cells after exposure to simulated gastric conditions. 198
Figure 5.5. Emulsion electrospun Eudragit L100 nanofibers limit protein release in simulated gastric fluid and protect proteins from pepsin-mediated activity loss. 200
Figure 5.6. Encapsulation of OVA in Eudragit L100 nanofibers prevents loss of $CD8^+$ activation ability upon exposure to simulated gastrointestinal digestion. 202
Figure 5.7. Effect of gastric protection of OVA in Eudragit L100 nanofibers on proliferation and polarization of $CD4^+$ T cells. 204
Figure 5.8. $CD8^+$ T cell responses to oral immunization with unprotected or gastric-protected antigen. 206
Figure 5.9. Gastric protection of oral antigen enhances $CD8^+$ T cell responses when co-delivered with mucosal adjuvant..... 207

LIST OF TABLES

Table 2.1. Mucosal pathogen route of entry, mode of transmission, and resulting disease. 24

Table 2.2. Immune responses to oral vaccine formulations with respect to protection from gastrointestinal digestion. 42

Table 2.3. Material-based approaches to modulate intestinal uptake and the effect on cellular processing and adaptive immune responses. 53

Table 2.4. Effects of immuno-modulating materials systems on immune responses after oral vaccination. 68

Table 3.1. Summary of protein-loaded electrospun fiber formulations and evaluation. 90

Table 3.2. Description and characterization of emulsion electrospun fiber formulations. 100

Table 4.1. Summary of adaptive immune responses elicited from orally delivered adjuvants. 173

ACKNOWLEDGEMENTS

I would first like the thank my advisor, Dr. Kim Woodrow, for continually providing me support, thoughtful and productive feedback throughout my work, encouraging me to seek after interesting and innovative science, and for giving me the opportunity to work on projects in which my passions of immunology and global health combine. I also thank my supervisory committee, Dr. James D. Bryers, Dr. Deborah H. Fuller, Dr. Hao Yuan Kueh, and Dr. Daniel M. Ratner, for their commitment to this project, their time and brilliant feedback, and to my development as a scientist. I would also like to acknowledge and thank my collaborators at the University of Washington, including Dr. Jaehyung Park, without whom I would not know half the immunology I do now, and Tiffany Ohlsen and Monica Macias Salas, the wonderful undergraduates I had the opportunity to mentor. Woodrow lab mates, past and present, have been unparalleled. Renuka Ramanathan, Emily Krogstad, Anna Blakney, and Shijie Cao provided mentorship and embodied the type of scientist I would strive to become. Rachel Creighton, Jamie Hernandez, and Hannah VanBenschoten were fantastic officemates, collaborators, and friends. All of you contributed your time, provided encouragement, were always there for feedback and troubleshooting advice, and kept the lab environment fun with lots of laughs and happy hours. This dissertation would not have been completed without you all. I also thank previous mentors who all made a significant impact on my scientific journey and helped push me along, especially to my undergraduate research advisor Dr. Nicholas Peppas who encouraged me in the pursuit of research and graduate school.

Part of my graduate work was spent in the lab of Dr. Laura Mackay at the Doherty Institute for Infection and Immunity in Melbourne, Australia. I cannot thank Dr. Mackay enough for the opportunity to conduct research in her lab and for her faith in me as an engineer coming into an immunology lab. To all of the members of the Mackay lab and other collaborators at the Doherty Institute, including Dr. Frank Carbone, Dr. Bill Heath,

Dr. Scott Mueller, and their lab members, thank you for making my experience unforgettable and contributing to my grow both as a scientist and as a person.

This dissertation would not have been possible, or really ever started, without the constant encouragement and unconditional support from my parents, Kevin and Terri Frizzell. They instilled in me the importance of hard work, the pursuit of knowledge, and passed on their travel bug that inspired me to seek international opportunities that made me a more well-rounded person. I thank my siblings, Emily and Colin, for showing me what it means to never give up in pursuit of your dreams and for always providing a good laugh at the expense of another family member. To have such a supportive family is an incredible blessing. To all of the friends I have made over the past 5 years, your friendship in both science and non-science related endeavors have provided me so much joy and inspiration. I could not have asked for a better cohort of friends to go through this journey with and know I have made lifelong friends. Finally, to my partner Adam, who has been with me side by side since submission of the NSF GRFP application that cemented my going to graduate school in Seattle and us starting long distance. I could not have done this without your never-failing love, support, advocacy, positivity, and countless sacrifices. May our adventures together never end.

I would like to acknowledge financial support from the National Science Foundation Graduate Research Fellowship Program, the National Science Foundation Graduate Research Opportunities Worldwide Fellowship Program, and from the Achievement Rewards for College Scientists (ARCS) Foundation.

DEDICATION

To the village that made this possible.

Chapter 1. SUMMARY AND SPECIFIC AIMS

1.1 Significance and Motivation

Oral vaccination is one of the most attractive administration routes due to increased patient compliance, the potential for mass vaccination, lower cost, and the elimination of the need for needles as sterile medical supplies in low resource settings are not always available [1]. Importantly, oral vaccination allows for the induction of immunity at mucosal surfaces, which enhances immune protection against mucosally-invading pathogens in contrast to traditional intramuscular vaccination routes, in which the development of mucosal immunity is limited [2]. Due to the lack of vaccines for many mucosal pathogens, these infections result in a high global burden of disease causing millions of deaths annually [3]. Most licensed intramuscular vaccines in the U.S. consist of inactivated pathogens or recombinant proteins, which are advantageous due to their safety profile [4]; however, such vaccines face significant challenges when delivered orally to mucosal surfaces, including: 1) cargo degradation by enzymes in the gastrointestinal tract, 2) low intestinal absorption, and 3) inability to overcome oral tolerance [5,6]. Materials-based strategies have been developed to address some of these barriers, but antigen uptake remains limited and mechanisms to overcome tolerance have not been elucidated [7–9]. Additionally, novel nanotechnology strategies are needed for the delivery of biotherapeutics that load therapeutics at high encapsulation efficiency, can stabilize the proteins upon storage, and are amenable to manufacturing scale-up for clinical use [10,11].

The first barrier to oral vaccines is the digestive gastrointestinal environment, which can denature and cleave protein-based antigens. In the field of allergy, correlations between the gastrointestinal enzyme digestion of proteins and their ability to elicit immune responses have been identified [12–14]. For orally-delivered protein antigens, protection from gastric digestion has been shown to activate the immune system in terms

of systemic antibody production in contrast to the lack of systemic antibodies observed without gastric protection [15]. However, many gaps remain in understanding how gastrointestinal digestion affects immune responses. The impact of gastrointestinal digestion on innate immune responses, which ultimately control adaptive immunity, has not been studied. Additionally, the impact of digestion on the activation of cytotoxic $CD8^+$ T cell responses is not fully understood. Questions remain regarding the need to protect protein antigens in gastric conditions, intestinal conditions, or both, as different proteases are found at each site that can differentially cleave immunogenic epitopes critical for immune responses. Further study of the role of gastrointestinal digestion will be critical for the design of oral vaccines and their carriers.

In terms of the barriers of low absorption and tolerance bias, insights from the field of mucosal immunology reveal the importance of intestinal epithelial cells in propagating immunogenic signals to condition dendritic cells (DCs) in the underlying lamina propria, which are responsible for inducing antigen-specific adaptive immune responses in the lymph nodes, and modulate antigen uptake [16–18]. Intestinal epithelial cells are responsible for conditioning antigen presenting cells in the gut to be tolerogenic, leading to the generation of regulatory adaptive immune responses. However, activation of epithelial cells by replicating pathogens or vaccine adjuvants can switch the nature of immune signals secreted into the surrounding tissue. Inflammatory cytokines and chemokines are the main soluble mediators in this process [19], where they condition innate immune cells to become inflammatory rather than tolerogenic and impact DC function to activate effector immunity. Chemokines can recruit immature dendritic cells and other antigen presenting cells to site of infection or vaccination, and specifically to the intestinal epithelium where DCs can internalize antigens present in the lumen. While potent parenteral adjuvants are known, the identification of adjuvants that can overcome the tolerogenic environment in the gut to activate immunity is still needed.

Here, we focused on the newly found importance of both gastrointestinal digestion and gut epithelial cells with a biomaterial vaccine delivery strategy for oral immunization. We hypothesized that pH-responsive nanofibers that protect antigens from gastrointestinal digestion with co-delivery of epithelial cell-activating adjuvants could address challenges associated with oral vaccine delivery. First, we developed and evaluated electrospun fibers to deliver proteins in a pH-dependent manner in conditions of pH > 6 to achieve release in the small intestine while retaining protein bioactivity. This platform was then used to prevent protein antigen degradation in harsh gastric conditions (barrier 1) to selectively deliver functional vaccine antigens to the small intestine. This platform was also used to study how protection from gastric digestion impacts less studied arms of the immune system, specifically DC and T cell responses. In the second arm of this work, we hypothesized that adjuvants capable of activating intestinal epithelial cells can initiate an inflammatory signaling cascade to expand the local DC population at the small intestinal epithelium. In this way, intestinal absorption of vaccine antigens from the lumen into dendritic cells may be increased (barrier 2). Additionally, vaccines containing mucosal adjuvants can stimulate intestinal epithelial cells to secrete inflammatory factors to overcome tolerance and ensure the activation of effector immune responses (barrier 3) [21,22].

1.2 Specific Aims

1.2.1 *Aim 1. Develop electrospun fibers for oral delivery of protein therapeutics.*

Here, we evaluated and characterized various electrospinning parameters, formulations, and methods to load proteins into polymeric nanofibers while retaining protein bioactivity and releasing the protein cargo with pH-dependency. Specifically, we developed this drug delivery platform with the polymer Eudragit L100, a co-polymer of methacrylic acid and methyl methacrylate, for its pH-sensitive dissolution at pH > 6. Maintenance of protein bioactivity is of critical importance when delivering therapeutic

biologics and we thus optimized a nanofiber platform to maintain protein bioactivity during formulation and upon storage. This electrospun fiber platform was also evaluated for the ability to protect loaded proteins in simulated gastric conditions from protease-mediated function loss. Overall, a biomaterial-based delivery platform using emulsion electrospinning was established to study and evaluate oral protein-based vaccines and therapeutics.

1.2.2 *Aim 2. Evaluate ability of adjuvants to stimulate innate and adaptive immune responses when used in an oral vaccine.*

A library of mucosal adjuvants was evaluated for their ability to stimulate intestinal epithelial cells as a strategy to increase DC migration to the intestinal epithelium, enhance uptake of antigens, and ultimately improve adaptive immune responses elicited by oral vaccines. We first identified adjuvants capable of inducing the production of DC-recruiting chemokines by intestinal epithelial cells *in vitro* and evaluated DC migration and recruitment in *in vitro* and *in vivo* models. Modulation of antigen uptake when adjuvants were co-delivered was also investigated both *in vitro* and *in vivo*. Additionally, the elicitation of adaptive systemic and mucosal immune responses of the identified adjuvant(s) were determined when administered orally with a protein antigen. Overall, this aim provided initial results on differential mechanisms of action of adjuvants after oral delivery, in particular their ability to induce the secretion of chemokines by intestinal epithelial cells, increase antigen internalization by multiple important cell populations, and drive different adaptive immune responses.

1.2.3 *Aim 3. Determine innate and adaptive immune responses to fiber-protected oral vaccines co-delivered with mucosal adjuvants.*

Last, we applied the protein-delivering nanofiber delivery platform developed in Aim 1 to study the effect gastrointestinal antigen digestion on oral vaccine immune

responses. First, we investigated how gastrointestinal digestion affects antigen immunogenicity in terms of DC maturation and presentation to $CD4^+$ and $CD8^+$ T cells *in vitro*. Based on the requirements to provide antigen protection in certain gastrointestinal conditions, we evaluated the ability of polymeric drug delivery platforms, namely nanoparticles and electrospun nanofibers, to prevent antigen digestion in gastrointestinal environments and retain immunogenicity. Finally, adaptive immune responses to oral vaccines delivered in the electrospun nanofiber carrier was evaluated with and without the co-delivery of effective adjuvants identified in Aim 2 to further potentiate immune responses. These studies ultimately provide insight into the formulation requirements of oral vaccines and their impact on immunologic outcomes.

1.3 Summary

Overall, this thesis developed a novel biomaterials strategy to enhance the immune responses elicited by oral vaccination using electrospun fibers to prevent vaccine degradation in the stomach and induce stimulation of intestinal epithelial cells by co-delivery of adjuvants to induce specific adaptive immune responses. We identified that antigen digestion by gastrointestinal proteases prevented DC maturation and presentation of antigenic epitopes that contain protease cleavage sites, leading to DCs being unable to activate epitope-specific T cells. In contrast to nanoparticles, emulsion electrospun fibers limited antigen release in simulated gastric conditions and provided protection of antigens from protease-mediated activity loss. Evaluation of adjuvants for use in oral vaccines identified CpG ODN to be an effective driver of antibody responses while the cationic polymer polyethyleneimine (PEI) increased the $CD8^+$ T cell response. When studied as an oral vaccine in mice, the strongest $CD8^+$ T cells responses in the intestine were induced when PEI was co-delivered with antigens formulated in the protective nanofiber delivery platform. These results indicated that protection of antigenic epitopes from digestion is

important in inducing T cell responses to orally-delivered antigens but only when proper immune activation through adjuvant co-delivery also achieved. Ultimately, this work both investigated and addressed barriers to oral vaccination by protecting the vaccine antigens from gastrointestinal digestion conditions in a pH-sensitive biomaterial carrier and investigating adjuvant-induced epithelial cell activation as a mechanism to recruited antigen presenting cells, increase vaccine uptake, and enhance adaptive immunity.

1.4 References

[1] M.M. Levine, G. Dougan, Optimism over vaccines administered via mucosal surfaces, Lancet. 351 (1998) 1375–1376. doi:10.1016/S0140-6736(05)79439-3.

[2] N. Lycke, Recent progress in mucosal vaccine development: potential and limitations, Nat. Rev. Immunol. 12 (2012) 592–605. doi:10.1038/nri3251.

[3] World Health Organization, World Health Statistics 2017 : Monitoring Health for The SDGs, 2017. doi:10.1017/CBO9781107415324.004.

[4] U.S. Vaccine Names | CDC, (2014). http://www.cdc.gov/vaccines/terms/usvaccines.html (accessed November 1, 2016).

[5] S. Wang, H. Liu, X. Zhang, F. Qian, Intranasal and oral vaccination with protein-based antigens: advantages, challenges and formulation strategies, Protein Cell. 6 (2015) 480–503. doi:10.1007/s13238-015-0164-2.

[6] M. Goldberg, I. Gomez-Orellana, Challenges for the oral delivery of macromolecules, Nat. Rev. Drug Discov. 2 (2003) 289–295. doi:10.1038/nrd1067.

[7] M. Yu, J. Wu, J. Shi, O.C. Farokhzad, Nanotechnology for protein delivery: Overview and perspectives, J. Control. Release. 240 (2016) 24–37. doi:10.1016/j.jconrel.2015.10.012.

[8] S. Mitragotri, P.A. Burke, R. Langer, Overcoming the challenges in administering biopharmaceuticals: formulation and delivery strategies, Nat. Rev. Drug Discov. 13 (2014) 655–672. doi:10.1038/nrd4363.

[9] R. Sharma, U. Agrawal, N. Mody, S.P. Vyas, Polymer nanotechnology based approaches in mucosal vaccine delivery: Challenges and opportunities, Biotechnol. Adv. 33 (2015) 64–79. doi:10.1016/j.biotechadv.2014.12.004.

[10] R. Duncan, H. Ringsdorf, R. Satchi-Fainaro, Polymer therapeutics--polymers as drugs, drug and protein conjugates and gene delivery systems: past, present and future opportunities., J. Drug Target. 14 (2006) 337–41. doi:10.1080/10611860600833856.

[11] D.J. Brayden, M.A. Jepson, A.W. Baird, Keynote review: intestinal Peyer's patch M cells and oral vaccine targeting., Drug Discov. Today. 10 (2005) 1145–57. doi:10.1016/S1359-

6446(05)03536-1.

[12] J.D. Astwood, J.N. Leach, R.L. Fuchs, Stability of food allergens to digestion in vitro, Nat. Biotechnol. 14 (1996) 1269–1273. doi:10.1038/nbt1096-1269.

[13] C.C. Bowman, M.K. Selgrade, Failure to Induce Oral Tolerance in Mice Is Predictive of Dietary Allergenic Potency among Foods with Sensitizing Capacity, Toxicol. Sci. 106 (2008) 435–443. doi:10.1093/toxsci/kfn200.

[14] G. Jordakieva, M. Kundi, E. Untersmayr, I. Pali-Schöll, B. Reichardt, E. Jensen-Jarolim, Country-wide medical records infer increased allergy risk of gastric acid inhibition, Nat. Commun. 10 (2019) 3298. doi:10.1038/s41467-019-10914-6.

[15] S. Jain, Activation patterns of murine B cells after oral administration of an encapsulated soluble antigen, Vaccine. 14 (1996) 42–48. doi:10.1016/0264-410X(95)00158-W.

[16] J. Farache, I. Koren, I. Milo, I. Gurevich, K.-W. Kim, E. Zigmond, G.C. Furtado, S.A. Lira, G. Shakhar, Luminal Bacteria Recruit CD103+ Dendritic Cells into the Intestinal Epithelium to Sample Bacterial Antigens for Presentation, Immunity. 38 (2013) 581–595. doi:10.1016/j.immuni.2013.01.009.

[17] M. Rescigno, M. Urbano, B. Valzasina, M. Francolini, G. Rotta, R. Bonasio, F. Granucci, J.-P. Kraehenbuhl, P. Ricciardi-Castagnoli, Dendritic cells express tight junction proteins and penetrate gut epithelial monolayers to sample bacteria, Nat. Immunol. 2 (2001) 361–367. doi:10.1038/86373.

[18] Y. Yin, T. Qin, X. Wang, J. Lin, Q. Yu, Q. Yang, CpG DNA assists the whole inactivated H9N2 influenza virus in crossing the intestinal epithelial barriers via transepithelial uptake of dendritic cell dendrites, Mucosal Immunol. 8 (2015) 799–814. doi:10.1038/mi.2014.110.

[19] R. McClure, P. Massari, TLR-Dependent Human Mucosal Epithelial Cell Responses to Microbial Pathogens., Front. Immunol. 5 (2014) 386. doi:10.3389/fimmu.2014.00386.

[20] H. Frizzell, T.J. Ohlsen, K.A. Woodrow, Protein-loaded emulsion electrospun fibers optimized for bioactivity retention and pH-controlled release for peroral delivery of biologic therapeutics, Int. J. Pharm. 533 (2017) 99–110. doi:10.1016/j.ijpharm.2017.09.043.

[21] S.L. Demento, W. Cui, J.M. Criscione, E. Stern, J. Tulipan, S.M. Kaech, T.M. Fahmy, Role of sustained antigen release from nanoparticle vaccines in shaping the T cell memory phenotype, Biomaterials. 33 (2012) 4957–4964. doi:10.1016/j.biomaterials.2012.03.041.

[22] S.-H. Kim, Y.-S. Jang, The development of mucosal vaccines for both mucosal and systemic immune induction and the roles played by adjuvants, Clin. Exp. Vaccine Res. 6 (2017) 15. doi:10.7774/cevr.2017.6.1.15.

Chapter 2. INTRODUCTION

Adapted from: **Frizzell, H.**, & Woodrow, K. A. Biomaterial approaches for understanding and overcoming immunological barriers to effective oral vaccination. *Submitted, in review.*

2.1 Background

2.1.1 *Mucosal vaccines*

Vaccines are the most effective way to reduce the spread of infectious diseases and are one of the biggest successes of global health. Annually, vaccines prevent 2-3 billion deaths worldwide [1]. The majority of vaccines are administered by intramuscular injection, which requires trained medical personnel and sterile equipment. In low-resource settings where the burden of infectious disease is concentrated, these requirements are not always readily available, adding challenges to widespread vaccination campaigns [2]. Additionally, alternative immunization methods that do not require as much time to administer are advantageous in situations of disease outbreak and epidemics. For example, 20 patients can be immunized orally in the same amount of time that 1 patient could be immunized by an injection [3]. The delivery of vaccines through the oral route is one way to increase access to vaccines in low-resources areas, improve immunization compliance, and improve infectious disease outbreak readiness.

2.1.1.1 Types of vaccine antigens

Vaccines in the United States and worldwide are predominately given by intramuscular injection. Only ~5% of the licensed vaccines in the U.S. are given orally, and all of the antigens in these vaccines are live-attenuated pathogens. Globally, oral

vaccines are used to protect against Rotavirus (live-attenuated), Poliomyelitis (live-attenuated), Typhoid (live-attenuated and delivered in enteric-coated capsules), and Cholera (killed whole cells). There exist only three World Health Organization-qualified oral vaccines that are not live-attenuated, all of which are used against Cholera. One is comprised of killed whole *Vibrio cholerae O1* bacterial cells and the adjuvant cholera toxin subunit B (Dukoral®) to be delivered in a buffer that requires buffer salt dissolution and mixing with the vaccine prior to administration. The other two are bivalent vaccines that consist of killed whole-cell *Vibrio cholerae* serogroups *O1* and *O139* (Shanchol™ and Euvichol®) and are packaged as a suspension that does not require an additional buffer. While these vaccines are approved for use by the World Health Organization, they are not FDA-approved for use in the U.S. In contrast to oral vaccine formulations, vaccine antigens in intramuscular immunizations are predominantly subunit proteins from the pathogen or killed pathogens. The differences in vaccine type between these two administration methods are due to physiochemical barriers and immune regulation in muscle tissue compared to mucosal surfaces. While vaccine injection directly into muscle tissue allows for immediate interaction of the vaccine antigen with local immune and antigen presenting cells, such as neutrophils, macrophages, and dendritic cells, orally-delivered vaccines must overcome the degradative environment of the GI tract as well as overcome immune tolerance before the vaccine antigen is able to interact with gut-associated immune cells. Thus, when the route of vaccine administration is oral, live-attenuated vaccines are most effective, as some are able to withstand the physiological environment and replicate in the intestinal tissue, eliciting a robust immune response. In contrast, the oral delivery of protein-based antigens used in intramuscular vaccines is not as effective at overcoming oral tolerance and generating immune protection [4]. However, next generation vaccines are moving away from delivering live-attenuated vaccines due to safety concerns as well as practical limitations, such as culture and storage difficulties, and are now focusing on protein-based subunit antigens. These antigens are non-infectious

portions of the pathogen against which the immune response is generated. Thus, new strategies must be developed to improve the efficacy of orally-delivered protein-based vaccines [3].

2.1.1.2 Mucosal adjuvants

One strategy to enhance the immune responses generated from mucosal vaccines is the use of adjuvants [5,6]. Adjuvants are commonly co-delivered with vaccine antigens to stimulate immune cells and direct them to generate robust effector immune responses [7]. The most common mucosal adjuvants include cholera toxin (CT) and heat-labile enterotoxin (LT). However, the clinical use of these adjuvants is limited due to their high toxicity. This unfavorable safety profile has motivated the development of non-toxic forms of these toxins that are currently in clinical trials. Depending on the adjuvant used, the nature of the adaptive immune responses can also be directed. When naïve T cells recognize an antigen that is presented to them by antigen presenting cells, they become activated and differentiate down a certain lineage depending on the types of signals that the antigen presenting cell secretes. Naïve $CD4^+$ T cells can differentiate down many pathways, including into T_H1, T_H2, T_H17, and T_{reg} cells. Each of these T cell types has a different function, with T_H1 cells contributing to the clearance of intracellular pathogens through production of IFN-γ and activation of $CD8^+$ T cells, T_H2 cells helping resolve extracellular parasite infections and inducing antibody production by B cells, T_H17 cells fighting extracellular bacteria and fungi, and T_{reg} cells suppressing the immune response against self or innocuous antigens. The signals that induce the activation of these transcription pathways can be controlled through the use of adjuvants. For example, the adjuvant monophosphoryl lipid A is known to activate the formation of T_H1 cells while the adjuvant alum (aluminum salts) is known to bias T_H2 responses [6]. Additionally, certain adjuvants are known to drive cytotoxic $CD8^+$ T cell responses, which are critical in combatting intracellular infections through their release of cytotoxins and binding of Fas (CD65) on the surface of infected cells leading to apoptosis.

The use of adjuvants for mucosal vaccination is also incredibly important due to the nature of immune suppression that exists at these sites, particularly the gut mucosa. The intestine is constantly exposed to food-based antigens and other substances that are not harmful. Thus, the existence of oral tolerance is critical to prevent over-activation of the immune system, in which robust inflammatory responses can be toxic to the tissue and allergies can occur to food substances. For protein-based vaccine antigens, tolerance is likely to occur due to the lack of immunostimulation and "danger signals" required. However, co-delivery of an adjuvant can instruct the gut-associated immune system to mount a protective response rather than tolerance [8,9].

2.1.2 *Organization of the mucosal immune system*

In addition to the logistical and practical advantages of oral immunizations, the route of vaccination is also critical in the elicitation of systemic and mucosal immunity [10]. Infectious pathogens enter the body primarily through mucosal surfaces, such as in the nasal mucosa after inhalation, the intestinal mucosa after ingestion, or the mucosa of the reproductive tract or rectum through sexual transmission (summarized in Table 2.1). In humans, these mucosal surfaces have a surface area of almost 400 m^2, an enormous area that our immune system must constantly survey to protect against infection. Due to this large feat, the mucosal immune system includes three-fourths of all the lymphocytes in the body and produces the majority of immunoglobulins. While each infectious disease has a unique pathophysiology, protection from many pathogens require robust immune defenses specifically at these mucosal surfaces. The infectious diseases that contribute to the most worldwide mortality are caused by mucosally-invading pathogens, leading to more than 9 million deaths annually [11].

Table 2.1. Mucosal pathogen route of entry, mode of transmission, and resulting disease. Table revised from [12] *and does not represent an exhaustive list of all mucosal infections.*

Mucosal route of entry	**Mode of transmission**	**Pathogen**	**Disease**
Mouth and respiratory tract	Inhalation or ingestion of infective material	Measles virus	Measles
		Influenza virus	Influenza
		Varicella-zoster	Chickenpox
		Epstein-Barr virus	Mononucleosis
		Streptococcus pyogenes	Tonsillitis
		Haemophilus influenzae	Pneumonia, meningitis
Gastrointestinal tract	Contaminated food or water	Rotavirus	Diarrhea
		Norovirus	Gastroenteritis
		Hepatitis A	Jaundice
		Salmonella enteritidis, S. typhimurium	Food poisoning
		Vibrio cholerae	Cholera
		Salmonella typhi	Typhoid fever
Reproductive tract and other	Sexual transmission/infected blood	Hepatitis B virus	Hepatitis B
		Human immunodeficiency virus (HIV)	Acquired immunodeficiency syndrome (AIDS)
	Sexual transmission	*Neisseria gonorrhoeae*	Gonorrhea
		Treponema pallidum	Syphilis

The systemic immune system includes primary lymphoid organs such as the spleen and lymph nodes and consists of networks of lymphatic vessels that drain excess fluid from tissues into lymph nodes and filter blood through the spleen. It is in these sites that

adaptive immune cells, T and B cells, are activated and generate antigen-specific immune responses. These responses primarily result in the increase of effector T cells and antibody-secreting B cells in circulation as well as the establishment of antigen-specific central memory cells [13]. In contrast to the organization and function of the systemic immune system, mucosal surfaces have their own organized lymphoid structures. The gastrointestinal tract, for example, has gut-associated lymphoid tissue, or GALT. The organization and function of the GALT will be further described in Section 2.1.2.1. Such a system also exists for the nasal-associated lymphoid tissue (NALT) and the skin-associated lymphoid tissue (SALT). In these lymphoid organs, immune responses differ in their homing abilities to specific mucosal sites and in the nature of the immune response. For example, immunity in the gut is primarily driven by secretory IgA in the mucus that lines the intestinal tract that can bind and neutralize pathogens in the lumen before they gain access to the intestinal epithelium.

Thus, the ability of vaccines to generate protection at these mucosal surfaces is of utmost importance to prevent infection at the point of pathogen entry; however, intramuscular vaccines are effective at establishing systemic immunity but do not elicit strong responses in mucosal tissues. In contrast, it is well accepted that vaccination at mucosal surfaces provides immunity at the location of the immunization [14]. Thus, the elicitation of immune responses can be targeted to certain sites based on the route of vaccination. Mucosal immunization can also induce immunity at other distant mucosal sites due to the connection of mucosal surfaces through the 'common mucosal immune system'. For example, it was shown that oral nanoparticle vaccines that were released in the large intestine were able to provide protection against viral challenge in both the vaginal tract and rectum [15]. Additionally, it has been shown that following transcutaneous skin vaccination, cells migrate to immune sites in the gut mucosa to present antigen, leading to the development of mucosal effector lymphocytes [16].

2.1.2.1 Gut-associated lymphoid tissue

Oral vaccination is able to access one of the largest mucosal surfaces in the body, the intestinal tract, making it an incredibly attractive site of immunization. The small intestine is lined by a single layer of columnar epithelium and is divided into three segments, the duodenum being the most proximal to the stomach, followed by the jejunum and the ileum. This epithelial structure is in contrast to that of other mucosal surfaces, such as the reproductive tract, which is composed of multi-layered stratified squamous epithelium. As mentioned, this anatomical site has its own organized lymphatic tissue, the GALT (Figure 2.1). Immune cells can be found scattered throughout the intestinal epithelium and lamina propria as well as in organized lymphatic tissues, Peyer's patches and mesenteric lymph nodes. Throughout the intestinal tissue also exist innate immune cells, such as macrophages and dendritic cells, and adaptive immune cells T and B cells. Additionally, intraepithelial lymphocytes (IELs), a heterogeneous population of antigen-experienced $CD4^+$ and $CD8^+$ T cells that express E-cadherin (CD103), are present between epithelial cells [17]. Due to the proximity of IELs to the intestinal lumen, these cells are one of the first lines of defense against enteric infections. The importance of intestinal epithelial cells themselves in mucosal immunity is discussed below.

In the underlying lamina propria, cells of interest include dendritic cells that make up ~5-10% of the total cells [18,19]. Importantly, these cells migrate from the lamina propria to the mesenteric lymph node, where they can interact with adaptive lymphocytes. There are three main DC populations in the intestinal lamina propria, $CD103^+CD11b^+$, $CD103^+CD11b^-$, and $CD103^-CD11b^+$ [20]. While the origin and function of these DC subtypes are still being investigated, they are thought to have differences in their location within the lamina propria (with $CD103^+$ DCs enriched at the epithelial layer), migration to MLNs, and of priming different T cell subsets [18,21]. Importantly, $CD103^+$ DCs are responsible for detection of inflammatory signals, acquiring and presenting antigen to T cells in MLNs, and have been shown to migrate to the epithelial cell layer to capture

antigens [22,23]. In addition to the IEL, T cells also exist in the lamina propria but display a different phenotype than IELs, with lamina propria T cells displaying an effector memory phenotype and regulatory phenotype [24]. In the lamina propria, IgA-secreting B cells are also present.

Organized lymphatic tissues in the intestine include Peyer's patches and mesenteric lymph nodes. In contrast to the lamina propria, DCs only make up 0.2% of the cells in the intestinal lymphoid tissues [21]. Peyer's patches are found along the length of the small intestine in the submucosa and are lined by a combination of columnar epithelial cells and specialized epithelial cells called M cells, which lack surface microvilli and a mucus layer. M cells are also able to transport antigens from the intestinal lumen to the underlying lymphoid tissue [25]. The follicle-associated epithelium (FAE) lining Peyer's patches is also infiltrated by immune cells such as T cells, B cells, macrophages, and dendritic cells. Below this epithelial layer exists the subepithelial dome (SED), which contains B cell follicles surrounded by T cell areas. In Peyer's patches, dendritic cells are localized in the SED and follicles. DCs can also be recruited to the FAE through epithelial cell secretion of chemokines [26]. In Peyer's patches, adaptive immunity can be activated by infiltrating antigens as well as by migratory DCs from the lamina propria. These primed T and B cells then drain to the mesenteric lymph node to amplify immune responses and enter circulation through the thoracic duct.

The mesenteric lymph nodes (mLNs) are the largest lymph nodes in the body and are where the presentation of orally-fed antigens predominately occurs [27]. The mLNs are the most critical lymphoid tissues for the development of mucosal immunity in the gut. Dendritic cells from both the intestinal lamina propria and Peyer's patches can migrate to the mLNs to present antigen within hours of antigen feeding and prime T cells that will then be directed back to the intestinal mucosa. This mucosal homing occurs when lymphocytes are primed specifically in the mesenteric lymph nodes through the downregulation integrin L-selectin, which directs cells to enter lymphoid tissues, and

upregulation of $\alpha_4\beta_7$, which allows cells to enter mucosal surfaces that express mucosal addressin cell-adhesion molecule 1 (MAD-CAM1) on their vasculature [28,29]. Lymphocytes primed in the mLNs are also recruited back to the intestinal tissue through expression of the chemokine receptor CCR9, whose ligand CCL25 is expressed by small intestinal epithelial cells [30,31]. These lymphocytes primed in the mLNs then distribute throughout the intestinal tissue, with mature IgA-secreting B cells present in the lamina propria, $CD4^+$ T cells primarily in the lamina propria, and $CD8^+$ T cells primarily in the epithelium. These cells function as both effector and memory cells to provide immunity during primary and secondary infection, respectively [32]. As the majority of oral antigens come from innocuous substances, many of the antigen-experienced T cells in the intestine are regulatory cells to maintain local tolerance to food-based and environmental antigens [33].

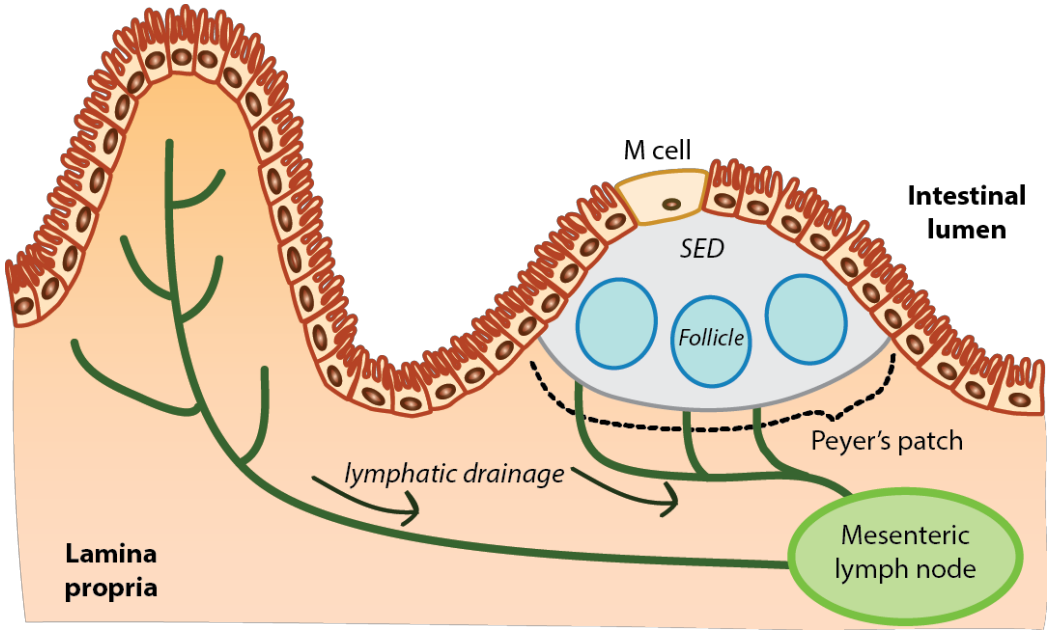

Figure 2.1. Organization of the gut-associated lymphoid tissue.

Intestinal epithelial cells have a critical role in mucosal immunity, as they are the first line of defense against pathogens and constantly provide signals to the underlying immune cells that dictate the development of tolerance or inflammation. At steady state, intestinal epithelial cells constitutively produce IL-10, TGF-β, thymic stromal

lymphopoietin (TSLP), and retinoic acid, which can condition both resident DCs and regulatory T cells to be unresponsive [25,34]. The signals produced by epithelial cells can be modulated by stimuli in the intestinal lumen, such as pathogen-associated molecular patterns. Recognition of microbial ligands by epithelial cells occurs through the activation of toll-like receptors (TLRs), NOD-like receptors (NLRs), and RIG-I-like receptors (RLRs). In addition to activating an inflammatory pathway that can lead to the generation of immunity, microbial recognition by epithelial cells through these receptors is also important for the regulation of intestinal homeostasis. Depending on the nature of the signals produced by the epithelial cells, both innate and adaptive immune responses can be controlled. In the context of generating immunity, inflammatory signals by epithelial cells can control DC phenotype and function. DCs lose their ability to produce the inflammatory cytokine IL-12, which polarizes T_H1 responses, when exposed to the tolerogenic immune signals expressed by epithelial cells. This anti-inflammatory state of DCs can be overcome by their exposure to microbial signals through the formation of transepithelial dendrites (TEDs), which is initiated by epithelial cell signaling [35]. It is thought that proper activation of DCs requires both direct pathogen recognition and inflammatory signals from epithelial cells [36].

Recruitment and expansion of antigen presenting cells at the intestinal epithelium is mediated by the production of the chemokine CCL20 by epithelial cells [37]. The CCL20 receptor CCR6 is expressed by immature dendritic cells and effector memory T and B cells. CCL20 production is constitutively expressed at low levels, but can be induced by the inflammatory cytokines IL-1β and TNF-α as well as pattern recognition receptor agonists that signal through NF-κB [38–41]. The recruitment of antigen presenting cells by epithelial cells can result in enhanced antigen internalization and has been shown to be essential for the generation of protective immunity [42].

2.1.3 *Defenses of the gastrointestinal tract*

As mentioned above, the development of effective oral vaccines is in large part challenging due to the significant physiochemical and immunological challenges that prevent parenteral vaccines from being administered orally, such as the harsh digestive environment of the gastrointestinal tract, limited absorption and bioavailability, and the immuno-tolerant nature of the gut. Vaccines delivered orally face many of the same obstacles as small molecule and biological therapeutics delivered by this route, and the physiological challenges of oral drug delivery have been reviewed elsewhere [4,43–45]. Here, we focus on how these barriers influence the immunologic function of oral vaccines and on the design of material-based systems to both understand and overcome challenges of oral immunization (Figure 2.2).

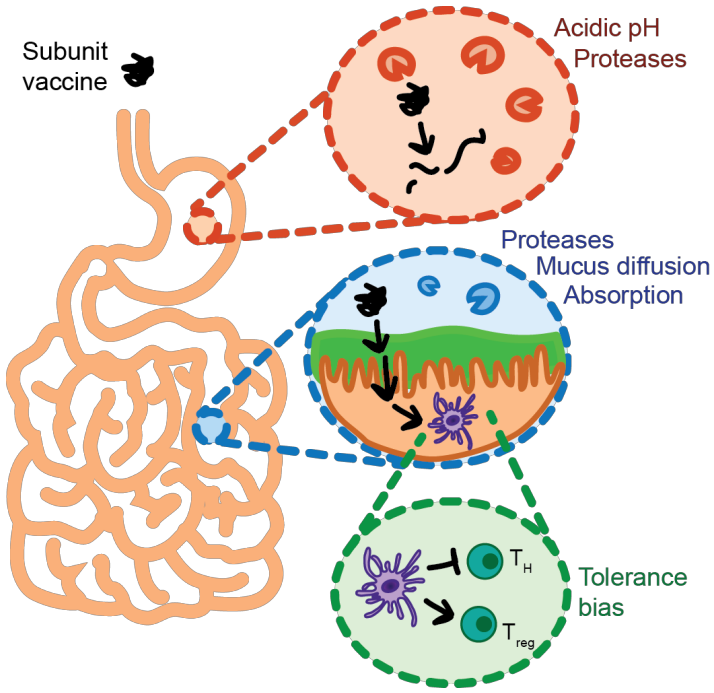

Figure 2.2. Physiochemical and immunological barriers of oral vaccines.

2.1.3.1 Digestive environment of gastrointestinal tract

Oral delivery of biologic-based therapeutics such as vaccines results in a degradative fate before reaching the epithelium for absorption, access to lymphoid organs,

and activation of antigen-specific lymphocytes. This is because a primary function of the gastrointestinal system is to digest food and absorb nutrients, and there exists high concentrations of enzymes and salts throughout the gastrointestinal tract that facilitates the breakdown of proteins, fats, and carbohydrates. The main enzyme responsible for protein digestion in the stomach is pepsin, which cleaves amide bonds to break down large protein molecules into polypeptides and is most active in acidic environments (max activity at pH 2.0). Trypsin, chymotrypsin, and peptidase present in the small intestine further break down digested proteins into tri- and dipeptides and single amino acids to facilitate absorption. Finally, the apical surface of intestinal enterocytes contains glycoproteins and enzymes, including glycosidases and protease-peptidases that form a brush border glycocalyx responsible for terminal digestion [46]. Ultimately, the presence of these enzymes results in cleavage of proteins at multiple sites, leading not only to their degradation but also the disruption of antigenic epitopes against which an immune response can be generated. Gastrointestinal enzyme-mediated degradation is known to influence the elicitation of an immune response. For example, substances with allergic potential are less susceptible to digestion by gastrointestinal enzymes, suggesting immunogenic epitopes are resistant to digestion [47]. Likewise, neutralizing stomach acidity to inhibit gastric enzymes leads to some tolerated foods inducing allergic responses [48–50]. These results suggest that gastrointestinal digestion can play a significant role in the immunogenicity of fed proteins. For vaccines, antigenic sequences that drive adaptive immune responses must be preserved to generate immune protection.

2.1.3.2 Limited access to epithelial layer and absorption

In addition to the acquisition of nutrients, the mucosal surface of the gastrointestinal tract also prevents infection by pathogens introduced through contaminated food and water sources. While beneficial to host protection, this same mechanism results in ineffective delivery of vaccines and large therapeutics. Commensal bacteria and mucus along the gastrointestinal tract pose a physical barrier for ingested substances to reach

the intestinal epithelium. Gut commensals occupy a nutrient-rich space along the lower gastrointestinal tract, where they live within and are supported by a hydrogel mucus network separating them from the intestinal epithelium to prevent an immune response against these innocuous bacteria. Glycoproteins that form the mucus matrix are continuously produced by intestinal Goblet cells and their secretion can be modulated by the presence of irritants and pathogens. The density and thickness of the mucus layer varies along the gastrointestinal tract. In rats, mucus thickness in the stomach is ~200 μm, decreases to ~100 μm in the small intestine, and increases to ~800 μm in the colon [51]. Mucus is a barrier to diffusion and can prevent luminal contents from accessing the epithelium for absorption. The mucus layer also protects the epithelium from the harsh digestive environment present in the stomach and intestinal lumen as well as from foreign microbes that have gained access to the gastrointestinal tract. Invading pathogens can become trapped in the integrated mucus network due to their size (mucus mesh pore size of ~300 nm in humans) and adhesion to the large, negatively-charged glycans [52]. Once trapped, these pathogens are subsequently cleared from the body through natural peristalsis. Orally delivered vaccines must diffuse through mucus in the intestinal lumen to be internalized and processed by cells. Failure of vaccines to access the epithelium results in their clearance and inability to initiate immune responses.

If and when substances diffuse through the mucus layer and reach the intestinal epithelium, small macromolecules can directly access cells in the lamina propria by paracellular transport across epithelial tight junctions, known as "paracellular leak" [53]. These pores are small (<5 nm) but can vary in diameter depending on the activation of different membrane transporters and on pathogen-induced damage, which leads to enhanced permeability. Hence, absorption of most vaccines requires active cellular transport. The use of certain pathways depends on the type of substance encountered and its physiochemical properties including shape, size, and charge. Luminal substances can be processed by epithelial enterocytes (~80% of small intestinal epithelial cells), mucus-

secreting Goblet cells, and microfold (M) cells in the follicle-associated epithelium (FAE) overlying Peyer's patches, which are organized secondary lymphoid structures uniquely present in the small intestine that are able to initiate adaptive immune responses. M cells have been shown to be a major mechanism of soluble antigen transcytosis and these cells can transport antigen directly to Peyer's patches [54]. However, the frequency of M cells is low in humans (5-10% of FAE cells), leading to research into alternative mechanisms of antigen uptake in the intestine [55]. Uptake of antigen by enterocytes can occur by receptor-mediated endocytosis, resulting in lysosomal degradation of the antigen or transcytosis into the interstitial space of the lamina propria. Enterocytes themselves are polarized, with their apical surface specialized for absorption across the large surface area of their microvilli. The membrane of the microvilli contains transport proteins for glucose and amino acids, and thus do not readily internalize large molecular weight proteins such as intact vaccine antigens. Goblet cells are a subset of intestinal epithelial cells that have been shown to internalize and shuttle proteins from the lumen, which was found to be the major transport pathway for protein antigens to access lamina propria dendritic cells (DCs) [56]. Intestinal macrophages have also been observed to acquire luminal antigens and transfer them to DCs through gap junctions [22,57,58]. Intestinal DCs and macrophages have been shown to acquire luminal antigens by extending dendrites through the epithelial layer [35,59,60], but the true phenotype of these antigen presenting cells and under what experimental conditions antigen uptake occurs by transepithelial dendrites is still under investigation [61,62]. How vaccine uptake in certain cell populations in the intestine and their propensity to activate immunity or tolerance will be discussed in subsequent sections.

While the gastrointestinal tract offers significant surface area for nutrient absorption, large molecular weight proteins have very limited absorption across the epithelium. Uptake of intact soluble antigen predominately occurs in specialized cells present in low frequency along the intestinal tract. Material-based and bioconjugation strategies have

achieved significantly enhanced intestinal absorption of orally delivered therapeutics and vaccines and are discussed in detail below.

2.1.3.3 Bias for tolerogenic immune responses

A main barrier to effective oral vaccination is the inclination for tolerogenic immune responses to be generated against orally delivered substances. This immunologic phenomenon known as oral tolerance is characterized by the lack of systemic immune response against an antigen that was initially introduced to the body through the oral route. The local tissue environment of the gastrointestinal tract is predisposed to induce tolerance to substance ingested orally likely as a mechanism to prevent erroneous immune responses to the abundance of innocuous food proteins and commensal bacteria encountered at this surface. Without this protective regulatory mechanism, chronic inflammation in the intestinal tract would likely occur in response to the myriad of substances ingested daily, resulting in pathologies similar to those observed in intestinal inflammatory diseases. However, inherent tolerogenic bias is detrimental to the function of vaccines designed to elicit protective immunity.

Immunologic hypo-responsiveness of the intestine is regulated by anti-inflammatory signals secreted by intestinal epithelial cells, which condition the underlying DCs that are responsible for activating antigen-specific adaptive immune responses [63]. At steady state, these DCs will induce the differentiation of naïve T cells into regulatory T cells (T_{reg}) expressing the transcription factor forkhead box P3 (Foxp3), which mediate oral tolerance [64]. At the same time, signals secreted by these DCs can suppress the differentiation pathway of naïve T cells to effector T cells [65]. This immunoregulatory phenotype of mucosal DCs prevents the mounting of inflammatory T_H1 responses [36,66]. The ability of DCs to overcome this limitation is thought to require innate recognition of pathogens by both epithelial cells and DCs, resulting in their activation. Intestinal tolerance is also controlled through byproducts from commensal bacteria, such as short chain fatty acids, as well as the presence of mucus that imparts anti-inflammatory properties on intestinal

epithelial and DCs [67]. Thus, upon uptake of orally delivered vaccines there is a higher threshold to activate effector immune responses and break oral tolerance. Specifically, both epithelial cells and DCs must be properly activated to develop protective immunity.

2.1.4 *Application of advanced materials to study intestinal immunology*

2.1.4.1 Role of gastrointestinal conditions and digestion

The development of effective oral vaccines will depend on successfully breaking oral tolerance and activating effector immune responses. The role of the digestive gastrointestinal environment on controlling tolerance versus immunity is an area of active investigation. Immunity provides protection against infection through activation of effector and helper T cells and the production of antibodies that can neutralize and clear the pathogen. Immunity can also take the form of an allergy if the recognized substance is innocuous, like a common food allergen such as nuts. In contrast, tolerance is the lack of immune response against a certain antigen. This may occur through the absence of an effector response or through active suppression of adaptive immunity. Studies on food allergens have found that antigens susceptible to gastrointestinal digestion elicit stronger tolerogenic responses whereas antigens that are resistant to gastrointestinal proteolysis induce inflammatory responses [50,68]. In support of this premise, studies show that direct inactivation of gastrointestinal proteases reduces antigen digestion, resulting in increased systemic and local antibody responses that more effectively clear parasites after challenge [69]. Resistance of substances to protease digestion has also been posed to play a role in the abrogation of oral tolerance and in disease pathogenesis linked to intestinal autoimmune diseases [70]. In Celiac disease, a proline-rich 33-mer peptide in gliadin, which is a component of gluten implicated in its toxicity, shows resistance to proteolysis by gastrointestinal enzymes and stimulates T cells isolated from the intestines of Celiac patients [70]. While these and other studies implicate antigen digestion on the elicitation of tolerance or immunity in the intestine, further investigation on how digestion of

antigens affects their uptake, presentation, and elicitation of adaptive immune responses will be critical questions to answer when designing oral vaccines.

Biomaterial formulation offers a unique functional approach to probing these questions. The ability of drug delivery systems to release their cargo in a controlled way provides a method to study vaccines upon exposure to specific gastrointestinal conditions. Various strategies for encapsulating antigens have demonstrated differential abilities to sequester their cargo from the external environment and to control their release in response to stimuli. Protection of vaccine cargo from gastrointestinal digestion by certain formulations may be one reason why higher immune stimulation is observed with materials-based vaccine systems after oral delivery [71]. Thus far, protein antigens have been encapsulated in various polymer- and lipid-based particle systems as well as pH-responsive platforms for oral delivery (Table 2.2) [3,43,72,73]. Here we review the ability of these systems to protect vaccines from gastrointestinal digestion through control of their release in specific gastrointestinal environments and analyze the effect of digestion protection on adaptive immune responses after oral delivery.

2.1.4.1.1 Protein engineered subunit vaccines to protect from digestion

Protein antigens can be engineered for enhanced stability in gastrointestinal conditions through expression in plants or modification of amino acid sequences. The antigen cholera toxin B subunit (CTB) was expressed in rice seed and ~75% of CTB was protected from pepsin digestion after 1 hour [74]. Oral delivery of CTB from rice seed did not increase serum IgG responses compared to soluble CTB, but fecal IgA titers were increased [74]. Virus-like particles (VLPs) were engineered to express protozoa-derived variant-specific surface proteins (VSPs) to protect VLP surface antigens from gastrointestinal digestion, which are otherwise rapidly degraded in the presence of gastrointestinal extracts [75]. The authors found that cysteine-rich motifs of the VSPs imparted resistance to both gastric and intestinal proteases [75]. Oral vaccination with VSP-coated VLPs generated significantly more serum antibodies and provided protection

against viral and tumor challenge while uncoated VLPs did not [75]. Since the VSPs alone were found to be inherently immunogenic, increasing production of inflammatory cytokines and the expression of stimulatory surface proteins on DCs, it is unknown if the strong immune responses were due to protection from gastrointestinal digestion or the immunostimulatory effects of the VSP-coated VLPs [75]. However, as the authors observed significant degradation of the surface antigen upon exposure to gastrointestinal conditions and no protective effects with uncoated VLPs, it is likely that the presence of undigested antigen is a requirement for the induction of antigen-specific immunity.

2.1.4.1.2 pH-responsive vaccine delivery systems

Retention of the structural conformation of protein antigens is critical for immunogenicity and this conformation can be compromised by acid-mediated protein denaturation [76]. pH-responsive polymeric systems take advantage of changes in pH throughout the gastrointestinal tract, where the highly acidic environment in the stomach gradually transitions to be more neutral in the small intestine. These polymers are insoluble in acidic conditions but soluble in neutral and alkaline conditions. Thus, pH-responsive systems are advantageous for preventing vaccine release in the stomach and delivery in the intestine, where the vaccine can be absorbed to initiate immune responses. Most commonly, Eudragit methacrylic acid methyl methacrylate co-polymers are used for their pH-dependent solubility transition. The pH of dissolution can be varied based on the co-polymer ratio. For release of cargo in the small intestine, Eudragit L 30 D-55, L 100-55 (dissolution above pH 5.5) and L 100 (dissolution above pH 6.0) are useful for their gastric-resistant properties to preserve antigen epitopes upon digestion.

Eudragit L 30 D-55 was used to encapsulate the protein antigen ovalbumin (OVA) in microparticles [71]. After oral administration, these particles elicited serum antibody responses in tolerized mice, whereas mice that received soluble OVA had suppressed serum antibody titers indicative of oral tolerance [71]. At the cellular level, restimulation of splenocytes from pre-tolerized mice that were orally vaccinated with Eudragit L 30 D-55

microparticle-encapsulated OVA led to a higher level of proliferation compared to mice that were fed soluble OVA [71]. Encapsulation of a whole cell killed vaccine in a Eudragit L 30 D-55 capsule was also effective in preventing vaccine release in simulated gastric conditions containing pepsin [77]. However, only a modest increase in serum IgA was observed when the vaccine was orally delivered in the capsule. Several aspects of this study confound our ability to discern the effect of gastric digestion on the resulting immune response. First, capsule delivery was not compared to vaccine administered in solution. Second, mice receiving the vaccine in solution were orally gavaged with sodium bicarbonate buffer to neutralize stomach acid, which results in both groups having reduced gastric digestion of the vaccine. Overall, these studies suggest that pH-responsive materials that protect vaccines from gastric digestion can improve the activation of adaptive immunity. More controlled studies that evaluate protection or release of the vaccine in different gastrointestinal conditions are needed to clearly demonstrate that digestion protection contributes to the generation of the observed immune responses.

2.1.4.1.3 Polymeric and liposomal nanoparticle delivery systems

Another strategy to protect vaccines from the gastrointestinal environment is to encapsulate them in nanoparticles. Nanoparticle properties, including size, charge, and hydrophobicity, are known to affect diffusion, uptake, and trafficking of vaccines [78,79]. Encapsulation of vaccines in nanoparticles can also sustain vaccine release over time depending on the polymer used [80]. Therefore, in addition to sequestering vaccines from the digestive gastrointestinal environment, nanoparticles also influence vaccine uptake and release kinetics compared to soluble delivery, both of which are known to affect adaptive immunity. For the purpose of identifying the effect of gastrointestinal digestion on the immune response, this attribute of nanoparticle formulation can be confounding. In this section, we highlight how well oral particulate delivery systems protect vaccines from release in gastrointestinal conditions to provide insight into the impact of digestion on immunity.

Nanoparticles can be synthesized from hydrophobic polymers, most notably poly(lactic glycolic acid) (PLGA), that are stable during transit through gastrointestinal fluids [81]. Encapsulation of Salmonella typhi outer membrane proteins (porins) in PLGA microparticles provided protection from acidic degradation [82]. After oral immunization, porins encapsulated in PLGA particles enhanced the number of antibody-secreting cells and germinal center B cells in gut-associated lymphoid organs compared to soluble delivery. In a separate study, nanoparticles composed of poly(lactic acid) (PLA) were co-polymerized with poly(ethylene glycol) (PEG) to enhance colloidal stability [83]. Co-polymerization reduced the release of encapsulated antigen in simulated gastrointestinal conditions with proteases [83]. Oral administration of PLA-PEG particles increased antigen-specific antibodies in the serum and mucosal secretions compared to PLA particles, likely due to the enhanced stability of these particles in gastrointestinal fluids [83].

pH-responsive polymers have also been used as coatings on nanoparticles encapsulating antigens. An oral PLGA nanoparticle vaccine was designed to be released in the small intestine by coating with Eudragit L 100 [15]. The aim of this study was to elucidate how release of PLGA nanoparticle vaccines in the small or large intestine through different Eudragit coatings would affect adaptive immunity. pH-responsive release of the nanoparticles in the small intestine resulted in a significant increase in the expansion of antigen-specific $CD8^+$ T cells compared to PLGA nanoparticle vaccines without the enteric coating [15]. Eudragit L 30 D-55-coated cellulose beads delivering OVA induced serum IgE antibodies in contrast to delivery of unencapsulated protein [50]. Antibody production in response to the vaccine without the Eudragit coating was not evaluated. Cubosomes, spray-dried nanoparticles composed of dextran, OVA, and the adjuvant Quil-A, were loaded in cylindrical microcontainers made of the photoresist SU-8 and coated with Eudragit L 100-55 for pH-dependent cubosome release [84]. Oral immunization with the microcontainer vaccine did not elicit humoral or cellular immune responses [84].

However, serum IgG was observed when cubosomes were delivered orally without encapsulation in microcontainers, which suggests that the microcontainers may hinder vaccine bioavailability. Thus, the impact of cubosome vaccine protection in gastric conditions is confounded by the reduced function observed when delivered in microcontainers.

Chitosan nanoparticles have also been explored for oral vaccine delivery and are additionally advantageous due to the mucoadhesive and absorption-enhancing properties of the polymer [85]. However, chitosan is soluble in acidic pH conditions and requires gastric stabilization. This can be achieved by using acid-resistant coatings such as alginic acid or lipid vesicles. Bovine serum albumin (BSA)-loaded chitosan nanoparticles were encapsulated in liposomes and niosomes [86]. While liposomes are composed of phospholipids and cholesterol, niosomes are composed of only cholesterol and surfactant. In contrast to chitosan, these lipid-coated vesicles are stable in the stomach but are digested by enzymes and bile salts in the small intestine. Lipid vesicle-encapsulation of chitosan particles enhanced their stability when exposed to simulated gastric conditions containing pepsin with ~70% vesicles remaining and ~65% residual antigen content after 2 hours [86]. In contrast, only ~35% residual antigen content was observed for uncoated chitosan nanoparticles in simulated gastric fluid [86]. Oral immunization with encapsulated chitosan nanoparticles in mice increased antigen-specific IgG levels in the serum and IgA levels in the intestine compared to both uncoated chitosan nanoparticles and soluble antigen delivery [86]. These results demonstrate that limiting antigen release in gastric conditions is favorable for the activation of humoral immunity. A different study investigated an oral vaccine composed of alginate-coated chitosan nanoparticles and showed enhanced protection of the antigen when incubated in acidic conditions for 2 hours compared to uncoated particles [87]. Oral immunization of mice with these alginate-coated chitosan particles resulted in higher plasma IgG and intestinal IgA titers compared to soluble vaccine delivery [87]. Mannosylated chitosan nanoparticles coated with Eudragit

L 100 prevented release of BSA antigen after incubation in simulated gastric fluid with pepsin for 2 hours. In contrast, uncoated particles released all of their BSA cargo in this time frame [88]. When administered *in vivo*, the Eudragit-coated mannosylated chitosan particles increased serum IgG and intestinal IgA titers compared to uncoated particles, similar to the results from previous studies [88]. Overall, these studies demonstrate that release of antigen in gastric conditions by chitosan particles, leading to antigen digestion, can be overcome through various gastric-resistant coating mechanisms resulting in improved immune responses after oral delivery.

In addition to polymer-based systems, particles composed of phospholipids have been studied as oral vaccines and are capable of eliciting immune responses when administered by this route. Lipid particles have favorable biocompatibility profiles and, depending on their fatty acid composition, can insert into the bilayer membrane of cells and interact with lipids present in mucus [89]. As lipids contain both hydrophobic and hydrophilic regions, lipid-based particles can incorporate molecules in their aqueous core and lipid bilayer. Where vaccines are loaded within liposomes can influence their release kinetics and their exposure to or protection from gastrointestinal conditions [90]. A recent study demonstrated the susceptibility of lipid particles to lose their physiochemical properties, such as size and surface charge, upon exposure to pepsin and bile salts present in the gastrointestinal tract, resulting in a reduction in efficacy when delivering siRNA [91]. These vulnerabilities are likely to impact the efficacy of liposome-based oral vaccines delivering protein antigens. To enhance stability, liposomes can be surface coated or incorporate bile salts in a platform termed "bilosomes" [92,93]. The enhanced stability of bilosomes has been shown to increase serum IgG titers compared to conventional liposomes without bile salts, supporting the importance of vesicle stability in gastric conditions and antigen retention on immunogenicity [94,95]. Future work may focus on the controlled design of these systems to further understand how liposome formulation

affects antigen protection, diffusion, and uptake leading to differences in immunologic responses.

The use of biomaterial-based delivery systems to encapsulate vaccines is clearly beneficial in eliciting immune responses after oral immunization. Preventing release of vaccines in the gastric environment, either through formulation in pH-responsive polymers like Eudragit or through coating of nanoparticle vaccines to impart gastric-resistance, enhances both cellular and humoral immunity. Critical limitations of these studies are the lack of extensive characterization of carrier-mediated digestion protection and the confounding effects of nanoparticle-mediated vaccine uptake and sustained release. Therefore, while these studies support a link between digestion protection and immunity, the relationship is not definitive. Additionally, many questions regarding the role and mechanism of gastrointestinal digestion on antigen immunogenicity and the elicitation of tolerance still remain. For example, how exactly does antigen digestion lead to a lack of immune responses? What are the contributions of gastric and intestinal digestion, respectively? Is protection of antigens from gastrointestinal digestion sufficient to activate immunity or is nanoparticle formulation also required to increase vaccine absorption and extend exposure? In general, advanced material delivery systems may answer outstanding questions regarding the balance of tolerance and immunity in the intestine with respect to antigen digestion.

Table 2.2. Immune responses to oral vaccine formulations with respect to protection from gastrointestinal digestion.

Strategy	Material	Gastric protection	Intestinal protection	Systemic immunity	Mucosal immunity	Confounding factors	Ref.
Protease-resistant protein coating		Y	Y	Increased IgG & protected against viral & tumor challenge	Increased IgA	Enhanced immunogenicity of variant-specific surface proteins	[75]
Expression in plants	Rice seed	Y, ~75% in SGF+pepsin	Not evaluated	No difference compared to soluble	Increased fecal IgA titers		[74]

pH-responsive delivery	Eudragit L 30 D-55 microparticles	Not evaluated	N/A	Induced IgG & proliferation of restimulated splenocytes		No evaluation of antigen release or digestion protection	[71]
	Eudragit L 30 D-55 capsules	Y, SGF+pepsin	N/A	Slight increase in IgA		Immune responses were not compared to vaccine delivered without capsule	[77]
NP formulation	PLGA NPs	Y, SGF	Not evaluated		Increased antibody-secreting cells and GC B cells	Nanoparticle formulation	[82]
	PLA-PEG NPs	Reduced release in SGF+pepsin	Reduced release in SIF+pancreatin	Increased IgG compared to PLA particles	Increased IgA compared to PLA particles	Nanoparticle formulation	[83]
Enteric-coated NP formulation	Eudragit L 100-coated PLGA NPs	Not evaluated	Not evaluated	Increased antigen-specific $CD8^+$ T cells compared to uncoated NPs		Nanoparticle formulation; Formulations included adjuvant	[15]
	Eudragit L 30 D-55-coated cellulose beads	Not evaluated	Not evaluated	Increased serum IgG		Nanoparticle formulation; No comparison to uncoated NPs	[50]
	Eudragit L 100-55-coated cubosome-loaded microcontainers	Intact lids in stomach extract	Dissolved lids in intestinal extract	No activation of systemic immunity		Nanoparticle formulation; Formulations included adjuvant; Microcontainers may limit vaccine release	[84]
	Eudragit L 100-coated chitosan NPs	Y, SGF+pepsin	Y, SIF+trypsin	Increased IgG compared to uncoated NPs	Increased intestinal IgA compared to uncoated NPs	Nanoparticle formulation	[88]
Liposome stabilization	Bilosome	Reduced release of antigen in SGF	Reduced release of antigen in SIF	Increased IgG		Nanoparticle formulation; No comparison to parent liposomes	[94,95]

NP, nanoparticle; SGF, simulated gastric fluid; SIF, simulated intestinal fluid; GC, germinal center.

2.1.4.2 Mechanisms of intestinal vaccine uptake

Once oral vaccines transit through the stomach into the intestinal lumen, the vaccine must then be internalized and processed by the appropriate cell types to activate

an immune response. As discussed above, there are a variety of mechanisms in which cells of the intestine uptake orally delivered substances. However, the internalization of full proteins larger than tripeptides is largely inefficient and only a few mechanisms of absorption are known. Many novel delivery platforms have been developed to both interrogate and target internalization pathways to increase vaccine absorption in the intestine (Figure 2.3). While these studies focus primarily on how oral drug delivery platform properties affect their biodistribution and uptake, examples that measure immunological outcomes will be highlighted. Here, we review and discuss how these material strategies affect vaccine uptake, processing and presentation by antigen presenting cells, and the subsequent polarization and magnitude of adaptive immunity. These findings are summarized in Table 2.3.

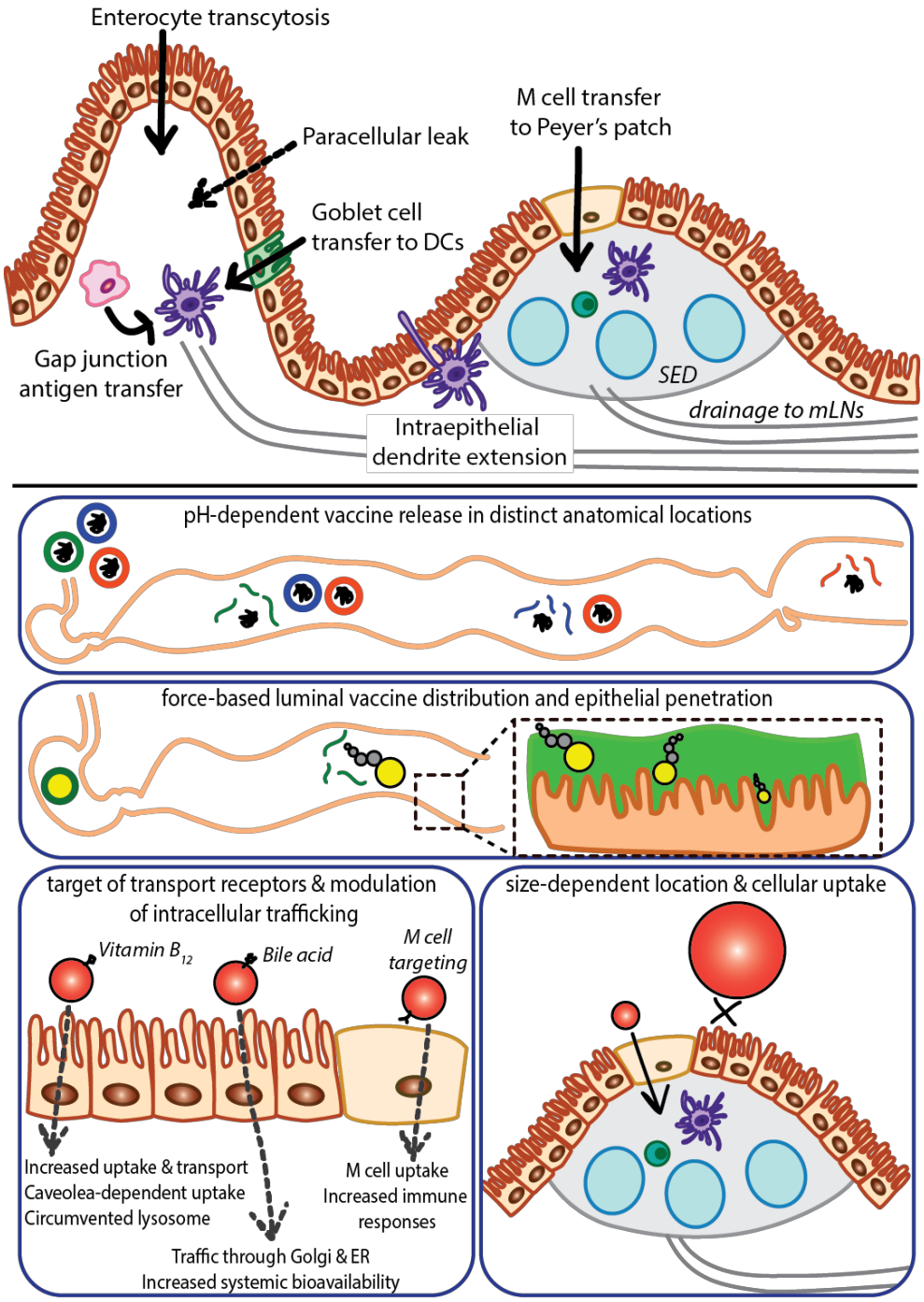

Figure 2.3. Mechanisms of intestinal vaccine absorption and vaccine delivery systems used to modulate uptake. Top panel: Known mechanisms of antigen uptake in the intestine. Bottom panel: Material-based systems to modulate vaccine delivery and uptake in the small intestine. DC, dendritic cell; SED, subepithelial dome; mLNs, mesenteric lymph nodes; ER, endoplasmic reticulum.

2.1.4.2.1 Passive cell targeting

Mechanisms of vaccine uptake in the small intestine have been investigated and exploited by material-based systems. Orally-delivered polystyrene nanoparticles of 200 nm size can gain access to the subepithelial dome (SED) of Peyer's patches and are internalized by DCs in the region [96]. Nanomaterial shape has been shown to affect gastrointestinal transit, uptake, and transport. The size of silica nanoparticles influenced uptake into intestinal Peyer's patches. Smaller particles (~100–200 nm) penetrated into the SED while larger particles (>1,000 nm) were found primarily on the luminal side of the epithelium [97]. Modulation of the size of vaccine nanocarriers can also affect transport through different epithelial cells. SED $CD11b^+$ macrophages internalized smaller silica particles (100, 180, and 365 nm) more effectively than larger particles. In contrast, M cells co-localized with particles of larger size (745 nm) [98]. The effect of size is critical to understand as difference cell types have distinct abilities to initiate immune responses. Additionally, size is known to influence cellular internalization pathways which has implications for antigen processing [99,100]. Indeed, the authors observed increased IgA production in the intestinal lumen after treatment with 925 nm particles (uptake in M cells) compared to 100 nm particles (uptake in macrophages) [98]. However, the number of IgA^+ cells in the Peyer's patches and IgA titers in bile secretions and Peyer's patches were higher in mice that received 100 nm particles compared to larger sizes [98]. In another study, mice were orally vaccinated with OVA-loaded PLGA nanoparticles of different diameters (1.3, 4.0, 7.5, and 14.0 µm). The 4 µm particles were found to induce the highest production of serum IgG at three different doses tested [101]. In terms of shape, polystyrene nanorods (~400 nm x ~150 nm) had higher retention in the gastrointestinal tract, increased penetration into villi, and were transported into mesenteric lymph compared to nanospheres of a similar size (~200 nm) [102]. These results demonstrate that the size of nanoparticle-delivering vaccines does impact which cells internalize the vaccine

and how well the lymphatic system is accessed, leading to differences in the magnitude and location of the adaptive immune response.

Studies on the uptake of oral drug delivery systems give additional insight into how nanomaterials can influence diffusion, uptake, and trafficking. Efficient diffusion of macromolecules through the mucus layer has been studied using spherical polystyrene particles of specific size, shape, and charge [79]. Carboxylate-modified polystyrene particles were used as mucoadhesive particles and demonstrated low distribution throughout the intestinal lumen and luminal invaginations. In contrast, PEG modification of the particles renders them mucus-penetrating and dramatically increased their distribution [103]. In terms of size, smaller PEG-modified particles (<100 nm) were more uniformly distributed in the colorectum compared to larger particles, which had lower tissue surface coverage [103]. Mucoadhesive particles are commonly used for oral drug delivery to increase residence time in the intestinal tract [44,104]. These findings on the relationship between size, mucoadhesion, and diffusion indicate that, while residence time may be increased with mucoadhesive particles, these particles will suffer from low distribution through the mucus layer with limited access to the epithelium. Importantly, a recent study observed that cationic polymeric nanoparticles were enveloped by a protein corona when exposed to simulated gastrointestinal conditions, which significantly reduced uptake of the particles by intestinal epithelial cells *in vitro* [105]. Findings from these studies are incredibly valuable for oral vaccines, in which the efficient absorption of antigens is critical to their immunologic function.

2.1.4.2.2 Targeting specialized epithelial cells and DCs

In addition to designing systems with specific physical properties to modulate uptake of oral vaccines, bioconjugation of particles with ligands can impart active cell targeting properties [106]. As enterocytes are the first cells to be encountered by vaccines in the intestinal lumen, enhancing uptake and transport in this cell population has been an attractive strategy [107]. After identifying the critical role of M cells and Goblet cells in

antigen transfer and the induction of adaptive immunity, many strategies have been developed to target these cells. Here, we comment on studies that correlate targeting with the elicitation of adaptive immune responses, but more curious readers can refer to comprehensive reviews on M cell targeting [108,109]. Targeting a protein vaccine to the M cell receptor glycoprotein 2 (GP2) through conjugating to the antigen-binding fragment region of an anti-GP2 antibody resulted in increased intestinal secretory IgA and better protection upon oral bacteria challenge [110]. Lectin conjugation of PLGA and polystyrene particles increased uptake by M cells and enhanced intestinal antigen-specific secretory IgA [111,112]. Targeting Goblet cells has only been investigated in the context of oral insulin delivery. Conjugation of trimethyl chitosan chloride nanoparticles with a Goblet cell-targeting peptide improved the bioavailability of orally-delivered insulin by 1.5-fold compared to untargeted particles [113]. As Goblet cells are also known to be central in transfer of luminal antigens in the intestine, the application of this targeting strategy for oral vaccines has much potential.

Another attractive targeting strategy for immunization is to accumulate vaccines in professional antigen presenting cells such as DCs [114]. Antigen processing by DCs ultimately determines the quality and quantity of the adaptive immune response [115]. This approach has been most widely studied for parenterally-administered vaccines, in which the vaccine accesses DCs directly in the tissue or in lymphoid organs [114]. Many strategies target C-type lectin receptors that are expressed on DCs. Lectin targeting induces endocytosis by DCs and can improve antigen presentation to T cells through access to lysosomes. In contrast to parenteral vaccinations, DC-targeting approaches have limitations for oral vaccine delivery. Multiple barriers must first be overcome for oral vaccines to be in the spatial vicinity of DCs, which reside below the epithelial layer in the lamina propria, to realize their targeting potential. Thus, the development of multi-functional systems that utilize strategies in series is likely required to target oral vaccines to DCs in the intestine. For example, certain mucosal adjuvants can recruit inflammatory

immune cell populations to the intestinal epithelium and induce DCs to extend transepithelial dendrites [22]. An oral vaccination regimen in which intestinal DCs are first recruited to the epithelium followed by their targeting with material-based strategies, as discussed above, may enhance vaccine accumulation in this important cell type. Additionally, new insights on DC subtypes in mucosal tissues has revealed populations more likely to induce tolerogenic or inflammatory responses [62,116]. How biomaterial vaccines are targeted to these different DC populations may have significant implications for oral immunization and the elicitation of protective immunity.

2.1.4.2.3 Targeting epithelial transport pathways

Oral drug delivery systems have also been designed to co-opt known transport pathways in the intestine, although few have been evaluated for oral immunization. Liposomes coated with layered sodium alginate and chitosan were conjugated to vitamin B_{12}, which in this study was used to impart surface roughness but is also known to be involved in intestinal absorption [117]. Conjugated liposomes demonstrated enhanced serum IgG and mucosal IgA titers after oral administration compared to soluble delivery of the antigen [118]. As the primary motivation of the study was the effect of surface roughness, a control particle without vitamin B_{12} was not included. Therefore, the contribution of targeting the vitamin B_{12} transport pathway in the development of antibodies could not be evaluated. In the oral delivery of insulin, a vitamin B_{12} derivative conjugated to dextran nanoparticles increased bioavailability compared to particles without modification [119]. Targeting strategies have also been shown to influence internalization and processing pathways in addition to enhancing uptake. Targeting vitamin B_{12} transport *in vitro* resulted in trafficking of polystyrene nanoparticles through a caveolae- rather than clathrin-dependent internalization pathway that was used for soluble B_{12} [120]. The internalization pathway for unconjugated nanoparticles was not evaluated. This pathway switch resulted in an avoidance of lysosomal processing, which could have implications for antigen presentation. PEG-PLGA nanoparticles modified with

a peptide ligand targeting heparan sulfate proteoglycans also modulated internalization pathways in intestinal epithelial cells *in vitro* [121]. Unmodified particles were shuttled through the lysosomal pathway while peptide-conjugated particles were transported through caveolae vesicles. This resulted in the particles avoiding lysosomal degradation and cell transcytosis [121]. Oral delivery of insulin with the peptide-modified particles resulted in higher therapeutic bioavailability compared to both free insulin and unmodified particle delivery [121].

To take advantage of bile acid transporters present on the apical side of intestinal enterocytes, the bile acid glycocholic acid has been conjugated to various nanoparticles. Bile acid-conjugated polystyrene particles demonstrated significant improvements in systemic bioavailability after oral dosing, with bioavailability being dependent on glycocholic acid density and particle size [122]. Intracellularly, bile acid-conjugated particles were transported through the endoplasmic reticulum and Golgi apparatus [122]. After release from the cell, conjugated particles gained access to the lymphatic system and were found in the liver at a lower percentage of the administered dose [122]. These results demonstrate that bile acid-conjugated particles have preferential access to the lymphatic system. While this study focused on the trafficking of the particles themselves, it will be important to understand how bile acid conjugation impacts trafficking of the therapeutics loaded within the delivery system. Additionally, targeting the bile acid transport pathway could affect the elicitation of immune responses and is important to investigate. These bioconjugate systems are useful tools to study how blood versus lymphatic drainage of orally-administered antigens can affect adaptive immunity, and investigating the role of the liver in oral tolerance is also alluring [123,124]. For example, one study surgically connected the mesenteric vein to the subhepatic inferior vena cava in rats to redirect intestinal drainage away from the liver. These animals were unable to mount tolerance to an orally-introduced antigen in contrast to control animals, suggesting that liver circulation is necessary for oral tolerance [125]. While surgically shunting veins

is an impractical clinical strategy to achieve immunity in response to oral vaccination, one could envision the use of advanced delivery systems to partition therapeutics through specific pathways and organs to control the activation of tolerance vs. immunity.

Oral drug and vaccine delivery platforms can also be conjugated to larger macromolecules, such as immunoglobulins, to access existing transport pathways. An HIV protein antigen was conjugated to secretory IgA to target transport through M cells, which bind and endocytose IgA [126]. This strategy increased antigen transport into Peyer's patches and heightened antibody production, memory B cells, and IFN-γ secreting cells compared to unconjugated antigen [126]. Conjugation of PLA-PEG nanoparticles with IgG fragments targeting the neonatal Fc Receptor (FcRn) pathway enhanced transport of insulin across the intestinal epithelium and into circulation [127]. Binding of IgG by FcRn is known to engage proinflammatory pathways, in contrast to the regulatory function of IgA complexes [128]. Targeting the intestinal FcRn transport pathway has not yet been studied as an oral vaccine. However, its utility in vaccination has been demonstrated at other mucosal surfaces. For example, intranasal delivery of antigens fused with the Fc region of IgG significantly increased antigen-specific immune response compared to antigen without Fc fusion [129,130]. It will be interesting to understand how FcRn pathway targeting influences the uptake of orally-delivered vaccines and the activation of adaptive immunity [131].

The ability of materials-based systems to both enhance and control cellular shuttling of therapeutics is a unique and powerful strategy. However, it is unknown how the use of different pathways influences antigen transport in epithelial cells and how this may affect subsequent immunologic outcomes. A recent review discusses the impact of cellular retention versus exocytosis of nanomaterial platforms on their efficacy [132]. The authors emphasize the importance of investigating not only cellular uptake but also recycling, which has been relatively understudied. While their review is focused predominately on gene delivery, many of the questions posed are important to consider for vaccine efficacy.

For oral vaccines, retention in or release from certain cell types will likely impact how robustly antigens are presented to adaptive immune cells, access lymphoid organs, and ultimately be cleared from the body.

2.1.4.2.4 Mechanical systems to modulate absorption

Novel devices offer an alternative approach to increase oral vaccine absorption by employing mechanical systems to facilitate penetration. A micromotor device was coated with a toxin antigen-inserted red blood cell membrane, further coated with chitosan, and enveloped in Eudragit L 100-55 [133]. In simulated gastrointestinal fluids, the enteric-coated device self-propelled in only intestinal conditions at a speed of ~150 μm sec^{-1} [133]. After oral administration, the micromotor device enhanced vaccine distribution and retention throughout the intestinal tract and within villi, resulting in enhanced fecal IgA titers compared to a static form of the same device [133]. These micromotors overcome a significant transport barrier in oral vaccination to effectively gain access to intestinal tissue and initiate immune responses. Other force-based technologies have been developed for gastrointestinal drug delivery. The self-orienting millimeter-scale applicator (SOMA) uses a self-orienting mechanism to deploy milliposts made of biodegradable polymers into the gastric mucosa [134]. Milliposts were shown to be capable of penetrating through the submucosa of stomach tissue *ex vivo* to facilitate drug delivery through the gastric wall [134]. In a separate example, a cylindrical pill with protruding microneedles around the surface was designed for oral drug delivery and demonstrated to be safe through gastrointestinal passage [135]. However, this device has yet to be evaluated for its ability to increase drug delivery across the intestine. It will be interesting to further study how the mechanical forces might have an adjuvant effect by modulating subsequent immune signaling and inflammatory responses. Epithelial cells are also known to be sensitive to mechanical stimulation, the physiologic effects of which depend on the nature of the mechanical disruption [136]. As mucus itself delivers immunoregulatory signals to

intestinal cells [67], if and how these mechanical systems interfere with this recognition pathway will be important to evaluate.

Using physiochemical, biologic, and mechanical attributes of material systems, vaccines can target a variety of cell types in the intestine. This can result in selective vaccine uptake in relevant cell populations and can exploit certain internalization pathways for desired immunological outcomes. The tunability of material-based systems is conducive for examining how distinct cellular pathways lead to differences in vaccine processing, presentation, and activation. Next generation oral vaccine delivery platforms can be better engineered and designed to achieve the most relevant functional outcomes upon expanding our fundamental understanding of these topics.

Table 2.3. Material-based approaches to modulate intestinal uptake and the effect on cellular processing and adaptive immune responses.

Design Feature	**Location of Uptake**	**Cellular Internalization & Processing**	**Immunological Outcomes**	**Reference**
Size				
100-200 nm NPs	SED	DCs, macrophages	IgA in Peyer's patches	[97]
~750 nm NPs	SED	M cells	IgA in intestinal lumen	[98]
>1000 nm NPs	Intestinal lumen (no epithelial transcytosis)			[97]
4 µm NPs			Increased serum IgG compared to 1.3, 7.5, & 14 µm NPs	[101]
Shape				
Rods vs. spheres	Rods enhanced intestinal retention & villi penetration	Rod increased lymphatic transport		[102]
Ligands				
Vitamin B12		Increased absorption & bioavailability; Caveolae-dependent internalization	Increased IgG and IgA	[118–120]
Bile acid		Transcytosis; lymphatic transport		[122]
Heparan sulfate		Caveolae vesicle transport & transcytosis		[121]

Secretory IgA	SED	M cells, DCs	Increased IgG, memory B cells, IFN-γ secreting cells	[126]
IgG Fc		Epithelial transport; access to circulation		[127]
M cell ligands		Uptake in M cells	Increased IgA & protection from bacterial challenge	[110–112]
Force				
Enteric micromotor	Increased retention & distribution		Increased IgA	[133]

NPs, nanoparticles; DCs, dendritic cells; SED, subepithelial dome.

2.1.4.3 Impact of oral vaccine delivery location and kinetics

Vaccine composition and delivery location can affect immunogenic responses to oral vaccines, both acutely and in the development of memory. The length of the small intestine is divided into the duodenum, jejunum, and ileum. Each of these segments are distinct cellularly and functionally, and immunologically discrete lymphoid organs drain different segments of the small intestine [137]. These lymphoid organs exhibit a gradient of inflammatory or tolerogenic responses to the same orally-derived antigen, highlighting the importance of where vaccine absorption occurs along the length of the intestine [137]. Once vaccines are inside cells within these locations, access to the cytosol and the kinetics of vaccine exposure can also affect immunologic responses. Physiological and immunological differences along the intestinal tract are highlighted in Figure 2.4. Through the application of advanced materials, how immunity is elicited throughout the intestinal tract and identifying the location most inductive of protective responses may be investigated. These functional systems also have the ability deliver antigens to distinct anatomical and cellular location, and to co-deliver physiochemically diverse agents such as adjuvants that can potentiate and direct immune responses [138]. Here, we review material-based platforms that have provided insight into how controlling the delivery location of oral vaccines and their release kinetics modulates innate and adaptive immunity. We will also discuss relevant observations from other mucosal and parenteral vaccine studies and their translation to oral immunization.

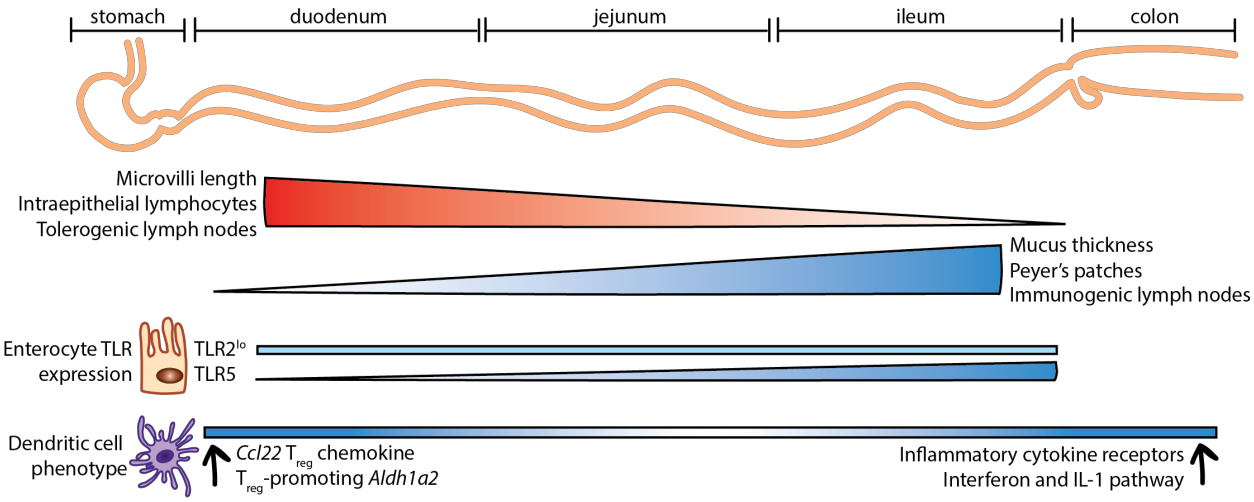

Figure 2.4. Physiological and immunological differences along the gastrointestinal tract.

2.1.4.3.1 Regional targeting of the intestinal tract

Physiological and immunological distinctions in regions of the small intestinal can be observed macro- and microscopically (Figure 2.4) [139,140]. For example, microvilli length, mucus thickness, and the presence of digestive enzymes vary depending on the anatomical function of the intestinal region. Immunologically, Peyer's patches and lymphoid follicles are found more frequently in the ileum compared to the upper small intestine, while intraepithelial lymphocytes decrease in number in more distal regions [141,142]. DC populations and expression of pathogen associated molecular pattern receptors also distribute to distinct regions of the intestine [143,144]. Mesenteric lymph nodes that drain more proximal regions of the small intestine induce the polarization of regulatory T cells while lymph nodes that drain the distal small intestine and the colon activate inflammatory and helper T cells [137]. These differences are critical to understand for the development of oral vaccines and suggest targeting vaccines to specific intestinal regions to achieve long-lasting immunity.

To understand the impact of regional vaccine delivery on the induction of immune responses, a radio controlled capsule oral vaccine was investigated in humans [145]. Controlled release of the vaccine in the jejunum and ileum generated systemic and mucosal

antigen-specific antibodies, with a higher response measured when the vaccine was released in the ileum [145]. These results support the notion that targeting distal regions of the small intestine, which drain to more inflammatory lymph nodes, can generate stronger immune responses. Another study used Eudragit-coated PLGA nanoparticle vaccines to understand the regional contribution of immunizing at the small and large intestine [15]. Release of the PLGA nanoparticles in the large intestine induced vaginal and rectal immunity, while small intestinal nanoparticle release resulted in local immune responses [15]. These results demonstrated the functional differences throughout the intestinal tract and highlighted the power of advanced materials systems to answer these fundamental vaccinology questions, many of which still remain to be investigated. Differences in pH along the small intestine could be further leveraged to take advantage of the propensity of certain intestinal regions to induce tolerance or immunity. Identification of compartmentalized intestinal immune responses were investigated by duodenal or ileal injection of antigen by a surgical procedure [137]. Through using an advanced delivery system, study of regional immunological mechanisms in the intestine could be achieved less invasively.

2.1.4.3.2 Mesenteric lymph node targeting

Material systems can also control vaccine access to lymph nodes where adaptive responses are initiated and directed. A range of immune cells can be accessed in lymph nodes that include antigen presenting cells and also T and B lymphocytes that are responsible for adaptive effector immune function. Vaccines can also traffic to specialized regions within the lymph nodes where T cell polarization and B cell affinity maturation take place. In the intestine, vaccines must first penetrate from the lumen, through the epithelium, and into the interstitium where lymphatic drainage occurs. At the same time, vaccines must avoid clearance through the vasculature system. Accumulation of vaccines in lymph nodes has been explored by controlling properties of material carriers and employing targeting strategies [146,147]. For orally-delivered systems, it has been observed

that nanoparticle functionalization with enterocyte-targeting ligands results in intracellular retention [148]. However, vaccine transcytosis from enterocytes is required to access draining lymphoid organs for the activation of adaptive immunity. Mesenteric lymph node targeting has been largely understudied and these results suggest novel strategies for lymph node targeting may be needed for this challenging administration route. As discussed above, much work in targeting M cells has identified properties of particulate systems that enhance uptake of orally delivered vaccines to Peyer's patches. It remains to be determined if another set of attributes is more appropriate for mesenteric lymph node targeting and how targeting lymph nodes versus Peyer's patches in the intestine influences the elicited immune responses.

2.1.4.3.3 Controlling subcellular delivery

Subcellular vaccine location is another important parameter in controlling immune outcomes. Vaccine antigens can be transported through distinct intracellular pathways that may result in antigen degradation, processing and presentation, transcytosis, or transfer to adjacent cells. Internalization pathways can be targeted by vaccine formulation and bioconjugation strategies, as mentioned above. Systems can also be designed to interfere with pathways after antigen internalization, of which the main strategy is endosomal escape. In vaccine delivery, successful endosomal escape is incredibly attractive to generate cytotoxic $CD8^+$ T cell responses to extracellular antigens. This is because the elicitation of a $CD4^+$ or $CD8^+$ T cell response is dependent on the context in which the lymphocyte sees the antigen. Most commonly, extracellular antigens are presented on MHC class II to $CD4^+$ T cells through lysosomal degradation pathways. Intracellular antigens can access MHC class I presentation to $CD8^+$ T cells through proteasomal degradation in the cytosol and transport to the endoplasmic reticulum. In most cases, extracellular antigens are not presented on MHC class I based on the mechanism of exogenous antigen uptake and processing. Thus, most vaccines elicit poor $CD8^+$ T cell responses on their own. As these responses are critical in combating viral infections and

cancers, systems that can interrogate lysosomal processing and access MHC class I processing machinery in the cytosol are desired. Most endosomal escape strategies use membrane-disrupting peptides, pH-sensitive polymers, and cationic lipids to destabilize endosomes and achieve release into the cytosol [149]. No endosomal escape-inducing systems have been applied to oral vaccines. Here, we discuss the promise of this strategy through review of parenteral vaccines and oral drug delivery platforms using this mechanism.

OVA was conjugated to poly(propyl acrylic acid) (PPAA) and formulated into nanoparticles with the cationic polymer poly(dimethylaminoethyl methacrylate) [150]. PPAA carriers undergo a pH-dependent protonation in the acidic environment of lysosomes that results in endosomal membrane disruption [151]. Delivery of OVA subcutaneously in the endosomal-disrupting particle dramatically increased the generation of $CD8^+$ T cells, serum antibody responses, and provided enhanced protection from tumor challenge compared to delivery in polymeric nanoparticles that did not induce endosomal escape [150]. Endosomal escape of antigens has recently been applied to oral biotherapeutics, predominately insulin delivery systems. A hydrophobic peptide HA2 was formulated in solid lipid nanoparticles to induce endosomal escape upon cellular internalization [152]. Incorporation of the peptide in the oil phase resulted in particles with peptide in the lipid corona, which increased endosomal escape *in vitro* compared to peptide encapsulated in the internal phase of the particles [152]. When the particles were injected in ligated intestinal loops, the highest transcytosis of the protein cargo was achieved with particles that had HA2 peptide in the lipid shell [152]. Enhanced endosomal escape resulted in significantly reduced blood glucose levels when delivering insulin compared to controls [152]. This study indicates that strategies for endosomal escape are promising for oral delivery of protein drugs and vaccines. However, since the particles were delivered directly into the intestine, the effect of exposure to gastric conditions could not be evaluated. Similar material-based platforms could be applied to study how

endosomal escape modulates antigen processing and presentation in intestinal cell populations, such as epithelial cells and DCs. As proof of concept, a *Salmonella* strain expressing influenza protein antigen was engineered to achieve endosomal escape and provided enhanced protection against viral challenge after oral administration compared to vaccination with the wildtype strain [153]. This study demonstrates the potential for endosomal escape-enhancing oral delivery systems to potentiate mucosal immune responses.

2.1.4.4 Pathogen biomimicry

The components of a vaccine are critical in directing immune responses, and mimicking the biophysical attributes of pathogens has been shown to be an effective way to activate immunity [138,154–156]. Pathogens express a variety of molecular patterns that cells detect through ligation of receptors that recognize distinct, evolutionary conserved patterns. Scientific understanding of these molecular patterns has led to the development of next-generation adjuvants to amplify the immune response, control the type of response, and establish immunologic memory critical for long-lasting protection from infection [157,158]. These adjuvants are commonly delivered as singular entities or in specific combinations to induce immune synergy [159,160]. In nature, these pathogen motifs are organized in specific spatial patterns and sensed concurrently, which is difficult to achieve with soluble delivery. Particle-based systems, composed of polymers, lipids, and viral proteins, have the unique capability to control the spatial and temporal presentation of these molecules and achieve their simultaneous delivery inside cells [155,161]. For example, protein nanoparticles presenting antigen complexes on their surface elicited significantly higher titers of neutralizing antibodies in mice and non-human primates compared to soluble delivery [162]. Studies have demonstrated that particle size and shape, presentation density, and antigen and adjuvant co-delivery have significant impacts on immune responses [163–165]. Here, we discuss the use of biomimicry in oral vaccine

delivery systems and review unique characteristics of intestinal immunology to be considered in the design of oral vaccines that utilize biomimicry.

Virus-like particles (VLPs) are the ultimate biomimicry strategy, in which structures of viral proteins form a non-pathogenic particle that is structurally similar to pathogenic viruses. This structure can present protein antigens on their surface to effectively crosslink B cell receptors and facilitate uptake in antigen presenting cells [166,167]. While VLPs have been incredibly impactful for injection-based vaccinations, their impact after oral administration has been less studied. VLPs delivering a DNA vaccine were developed from hepatitis E virus for oral delivery [168]. Mucosal adaptive immune responses were highest in mice that had been vaccinated orally with VLPs in comparison to unencapsulated DNA [168]. Orally-delivered VLPs also induced systemic antibody responses to a similar degree as VLPs delivered subcutaneously, demonstrating the highly immunogenic nature of this vaccine delivery system [168]. A novel VLP system utilizing gastrointestinal digestion-resistant surface proteins induced robust activation of systemic and mucosal immune responses upon oral immunization [75]. This resulted protection against influenza challenge while delivery of the vaccine without the digestion-resistant proteins did not [75]. This study observed that the digestion-resistant surface proteins were paramount to the immunogenicity of the platform. VLPs that did not express these surface proteins were less effective in eliciting immunity [75].

In addition to VLPs, polymeric and lipid particles can be synthesized as biomimetic particles. One study investigated the effect of co-encapsulation of antigen and adjuvant in PLGA nanoparticles for oral immunization and observed higher serum antibody titers compared to particle delivery of antigen only [169]. As many biomimicking platforms incorporate adjuvants that antagonize specific pattern recognition receptors, it is important to remember that potent adjuvant combinations for parenteral vaccine formulations may not be as effective mucosally. Distinct expression profiles of pathogen pattern-recognition receptors (PRRs) are observed among different cell types and

locations. The PRR expression profiles of DCs have been most widely studied, due to the role of these cells in bridging innate and adaptive immunity. Parenteral vaccines are able directly access these cells and are thus designed with the PRR profiles of DCs in mind. However, mucosal vaccines first interact with epithelial cells lining these surfaces, which may require different design considerations. Intestinal epithelial cells are known to express a subset of toll-like receptors and expression is polarized [144,170]. The TLR agonist flagellin, known to activate intestinal epithelial cells [40], and the C-type lectin receptor ligand mannosamine, known to target and activate DCs [171], were conjugated to polyanhydride nanoparticles [172]. Upon oral delivery, increased antigen-specific antibody titers were observed from the biomimicking particles compared to particles without ligand decoration [172]. Immunity generated in response to soluble co-delivery of antigen and adjuvant was not reported. Thus, it is not clear the role of antigen and adjuvant co-presentation by the vaccine-delivering particle on the enhanced immune responses. This ability of material-based systems to potentiate immune responses and mimic attributes of infectious pathogens is incredibly powerful. The utilization of advanced material systems to mimic biophysical attributes has significant potential to expand our understanding of oral vaccine requirements to activate immunity.

2.1.4.4.1 Controlling vaccine kinetics

Natural infections are known to have varying pathogen loads over time and infection kinetics dictate the timing and type of immune response for proper pathogen elimination [173,174]. Non-replicating vaccines, which have shown limited ability to induce immunity when administered orally, deliver a bolus of antigen to the body and do not mirror the kinetics of naturally occurring infections. It is possible that the immunologic processes necessary for protection are not activated due to differences in vaccine kinetics. For example, the timescale of naïve T cell differentiation into effector T cells is on the order of days. B cell class switching and somatic hypermutation depend on the continued exposure to antigen over time to develop high-affinity receptors. Indeed, modulating

parenteral vaccine delivery kinetics has shown to result in differences in both the $CD8^+$ T cell [174] and antibody [175] response. Exponentially increasing vaccine dosing regimens were found to activate the highest adaptive immune responses. Enhanced responses were due to prolonged antigenic stimulation of T and B cells, resulting in increased germinal center B cell responses. To achieve such kinetics for oral immunizations, the timescale of adaptive immune generation must be reconciled with the short residence time of orally delivered vaccines.

Oral immunization with cholera toxin conjugated with a small molecule hapten required repeat doses to generate intestinal IgA [176]. The authors note that the time between doses was not as critical as the number of immunizations in eliciting mucosal antibodies. This study identified that repeat doses were necessary to select and expand high affinity antibody-producing plasma cells in the intestine, which was initiated in Peyer's patch germinal centers [176]. Thus, these results indicate sustained vaccine exposure is also required for oral immunization. For clinical use, the development of an advanced delivery system to achieve such dosing kinetics will be advantageous. Material-based systems can control vaccine release rates and importantly, sustained release kinetics can be realized.

While most studies investigating antigen kinetics and persistence use parenteral vaccine administration, there are a few of note that investigate kinetics for oral vaccination. Alginate-coated chitosan nanoparticles of different molecular weights demonstrated distinct antigen release kinetics and were compared as oral vaccines [87]. The authors observed that lower molecular weight chitosan formulations, which had a more sustained release profile compared to higher molecular weight formulation, elicited higher antibody titers [87]. While it is not known if the varying molecular weights of the formulations led to other important differences *in vivo*, such as vaccine absorption, this study suggests that the dependence of the immune response on vaccine kinetics observed for parenteral vaccination may also be true for mucosal vaccines. Enteric-coated plant-

based microcapsules have also demonstrated sustained release kinetics in simulated intestinal fluid over 8 hours [177]. However, this platform has yet to be evaluated for the elicitation of immune responses.

Modulation of vaccine delivery kinetics at mucosal surfaces can also be achieved using mucoadhesive systems to prolong vaccine residence time. As discussed above, oral vaccine delivery systems that are themselves mucoadhesive may have limited diffusion through the mucus barrier, ultimately resulting in vaccine clearance. Rather, some material solutions may include adhesive depots that sustain vaccine release while simultaneously extending residence time or a delivery system that provides a constant source of antigen upstream of inductive sites in the intestine. Such advanced technologies have been designed for oral therapeutic delivery and have relevance to questions regarding the effect of vaccine kinetics on oral immunization. Planar microdevices were developed to achieve unidirectional release of the small molecule drug acyclovir to increase oral bioavailability [178]. Lectin conjugation of the microdevices increased mucoadhesion, resulting in retention of the devices in the small intestine over two hours [178]. In contrast, microparticles were found in the colon at this time point [178]. These results support the application of such mucoadhesive devices to extend vaccine persistence compared to traditional particle-based platforms. The same group also designed planar microdevices with nanostraw membranes to increase intestinal adhesion and modulate drug release by controlling the nanostraw diameter [179]. As these devices were only evaluated *ex vivo*, how these modified microdevices affect drug uptake *in vivo* is still to be determined. One limitation of mucoadhesive devices is their dependence on mucus, which is rapidly turned over in the gastrointestinal tract. A device that does not depend on mucoadhesion for retention, such as the recently engineered star-shaped drug delivery device that sits at the pylorus [180], could achieve sustained vaccine dosing in the intestine over much longer time scales. This device was able to sustained the release of an anti-malaria small molecule drug for up to 14 days [180]. Using such a device to deliver a continuous vaccine dose in

the gastrointestinal tract independent of mucus adhesion is powerful in the effort to develop effective oral vaccines. The vaccine released from this system will also need to overcome subsequent barriers to activate immunity as discussed above, such as mucus diffusion, intestinal absorption, and immune activation.

Achieving specific vaccine release profiles through the use of material-based systems has proven favorable to amplify immune responses. Studies thus far indicate that extended persistence of vaccines through sustained release is required for high affinity adaptive immunity. Gaps remain for oral vaccines, in which the relationship between vaccine kinetics and immune responses have not been established.

2.1.4.5 Material immunomodulation

The gut is known to be an immunosuppressive site, where immune responses skew towards having regulatory functions. Ensuring proper activation of inflammatory responses is critical for oral vaccines to generate immunity and not tolerance [181]. The use of adjuvants has proved to be effective in driving the quality of immune responses to vaccines, especially for conjugate, killed, or inactivated antigen vaccines. Development of adjuvants specifically for vaccination at mucosal surfaces is an area of active focus [6,10]. Adjuvant mechanism of action, potency, and safety profile are key considerations for mucosal administration. One of the most effective and established mucosal adjuvants is cholera toxin; however, toxicity has hindered its clinical use. Next-generation vaccine adjuvants focus on exploiting newly identified pattern recognition receptors, such as Toll-like receptors (TLRs), NOD-like receptors (NLRs), and retinoic acid-inducible gene-like receptors (RLRs). These adjuvants are highly specific to the activation of certain immunologic pathways that allows tailoring of the generated immune responses [182]. In addition to known pathogen recognition receptor ligands, biomaterial systems themselves have also been shown to interact with the body in an immuno-stimulatory or -regulatory manner depending on their physiochemical properties. These findings were first observed in the field of regenerative medicine but have relevance for material-based

immunotherapies [183]. The ability of biomaterials to modulate inflammatory pathways may achieve increased activation of immune cells at the same time that a vaccine is delivered. These systems may also elucidate new ways to stimulate immunity in addition to the use of traditional adjuvants [184]. Here, we discuss biomaterials with intrinsic adjuvant properties, highlight examples of mucosal immunomodulation by these materials, and comment on their utility as novel oral vaccine platforms. Novel material-based adjuvants that have been used in oral vaccine formulations are summarized in Table 2.4.

The intrinsic immunogenicity of biomaterials is driven by physiochemical attributes, particularly shape, charge, surface chemistry, hydrophobicity, and molecular weight. Changing material properties has been shown to modulate the secretion of cytokines, DC maturation, inflammasome activation, and complement activation. For example, increasing the hydrophobicity of head groups on gold nanoparticles correlated with increased gene expression of a panel of inflammatory cytokines [185]. Activation of DCs was shown to be modulated by nanoparticle surface chemistry, with some formulations inducing suppressive responses [186]. The properties of material-based delivery systems also play a role in the activation of the complement pathway, which can lead to recognition by the immune system and modulate adaptive immunity [187–189]. Activation of complement by biomaterial carriers can also limit their clinical translation due to immune system recognition leading to allergic responses and accelerated clearance [190]. Thus, designing materials to interact with the immune system must be balanced to achieve stimulatory function while limiting adverse events. While the mechanism of immune-modulation by materials is not fully understood, specific physical attributes of materials have been shown to act through inflammasome activation and TLR-dependent signaling. Inflammasome complexes form in the cytosol upon sensing of pathogen-associated motifs, which results in an inflammatory signal cascade and programmed cell death as part of the antimicrobial response [191]. Polymeric particles composed of polystyrene and PLGA increased production of the inflammasome-dependent cytokine IL-1β by DCs *in vitro* and

this effect was dependent on particle size [192]. Polyethyleneimine (PEI), a highly branched cationic polymer, exhibits adjuvant and inflammasome-activating properties [193,194]. Nanogels composed of pyridine-poly(hydroxyethyl methacrylate) also demonstrated intrinsic adjuvant effects that acted through TLR2 signaling, leading to enhanced germinal center B cell responses [195]. The authors hypothesized the TLR2-mediated activity to be due to the aromatic, hydrophobic portions of the nanomaterial. Material shape can also control the type of immune response generated. Small, spherical polystyrene particles were found to bias the immune response towards type-I (protective, cell-mediated response) while rod-shaped polystyrene particles induced type-II responses (humoral and resolution of inflammation) after subcutaneous immunization [196]. These polymeric systems demonstrate their multi-parameter utility for therapeutic delivery and their promise to address multiple barriers for oral vaccine delivery due to their physiochemical properties, including activation of inflammatory pathways.

Natural polymers and their derivatives have also been investigated for use as mucosal adjuvants. Chitosan and N-trimethyl chitosan (TMC) nanoparticles enhanced antibody responses following intraduodenal administration, which may be due to the intrinsic immunostimulatory effect of TMC observed on monocyte-derived DCs *in vitro* [197]. This study also found that TMC particles had enhanced epithelial transport *in vitro* and *ex vivo* [197]. Additionally, chitosan is known to activate the inflammasome [198]. The specific contributions of immune stimulation versus increased uptake of chitosan-based particles on enhanced adaptive immunity after oral vaccination is still unknown. Orally-delivered chitosan nanoparticle vaccines increased antibody titers compared to soluble antigen, with higher responses in groups vaccinated with chitosan nanoparticles encapsulated in either liposomes and niosomes that were used to enhance their stability in acidic environments [86]. These results suggest that both gastrointestinal stability and intrinsic immuno-stimulation contributes to activation of adaptive immunity upon oral immunization. TMC particles were also found to uniquely activate DCs *in vitro* and induce

serum IgG and secretory IgA production compared to PLGA particles when administered nasally [199]. Calcium carbonate microparticles encapsulating antigenic peptide nanofibers induced DC maturation and IL-1β production *in vitro*, which was dependent on calcium carbonate microparticle formulation of the peptide nanofibers [200]. This trend was recapitulated *in vivo* following oral administration, where calcium carbonate-peptide nanofibers induced the highest levels of systemic and mucosal antibodies followed by unencapsulated peptide nanofibers [200]. Microparticles made of β-glucan, which is a pathogen-associated molecular pattern known to modulate innate immunity, altered epithelial gene expression of inflammatory cytokines, pattern recognition receptors, and costimulatory molecules [201]. The authors observed the induction of mixed T_H1/T_H17 responses in the spleens of mice orally vaccinated with β-glucan particles that was not observed with soluble antigen delivery [201]. As epithelial cells have been shown to direct innate immune responses to oral antigens, the use of material properties to control their signaling profiles from tolerogenic to inflammatory has significant implications for oral vaccines. Immune stimulating complexes (ISCOMs) are self-assembling lipid nanoparticles that contain the immunostimulant saponin. ISCOMs can be loaded with vaccine components and prevent the induction of oral tolerance to the protein antigen ovalbumin after oral delivery [202]. While the particulate shape of ISCOMs can modulate vaccine uptake, parenteral injection of these complexes demonstrate their inherent immunogenic effects, in which innate immune cells and inflammatory signaling pathways are activated [203]. The mechanism of action of ISCOMs has not been fully elucidated, but is thought to be due to functional group hydrophobicity and conformation leading to endosomal membrane destabilization, cytoplasmic delivery of antigen, and robust activation of DCs [204].

Exploring the full breadth of physiochemical features of material-based systems will be significant for oral vaccine delivery to identify the most effective stimulatory systems to achieve immunity. Additionally, material systems can be used to selectively

activate and uncover signaling pathways in the gut that result in differences in immune responses. How these platforms modulate intestinal epithelial cell signaling, signals in the tissue microenvironment, and the recruitment and activation of different antigen presenting cell populations will be central to evaluate for oral vaccines.

Table 2.4. Effects of immuno-modulating materials systems on immune responses after oral vaccination.

Material	**Adjuvant mechanisms**	**Adaptive immunity**	**Reference**
Chitosan-based nanoparticles	DC maturation	Antibody response	[86,197–199]
Calcium carbonate nanofibers	DC maturation; inflammatory cytokines	Systemic and mucosal antibodies	[200]
β-glucan microparticles	Epithelial gene expression (inflammatory cytokines, PRRs, costimulatory molecules)	Mixed T_H1/T_H17 responses	[201]
Immune-stimulating complexes (ISCOMs)	Endosome destabilization, DC activation	Overcome oral tolerance	[202,203]

2.1.5 *Applied immunology*

Another strategy to improve the efficacy of orally delivered vaccines is through delivery of chemokines, cytokines, and novel adjuvants. The development of mucosal adjuvants is currently a big focus of the field due to the necessity to activate inflammatory responses from immune cells at mucosal surfaces while reducing toxicity. During natural infection as well as upon administration of established adjuvants such as cholera toxin and aluminum hydroxide, it has been shown that activation of intestinal epithelial cells results in the production of DC-attracting chemokines [22,205–207]. This activation is largely due to the ligation of different receptors on the surface of epithelial cells that serve as "danger signals". The identification of such ligands, for example TLRs, NLRs, and RLRs, has allowed for the evaluation of many new immunomodulatory agents for this purpose. The oral administration of the TLR-9 agonist CpG ODN was shown to increase the frequency of DC transepithelial dendrites into the small intestinal lumen, which resulted in an increase in antigen uptake and enhanced antibody and T cell responses [208]. The authors hypothesized that DC recruitment was due to the enhanced production

of the chemokine CCL20 at the apical side of epithelial cells. The TLR-7/8 ligand Resiquimod (R-848) can also expand the DC population in the small intestinal lamina propria and MLNs, which was found to be mediated by the inflammatory cytokine TNF-α [209]. Flagellin, a TLR-5 agonist, has been shown to induce epithelial cell production of CCL20 and trigger migration of immature DCs *in vitro* [40]. The ability of new adjuvants to recruit antigen presenting cells has also been demonstrated at other mucosal sites. Following intranasal administration of the cationic polymer polyethyleneimine (PEI), dendritic cell trafficking to the draining lymph nodes could be enhanced and vaccine delivery with this adjuvant resulted in higher IgA and IgG titers as well as protection from viral challenge [210]. Importantly, this recruitment of DCs at mucosal tissues can lead to enhanced activation of adaptive immune responses and the development of protective immunity.

In addition to delivering chemokine-inducing agents such as adjuvants, the delivery of chemokines themselves have been used as a strategy for a variety of immunomodulatory applications. Chemokines and cytokines also been used in implanted materials to induce the migration of certain cell types into the introduced device [211,212]. Vaginal administration of the chemokine GM-CSF resulted in an increase of the total DCs in the mucosal tissue [213]. However, it is clear that, due to the different mechanisms of immune activation of each agent, their use must be carefully selected based on the administration route and aims of the study. While it is known that certain adjuvants can induce the secretion of chemokines by intestinal epithelial cells, the optimal adjuvant for this purpose has not been evaluated for oral vaccine delivery nor has the role of other inflammatory signals, such as CCL2, CCL7, CCL8, CCL22, and IFN-γ in stimulating these responses.

2.2 Conclusions

The development of effective next-generation oral vaccines has significant potential to increase immunization access in low resource settings by eliminating the need for

trained medical personnel and sterile needles as well as to develop strategies to generate protective immunity at mucosal sites to prevent the spread of infectious disease. Currently, millions of people die every year from pathogens that infect the body at these mucosal surfaces. While we have existing vaccines for some of these pathogens, immunization campaign logistics limit the use of injection-based vaccines in developing regions. Additionally, the use of protein-based antigens is necessary for pathogens in which their attenuation is not possible or there is a risk of vaccine reversion to a virulent form. However, there exists no licensed non-live oral vaccine in the United States. The oral delivery of protein-based vaccines is not a trivial task and one that has been investigated for decades. The use of biomaterials-based approaches has shown to be advantageous in addressing the chemical barriers upon oral delivery, such as the harsh GI environment, and in improving vaccine uptake and immune responses. With the recent advancements in immunology, we have new understandings about the mechanisms of antigen uptake by mucosal immune cells, how to elicit protection at mucosal surfaces, and the establishment of tissue-resident memory cells that are crucial in preventing infection following immunization. We believe that interdisciplinary collaborations utilizing both biomaterial delivery strategies and applied immunology will lead to novel oral vaccine approaches.

2.3 References

[1] WHO; UNICEF; World Bank, State of the world's vaccines and immunization, 3rd ed., 2009.

[2] S. Mitragotri, Immunization without needles., Nat. Rev. Immunol. 5 (2005) 905–16. doi:10.1038/nri1728.

[3] C.J.H. Davitt, E.C. Lavelle, Delivery strategies to enhance oral vaccination against enteric infections, Adv. Drug Deliv. Rev. 91 (2015) 52–69. doi:10.1016/j.addr.2015.03.007.

[4] S. Wang, H. Liu, X. Zhang, F. Qian, Intranasal and oral vaccination with protein-based antigens: advantages, challenges and formulation strategies, Protein Cell. 6 (2015) 480–503. doi:10.1007/s13238-015-0164-2.

[5] M.F. Pasetti, J.K. Simon, M.B. Sztein, M.M. Levine, Immunology of gut mucosal vaccines, Immunol. Rev. 239 (2011) 125–148. doi:10.1111/j.1600-065X.2010.00970.x.

[6] E. Bergmann-Leitner, W. Leitner, Adjuvants in the Driver's Seat: How Magnitude, Type, Fine Specificity and Longevity of Immune Responses Are Driven by Distinct Classes of

Immune Potentiators, Vaccines. 2 (2014) 252–296. doi:10.3390/vaccines2020252.
[7] N. Lycke, Recent progress in mucosal vaccine development: potential and limitations, Nat. Rev. Immunol. 12 (2012) 592–605. doi:10.1038/nri3251.
[8] C.O. Elson, W. Ealding, Cholera toxin feeding did not induce oral tolerance in mice and abrogated oral tolerance to an unrelated protein antigen., J. Immunol. 133 (1984) 2892–7. http://www.ncbi.nlm.nih.gov/pubmed/6491278.
[9] J.D. Clements, N.M. Hartzog, F.L. Lyon, Adjuvant activity of Escherichia coli heat-labile enterotoxin and effect on the induction of oral tolerance in mice to unrelated protein antigens., Vaccine. 6 (1988) 269–77. doi:10.1016/0264-410x(88)90223-x.
[10] K.A. Woodrow, K.M. Bennett, D.D. Lo, Mucosal Vaccine Design and Delivery, Annu. Rev. Biomed. Eng. 14 (2012) 17–46. doi:10.1146/annurev-bioeng-071811-150054.
[11] World Health Organization, The Global Burden of Disease: 2004 update, 2004 Updat. (2008) 146. doi:10.1038/npp.2011.85.
[12] C. Murphy, K., Travers, P., Walport, M., & Janeway, Janeway's immunobiology (8th ed.)., 2012.
[13] I.M. Belyakov, J.D. Ahlers, What Role Does the Route of Immunization Play in the Generation of Protective Immunity against Mucosal Pathogens?, J. Immunol. 183 (2009) 6883–6892. doi:10.4049/jimmunol.0901466.
[14] J. Holmgren, C. Czerkinsky, Mucosal immunity and vaccines, Nat. Med. 11 (2005) S45–S53. doi:10.1038/nm1213.
[15] Q. Zhu, J. Talton, G. Zhang, T. Cunningham, Z. Wang, R.C. Waters, J. Kirk, B. Eppler, D.M. Klinman, Y. Sui, S. Gagnon, I.M. Belyakov, R.J. Mumper, J.A. Berzofsky, Large intestine-targeted, nanoparticle-releasing oral vaccine to control genitorectal viral infection, Nat. Med. 18 (2012) 1291–1296. doi:10.1038/nm.2866.
[16] I.M. Belyakov, S.A. Hammond, J.D. Ahlers, G.M. Glenn, J.A. Berzofsky, Transcutaneous immunization induces mucosal CTLs and protective immunity by migration of primed skin dendritic cells, J. Clin. Invest. 113 (2004) 998–1007. doi:10.1172/JCI200420261.
[17] H. Cheroutre, F. Lambolez, D. Mucida, The light and dark sides of intestinal intraepithelial lymphocytes, Nat. Rev. Immunol. 11 (2011) 445–456. doi:10.1038/nri3007.
[18] B. Koscsó, K. Gowda, T.D. Schell, M. Bogunovic, Purification of dendritic cell and macrophage subsets from the normal mouse small intestine, J. Immunol. Methods. 421 (2015) 1–13. doi:10.1016/j.jim.2015.02.013.
[19] R. Ohue, M. Nakamoto, N. Kitabatake, F. Tani, Changes in lamina propria dendritic cells on the oral administration of exogenous protein antigens during weaning, Cytotechnology. 64 (2012) 221–230. doi:10.1007/s10616-011-9351-z.
[20] E.K. Persson, C.L. Scott, A.M. Mowat, W.W. Agace, Dendritic cell subsets in the intestinal lamina propria: Ontogeny and function, Eur. J. Immunol. 43 (2013) 3098–3107. doi:10.1002/eji.201343740.
[21] S. Milling, U. Yrlid, V. Cerovic, G. MacPherson, Subsets of migrating intestinal dendritic cells, Immunol. Rev. 234 (2010) 259–267. doi:10.1111/j.0105-2896.2009.00866.x.
[22] J. Farache, I. Koren, I. Milo, I. Gurevich, K.-W. Kim, E. Zigmond, G.C. Furtado, S.A. Lira, G. Shakhar, Luminal Bacteria Recruit CD103+ Dendritic Cells into the Intestinal Epithelium to Sample Bacterial Antigens for Presentation, Immunity. 38 (2013) 581–595. doi:10.1016/j.immuni.2013.01.009.
[23] E. Jaensson, H. Uronen-Hansson, O. Pabst, B. Eksteen, J. Tian, J.L. Coombes, P.L.

Berg, T. Davidsson, F. Powrie, B. Johansson-Lindbom, W.W. Agace, Small intestinal CD103+ dendritic cells display unique functional properties that are conserved between mice and humans, J. Exp. Med. 205 (2008) 2139–2149. doi:10.1084/jem.20080414.

[24] A.M. Mowat, W.W. Agace, Regional specialization within the intestinal immune system, Nat. Rev. Immunol. 14 (2014) 667–685. doi:10.1038/nri3738.

[25] L.W. Peterson, D. Artis, Intestinal epithelial cells: regulators of barrier function and immune homeostasis., Nat. Rev. Immunol. 14 (2014) 141–53. doi:10.1038/nri3608.

[26] A. Iwasaki, B.L. Kelsall, Localization of distinct Peyer's patch dendritic cell subsets and their recruitment by chemokines macrophage inflammatory protein (MIP)-3alpha, MIP-3beta, and secondary lymphoid organ chemokine., J. Exp. Med. 191 (2000) 1381–94. doi:10.1084/jem.191.8.1381.

[27] A.J. Macpherson, K. Smith, Mesenteric lymph nodes at the center of immune anatomy, J. Exp. Med. 203 (2006) 497–500. doi:10.1084/jem.20060227.

[28] C. Berlin, E.L. Berg, M.J. Briskin, D.P. Andrew, P.J. Kilshaw, B. Holzmann, I.L. Weissman, A. Hamann, E.C. Butcher, α4β7 integrin mediates lymphocyte binding to the mucosal vascular addressin MAdCAM-1, Cell. 74 (1993) 185–195. doi:10.1016/0092-8674(93)90305-A.

[29] E.C. Butcher, M. Williams, K. Youngman, L. Rott, M. Briskin, Lymphocyte Trafficking and Regional Immunity, Adv. Immunol. 72 (1999) 209–253. doi:10.1016/S0065-2776(08)60022-X.

[30] E.P. Bowman, N.A. Kuklin, K.R. Youngman, N.H. Lazarus, E.J. Kunkel, J. Pan, H.B. Greenberg, E.C. Butcher, The intestinal chemokine thymus-expressed chemokine (CCL25) attracts IgA antibody-secreting cells, J. Exp. Med. 195 (2002) 269–275. doi:10.1084/jem.20010670.

[31] D.J. Campbell, E.C. Butcher, Rapid Acquisition of Tissue-specific Homing Phenotypes by CD4 + T Cells Activated in Cutaneous or Mucosal Lymphoid Tissues, J. Exp. Med. 195 (2002) 135–141. doi:10.1084/jem.20011502.

[32] A.M. Mowat, Anatomical basis of tolerance and immunity to intestinal antigens, Nat. Rev. Immunol. 3 (2003) 331–341. doi:10.1038/nri1057.

[33] U.Y. Khoo, I.E. Proctor, A.J. Macpherson, CD4+ T cell down-regulation in human intestinal mucosa: evidence for intestinal tolerance to luminal bacterial antigens., J. Immunol. 158 (1997) 3626–34. http://www.jimmunol.org/content/158/8/3626 (accessed October 17, 2017).

[34] M. Rimoldi, M. Chieppa, V. Salucci, F. Avogadri, A. Sonzogni, G.M. Sampietro, A. Nespoli, G. Viale, P. Allavena, M. Rescigno, Intestinal immune homeostasis is regulated by the crosstalk between epithelial cells and dendritic cells, Nat. Immunol. 6 (2005) 507–514. doi:10.1038/ni1192.

[35] M. Chieppa, M. Rescigno, A.Y.C. Huang, R.N. Germain, Dynamic imaging of dendritic cell extension into the small bowel lumen in response to epithelial cell TLR engagement., J. Exp. Med. 203 (2006) 2841–52. doi:10.1084/jem.20061884.

[36] A. Iwasaki, Mucosal Dendritic Cells, Annu. Rev. Immunol. 25 (2007) 381–418. doi:10.1146/annurev.immunol.25.022106.141634.

[37] N. Kulkarni, M. Pathak, G. Lal, Role of chemokine receptors and intestinal epithelial cells in the mucosal inflammation and tolerance, J. Leukoc. Biol. 101 (2016) 377–394. doi:10.1189/jlb.1RU0716-327R.

[38] S. Fujiie, K. Hieshima, D. Izawa, T. Nakayama, R. Fujisawa, H. Ohyanagi, O. Yoshie, Proinflammatory cytokines induce liver and activation-regulated chemokine/macrophage inflammatory protein-3alpha/CCL20 in mucosal epithelial cells through NF-kappaB., Int. Immunol. 13 (2001) 1255–1263. doi:10.1093/intimm/13.10.1255.

[39] P. Dutta, A. Ta, B.K. Thakur, N. Dasgupta, S. Das, Biphasic Ccl20 regulation by Toll-like receptor 9 through the activation of ERK-AP-1 and non-canonical NF-κB signaling pathways, Biochim. Biophys. Acta - Gen. Subj. 1861 (2017) 3365–3377. doi:10.1016/j.bbagen.2016.08.019.

[40] F. Sierro, B. Dubois, A. Coste, D. Kaiserlian, J.P. Kraehenbuhl, J.C. Sirard, Flagellin stimulation of intestinal epithelial cells triggers CCL20-mediated migration of dendritic cells., Proc. Natl. Acad. Sci. U. S. A. 98 (2001) 13722–7. doi:10.1073/pnas.241308598.

[41] Y. Sugiura, K. Kamdar, S. Khakpour, G. Young, W.J. Karpus, R.W. DePaolo, TLR1-induced chemokine production is critical for mucosal immunity against Yersinia enterocolitica, Mucosal Immunol. 6 (2013) 1101–9. doi:10.1038/mi.2013.5.

[42] M. Le Borgne, N. Etchart, A. Goubier, S. a. Lira, J.C. Sirard, N. Van Rooijen, C. Caux, S. Aït-Yahia, A. Vicari, D. Kaiserlian, B. Dubois, Dendritic cells rapidly recruited into epithelial tissues via CCR6/CCL20 are responsible for CD8+ T cell crosspriming in vivo, Immunity. 24 (2006) 191–201. doi:10.1016/j.immuni.2006.01.005.

[43] J.E. Vela Ramirez, L.A. Sharpe, N.A. Peppas, Current state and challenges in developing oral vaccines, Adv. Drug Deliv. Rev. 114 (2017) 116–131. doi:10.1016/j.addr.2017.04.008.

[44] L.M. Ensign, R. Cone, J. Hanes, Oral drug delivery with polymeric nanoparticles: The gastrointestinal mucus barriers, Adv. Drug Deliv. Rev. 64 (2012) 557–570. doi:10.1016/j.addr.2011.12.009.

[45] P. Lundquist, P. Artursson, Oral absorption of peptides and nanoparticles across the human intestine: Opportunities, limitations and studies in human tissues, Adv. Drug Deliv. Rev. 106 (2016) 256–276. doi:10.1016/j.addr.2016.07.007.

[46] G. Semenza, Anchoring and Biosynthesis of Stalked Brush Border Membrane Proteins: Glycosidases and Peptidases of Enterocytes and Renal Tubuli, Annu. Rev. Cell Biol. 2 (1986) 255–313. doi:10.1146/annurev.cellbio.2.1.255.

[47] J.D. Astwood, J.N. Leach, R.L. Fuchs, Stability of food allergens to digestion in vitro, Nat. Biotechnol. 14 (1996) 1269–1273. doi:10.1038/nbt1096-1269.

[48] E. Untersmayr, N. Bakos, I. Schöll, M. Kundi, F. Roth-Walter, K. Szalai, A.B. Riemer, H.J. Ankersmit, O. Scheiner, G. Boltz-Nitulescu, E. Jensen-Jarolim, Anti-ulcer drugs promote IgE formation toward dietary antigens in adult patients, FASEB J. 19 (2005) 656–658. doi:10.1096/fj.04-3170fje.

[49] I. Pali-Schöll, E. Jensen-Jarolim, Anti-acid medication as a risk factor for food allergy, Allergy Eur. J. Allergy Clin. Immunol. 66 (2011) 469–477. doi:10.1111/j.1398-9995.2010.02511.x.

[50] C.C. Bowman, M.K. Selgrade, Failure to Induce Oral Tolerance in Mice Is Predictive of Dietary Allergenic Potency among Foods with Sensitizing Capacity, Toxicol. Sci. 106 (2008) 435–443. doi:10.1093/toxsci/kfn200.

[51] C. Atuma, V. Strugala, A. Allen, L. Holm, The adherent gastrointestinal mucus gel layer: thickness and physical state in vivo, Am. J. Physiol. Liver Physiol. 280 (2001) G922–G929. doi:10.1152/ajpgi.2001.280.5.G922.

[52] S.K. Lai, Y.-Y. Wang, K. Hida, R. Cone, J. Hanes, Nanoparticles reveal that human

cervicovaginal mucus is riddled with pores larger than viruses, Proc. Natl. Acad. Sci. 107 (2010) 598–603. doi:10.1073/pnas.0911748107.

[53] L. Shen, C.R. Weber, D.R. Raleigh, D. Yu, J.R. Turner, Tight Junction Pore and Leak Pathways: A Dynamic Duo, Annu. Rev. Physiol. 73 (2011) 283–309. doi:10.1146/annurev-physiol-012110-142150.

[54] R.L. Owen, Sequential Uptake of Horseradish Peroxidase by Lymphoid Follicle Epithelium of Peyer's Patches in the Normal Unobstructed Mouse Intestine: An Ultrastructural Study, Gastroenterology. (1977). doi:10.1016/S0016-5085(77)80254-0.

[55] M.A. Jepson, M. Ann Clark, Studying M cells and their role in infection, Trends Microbiol. 6 (1998) 359–365. doi:10.1016/S0966-842X(98)01337-7.

[56] J.R. McDole, L.W. Wheeler, K.G. McDonald, B. Wang, V. Konjufca, K.A. Knoop, R.D. Newberry, M.J. Miller, Goblet cells deliver luminal antigen to CD103+ dendritic cells in the small intestine, Nature. 483 (2012) 345–349. doi:10.1038/nature10863.

[57] H. Lelouard, M. Fallet, B. De Bovis, S. Méresse, J. Gorvel, Peyer's patch dendritic cells sample antigens by extending dendrites through M cell-specific transcellular pores, Gastroenterology. 142 (2012) 592–601. doi:10.1053/j.gastro.2011.11.039.

[58] E. Mazzini, L. Massimiliano, G. Penna, M. Rescigno, Oral Tolerance Can Be Established via Gap Junction Transfer of Fed Antigens from CX3CR1+ Macrophages to CD103+ Dendritic Cells, Immunity. 40 (2014) 248–261. doi:10.1016/j.immuni.2013.12.012.

[59] M. Rescigno, M. Urbano, B. Valzasina, M. Francolini, G. Rotta, R. Bonasio, F. Granucci, J.-P. Kraehenbuhl, P. Ricciardi-Castagnoli, Dendritic cells express tight junction proteins and penetrate gut epithelial monolayers to sample bacteria, Nat. Immunol. 2 (2001) 361–367. doi:10.1038/86373.

[60] J.H. Niess, S. Brand, X. Gu, L. Landsman, S. Jung, B.A. McCormick, J.M. Vyas, M. Boes, H.L. Ploegh, J.G. Fox, D.R. Littman, H.C. Reinecker, CX3CR1-mediated dendritic cell access to the intestinal lumen and bacterial clearance, Science (80-.). (2005). doi:10.1126/science.1102901.

[61] M. Regoli, E. Bertelli, M. Gulisano, C. Nicoletti, The Multifaceted Personality of Intestinal CX 3 CR1 + Macrophages, Trends Immunol. 38 (2017) 879–887. doi:10.1016/j.it.2017.07.009.

[62] A.J. Stagg, Intestinal Dendritic Cells in Health and Gut Inflammation, Front. Immunol. 9 (2018) 2883. doi:10.3389/fimmu.2018.02883.

[63] J.M. Allaire, S.M. Crowley, H.T. Law, S.-Y. Chang, H.-J. Ko, B.A. Vallance, The Intestinal Epithelium: Central Coordinator of Mucosal Immunity, Trends Immunol. 39 (2018) 677–696. doi:10.1016/j.it.2018.04.002.

[64] U. Hadis, B. Wahl, O. Schulz, M. Hardtke-Wolenski, A. Schippers, N. Wagner, W. Müller, T. Sparwasser, R. Förster, O. Pabst, Intestinal Tolerance Requires Gut Homing and Expansion of FoxP3+ Regulatory T Cells in the Lamina Propria, Immunity. 34 (2011) 237–246. doi:10.1016/j.immuni.2011.01.016.

[65] C.-M. Sun, J.A. Hall, R.B. Blank, N. Bouladoux, M. Oukka, J.R. Mora, Y. Belkaid, Small intestine lamina propria dendritic cells promote de novo generation of Foxp3 T reg cells via retinoic acid, J. Exp. Med. 204 (2007) 1775–1785. doi:10.1084/jem.20070602.

[66] M.F. Neurath, S. Finotto, L.H. Glimcher, The role of Th1/Th2 polarization in mucosal immunity, Nat. Med. 8 (2002) 567–573. doi:10.1038/nm0602-567.

[67] B. Huang, J.R. Yeiser, A. Cerutti, K. Chen, A. Bigas, L. Cassis, M. Cols, A. Velcich, L.

Comerma, L. Mayer, H. Xiong, V.U. Bornstein, M. Shan, B. He, J.M. Blander, A.C. Walland, L.H. Augenlicht, M. Gentile, C. Berin, Mucus Enhances Gut Homeostasis and Oral Tolerance by Delivering Immunoregulatory Signals, Science (80-.). 342 (2013) 447–453. doi:10.1126/science.1237910.

[68] A. Wakabayashi, Y. Kumagai, E. Watari, M. Shimizu, M. Utsuyama, K. Hirokawa, H. Takahashi, Importance of gastrointestinal ingestion and macromolecular antigens in the vein for oral tolerance induction, Immunology. 119 (2006) 167–177. doi:10.1111/j.1365-2567.2006.02418.x.

[69] A.E. Ibañez, L.M. Coria, M.V. Carabajal, M.V. Delpino, G.S. Risso, P.G. Cobiello, J. Rinaldi, P. Barrionuevo, L. Bruno, F. Frank, S. Klinke, F.A. Goldbaum, G. Briones, G.H. Giambartolomei, K.A. Pasquevich, J. Cassataro, A bacterial protease inhibitor protects antigens delivered in oral vaccines from digestion while triggering specific mucosal immune responses, J. Control. Release. 220 (2015) 18–28. doi:10.1016/j.jconrel.2015.10.011.

[70] L. Shan, Ø. Molberg, I. Parrot, F. Hausch, F. Filiz, G.M. Gray, L.M. Sollid, C. Khosla, Structural basis for gluten intolerance in celiac sprue., Science. 297 (2002) 2275–9. doi:10.1126/science.1074129.

[71] K.S. Barone, M.R. Reilly, M.P. Flanagan, J.G. Michael, Abrogation of oral tolerance by feeding encapsulated antigen, Cell. Immunol. 199 (2000) 65–72. doi:10.1006/cimm.1999.1603.

[72] P. Sahdev, L.J. Ochyl, J.J. Moon, Biomaterials for nanoparticle vaccine delivery systems, Pharm. Res. 31 (2014) 2563–2582. doi:10.1007/s11095-014-1419-y.

[73] A. des Rieux, V. Fievez, M. Garinot, Y.-J. Schneider, V. Préat, Nanoparticles as potential oral delivery systems of proteins and vaccines: A mechanistic approach, J. Control. Release. 116 (2006) 1–27. doi:10.1016/j.jconrel.2006.08.013.

[74] T. Nochi, H. Takagi, Y. Yuki, L. Yang, T. Masumura, M. Mejima, U. Nakanishi, A. Matsumura, A. Uozumi, T. Hiroi, S. Morita, K. Tanaka, F. Takaiwa, H. Kiyono, Rice-based mucosal vaccine as a global strategy for cold-chain- and needle-free vaccination, Proc. Natl. Acad. Sci. 104 (2007) 10986–10991. doi:10.1073/pnas.0703766104.

[75] B. Bellier, A.H. Tenaglia, C.G. Prucca, T. Sparwasser, M.C. Serradell, P.R. Gargantini, A. Saura, L.L. Rupil, D. Klatzmann, J. Echenique, P.G. Carranza, N. Reinoso-Vizcaino, E.A. Fernández, L. Berod, R.R. Tonelli, J.P. Petiti, R.A. Martino, E. Piaggio, H.D. Luján, Efficient oral vaccination by bioengineering virus-like particles with protozoan surface proteins, Nat. Commun. 10 (2019) 361. doi:10.1038/s41467-018-08265-9.

[76] S. Scheiblhofer, J. Laimer, Y. Machado, R. Weiss, J. Thalhamer, Influence of protein fold stability on immunogenicity and its implications for vaccine design, Expert Rev. Vaccines. 16 (2017) 479–489. doi:10.1080/14760584.2017.1306441.

[77] C.J.H. Davitt, E.A. McNeela, S. Longet, J. Tobias, V. Aversa, C.P. McEntee, M. Rosa, I.S. Coulter, J. Holmgren, E.C. Lavelle, A novel adjuvanted capsule based strategy for oral vaccination against infectious diarrhoeal pathogens, J. Control. Release. 233 (2016) 162–173. doi:10.1016/j.jconrel.2016.05.001.

[78] A.A. Date, J. Hanes, L.M. Ensign, Nanoparticles for oral delivery: Design, evaluation and state-of-the-art, J. Control. Release. 240 (2016) 504–526. doi:10.1016/j.jconrel.2016.06.016.

[79] J. Wong, R. Gogoi, A. Banerjee, S. Mitragotri, J. Qi, Role of nanoparticle size, shape and

surface chemistry in oral drug delivery, J. Control. Release. 238 (2016) 176–185. doi:10.1016/j.jconrel.2016.07.051.

[80] A.E. Gregory, R. Titball, D. Williamson, Vaccine delivery using nanoparticles, Front. Cell. Infect. Microbiol. 3 (2013) 1–13. doi:10.3389/fcimb.2013.00013.

[81] M.-C. Chen, K. Sonaje, K.-J. Chen, H.-W. Sung, A review of the prospects for polymeric nanoparticle platforms in oral insulin delivery, Biomaterials. 32 (2011) 9826–9838. doi:10.1016/j.biomaterials.2011.08.087.

[82] J.M. Carreño, C. Perez-Shibayama, C. Gil-Cruz, A. Printz, R. Pastelin, A. Isibasi, D. Chariatte, Y. Tanoue, C. Lopez-Macias, B. Gander, B. Ludewig, PLGA-microencapsulation protects Salmonella typhi outer membrane proteins from acidic degradation and increases their mucosal immunogenicity, Vaccine. 34 (2016) 4263–4269. doi:10.1016/j.vaccine.2016.05.036.

[83] A.K. Jain, A.K. Goyal, N. Mishra, B. Vaidya, S. Mangal, S.P. Vyas, PEG-PLA-PEG block copolymeric nanoparticles for oral immunization against hepatitis B, Int. J. Pharm. 387 (2010) 253–262. doi:10.1016/j.ijpharm.2009.12.013.

[84] A. Boisen, B. Gibson, C. von Halling Laier, S. Hook, L.H. Nielsen, T. Rades, J.A.S. Moreno, Microcontainers for protection of oral vaccines, in vitro and in vivo evaluation, J. Control. Release. 294 (2018) 91–101. doi:10.1016/j.jconrel.2018.11.030.

[85] M. Thanou, J.. Verhoef, H.. Junginger, Oral drug absorption enhancement by chitosan and its derivatives, Adv. Drug Deliv. Rev. 52 (2001) 117–126. doi:10.1016/S0169-409X(01)00231-9.

[86] S. Jain, R.K. Sharma, S.P. Vyas, Chitosan nanoparticles encapsulated vesicular systems for oral immunization: preparation, in-vitro and in-vivo characterization, J. Pharm. Pharmacol. 58 (2006) 303–310. doi:10.1211/jpp.58.3.0003.

[87] S. Biswas, M. Chattopadhyay, K.K. Sen, M.K. Saha, Development and characterization of alginate coated low molecular weight chitosan nanoparticles as new carriers for oral vaccine delivery in mice, Carbohydr. Polym. 121 (2015) 403–410. doi:10.1016/j.carbpol.2014.12.044.

[88] B. Xu, W. Zhang, Y. Chen, Y. Xu, B. Wang, L. Zong, Eudragit® L100-coated mannosylated chitosan nanoparticles for oral protein vaccine delivery, Int. J. Biol. Macromol. 113 (2018) 534–542. doi:10.1016/j.ijbiomac.2018.02.016.

[89] A. Puri, K. Loomis, B. Smith, J.-H. Lee, A. Yavlovich, E. Heldman, R. Blumenthal, Lipid-based nanoparticles as pharmaceutical drug carriers: from concepts to clinic., Crit. Rev. Ther. Drug Carrier Syst. 26 (2009) 523–80. doi:10.1615/CritRevTherDrugCarrierSyst.v26.i6.10.

[90] P. Severino, T. Andreani, A.S. Macedo, J.F. Fangueiro, M.H.A. Santana, A.M. Silva, E.B. Souto, Current State-of-Art and New Trends on Lipid Nanoparticles (SLN and NLC) for Oral Drug Delivery, J. Drug Deliv. 2012 (2012) 1–10. doi:10.1155/2012/750891.

[91] R.L. Ball, P. Bajaj, K.A. Whitehead, Oral delivery of siRNA lipid nanoparticles: Fate in the GI tract, Sci. Rep. 8 (2018) 1–12. doi:10.1038/s41598-018-20632-6.

[92] K. Iwanaga, S. Ono, K. Narioka, K. Morimoto, M. Kakemi, S. Yamashita, M. Nango, N. Oku, Oral delivery of insulin by using surface coating liposomes. Improvement of stability of insulin in GI tract, Int. J. Pharm. 157 (1997) 73–80. doi:10.1016/S0378-5173(97)00237-8.

[93] A. Shukla, V. Mishra, P. Kesharwani, Bilosomes in the context of oral immunization:

development, challenges and opportunities, Drug Discov. Today. 21 (2016) 888–899. doi:10.1016/j.drudis.2016.03.013.
[94] A. Shukla, K. Khatri, P.N. Gupta, A.K. Goyal, A. Mehta, S.P. Vyas, Oral immunization against hepatitis B using bile salt stabilized vesicles (bilosomes)., J. Pharm. Pharm. Sci. 11 (2008) 59–66. http://www.ncbi.nlm.nih.gov/pubmed/18445364 (accessed March 26, 2019).
[95] M. Conacher, J. Alexander, J.M. Brewer, Oral immunisation with peptide and protein antigens by formulation in lipid vesicles incorporating bile salts (bilosomes), Vaccine. 19 (2001) 2965–2974. doi:10.1016/S0264-410X(00)00537-5.
[96] V.K. Shreedhar, B.L. Kelsall, M.R. Neutra, Cholera toxin induces migration of dendritic cells from the subepithelial dome region to T- and B-cell areas of Peyer's patches, Infect. Immun. 71 (2003) 504–509. doi:10.1128/IAI.71.1.504-509.2003.
[97] A. Awaad, M. Nakamura, K. Ishimura, Imaging of size-dependent uptake and identification of novel pathways in mouse Peyer's patches using fluorescent organosilica particles, Nanomedicine Nanotechnology, Biol. Med. 8 (2012) 627–636. doi:10.1016/j.nano.2011.08.009.
[98] M. Nakamura, Awaad, Ishimura, Histochemical and biochemical analysis of the size-dependent nanoimmunoresponse in mouse Peyer's patches using fluorescent organosilica particles, Int. J. Nanomedicine. (2012) 1423. doi:10.2147/IJN.S28675.
[99] S.E.A. Gratton, P.A. Ropp, P.D. Pohlhaus, J.C. Luft, V.J. Madden, M.E. Napier, J.M. DeSimone, The effect of particle design on cellular internalization pathways, Proc. Natl. Acad. Sci. 105 (2008) 11613–11618. doi:10.1073/pnas.0801763105.
[100] J.S. Blum, P.A. Wearsch, P. Cresswell, Pathways of Antigen Processing, Annu. Rev. Immunol. 31 (2013) 443–473. doi:10.1146/annurev-immunol-032712-095910.
[101] T. Uchida, S. Goto, Oral delivery of poly(lactide-co-glycolide) microspheres containing ovalbumin as vaccine formulation: particle size study., Biol. Pharm. Bull. 17 (1994) 1272–6. doi:10.1248/bpb.17.1272.
[102] D. Li, J. Zhuang, H. He, S. Jiang, A. Banerjee, Y. Lu, W. Wu, S. Mitragotri, L. Gan, J. Qi, Influence of Particle Geometry on Gastrointestinal Transit and Absorption following Oral Administration, ACS Appl. Mater. Interfaces. 9 (2017) 42492–42502. doi:10.1021/acsami.7b11821.
[103] K. Maisel, L. Ensign, M. Reddy, R. Cone, J. Hanes, Effect of surface chemistry on nanoparticle interaction with gastrointestinal mucus and distribution in the gastrointestinal tract following oral and rectal administration in the mouse, J. Control. Release. 197 (2015) 48–57. doi:10.1016/j.jconrel.2014.10.026.
[104] R. Schwarz, A. Kaspar, J. Seelig, B. Künnecke, Gastrointestinal transit times in mice and humans measured with 27Al and 19F nuclear magnetic resonance, Magn. Reson. Med. (2002). doi:10.1002/mrm.10207.
[105] Q. Peng, J. Liu, T. Zhang, T.X. Zhang, C.L. Zhang, H. Mu, Digestive Enzyme Corona Formed in the Gastrointestinal Tract and Its Impact on Epithelial Cell Uptake of Nanoparticles, Biomacromolecules. 20 (2019) 1789–1797. doi:10.1021/acs.biomac.9b00175.
[106] S. Longet, M.L.E. Lundahl, E.C. Lavelle, Targeted Strategies for Mucosal Vaccination, Bioconjug. Chem. 29 (2018) 613–623. doi:10.1021/acs.bioconjchem.7b00738.
[107] B. Devriendt, B.G. De Geest, B.M. Goddeeris, E. Cox, Crossing the barrier: Targeting epithelial receptors for enhanced oral vaccine delivery, J. Control. Release. 160 (2012)

431–439. doi:10.1016/j.jconrel.2012.02.006.
[108] S.-H. Kim, Y.-S. Jang, Antigen targeting to M cells for enhancing the efficacy of mucosal vaccines, Exp. Mol. Med. 46 (2014) e85–e85. doi:10.1038/emm.2013.165.
[109] J. Firdous, M.A. Islam, A. Hasan, A.Z.M. Badruddoza, S. Guillemette, M. Azad, E. Reesor, M. Lim, C.S. Cho, W. Cao, M cell targeting engineered biomaterials for effective vaccination, Biomaterials. 192 (2018) 75–94. doi:10.1016/j.biomaterials.2018.10.041.
[110] H. Shima, T. Watanabe, S. Fukuda, S.I. Fukuoka, O. Ohara, H. Ohno, A novel mucosal vaccine targeting Peyer's patch M cells induces protective antigen-specific IgA responses, Int. Immunol. 26 (2014) 619–625. doi:10.1093/intimm/dxu061.
[111] N. Hussain, P.U. Jani, A.T. Florence, Enhanced oral uptake of tomato Lectin-Conjugated nanoparticles in the rat, Pharm. Res. 14 (1997) 613–618. doi:10.1023/A:1012153011884.
[112] P.N. Gupta, K. Khatri, A.K. Goyal, N. Mishra, S.P. Vyas, M-cell targeted biodegradable PLGA nanoparticles for oral immunization against hepatitis B, J. Drug Target. 15 (2007) 701–713. doi:10.1080/10611860701637982.
[113] Y. Jin, Y. Song, X. Zhu, D. Zhou, C. Chen, Z. Zhang, Y. Huang, Goblet cell-targeting nanoparticles for oral insulin delivery and the influence of mucus on insulin transport, Biomaterials. 33 (2012) 1573–1582. doi:10.1016/j.biomaterials.2011.10.075.
[114] S.T. Reddy, M.A. Swartz, J.A. Hubbell, Targeting dendritic cells with biomaterials: developing the next generation of vaccines, Trends Immunol. 27 (2006) 573–579. doi:10.1016/j.it.2006.10.005.
[115] A. Iwasaki, R. Medzhitov, Control of adaptive immunity by the innate immune system, Nat. Immunol. 16 (2015) 343–353. doi:10.1038/ni.3123.
[116] S.-Y. Chang, H.-J. Ko, M.-N. Kweon, Mucosal dendritic cells shape mucosal immunity., Exp. Mol. Med. 46 (2014) e84. doi:10.1038/emm.2014.16.
[117] M.J. Nielsen, M.R. Rasmussen, C.B.F. Andersen, E. Nexø, S.K. Moestrup, Vitamin B12 transport from food to the body's cells—a sophisticated, multistep pathway, Nat. Rev. Gastroenterol. Hepatol. 9 (2012) 345–354. doi:10.1038/nrgastro.2012.76.
[118] A.K. Verma, S. Sharma, P. Gupta, D. Singodia, S. Kansal, V. Sharma, P.R. Mishra, Vitamin B 12 grafted layer-by-layer liposomes bearing HBsAg facilitate oral immunization: Effect of modulated biomechanical properties, Mol. Pharm. 13 (2016) 2531–2542. doi:10.1021/acs.molpharmaceut.6b00274.
[119] K.B. Chalasani, G.J. Russell-Jones, S.K. Yandrapu, P. V. Diwan, S.K. Jain, A novel vitamin B12-nanosphere conjugate carrier system for peroral delivery of insulin, J. Control. Release. 117 (2007) 421–429. doi:10.1016/j.jconrel.2006.12.003.
[120] R. Fowler, D. Vllasaliu, F.F. Trillo, M. Garnett, C. Alexander, H. Horsley, B. Smith, I. Whitcombe, M. Eaton, S. Stolnik, Nanoparticle transport in epithelial cells: Pathway switching through bioconjugation, Small. 9 (2013) 3282–3294. doi:10.1002/smll.201202623.
[121] Y. Zheng, J. Wu, W. Shan, L. Wu, R. Zhou, M. Liu, Y. Cui, M. Zhou, Z. Zhang, Y. Huang, Multifunctional Nanoparticles Enable Efficient Oral Delivery of Biomacromolecules via Improving Payload Stability and Regulating the Transcytosis Pathway, ACS Appl. Mater. Interfaces. 10 (2018) 34039–34049. doi:10.1021/acsami.8b13707.
[122] K.S. Kim, K. Suzuki, H. Cho, Y.S. Youn, Y.H. Bae, Oral Nanoparticles Exhibit Specific High-Efficiency Intestinal Uptake and Lymphatic Transport, ACS Nano. 12 (2018) 8893–8900. doi:10.1021/acsnano.8b04315.

[123] A. Limmer, J. Ohl, C. Kurts, H.G. Ljunggren, Y. Reiss, M. Groettrup, F. Momburg, B. Arnold, P.A. Knolle, Efficient presentation of exogenous antigen by liver endothelial cells to CD8+ T cells results in antigen-specific T-cell tolerance, Nat. Med. 6 (2000) 1348–1354. doi:10.1038/82161.

[124] A.W. Thomson, P.A. Knolle, Antigen-presenting cell function in the tolerogenic liver environment, Nat. Rev. Immunol. 10 (2010) 753–766. doi:10.1038/nri2858.

[125] R. Yang, Q. Liu, J.L. Grosfeld, M.D. Pescovitz, Intestinal venous drainage through the liver is a prerequisite for oral tolerance induction, J. Pediatr. Surg. 29 (1994) 1145–1148. doi:10.1016/0022-3468(94)90297-6.

[126] N. Rochereau, V. Pavot, B. Verrier, A. Ensinas, C. Genin, B. Corthésy, S. Paul, Secretory IgA as a vaccine carrier for delivery of HIV antigen to M cells., Eur. J. Immunol. 45 (2015) 773–9. doi:10.1002/eji.201444816.

[127] E.M. Pridgen, F. Alexis, T.T. Kuo, E. Levy-Nissenbaum, R. Karnik, R.S. Blumberg, R. Langer, O.C. Farokhzad, Transepithelial Transport of Fc -Targeted Nanoparticles by the Neonatal Fc Receptor for Oral Delivery, Sci Transl Med. 5 (2013) 213–167. doi:10.1126/scitranslmed.3007049.

[128] S. Bournazos, D.J. DiLillo, J. V. Ravetch, The role of Fc–FcγR interactions in IgG-mediated microbial neutralization, J. Exp. Med. 212 (2015) 1361–1369. doi:10.1084/jem.20151267.

[129] D.C. Roopenian, X. Zhu, S. Palaniyandi, X. Liu, Y. Bai, C.D. Pauza, Y. Wang, R. Zeng, L. Lu, A Neonatal Fc Receptor-Targeted Mucosal Vaccine Strategy Effectively Induces HIV-1 Antigen-Specific Immunity to Genital Infection, J. Virol. 85 (2011) 10542–10553. doi:10.1128/jvi.05441-11.

[130] L. Ye, R. Zeng, Y. Bai, D.C. Roopenian, X. Zhu, Efficient mucosal vaccination mediated by the neonatal Fc receptor, Nat. Biotechnol. 29 (2011) 158–165. doi:10.1038/nbt.1742.

[131] J. Qi, J. Zhuang, Y. Lv, Y. Lu, W. Wu, Exploiting or overcoming the dome trap for enhanced oral immunization and drug delivery, J. Control. Release. 275 (2018) 92–106. doi:10.1016/j.jconrel.2018.02.021.

[132] U.R. Dahiya, M. Ganguli, Exocytosis - a putative road-block in nanoparticle and nanocomplex mediated gene delivery, J. Control. Release. 303 (2019) 67–76. doi:10.1016/j.jconrel.2019.04.012.

[133] D. Ran, M. Beltrán-Gastélum, E. Karshalev, P. Angsantikul, R.H. Fang, J. Zhou, X. Wei, L. Zhang, J. Wang, B. Esteban-Fernández de Ávila, Biomimetic Micromotor Enables Active Delivery of Antigens for Oral Vaccination, Nano Lett. 19 (2019) 56. doi:10.1021/acs.nanolett.8b05051.

[134] A. Abramson, E. Caffarel-Salvador, M. Khang, D. Dellal, D. Silverstein, Y. Gao, M.R. Frederiksen, A. Vegge, F. Hubálek, J.J. Water, A. V. Friderichsen, J. Fels, R.K. Kirk, C. Cleveland, J. Collins, S. Tamang, A. Hayward, T. Landh, S.T. Buckley, N. Roxhed, U. Rahbek, R. Langer, G. Traverso, An ingestible self-orienting system for oral delivery of macromolecules, Science (80-.). 363 (2019) 611–615. doi:10.1126/science.aau2277.

[135] G. Traverso, C.M. Schoellhammer, A. Schroeder, R. Maa, G.Y. Lauwers, B.E. Polat, D.G. Anderson, D. Blankschtein, R. Langer, Microneedles for drug delivery via the gastrointestinal tract, J. Pharm. Sci. 104 (2015) 362–367. doi:10.1002/jps.24182.

[136] C.P. Gayer, M.D. Basson, The effects of mechanical forces on intestinal physiology and pathology, Cell. Signal. 21 (2009) 1237–1244. doi:10.1016/j.cellsig.2009.02.011.

[137] D. Esterhazy, M.C. Canesso, P.A. Muller, A. Lockhart, L. Mesin, A.M. Faria, D. Mucida, Compartmentalized lymph node drainage dictates intestinal adaptive immune responses, Nature. (2018) 299628. doi:10.1101/299628.
[138] D.J. Irvine, M.A. Swartz, G.L. Szeto, Engineering synthetic vaccines using cues from natural immunity, Nat. Mater. 12 (2013) 978–990. doi:10.1038/nmat3775.
[139] T.T. Kararli, Comparison of the gastrointestinal anatomy, physiology, and biochemistry of humans and commonly used laboratory animals, Biopharm. Drug Dispos. 16 (1995) 351–380. doi:10.1002/bdd.2510160502.
[140] A. Ermund, A. Schütte, M.E. V. Johansson, J.K. Gustafsson, G.C. Hansson, Studies of mucus in mouse stomach, small intestine, and colon. I. Gastrointestinal mucus layers have different properties depending on location as well as over the Peyer's patches, Am. J. Physiol. Liver Physiol. (2013). doi:10.1152/ajpgi.00046.2013.
[141] C. Jung, J.-P. Hugot, F. Barreau, Peyer's Patches: The Immune Sensors of the Intestine, Int. J. Inflam. 2010 (2010) 1–12. doi:10.4061/2010/823710.
[142] W.W. Agace, K.D. McCoy, Regionalized Development and Maintenance of the Intestinal Adaptive Immune Landscape, Immunity. 46 (2017) 532–548. doi:10.1016/j.immuni.2017.04.004.
[143] T.L. Denning, B.A. Norris, O. Medina-Contreras, S. Manicassamy, D. Geem, R. Madan, C.L. Karp, B. Pulendran, Functional Specializations of Intestinal Dendritic Cell and Macrophage Subsets That Control Th17 and Regulatory T Cell Responses Are Dependent on the T Cell/APC Ratio, Source of Mouse Strain, and Regional Localization, J. Immunol. 187 (2011) 733–747. doi:10.4049/jimmunol.1002701.
[144] A.E. Price, K. Shamardani, K.A. Lugo, J. Deguine, A.W. Roberts, B.L. Lee, G.M. Barton, A Map of Toll-like Receptor Expression in the Intestinal Epithelium Reveals Distinct Spatial, Cell Type-Specific, and Temporal Patterns, Immunity. 49 (2018) 560-575.e6. doi:10.1016/j.immuni.2018.07.016.
[145] L. Kim, C.J. Martinez, K.A. Hodgson, G.R. Trager, J.R. Brandl, E.P. Sandefer, W.J. Doll, D. Liebowitz, S.N. Tucker, Systemic and mucosal immune responses following oral adenoviral delivery of influenza vaccine to the human intestine by radio controlled capsule, Sci. Rep. 6 (2016) 37295. doi:10.1038/srep37295.
[146] N.L. Trevaskis, L.M. Kaminskas, C.J.H. Porter, From sewer to saviour — targeting the lymphatic system to promote drug exposure and activity, Nat. Rev. Drug Discov. 14 (2015) 781–803. doi:10.1038/nrd4608.
[147] A. Schudel, D.M. Francis, S.N. Thomas, Material design for lymph node drug delivery, Nat. Rev. Mater. (2019). doi:10.1038/s41578-019-0110-7.
[148] A.T. Florence, Nanoparticle uptake by the oral route: Fulfilling its potential?, Drug Discov. Today Technol. 2 (2005) 75–81. doi:10.1016/j.ddtec.2005.05.019.
[149] P.L. Leopold, Endosomal Escape Pathways for Delivery of Biologics, in: Lysosomes Biol. Dis. Ther., John Wiley & Sons, Inc., Hoboken, NJ, USA, 2016: pp. 383–407. doi:10.1002/9781118978320.ch16.
[150] S. Foster, C.L. Duvall, E.F. Crownover, A.S. Hoffman, P.S. Stayton, Intracellular delivery of a protein antigen with an endosomal-releasing polymer enhances CD8 T-cell production and prophylactic vaccine efficacy, Bioconjug. Chem. 21 (2010) 2205–2212. doi:10.1021/bc100204m.
[151] R.A. Jones, C.Y. Cheung, F.E. Black, J.K. Zia, P.S. Stayton, A.S. Hoffman, M.R.

Wilson, Poly(2-alkylacrylic acid) polymers deliver molecules to the cytosol by pH-sensitive disruption of endosomal vesicles., Biochem. J. 372 (2003) 65–75. doi:10.1042/BJ20021945.

[152] Y. Xu, Y. Zheng, L. Wu, X. Zhu, Z. Zhang, Y. Huang, Novel Solid Lipid Nanoparticle with Endosomal Escape Function for Oral Delivery of Insulin, ACS Appl. Mater. Interfaces. 10 (2018) 9315–9324. doi:10.1021/acsami.8b00507.

[153] S. Ashraf, W. Kong, S. Wang, J. Yang, R. Curtiss, Protective cellular responses elicited by vaccination with influenza nucleoprotein delivered by a live recombinant attenuated Salmonella vaccine, Vaccine. 29 (2011) 3990–4002. doi:10.1016/j.vaccine.2011.03.066.

[154] J.-W. Yoo, D.J. Irvine, D.E. Discher, S. Mitragotri, Bio-inspired, bioengineered and biomimetic drug delivery carriers, Nat. Rev. Drug Discov. 10 (2011) 521–535. doi:10.1038/nrd3499.

[155] J.A. Rosenthal, L. Chen, J.L. Baker, D. Putnam, M.P. DeLisa, Pathogen-like particles: biomimetic vaccine carriers engineered at the nanoscale, Curr. Opin. Biotechnol. 28 (2014) 51–58. doi:10.1016/j.copbio.2013.11.005.

[156] M.L. Bookstaver, S.J. Tsai, J.S. Bromberg, C.M. Jewell, Improving Vaccine and Immunotherapy Design Using Biomaterials, Trends Immunol. 39 (2018) 135–150. doi:10.1016/j.it.2017.10.002.

[157] D.T. O'Hagan, N.M. Valiante, Recent advances in the discovery and delivery of vaccine adjuvants, Nat. Rev. Drug Discov. 2 (2003) 727–735. doi:10.1038/nrd1176.

[158] M.J. Bevan, Understand memory, design better vaccines, Nat. Immunol. 12 (2011) 463–465. doi:10.1038/ni.2041.

[159] G. Napolitani, A. Rinaldi, F. Bertoni, F. Sallusto, A. Lanzavecchia, Selected Toll-like receptor agonist combinations synergistically trigger a T helper type 1-polarizing program in dendritic cells., Nat. Immunol. 6 (2005) 769–76. doi:10.1038/ni1223.

[160] J. Garaude, A. Kent, N. van Rooijen, J.M. Blander, Simultaneous Targeting of Toll- and Nod-Like Receptors Induces Effective Tumor-Specific Immune Responses, Sci. Transl. Med. 4 (2012) 120ra16-120ra16. doi:10.1126/scitranslmed.3002868.

[161] T.J. Moyer, A.C. Zmolek, D.J. Irvine, Beyond antigens and adjuvants: Formulating future vaccines, J. Clin. Invest. 126 (2016) 799–808. doi:10.1172/JCI81083.

[162] W. Bu, M.G. Joyce, H. Nguyen, D. V Banh, F. Aguilar, Z. Tariq, M.L. Yap, Y. Tsujimura, R.A. Gillespie, Y. Tsybovsky, S.F. Andrews, S.R. Narpala, A.B. McDermott, M.G. Rossmann, Y. Yasutomi, G.J. Nabel, M. Kanekiyo, J.I. Cohen, Immunization with Components of the Viral Fusion Apparatus Elicits Antibodies That Neutralize Epstein-Barr Virus in B Cells and Epithelial Cells, Immunity. 50 (2019) 1–12. doi:10.1016/j.immuni.2019.03.010.

[163] E. Schlosser, M. Mueller, S. Fischer, S. Basta, D.H. Busch, B. Gander, M. Groettrup, TLR ligands and antigen need to be coencapsulated into the same biodegradable microsphere for the generation of potent cytotoxic T lymphocyte responses, Vaccine. 26 (2008) 1626–1637. doi:10.1016/j.vaccine.2008.01.030.

[164] C.H. Kapadia, S. Tian, J.L. Perry, J.C. Luft, J.M. DeSimone, Role of Linker Length and Antigen Density in Nanoparticle Peptide Vaccine, ACS Omega. 4 (2019) 5547–5555. doi:10.1021/acsomega.8b03391.

[165] J.A. Leleux, P. Pradhan, K. Roy, Biophysical Attributes of CpG Presentation Control TLR9 Signaling to Differentially Polarize Systemic Immune Responses, Cell Rep. 18

(2017) 700–710. doi:10.1016/j.celrep.2016.12.073.
[166] R. Noad, P. Roy, Virus-like particles as immunogens., Trends Microbiol. 11 (2003) 438–44. doi:10.1016/S0966-842X(03)00208-7.
[167] L.H.L. Lua, N.K. Connors, F. Sainsbury, Y.P. Chuan, N. Wibowo, A.P.J. Middelberg, Bioengineering virus-like particles as vaccines, Biotechnol. Bioeng. 111 (2014) 425–440. doi:10.1002/bit.25159.
[168] S. Takamura, M. Niikura, T.C. Li, N. Takeda, S. Kusagawa, Y. Takebe, T. Miyamura, Y. Yasutomi, DNA vaccine-encapsulated virus-like particles derived from an orally transmissible virus stimulate mucosal and systemic immune responses by oral administration, Gene Ther. 11 (2004) 628–635. doi:10.1038/sj.gt.3302193.
[169] F. Sarti, G. Perera, F. Hintzen, K. Kotti, V. Karageorgiou, O. Kammona, C. Kiparissides, A. Bernkop-Schnürch, In vivo evidence of oral vaccination with PLGA nanoparticles containing the immunostimulant monophosphoryl lipid A, Biomaterials. 32 (2011) 4052–4057. doi:10.1016/j.biomaterials.2011.02.011.
[170] M.T. Abreu, Toll-like receptor signalling in the intestinal epithelium: how bacterial recognition shapes intestinal function, Nat Rev Immunol. 10 (2010) 131–144. doi:10.1038/nri2707.
[171] M.J. Robinson, D. Sancho, E.C. Slack, S. LeibundGut-Landmann, C.R. e Sousa, Myeloid C-type lectins in innate immunity, Nat. Immunol. 7 (2006) 1258–1265. doi:10.1038/ni1417.
[172] H.H. Salman, J.M. Irache, C. Gamazo, Immunoadjuvant capacity of flagellin and mannosamine-coated poly(anhydride) nanoparticles in oral vaccination, Vaccine. 27 (2009) 4784–4790. doi:10.1016/j.vaccine.2009.05.091.
[173] A.S. Perelson, Modelling viral and immune system dynamics, Nat. Rev. Immunol. 2 (2002) 28–36. doi:10.1038/nri700.
[174] T. Storni, G. Senti, P. Johansen, V. Manolova, R.F. Speck, T. Gerlach, B. Müllhaupt, Z. Qiu, L. Rettig, A. Bot, K.A. Smith, T.M. Kündig, K.S. Lang, A. Der-Sarkissian, Antigen kinetics determines immune reactivity, Proc. Natl. Acad. Sci. 105 (2008) 5189–5194. doi:10.1073/pnas.0706296105.
[175] S. Kumari, J. Crampton, M.B. Melo, D.G. Anderson, D.J. Irvine, J.M. Pelet, J.K. Hu, M. Kang, S. Crotty, A.K. Chakraborty, R. Langer, R.W. Sanders, V.M. Ruda, A.D. Baldeon, H.H. Tam, J.P. Moore, M.H. Foley, Sustained antigen availability during germinal center initiation enhances antibody responses to vaccination, Proc. Natl. Acad. Sci. 113 (2016) E6639–E6648. doi:10.1073/pnas.1606050113.
[176] P. Bergqvist, A. Stensson, L. Hazanov, A. Holmberg, J. Mattsson, R. Mehr, M. Bemark, N.Y. Lycke, Re-utilization of germinal centers in multiple Peyer's patches results in highly synchronized, oligoclonal, and affinity-matured gut IgA responses, Mucosal Immunol. 6 (2013) 122–135. doi:10.1038/mi.2012.56.
[177] M.G. Potroz, R.C. Mundargi, J.J. Gillissen, E.L. Tan, S. Meker, J.H. Park, H. Jung, S. Park, D. Cho, S.I. Bang, N.J. Cho, Plant-Based Hollow Microcapsules for Oral Delivery Applications: Toward Optimized Loading and Controlled Release, Adv. Funct. Mater. 27 (2017) 1–12. doi:10.1002/adfm.201700270.
[178] C.B. Fox, A. Ma, H.D. Chirra, J.M. Wade, L. Shao, N. Ciaccio, T.A. Desai, Planar Microdevices for Enhanced In Vivo Retention and Oral Bioavailability of Poorly Permeable Drugs, Adv. Healthc. Mater. 3 (2014) 1648–1654.

doi:10.1002/adhm.201300676.
[179] C.B. Fox, Y. Cao, C.L. Nemeth, H.D. Chirra, R.W. Chevalier, A.M. Xu, N.A. Melosh, T.A. Desai, Fabrication of Sealed Nanostraw Microdevices for Oral Drug Delivery, ACS Nano. 10 (2016) 5873–5881. doi:10.1021/acsnano.6b00809.
[180] H. Mazdiyasni, T. Bensel, B. Nikolic, L. Kogan, L. Wood, T.M. Grant, S. Zhang, P.A. Eckhoff, H.C. Slater, R. Langer, G. Traverso, J. Daily, E.A. Wenger, H.M. Hurowitz, R. Barman, L. Booth, D. Minahan, S. Mo, C. Cleveland, Y.-A.L. Lee, T. Tai, M. Jafari, A.M. Bellinger, Oral, ultra–long-lasting drug delivery: Application toward malaria elimination goals, Sci. Transl. Med. 8 (2016) 365ra157-365ra157. doi:10.1126/scitranslmed.aag2374.
[181] A.M.I. Mowat, To respond or not to respond - A personal perspective of intestinal tolerance, Nat. Rev. Immunol. 18 (2018) 405–415. doi:10.1038/s41577-018-0002-x.
[182] D.R. Frederick, J.A. Goggins, L.M. Sabbagh, L.C. Freytag, J.D. Clements, J.B. McLachlan, Adjuvant selection regulates gut migration and phenotypic diversity of antigen-specific CD4 + T cells following parenteral immunization, Mucosal Immunol. 11 (2018) 549–561. doi:10.1038/mi.2017.70.
[183] A. Vishwakarma, N.S. Bhise, M.B. Evangelista, J. Rouwkema, M.R. Dokmeci, A.M. Ghaemmaghami, N.E. Vrana, A. Khademhosseini, Engineering Immunomodulatory Biomaterials To Tune the Inflammatory Response, Trends Biotechnol. 34 (2016) 470–482. doi:10.1016/j.tibtech.2016.03.009.
[184] E.J. Ryan, L.M. Daly, K.H.G. Mills, Immunomodulators and delivery systems for vaccination by mucosal routes, Trends Biotechnol. 19 (2001) 293–304. doi:10.1016/S0167-7799(01)01670-5.
[185] D.F. Moyano, M. Goldsmith, D.J. Solfiell, D. Landesman-Milo, O.R. Miranda, D. Peer, V.M. Rotello, Nanoparticle hydrophobicity dictates immune response, J. Am. Chem. Soc. 134 (2012) 3965–3967. doi:10.1021/ja2108905.
[186] M.A. Shahbazi, T.D. Fernández, E.M. Mäkilä, X. Le Guével, C. Mayorga, M.H. Kaasalainen, J.J. Salonen, J.T. Hirvonen, H.A. Santos, Surface chemistry dependent immunostimulative potential of porous silicon nanoplatforms, Biomaterials. 35 (2014) 9224–9235. doi:10.1016/j.biomaterials.2014.07.050.
[187] S.T. Reddy, A.J. Van Der Vlies, E. Simeoni, V. Angeli, G.J. Randolph, C.P. O'Neil, L.K. Lee, M.A. Swartz, J.A. Hubbell, Exploiting lymphatic transport and complement activation in nanoparticle vaccines, Nat. Biotechnol. 25 (2007) 1159–1164. doi:10.1038/nbt1332.
[188] S.N. Thomas, A.J. van der Vlies, C.P. O'Neil, S.T. Reddy, S.S. Yu, T.D. Giorgio, M.A. Swartz, J.A. Hubbell, Engineering complement activation on polypropylene sulfide vaccine nanoparticles, Biomaterials. 32 (2011) 2194–2203. doi:10.1016/j.biomaterials.2010.11.037.
[189] I. Hamad, O. Al-Hanbali, A.C. Hunter, K.J. Rutt, T.L. Andresen, S.M. Moghimi, Distinct polymer architecture mediates switching of complement activation pathways at the nanosphere-serum interface: Implications for stealth nanoparticle engineering, ACS Nano. 4 (2010) 6629–6638. doi:10.1021/nn101990a.
[190] F. Chen, G. Wang, J.I. Griffin, B. Brenneman, N.K. Banda, V.M. Holers, D.S. Backos, L. Wu, S.M. Moghimi, D. Simberg, Complement proteins bind to nanoparticle protein corona and undergo dynamic exchange in vivo, Nat. Nanotechnol. (2017).

doi:10.1038/nnano.2016.269.
[191] H. Guo, J.B. Callaway, J.P.Y. Ting, Inflammasomes: mechanism of action, role in disease, and therapeutics, Nat. Med. 21 (2015) 677–687. doi:10.1038/nm.3893.
[192] F.A. Sharp, D. Ruane, B. Claass, E. Creagh, J. Harris, P. Malyala, M. Singh, D.T. O'Hagan, V. Pétrilli, J. Tschopp, L.A.J. O'Neill, E.C. Lavelle, Uptake of particulate vaccine adjuvants by dendritic cells activates the NALP3 inflammasome., Proc. Natl. Acad. Sci. U. S. A. 106 (2009) 870–5. doi:10.1073/pnas.0804897106.
[193] Q. Hu, F. Zhao, F. Guo, C. Wang, Z. Fu, Polymeric Nanoparticles Induce NLRP3 Inflammasome Activation and Promote Breast Cancer Metastasis, Macromol. Biosci. 17 (2017) 1–8. doi:10.1002/mabi.201700273.
[194] N.C. Sheppard, S.A. Brinckmann, K.H. Gartlan, M. Puthia, C. Svanborg, G. Krashias, S.C. Eisenbarth, R.A. Flavell, Q.J. Sattentau, F. Wegmann, Polyethyleneimine is a potent systemic adjuvant for glycoprotein antigens, Int. Immunol. 26 (2014) 531–538. doi:10.1093/intimm/dxu055.
[195] M.J. Mosquera, S. Kim, H. Zhou, T.T. Jing, M. Luna, J.D. Guss, P. Reddy, K. Lai, C.A. Leifer, I.L. Brito, C.J. Hernandez, A. Singh, Immunomodulatory nanogels overcome restricted immunity in a murine model of gut microbiome–mediated metabolic syndrome, Sci. Adv. 5 (2019) eaav9788. doi:10.1126/sciadv.aav9788.
[196] S. Kumar, A.C. Anselmo, A. Banerjee, M. Zakrewsky, S. Mitragotri, Shape and size-dependent immune response to antigen-carrying nanoparticles, J. Control. Release. 220 (2015) 141–148. doi:10.1016/j.jconrel.2015.09.069.
[197] B. Slütter, L. Plapied, V. Fievez, M. Alonso Sande, A. des Rieux, Y.J. Schneider, E. Van Riet, W. Jiskoot, V. Préat, Mechanistic study of the adjuvant effect of biodegradable nanoparticles in mucosal vaccination, J. Control. Release. 138 (2009) 113–121. doi:10.1016/j.jconrel.2009.05.011.
[198] C.A. Specht, S.M. Levitz, V.A.K. Rathinam, C.K. Lee, G.J. Healy, C.H. Taron, C.L. Bueter, Chitosan but Not Chitin Activates the Inflammasome by a Mechanism Dependent upon Phagocytosis, J. Biol. Chem. 286 (2011) 35447–35455. doi:10.1074/jbc.m111.274936.
[199] B. Slütter, S. Bal, C. Keijzer, R. Mallants, N. Hagenaars, I. Que, E. Kaijzel, W. van Eden, P. Augustijns, C. Löwik, J. Bouwstra, F. Broere, W. Jiskoot, Nasal vaccination with N-trimethyl chitosan and PLGA based nanoparticles: Nanoparticle characteristics determine quality and strength of the antibody response in mice against the encapsulated antigen, Vaccine. 28 (2010) 6282–6291. doi:10.1016/j.vaccine.2010.06.121.
[200] A. Paulucci, V. Pinchuk, J.S. Rudra, Peptide nanofiber–CaCO3 composite microparticles as adjuvant-free oral vaccine delivery vehicles, J. Mater. Chem. B. 4 (2016) 1640–1649. doi:10.1039/C5TB01623A.
[201] R. De Smet, T. Demoor, S. Verschuere, M. Dullaers, G.R. Ostroff, G. Leclercq, L. Allais, C. Pilette, M. Dierendonck, B.G. De Geest, C.A. Cuvelier, β-Glucan microparticles are good candidates for mucosal antigen delivery in oral vaccination, J. Control. Release. 172 (2013) 671–678. doi:10.1016/j.jconrel.2013.09.007.
[202] A.M. Mowat, K.J. Maloy, A.M. Donachie, Immune-stimulating complexes as adjuvants for inducing local and systemic immunity after oral immunization with protein antigens., Immunology. 80 (1993) 527–34. https://www.ncbi.nlm.nih.gov/pmc/articles/PMC1422256/pdf/immunology00091-

0019.pdf (accessed April 12, 2019).
[203] A.M. Mowat, R.E. Smith, A.M. Donachie, E. Furrie, D. Grdic, N. Lycke, Oral vaccination with immune stimulating complexes., Immunol. Lett. 65 (1999) 133–40. doi:10.1016/S0165-2478(98)00136-9.
[204] R.L. Coffman, A. Sher, R.A. Seder, Vaccine adjuvants: putting innate immunity to work., Immunity. 33 (2010) 492–503. doi:10.1016/j.immuni.2010.10.002.
[205] G. Auray, S. Lacroix-Lamandé, R. Mancassola, I. Dimier-Poisson, F. Laurent, Involvement of intestinal epithelial cells in dendritic cell recruitment during C. parvum infection, Microbes Infect. 9 (2007) 574–582. doi:10.1016/j.micinf.2007.01.026.
[206] F. Anjuère, C. Luci, M. Lebens, D. Rousseau, C. Hervouet, G. Milon, J. Holmgren, C. Ardavin, C. Czerkinsky, In vivo adjuvant-induced mobilization and maturation of gut dendritic cells after oral administration of cholera toxin., J. Immunol. 173 (2004) 5103–5111. doi:10.4049/jimmunol.173.8.5103.
[207] A.S. McWilliam, S. Napoli, A.M. Marsh, F.L. Pemper, D.J. Nelson, C.L. Pimm, P.A. Stumbles, T.N. Wells, P.G. Holt, Dendritic cells are recruited into the airway epithelium during the inflammatory response to a broad spectrum of stimuli., J. Exp. Med. 184 (1996) 2429–32. doi:10.1084/jem.184.6.2429.
[208] Y. Yin, T. Qin, X. Wang, J. Lin, Q. Yu, Q. Yang, CpG DNA assists the whole inactivated H9N2 influenza virus in crossing the intestinal epithelial barriers via transepithelial uptake of dendritic cell dendrites, Mucosal Immunol. 8 (2015) 799–814. doi:10.1038/mi.2014.110.
[209] U. Yrlid, S.W.F. Milling, J.L. Miller, S. Cartland, C.D. Jenkins, G.G. MacPherson, Regulation of Intestinal Dendritic Cell Migration and Activation by Plasmacytoid Dendritic Cells, TNF-alpha and Type 1 IFNs after Feeding a TLR7/8 Ligand, J. Immunol. 176 (2006) 5205–5212. doi:10.4049/jimmunol.176.9.5205.
[210] F. Wegmann, K.H. Gartlan, a M. Harandi, S. a Brinckmann, M. Coccia, W.R. Hillson, W.L. Kok, S. Cole, L.P. Ho, T. Lambe, M. Puthia, C. Svanborg, E.M. Scherer, G. Krashias, a Williams, J.N. Blattman, P.D. Greenberg, R. a Flavell, a E. Moghaddam, N.C. Sheppard, Q.J. Sattentau, Polyethyleneimine is a potent mucosal adjuvant for viral glycoprotein antigens, Nat Biotechnol. 30 (2012) 883–888. doi:10.1038/nbt.2344.
[211] J. Kim, D.J. Mooney, In vivo modulation of dendritic cells by engineered materials: Towards new cancer vaccines, Nano Today. 6 (2011) 466–477. doi:10.1016/j.nantod.2011.08.005.
[212] Y. Wang, D.J. Irvine, Engineering chemoattractant gradients using chemokine-releasing polysaccharide microspheres, Biomaterials. 32 (2011) 4903–4913. doi:10.1016/j.biomaterials.2011.03.027.
[213] R. Ramanathan, J. Park, S.M. Hughes, W.R. Lykins, H.R. Bennett, F. Hladik, K. a. Woodrow, Effect of Mucosal Cytokine Administration on Selective Expansion of Vaginal Dendritic Cells to Support Nanoparticle Transport, Am. J. Reprod. Immunol. 74 (2015) 333–344. doi:10.1111/aji.12409.

Chapter 3. ELECTROSPUN FIBERS FOR ORAL DELIVERY OF PROTEIN BIOTHERAPEUTICS

Adapted from: **Frizzell, H.**, Ohlsen, T. J., & Woodrow, K. A. (2017). Protein-loaded emulsion electrospun fibers optimized for bioactivity retention and pH-controlled release for peroral delivery of biologic therapeutics. I*nternational Journal of Pharmaceutics*, *533*(1), 99-110.

3.1 Abstract

Biologics are the most rapidly growing class of therapeutics, but commonly suffer from low stability. Peroral administration of these therapeutics is an attractive delivery route; however, this route introduces unique physiological challenges that increase the susceptibility of proteins to lose function. Formulation of proteins into biomaterials, such as electrospun fibers, is one strategy to overcome these barriers, but such platforms need to be optimized to ensure protein stability and maintenance of bioactivity during the formulation process. This work develops an emulsion electrospinning method to load proteins into Eudragit L100 fibers for peroral delivery. Horseradish peroxidase and alkaline phosphatase are encapsulated with high efficiency into fibers and released with pH-specificity. Recovery of protein bioactivity is enhanced through reduction of the emulsion aqueous phase and the inclusion of a hydrophilic polymer excipient. Finally, we show that formulation of proteins in lyophilized electrospun fibers extends the therapeutic shelf life compared to aqueous storage. Thus, this platform shows promise as a novel dosage form for the peroral delivery of biotherapeutics.

3.2 Introduction

While the development of biological products has increased dramatically in the last three decades, the delivery of protein therapeutics remains particularly challenging [1]. Proteins are large macromolecules that require a precise 3D structure to carry out their function. Due to this structural complexity, loss of protein activity can occur in response to a variety of factors that cause protein stress and changes in conformation such as temperature, pH, ultraviolet light, and interaction with organic solvents. In the clinical application of such biopharmaceutics, the route of administration introduces a variety of these unique challenges. Peroral administration, through swallowing of a solution or pill, is one of the most attractive routes for therapeutic delivery, as patient comfort is increased, the use of needles is eliminated, and local delivery to the gastrointestinal tract can be achieved, reducing systemic side effects [2]. However, peroral delivery of proteins is difficult due to the inherent barrier of the acidic environment of the stomach, which can result in protein degradation, leading to low bioavailability and the need for multiple doses [3,4]. Recently, a variety of nanotechnology platforms utilizing biomaterials have been developed to overcome these challenges in biologic formulation and peroral delivery to the gut [5,6]. Alternative approaches include conjugating therapeutic proteins with protective polymers or engineering proteins to modify the amino acid structure to reduce the susceptibility of the protein to protease cleavage [7,8].

Electrospinning is a technique that has been explored in the pharmaceutical nanotechnology field to develop materials as scaffolds for tissue engineering and for the delivery of small molecule therapeutics [9]. The electrospinning platform has many advantages compared to other formulations such as particulates, films, and tablets, including the versatility of polymers that can be employed to tailor release kinetics and therapeutic targeting for specific applications, high encapsulation efficiency, which is critical when loading high-cost therapeutics, high surface-area-to-volume ratio for enhanced interaction with the tissue of interest, and ease of production [9–11]. In the last

10 years, electrospun nanofibers have been investigated for the delivery of larger, less stable therapeutics such as protein biologics and have proven to be advantageous in terms of controlled delivery and enhancing protein stability [12]. While protein encapsulation into nanofibers has been primarily developed for the production of bioactive scaffolds, we expect this platform holds promise for the targeted delivery of proteins to the gut.

Proteins can be loaded into electrospun nanofibers by a method called emulsion electrospinning, which forms core-shell nanofibers from an emulsion comprised of an organic phase (containing polymer), surfactant, and aqueous phase (containing protein) [13]. In the emulsion electrospinning process, a high voltage is applied to the solution as it is pumped out of a needle and syringe until electrostatic forces overcome droplet surface tension. This results in the formation of a Taylor cone and the ejection of a polymer jet that is electrically charged [14,15]. As this charged jet moves through an electric field to be deposited onto a grounded collector as elongated fibers, the organic solvent evaporates more quickly than water and the emulsion droplets move inward and are stretched to form fibers with a continuous core surrounded by a viscous polymer shell [16,17]. This architecture is advantageous for enhancing protein stability and controlled protein release compared to blend electrospinning, which directly exposes proteins to organic solvents and exhibits burst release kinetics [12].

However, since in emulsion electrospinning proteins in the aqueous phase may still interact with organic solvents throughout the process, maintenance of protein bioactivity and stability must be optimized to prevent loss of protein structure, and thus function. In many studies that load non-enzymatic proteins into electrospun fibers, function is demonstrated but protein activity is not able to be quantified [18–22], and only a few studies have investigated the effects of emulsion electrospinning solution and processing parameters on maintaining protein bioactivity [23–25] (summarized in Table 3.1). Learning from these studies, it is clear that many parameters can significantly affect protein loading and activity and that the main challenges of high protein loading efficiency

and bioactivity preservation still remain. In particular, previous studies have elucidated that each delivery system must be optimized based on electrospinning method, processing parameters, and the polymers and proteins used to ensure appropriate formulation of active, stable proteins in nanofibers. Additionally, the stability of therapeutic proteins loaded in electrospun fibers over time has not been widely studied. This shelf life is critical to evaluate, understand, and improve for the translation of such protein delivery platforms to clinical use.

The methacrylic acid and methyl methacrylate co-polymer Eudragit L100 has been used in clinical settings as a capsule for the peroral delivery of therapeutics as it demonstrates pH-dependent solubility in neutral and basic conditions. This polymer has been applied to electrospinning and Eudragit-based nanofibers have been used for small molecule drug delivery, stent coatings, antibacterial mats, and contrast agents for imaging [26–30]. In the space of protein therapeutics, one study loaded human growth hormone into Eudragit fibers using blend electrospinning for buccal drug delivery and demonstrated successful fabrication and wound healing function, but did not investigate how protein function was affected by the process [21].

The encapsulation of more diverse proteins, such as larger protein antigens or complex therapeutic antibodies, into Eudragit fibers has not been investigated nor has the emulsion electrospinning of protein-loaded Eudragit fibers, which can address problems in loss of protein function during formulation. The development of such a system would be advantageous for the delivery of proteins to targets in the intestinal tract, either to improve patient comfort in therapeutic administration, to access the mucosal immune system, or to address intestine-specific diseases [31–33]. Thus, in this study we aimed to optimize the electrospinning of two diverse proteins into Eudragit L100 nanofibers. Specifically, we investigated the solution and processing parameters of emulsion electrospinning to achieve high protein loading into nanofibers, retention of protein bioactivity during the electrospinning process and in simulated gastric fluids, extended

formulation stability, and pH-controlled protein release for future applications in peroral delivery of biotherapeutics to the intestinal tract.

Table 3.1. Summary of protein-loaded electrospun fiber formulations and evaluation. N, not used in study; ND, not disclosed in methods. N/A, not applicable; BSA, bovine serum albumin; T3, thyroid hormone triiodo-thyronine. EGF, epidermal growth factor; MSC, mesenchymal stem cells.

Polymer	Protein	Surfactant	Loading (wt%)	Aqueous Phase %	Activity Assay	Shelf Life	Ref.
Eudragit L100	Human growth hormone	N	0.1%	N/A	Cell proliferation	N	[21]
PCL/PEG	Lysozyme-oleate complexes	N	2.5%	N/A	95%, turbidity assay	90%, 1 month	[34]
PLA/PCL	Nerve growth factor	0.4%	N/A	N/A	Cell differentiation	N	[22]
PCL/PEO	Lysozyme	0.025 – 0.4%	0.2%	1%	Osteogenic differentiation	N	[24]
PDLLA	Laccase	Y	0.1%	ND	67%, substrate activity assay	N	[35]
PCL/PEO	Lysozyme	N	1%	6.25%	95%, lysis activity assay	N	[36]
PCL	Alkaline phosphatase	N	ND	25%	50%, substrate activity at 1h	N	[37]
PLGA	BSA, T3, insulin, EGF	N	ND	10%	33-40%, bioactivity assay, MSC differentiation	N	[38]
PDLA	Lysozyme	N	1 – 5%	ND	70-90%, turbidity assay	N	[39]
PELA	Lysozyme	N	ND	0.5 – 5%	30-60%, turbidity assay	N	[40]
PCL	Trypsin	Y	ND	5%	40-60%, catalytic activity assay	60%, 2 weeks 40%, 4 weeks	[23]

3.3 Materials and Methods

3.3.1 *Materials*

Eudragit L100 was a gift from Evonik Industries (Essen, Germany). *N,N*-Dimethylformamide (DMF) (anhydrous, 99.8%), poly(vinyl alcohol) (PVA, used in studies as an excipient) (30,000-70,000 g mol^{-1}, 87-95% hydrolyzed), poly(vinyl alcohol) (PVA, used in studies for electrospinning) (89,000-124,000 g mol^{-1}, 89% hydrolyzed), Tween 20 (polysorbate 20), albumin–fluorescein isothiocyanate conjugate (FITC-BSA), alkaline phosphatase (AP) from bovine intestinal mucosa (~160 kDa, ≥10 DEA units mg^{-1} solid), sodium hydroxide (NaOH) (50% in H_2O), alkaline phosphatase yellow (pNPP) liquid substrate system, magnesium chloride ($MgCl_2$) (anhydrous, ≥98%), and pepsin from porcine gastric mucosa (≥2,500 units/mg protein) were purchased from Sigma-Aldrich (St. Louis, MO, USA). Horseradish peroxidase (HRP) (~44 kDa), Micro BCA™ Protein Assay Kit, and Karl Fischer titration reagents AQUASTAR™ CombiMethanol and Combititrant 5 were purchased from Thermo Fisher Scientific (Waltham, MA, USA). Hydrochloric acid (HCl) (36.5%-38.0%) was purchased from Avantor Performance Materials (Center Valley, PA, USA). Dulbecco's Phosphate-Buffered Saline (PBS) was purchased from Corning Inc. (Corning, NY, USA). TMB substrate set was purchased from BioLegend (San Diego, CA, USA). Tris-HCl (Tris-hydrochloride, molecular biology grade) was purchased from Promega (Madison, WI, USA). Sodium chloride (NaCl) was purchased from EMD Millipore (Gibbstown, NJ, USA). Ethanol (EtOH) (200 proof) was purchased from the University of Washington's chemistry supply store.

3.3.2 *Emulsion Electrospinning*

Eudragit L100 was dissolved at 15% (wt/vol) in a solution of 4:1 (vol:vol) EtOH:DMF. Non-ionic surfactant Tween 20 was added to the stirring Eudragit solution at 0.4% (vol/vol) in 20 mL glass scintillation vials. Aqueous protein solutions were

dropped into the stirring Eudragit and surfactant solution at either 5% or 20% (vol/vol). Theoretical protein loading was kept constant at 1 wt%. The solution was emulsified for 10 minutes by constant stirring at high speed then loaded into a 1 mL glass syringe with a 21G stainless steel blunt needle for electrospinning on a needle rig set-up utilizing a syringe pump and voltage source. We chose high speed stirring over sonication for emulsification, as sonication has been shown to have an effect on secondary protein structure [41]. The solution was electrospun onto a wax paper substrate on a grounded metal collector at a distance of 10-12 cm. A constant voltage of 12.5 kV was applied, and the flow rate was varied between formulations to determine its effect on protein bioactivity. Low and high flow rate formulations were electrospun at 25 and 40 μL min^{-1}, respectively. Electrospinning was performed at room temperature in a fume hood. Protein-loaded fibers were stored in sealed bags at room temperature unless stated otherwise.

3.3.3 *Characterization of Protein-Loaded Electrospun Fibers*

3.3.3.1 Microscopy of Protein-Loaded Electrospun Fibers

Electrospun fibers were characterized using scanning electron microscopy (SEM) using a Sirion XL30 SEM and transmission electron microscopy (TEM) using a Tecnai G2 F20 Supertwin operating at 200 kV (Molecular Analysis Facility, University of Washington). For SEM imaging, fiber samples were mounted on carbon tape and sputter coated with gold and palladium before imaging. Image settings of 5 kV, spot size of 2, and a working distance of 5 mm were used. Fiber diameters were measured using ImageJ software (NIH) by bi-sectioning each image diagonally with a line and manually measuring diameters for fibers that intersected the line. At least 30 fibers were measured per fiber formulation sample. Samples for TEM imaging were prepared by electrospinning fibers onto copper-coated TEM grids.

The location of protein within the fibers was determined by electrospinning FITC-BSA into Eudragit L100 as described above. Briefly, FITC-BSA was dissolved in PBS at

a concentration of 1 mg ml^{-1} and dropped into a spinning solution of 15 wt% Eudragit L100 in 4:1 DMF:EtOH (vol:vol) and Tween 20 (0.4 vol%). FITC-BSA was added to achieve emulsions with 5% and 20% aqueous phases. Emulsification proceeded for 10 minutes and was then loaded into a 1 mL glass syringe with a 21G stainless steel blunt needle for electrospinning on a needle rig set-up utilizing a syringe pump and voltage source. The solution was electrospun at a constant voltage of 12.5 kV and a flow rate of 25 μL min^{-1} onto a wax paper substrate on a grounded metal collector at a distance of 10-12 cm. Electrospinning was performed at room temperature in a fume hood. Protein-loaded fibers were transferred to glass slides and imaged using a Nikon Eclipse Ti microscope (Nikon, Melville, NY) equipped with an Andor (model number DR-328G-C01-SIL) fluorescence camera (Andor, Belfast, UK).

3.3.3.2 Kinetics of Protein Release in Dynamic pH Conditions

Protein release from fibers was investigated under dynamic pH conditions, mimicking oral-to-intestinal transit after ingestion, focused on the lower stomach and small intestine. Fiber samples were cut, massed, and placed in 20 mL scintillation vials. Three samples from the fiber mat were analyzed for each formulation. Phosphate buffered saline (PBS) (1x) was pH-adjusted to 2 using 1M HCl and added to the scintillation vials at 2 mg fiber/mL PBS. Vials were placed on an orbital shaker (150 rpm) at 37 °C. At each time point, aliquots were removed for analysis and the volume was replaced with PBS pH 2. After the 4-hour time point sample was taken, the volume was replaced with PBS pH 7 and 1M NaOH to increase the pH to 7. The pH change was verified for one representative sample. Volume replacement was performed with PBS pH 7 for the remainder of the time points. The Micro BCA assay was used to determine protein concentrations released over time using a standard curve with known protein concentrations and performed according to the manufacturer's instructions. Protein standards in PBS pH 2 and 7 and in solutions of blank Eudragit L100 electrospun fibers dissolved in PBS pH 7 were included to account for assay interference. Sample dilution

during the experiment was accounted for by incorporating the mass removed from each time point in data analysis calculations.

3.3.3.3 Protein Encapsulation Efficiency

Encapsulation efficiency was calculated based on the amount of protein recovered from the fiber after 24 hours of incubation in PBS pH 7 at 37 °C when the fiber was fully dissolved using equation (1).

$$Encapsulation\ efficiency\ (\%) = \frac{Recovered\ protein\ mass\ (mg)}{Theoretical\ protein\ mass\ loaded\ (mg)} \times\ 100 \qquad (1)$$

3.3.4 *Quantification of Bioactivity of Proteins Released from Emulsion Electrospun Fibers*

Bioactivity retention of encapsulated proteins was determined by kinetic colorimetric substrate assays of the proteins recovered from each fiber formulation at day 0, 1 week, and 4 weeks. Three samples from the fiber mat were analyzed for each formulation. For HRP activity quantification, fibers were massed (5 ± 1 mg) and placed in 20 mL scintillation vials. PBS (1x, pH-unadjusted) was added for a fiber concentration of 0.5 mg mL^{-1} and vials were placed on a tube rotator at room temperature for 30 minutes or until fully dissolved. Serial dilutions were performed to achieve an HRP concentration of 5 ng mL^{-1}. To a 96-well clear, flat bottom plate, 100 µL of each sample or freshly prepared 5 ng mL^{-1} HRP controls were added per well and 50 µL of TMB substrate solution (1:1 Substrate A:Substrate B, vol:vol) was added to start the assay. Change in absorbance at 652 nm was monitored every 15 seconds using a Tecan Infinite 200 PRO microplate reader (Männedorf, Switzerland) over 10 minutes. For AP activity quantification, fibers were massed (5 ± 1 mg) and placed in 20 mL scintillation vials. AP buffer (100 mM Tris-HCl, 100 mM NaCl, 5 mM $MgCl_2$, 0.05 vol% Tween 20, pH 9.5) was added for a fiber concentration of 1 mg mL^{-1} (10 µg mL^{-1} AP concentration) and vials were placed on a tube rotator at room temperature for 30 minutes or until fully dissolved.

To a 96-well clear, flat bottom plate, 100 µL of each sample or freshly prepared 10 µg mL^{-1} AP controls were added per well and 100 µL of 10x diluted pNPP substrate solution was added to start the assay. Change in absorbance at 405 nm was monitored every 15 seconds using a Tecan Infinite 200 PRO microplate reader over 10 minutes. For both proteins, the maximum increase in absorbance per minute (max slope) from the initial linear portion was determined and the retained protein bioactivity from the fibers was calculated using equation (2).

$$\%\, Bioactivity = \frac{Max\ slope_{sample}}{Max\ slope_{standard}} \times 100 \quad (2)$$

To determine the stability of proteins in the fibers over time, fibers were stored in sealed bags at room temperature for 4 weeks and assayed for activity at weeks 1 and 4. HRP (5 ng mL^{-1}) and AP (10 µg mL^{-1}) in PBS at room temperature were used as controls stored in aqueous conditions for the stability studies.

3.3.5 *Bioactivity in Simulated Gastric Fluid*

HRP was loaded into Eudragit L100 nanofibers using emulsion electrospinning with a 5% aqueous phase. Fibers were massed and incubated in simulated gastric fluid (SGF) (1 mg mL^{-1} pepsin, 300 mM NaCl, pH 1.5) at a fiber concentration of 1 mg mL^{-1} at 37 °C for 1 hour. HRP in soluble form was incubated in SGF at a concentration of 10 µg mL^{-1} under the same conditions. Following incubation, samples were diluted to an HRP concentration of 5 ng mL^{-1} in PBS and the enzyme bioactivity was determined using the bioactivity assay as described above. Controls of freshly prepared HRP and HRP released from fibers immediately after electrospinning were evaluated for bioactivity.

3.3.6 *Characterization of Lyophilized Electrospun Fibers*

3.3.6.1 Quantification of Fiber Water Content

Water content of each fiber formulation was determined by Karl Fischer titration using a V20 Volumetric KF Titrator (Mettler-Toledo, Columbus, OH, USA). Briefly, a

titration beaker was filled with solvent (CombiMethanol) and a pre-massed fiber sample (10 – 20 mg) was added to the stirring solution. A colorimetric titration was then automatically performed using titrant reagent (Combititrant 5) and the percent water content of the total sample mass was determined by the software. Three samples from the fiber mat were analyzed for each formulation. The water content of protein-loaded fibers was analyzed immediately after electrospinning, one day after electrospinning stored at room temperature, and one day after electrospinning stored under lyophilization. After lyophilization overnight, fibers were removed from vacuum and stored in the same conditions as the non-lyophilized fibers at room temperature for a total storage time of 7 days.

3.3.6.2 Quantification of Bioactivity of Proteins Released from Lyophilized Electrospun Fibers

Bioactivity of the proteins recovered from electrospun fibers with or without one-time lyophilization was determined by kinetic colorimetric assays as described above.

3.3.7 *Blend Electrospinning*

Alkaline phosphatase was added to a 7.14 wt% solution of poly(vinly alcohol) (PVA) (M.W. 89 – 124 kDa, 89% hydrolyzed) in water and electrospun into nanofibers using a small-scale electrospinning set-up as described above for emulsion electrospinning.

To determine the stability of alkaline phosphatase when stored in PVA fibers fabricated using blend electrospinning, fibers were stored in heat-sealed bags at 40 °C. Activity of AP was measured after 7 and 17 days of storage and compared to the activity of a freshly prepared solution of AP of equivalent concentration. AP activity was determined as previously described above.

3.3.8 *Antigen Functionality Assay*

A murine dendritic cell line DC2.4 was cultured in RPMI 1640 (Cellgro, Manassas, VA) supplemented with 2 mM L-glutamine (Cellgro), 10 mM HEPES (Cellgro), 10% fetal bovine serum, 100 U mL^{-1} penicillin, and 100 μg mL^{-1} streptomycin (all from Invitrogen, Carlsbad, CA). DC2.4s were seeded at 5 x 10^4 per well in a flat bottom 96-well plate overnight. The antigen ovalbumin (OVA) (InvivoGen, San Diego, CA) was emulsion electrospun into fibers with a 20% aqueous phase. After electrospinning, residual solvents were removed from the fibers through drying in a fume hood followed by lyophilization for 1 hour. Fibers were dissolved in complete medium at an OVA concentration of 100 μg mL^{-1}. OVA recovered from electrospun fibers or non-formulated, soluble OVA was added DC2.4 cells at a concentration of 100 μg mL^{-1}. Inclusion of LPS (1 μg mL^{-1}) (InvivoGen, San Diego, CA) was used as a positive control. After 24-hours, the supernatant was removed and the cells were washed three times with pre-warmed PBS. B3Z T cells, a lacZ-inducible CD8+ T cell hybridoma expressing a T cell receptor specific for $OVA_{257-264}$ [42], were added to each well at 5 x 10^4 and co-cultured for 24 hours. The plate was then centrifuged at 500 *x g* for 2 minutes and the culture medium was removed. Lysis buffer (0.15 mM chlorophenol red β-d-galactopyranoside (Roche, Basel, Switzerland), 9 mM $MgCl_2$, 0.125% Triton-X100, and 100 μM 2-mercaptoethanol (Invitrogen) in PBS) was added to each well and plates were incubated at 37 °C for 2 hours. The plates were read at 570 nm using a Tecan Infinite 200 PRO microplate reader.

3.3.9 *In Vitro Mucoadhesion Tests*

Eudragit L100 fiber mats were punched into 0.75" samples and attached to a metal mount and connected to the Instron load cell. Fibers were lowered into a 2% mucin (mucin from porcine stomach, type II, Sigma-Aldrich) solution in PBS at a contact force of 0.05 – 0.1 N and incubated for 5 minutes to allow for fiber wetting and mucin interaction. Following the incubation, the load cell was vertically displaced at a constant speed of 6

mm min^{-1} and the detachment force was measured over time using Instron Bluehill software. The work of adhesion between the fibers and the mucin solution was calculated from the area under the detachment force vs. extension curve.

To determine hydrogel swelling properties of Eudragit L100, fibers were placed in 2% mucin solutions in PBS at 37 °C and mass was determined at various time points. The ratio of wet mass to dry mass was calculated using the equation:

$$Swelling\ ratio = \frac{m_{wet}}{m_{dry}} \quad (3)$$

3.3.10 *Fiber Micronization and In Vivo Retention in Gastrointestinal Tract*

To allow for oral gavage into mice, Eudragit-L100 fibers loaded with BSA-Dylight800 were micronized into particulates < 800 nm, the diameter of an 18 G gavage needle. Fibers were added to a blender (Blendtec, Orem, UT, USA) with 200 mL water (pH 2) and blended using the following regimen: 1X ice crush, 1X ice cream for two cycles. Micronized fibers were then separated by flowing the solution through a 250 μm stainless steel sieve (VWR, Radnor, PA, USA). Fibers were then vacuum dried using a 1.2 μm nylon filter paper (Merck Millipore Ltd., Tulagreen, Ireland) and house vacuum. Micronized fibers were resuspended in PBS pH 2 and 200 μL was orally administered to 6-8-week-old, female C57BL/6 mice (Charles River, Wilmington, MA) by a 22 G gavage needle (Braintree Scientific, Braintree, MA) at a dose of 50 μg BSA per mouse. At the indicated time points, mice were sacrificed using CO_2 asphyxiation and the gastrointestinal tract was dissected. The organs were placed on black drawing paper (Artagain®400 Series, Strathmore) and imaged using a Xenogen IVIS Spectrum In Vivo Imaging System (PerkinElmer, Waltham, MA, USA) at an excitation/emission of 777/794 nm. The average radiance (p/sec/cm^2/sr) of the gastrointestinal tract was determined for each time point.

3.3.11 *Statistical Analysis*

Results were expressed as the mean ± standard deviation. When comparing outcomes between groups, statistical analysis was performed by one-way or two-way analysis of variance (ANOVA) using Tukey's or Sidak's multiple comparison post-test. Statistical analyses were performed using GraphPad Prism 6 software. Statistical significance was defined as $p < 0.05$ (*).

3.4 Results and Discussion

3.4.1 *Characterization of Protein-Loaded Eudragit L100 Emulsion Electrospun Fibers*

Two model proteins were loaded into Eudragit L100 fibers through an emulsion electrospinning method using a non-ionic surfactant. Horseradish peroxidase (HRP, ~44 kDa) and alkaline phosphatase (AP, ~160 kDa) were chosen due to their difference in molecular weight, number of subunits, and isoelectric point. In addition, both enzymes are well-characterized and have developed colorimetric activity assays [43,44]. In our studies, HRP and AP also serve as surrogates for more therapeutically relevant proteins. Emulsion electrospinning with a non-ionic surfactant was utilized to incorporate an aqueous protein solution into an organic polymer solution while reducing exposure of the proteins to the organic solvent interface (Figure 3.1A). This strategy has been shown to enhance the bioactivity of the proteins recovered from emulsion electrospun fibers [24]. The percent aqueous phase in the emulsion (5 and 20 vol%) and the electrospinning flow rate (25 and 40 μL min^{-1}) were varied in each formulation to maximize protein loading and material productivity, respectively (Table 3.2).

Table 3.2. Description and characterization of emulsion electrospun fiber formulations. [a]Data reported as the average of n=3 fiber samples ± standard deviation.

Fiber Description				Fiber Characterization	
Formulation Name	Protein Encapsulated	Protein M.W. (kDa)	Aqueous Phase (%)	[a]Fiber Diameter (nm)	[a]Encapsulation Efficiency (%)
EEHRP5	HRP	44	5	368 ± 101	97.21 ± 2.71
EEHRP20	HRP	44	20	617 ± 247	96.40 ± 1.03
EEAP5	AP	160	5	578 ± 116	94.76 ± 4.05
EEAP20	AP	160	20	1031 ± 289	96.19 ± 3.42

All formulations were successful at forming electrospun Eudragit L100 fibers as confirmed by scanning electron microscopy (Figure 3.1B-E). Fiber diameters were in the range of 300-1300 nm and were dependent on the molecular weight of protein loaded and the percent aqueous phase. An increase in the protein molecular weight and percent aqueous phase resulted in fibers with slightly larger average diameters. Flow rate did not have a significant effect on fiber diameter for either protein encapsulated. Using this method, proteins were loaded into Eudragit L100 fibers with very high encapsulation efficiencies, above 95% for all formulations (Table 3.2).

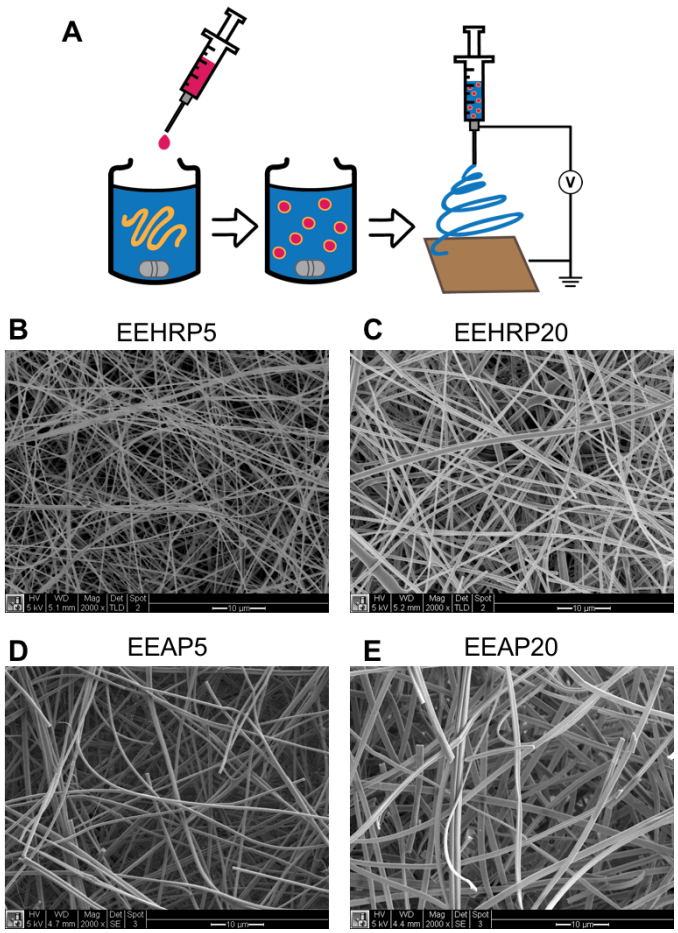

Figure 3.1. Scanning electron microscopy characterization of emulsion electrospun fiber morphology. A) Schematic of emulsion electrospinning process. B) EEHRP5: HRP loading, 5% aqueous phase. C) EEHRP20: HRP loading, 20% aqueous phase. D) EEAP5: AP loading, 5% aqueous phase. E) EEAP20: AP loading, 20% aqueous phase. All images taken at 2000X magnification.

To determine the location of the protein in the nanofibers, we utilized bovine serum albumin (BSA) as a representative non-enzymatic protein with a similar molecular weight to HRP (~66 kDa). Transmission electron microscopy (TEM) imaging of the emulsion electrospun fibers revealed sections of aqueous core surrounded by polymer shell for both the 5% (Figure 3.2A) and 20% aqueous phase (Figure 3.2B) fibers. This core-shell architecture has been observed for emulsion electrospun fibers encapsulating a variety of proteins [39,40] and small molecule drugs [28]. As such, we expect that the fiber

architecture observed with the incorporation of BSA is representative for HRP- and AP-loaded emulsion electrospun fibers. Due to the low percentage of the aqueous phase in our emulsions, it is feasible that aqueous emulsion droplets are pulled and elongated in the electric field during the electrospinning process to create discrete protein-loaded aqueous pockets. In fact, upon increasing the aqueous phase from 5% to 20%, we observed more continuous aqueous cores that may reflect the increased aqueous volume relative to the organic/polymer phase or larger aqueous droplets in the emulsion. Loading fibers with FITC-BSA confirmed the presence of protein throughout the nanofibers and showed protein partitioning within the discrete aqueous pockets in the polymeric fiber (Figure 3.2C,D), further validating the core-shell structure of the fibers where protein is located within a polymer shell rather than throughout the polymer matrix.

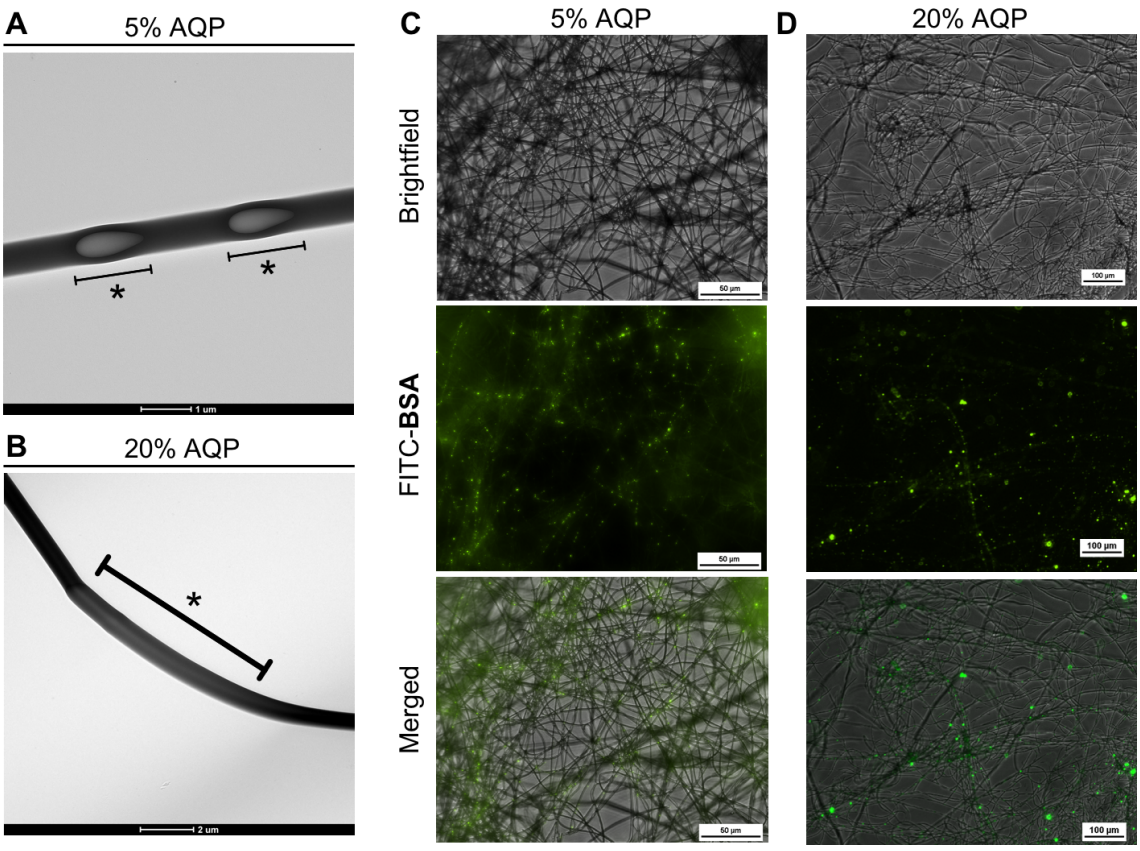

Figure 3.2. Core/shell architecture of emulsion electrospun fibers. Transmission scanning microscopy images of Eudragit L100/BSA electrospun fibers from A) 5% aqueous phase, scale bar 1 µm, and B) 20% aqueous phase, scale bar 2 µm, emulsions. An asterisk indicates the location

of an aqueous core. Fluorescence microscopy images of Eudragit L100/FITC-BSA electrospun fibers from C) a 5% aqueous phase emulsion, scale bar 50 μm, and D) a 20% aqueous phase emulsion, scale bar 10 μm.

Maximizing biologic therapeutic loading into biomaterials is important for reducing the total dosing amount, but protein loading is commonly limited by solubility. In emulsion electrospinning, high protein loading can theoretically be achieved by increasing the volume fraction of the protein aqueous phase; however, the ability of solutions to be successfully electrospun into fibers is also limited by this parameter. Thus, we investigated emulsions composed of the maximum aqueous phase percentage without compromising electrospinnability of the solution, which we found to be 20%. Using this emulsion composition, proteins could be loaded into Eudragit-L100 fibers as high as 6.25% (wt/wt), based on the polymer solution weight percent and maximum protein solubility. The electrospinning parameter flow rate has an impact on material manufacturing time, and we demonstrated successful protein loading into electrospun fibers at both flow rates tested. The high encapsulation efficiencies achieved (>95%) using this process also demonstrate the manufacturing advantage of this platform for delivery of biotherapeutics, which can be a limitation of other nanotechnology approaches such as particulate systems [45,46].

3.4.2 *pH-Controlled Protein Release of Electrospun Eudragit L100 Fibers*

Next, we tested the ability of our protein-loaded Eudragit L100 fibers to release their protein cargo with pH-dependent kinetics. Such material solubility characteristics are desirable for peroral delivery of proteins, in which fibers can protect proteins from the acidic environment of the stomach while in transit through the gastrointestinal tract. Eudragit L100 was selected because of its favorable pH-dependent dissolution profile. The carboxyl group of Eudragit L100 has an apparent pKa of ˜6, which causes it to be protonated and insoluble in acidic pH but ionized and soluble in neutral or basic conditions

[47]. After peroral administration via swallowing, the material first passes through the stomach (pH 1.5 – 3.5) followed by transit through the intestine, where the pH gradually increases to $>$ 6 [48]. Thus, Eudragit L100 fibers can selectively deliver the formulated proteins by means of fiber dissolution in neutral and basic environments. We verified this pH-controlled release of our four main formulations through an experiment mimicking the pH profile encountered and transit time of the material after oral ingestion [49], in which the residence time of the material in the oral cavity and esophagus is negligible, although this is known to vary between and within individuals [50]. Analysis of protein release from the fiber at 37 °C under mild shaking showed that $<$5% of the loaded protein was released over 4 hours in acidic conditions (PBS pH 2). In contrast, upon pH increase above 6, fibers released their cargo with burst-release kinetics resulting in ˜100% protein release within 1 hour of pH change (Figure 3.3A,B). Qualitatively, this burst-release behavior corresponded to fiber dissolution. In PBS pH 2, Eudragit L100 fiber mats did not dissolve and maintained their macroscopic structure (Figure 3.3C) and when the solution pH was increased to 7, fibers dissolved within 1 hour (Figure 3.3D). Qualitative observations indicated that time to fiber dissolution was a function of fiber mat thickness, in which thicker fibers mats required longer time to fully wet and dissolve, resulting in delayed release of the protein. Drug release rates from electrospun fibers were found to be dependent on the rate of water diffusion into the material, which can be affected by a variety of factors including fiber mat thickness, degree of hydrophobicity, and polymer crystallinity [51–54]. This correlation of sustained drug release with fiber mat thickness was observed for protein release from EEHRP fibers, in which the variability in release rates observed was due to differences in the thickness of each fiber mat sample.

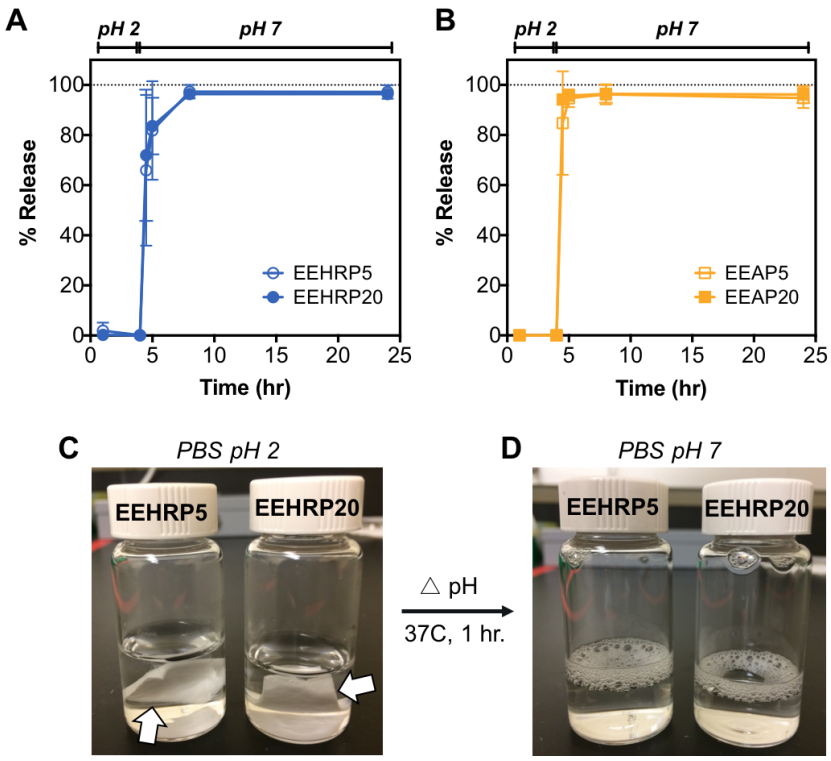

Figure 3.3. pH-controlled release of proteins from Eudragit L100 nanofibers. Kinetics of A) HRP and B) AP release from Eudragit L100 fibers in PBS pH 2 and 7 over 24 hours. Data is representative of results from n=3 fiber punches per formulation and presented as mean ± standard deviation. Qualitative observations of macroscopic fiber mat structure C) intact in PBS pH 2 and D) dissolved upon pH increase to 7.

In our experimental timeframe, we observed that protein release was dependent on fiber dissolution, rather than protein diffusion out of the fiber matrix, as we detected little to no protein released at pH 2 over 4 hours. This observation supports the core-shell structure of the fibers, in which protein is located in the fiber core surrounded by a polymer shell rather than being surface-associated, which would result in a higher rate of protein release in the absence of fiber dissolution. Yang *et al.* detected between ~3-30% surface-associated protein content for their poly(ethylene glycol)-poly(DL-lactide) (PELA)/lysozyme emulsion electrospun fibers, which they found to be dependent on polymer matrix, inclusion of excipients, and aqueous/organic volume ratio [40]. The lowest

surface-associated protein content was achieved by including a dispersion excipient in the aqueous phase and by decreasing the aqueous/organic ratio. In our system, we observed <5% surface-associated protein content at both 5% and 20% aqueous phases and without including excipients. This characteristic is favorable for controlled-release systems in which non-specific, premature protein delivery is minimized. For peroral delivery, entrapment of the therapeutic within the polymer shell can shield proteins from digestive enzymes in the stomach, such as the protease pepsin. Additionally, high mucus turnover in the intestinal tract poses a challenge to delivery systems by reducing the bioavailable dose due to clearance of the therapeutic during mucus turnover before its absorption [55]. Finally, some materials-based delivery platforms with sustained release kinetics suffer from incomplete protein release in the time frame from oral ingestion to clearance from the body, further limiting the effective dose that is released at the target site. In contrast, rapid and complete protein release from our fiber delivery system, triggered by a change in pH, can be advantageous for delivery to the intestinal tract by ensuring the full therapeutic dose is released and bioavailable.

3.4.3 *Bioactivity Retention of Proteins Electrospun in Eudragit L100 Fibers by Emulsion Electrospinning*

Retention of protein bioactivity is important when electrospinning biologics in organic solvents and is currently a major challenge for electrospinning proteins [12]. We aimed to maximize retention of protein bioactivity after being electrospun into Eudragit L100 fibers by investigating the effect of flow rate, percent aqueous phase, and incorporation of hydrophilic polymer excipients in the aqueous phase during the emulsion electrospinning process.

The aqueous phase percentage in the emulsion dictates the maximum loading of the therapeutic of interest since the protein concentration in this phase is limited by its solubility. We hypothesized that increasing the aqueous fraction in the emulsion would

result in a higher loss of protein bioactivity due to an increased aqueous/organic interface and protein/solvent interactions. This relationship between percent aqueous phase and protein activity has been observed in other protein-fiber systems [40]. We utilized colorimetric activity assays to determine the initial rate of substrate conversion of proteins released from the electrospun fibers compared to unformulated protein controls. Representative kinetic activity assays are shown for HRP (Figure 3.4A) and AP (Figure 3.4B). For HRP-loaded fibers, ~90% enzymatic activity was retained for EEHRP5 and EEHRP20 fibers at each flow rate tested (Figure 3.4C,D). There was no significant effect of aqueous phase percentage on HRP bioactivity recovered at either flow rate, or a significant effect of flow rate with the same formulation. These data conclude that HRP can be electrospun from emulsions with higher aqueous phase percentages and at higher flow rates to increase protein loading and material productivity, respectively, without compromising bioactivity. For AP-loaded fibers we observed a significant decrease in AP bioactivity upon increase of aqueous phase percentage from 5% (EEAP5) to 20% (EEAP20) for both flow rates tested, from ~80% to ~50% (Figure 3.4C,D). As was observed with HRP-fibers, there was no significant difference between recovered AP bioactivity of the same formulation at different electrospinning flow rates. Overall, we recovered less bioactivity from AP-loaded fibers than from HRP-loaded fibers, which we hypothesize is due to the larger molecular weight and multimeric structure of AP. In contrast to HRP, an increase of the percent aqueous phase in the emulsion compromised AP activity, which limits the protein loading capacity of the system. However, AP can still be electrospun at higher flow rates to increase productivity without resulting in further activity loss.

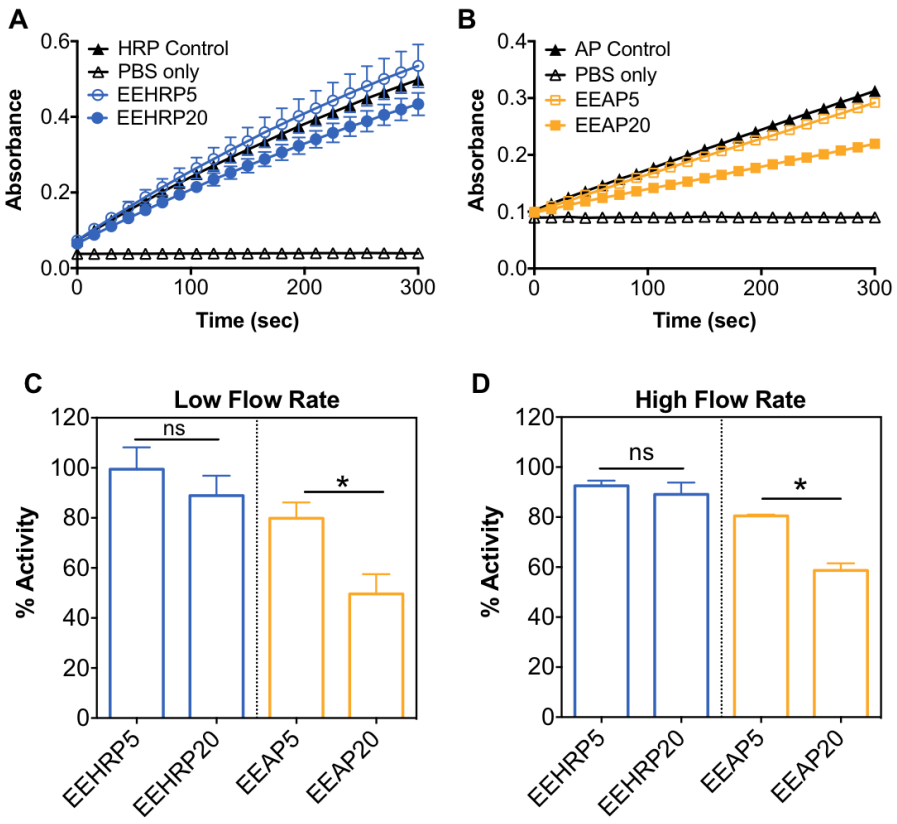

*Figure 3.4. Bioactivity of proteins released from Eudragit L100 nanofibers prepared from emulsions with lower aqueous phase percentages. Representative kinetic enzymatic activity of A) HRP and B) AP recovered from electrospun fibers compared to non-electrospun fresh protein controls. Percent bioactivity recovered from HRP- and AP-loaded fibers with different aqueous phases percentages electrospun at C) 25 μL min^{-1} (low) and D) 40 μL min^{-1} (high) flow rates. Data is representative of results from n=3 fiber punches per formulation and presented as mean ± standard deviation. *$p<0.05$.*

Since we observed loss of protein bioactivity after emulsion electrospinning, we sought to protect the proteins through inclusion of a hydrophilic polymer poly(vinyl alcohol) (PVA) in the aqueous protein solution. This technique is used to induce the preferential interaction of the protein with the hydrophilic polymer, preventing conformational changes that would otherwise occur through interaction with the organic solvent interface [12]. For both HRP- and AP-loaded Eudragit L100 fibers, PVA had no

measurable effect on protein bioactivity for the low electrospinning flow rate tested (Figure 3.5A). However, when fibers were electrospun at the higher flow rate, inclusion of PVA increased the recovered bioactivity from ~90% to 100% for EEHRP20 and from ~60% to 75% for EEAP20 (Figure 3.5B). PVA did not have an effect on 5% aqueous phase fibers at either flow rate. Overall, our results indicate that incorporating PVA is favorable for emulsion electrospinning of proteins from solutions with high aqueous phase percentages, which may be necessary when high protein loading is desired.

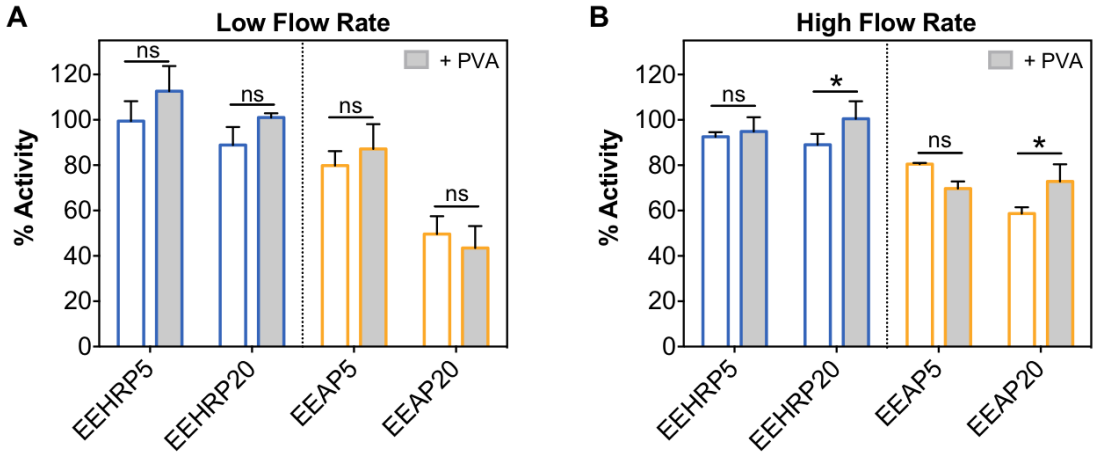

*Figure 3.5. Inclusion of hydrophilic polymer poly(vinyl alcohol) can enhance bioactivity retention from high aqueous phase emulsion formulations electrospun at high flow rates. Percent bioactivity recovered from HRP- and AP-loaded fibers with or without the inclusion of PVA (1% w/w) in the protein solution electrospun at A) 25 μL min^{-1} (low) and B) 40 μL min^{-1} (high) flow rates. Data is representative of results from n=3 fiber punches per formulation and presented as mean ± standard deviation. *p<0.05.*

There have been few studies investigating the effect of emulsion electrospinning parameters on the bioactivity recovered of proteins released from electrospun fibers. In one study that loaded AP into electrospun polycaprolactone fibers, ~50% activity retention was reported based on an end-point measured absorbance value taken at 1 hour of progression of a colorimetric assay [37], which does not account for differences in initial conversion rates. In cases where the enzymatic reaction is substrate-limited, progression

to a maximum absorbance value will occur as the substrate is consumed and the reaction rate goes to zero, even if the enzyme is functioning at <100%. This is in contrast to the initial rate of absorbance change over time that was used in our calculations, which discerns changes in enzyme activity based on the rate of product conversion per unit time in the initial linear region. Lysozyme is another enzyme commonly used to probe protein loading and bioactivity when formulated into electrospun fibers, and retention values in the range of ~30 – 95% have been reported [24,36,39,40]. However, these studies all use various polymers, solvents, aqueous phase percentages, and loading amounts. Yang *et al.* observed that lysozyme bioactivity was dependent on the emulsion aqueous/organic volume ratio, but their study focused on aqueous phases only up to 5% [40]. The enzyme trypsin has also been electrospun into polycaprolactone fibers and ~66% bioactivity retention was reported after emulsion electrospinning from a 5% aqueous phase emulsion [23]. Place *et al.* loaded the protein fibroblast growth factor-2 (FGF-2) into electrospun fibers using the polymer chitosan, comparing emulsion electrospinning with a two-phase electrospinning method [25]. While protein bioactivity was not determined quantitatively, they found that treatment of cells with FGF-2-loaded electrospun fibers resulted in similar cell activity as when cells were treated with soluble FGF-2. Interestingly, this study did not detect any protein that was incorporated into emulsion electrospun fibers by enzyme-linked immunosorbent assay, in contrast to incorporation of 20% of the total protein input when electrospun by A/O two-phase electrospinning. This measure can be viewed as a surrogate for protein conformation and thus related to protein activity. Their study used similar emulsion electrospinning parameters as in our study (10% aqueous phase, non-ionic surfactant), and the lack of bioactive protein detected from their emulsion electrospun fibers may be due to the differences in polymers and organic solvents used or the inherent instability of growth factor proteins, which have half-lives on the order of minutes [56]. A study by Peh *et al.* loaded multiple proteins into poly(lactic-co-glycolic acid) emulsion electrospun fibers with a 10% aqueous phase and found that the bioactivity

recovered was highly dependent on the protein [38], as is supported by the results of our study. Finally, many studies incorporating proteins into electrospun fibers for wound healing and tissue engineering demonstrate function of the encapsulated proteins but bioactivity retention is not quantified due to the non-enzymatic nature of the protein investigated [18–22]. While it is difficult draw conclusions from studies evaluating different systems, we demonstrated that protein bioactivity is dependent on aqueous phase percentage in the emulsion as well as on the protein loaded when emulsion electrospinning Eudragit L100 fibers.

3.4.4 *Bioactivity of Proteins Encapsulated in Eudragit L100 Fibers in Simulated Gastric Fluid*

As we observed localization of the incorporated proteins in aqueous pockets in the nanofibers surrounded by polymer, we sought determine if this microarchitecture could provide protection of the proteins in simulated gastric fluid (SGF) with pepsin. HRP was loaded into fibers using a 5% aqueous phase emulsion and 100% HRP activity was verified immediately after electrospinning, as previously observed using this formulation. HRP was then incubated in SGF (pH 1.5) with pepsin (1 mg mL^{-1}) for 1 hour at 37 °C. Unformulated HRP lost ~90% of its bioactivity following incubation in SGF while HRP formulated in fibers only lost ~25% bioactivity (Figure 3.6). These results indicate that electrospinning proteins into Eudragit nanofibers can prevent protein degradation and loss of therapeutic protein activity in the harsh acidic and enzymatic conditions of the stomach. We hypothesize that since the nanofibers are insoluble in acidic conditions, the proteins sequestered in the aqueous pockets are not exposed to the degradative external environment. This attribute is advantageous for oral protein delivery, as more bioactive protein will be released in the intestines after transit through the stomach when formulated in Eudragit nanofibers compared to aqueous delivery. The mild activity loss of the enzyme-loaded fibers in these conditions may be due to protein release from the

fibers. Although we found <5% protein release in gastric pH conditions, the digestive enzyme pepsin was not included in the experiments and may increase protein release from the fibers. Alternatively, while the fibers were washed in water at pH 2.0 following simulated gastric fluid incubation, it may be possible that residual pepsin was fiber-associated and transferred into neutral PBS solution in which the activity assay was performed, causing degradation of the released protein.

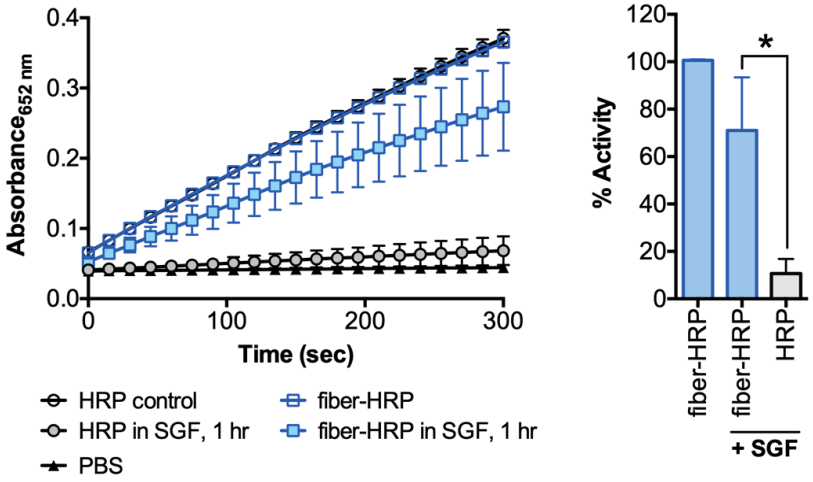

*Figure 3.6. Bioactivity of HRP after incubation in simulated gastric fluid for 1 hour in soluble or emulsion electrospun Eudragit L100 fiber formulation. Data representative of results from n=3 fiber punches per formulation and presented as mean ± standard deviation. *p<0.05.*

As no electrospun fiber systems have been designed for peroral delivery of proteins, the degree of protein activity protection in the gastric environment of our fiber system compared to other polymeric fibers cannot be evaluated. However, nano- and microparticle systems for oral protein delivery have been designed and undergone such evaluations. Kim *et al.* designed microparticle hydrogels for oral insulin delivery and found that, depending on the microparticle composition, between 15 – 75% of the insulin activity could be retained after incubation in simulated gastric fluids with pepsin [57]. Crosslinked chitosan nanoparticles were found to partially protect the encapsulated protein in gastric conditions *in vitro*, in which ~40% of the protein activity was lost within 30 minutes and ~60%

within 2 hours [58]. Kumar *et al.* observed ~50% activity retention in simulated gastric conditions for pore-containing Eudragit S100 microparticles encapsulating lactase [59]. Protection of proteins in gastric fluids has also been demonstrated, but not quantified, for alginate-chitosan microspheres [60]. Alternative approaches to maintaining the activity of orally delivered proteins involve conjugation with polymers to inhibit protease access to the proteins in the stomach and engineering proteins to be more robust against protease activity through amino acid substitution. Systems utilizing these approaches have demonstrated maintenance of protein activity in simulated gastric conditions *in vitro* and *in vivo* [61,62]. Such protein conjugation and manipulation are commonly explored for therapeutic proteins whose site of action is in the stomach, such as proteins for the treatment of lactose and gluten intolerance, rather than for proteins which either act in or are absorbed in the intestinal tract. Fuhrmann *et al.* synthesized protein-polymer conjugates, which were stable and exhibited activity in simulated intestinal fluid. However, protein activity was lost within 5 minutes of incubation in simulated gastric fluid with pepsin, indicating the inability of all polymers tested (poly-(3,5-bis(3-aminopropoxy)benzyl)-methacrylate, a-poly(D-lysine), methoxy poly(ethylene glycol), and poly(acrylic acid)) to protect the protein from deactivation [61]. Similarly, Turner *et al.* conjugated branched poly(ethylene glycol) to the enzyme β-galactosidase and found that the residual activity could be improved from 31% without PEG conjugation to 52% with PEG conjugation after incubation in SGF with pepsin [62]. In summary, these results indicate that full protection of proteins in the gastric environment is still an elusive task. However, our materials show promise in their ability to preserve ~75% protein bioactivity in such harsh conditions, better than or comparable to other materials-based approaches.

3.4.5 *Evaluation and Extension of Protein-Loaded Fiber Shelf Life*

One advantage of delivering therapeutics in fibers is the production of a solid dosage form that is not subject to complications faced by soluble protein storage such as

aggregation and hydrolysis. Commonly, protein therapeutics must be used within hours of solubilization and other nanotechnology platforms for protein delivery require fresh production due to low colloidal stability in solution or require refrigerated or desiccated storage conditions [63,64]. The manufacture of shelf-stable biologics is very desirable, and we hypothesized that the incorporation of proteins into electrospun fibers could extend their storage lifetime through enhanced stabilization and protection. We found that storage of HRP in all fiber formulations at room temperature resulted in 30x higher bioactivities recovered after 1 week compared to soluble storage of the protein (Figure 3.7A). Recovered bioactivity of HRP was also significantly increased when stored out to 4 weeks in fibers made from 5% (1.5x), but not 20%, aqueous phase emulsions (Figure 3.7A). For AP, the benefit of storage in fibers was not observed as bioactivity decay kinetics were similar to that of AP storage in aqueous solution (Figure 3.7B).

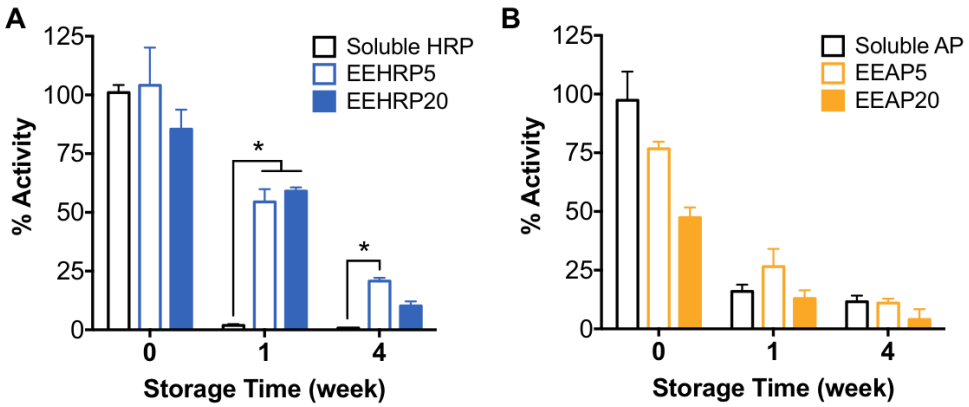

*Figure 3.7. Stability of proteins is enhanced or maintained by formulation into electrospun fibers. Bioactivity decay of A) HRP and B) AP recovered from electrospun fibers after storage at room temperature for 1 and 4 weeks compared to storage in aqueous solution (soluble). Data representative of results from n=3 fiber punches per formulation and presented as mean ± standard deviation. *p<0.05.*

To further extend the shelf life of these protein-loaded fibers, we investigated the contribution of residual water in the fibers. We hypothesized that any remaining water in the aqueous pockets of the fiber could result in increased mobility of the protein and thus

increase the probability of conformational change and activity loss [65]. Water content of protein-loaded fibers was measured immediately after electrospinning and after one day of storage at room temperature or under lyophilization. For HRP- and AP-fibers produced from 5% aqueous phase emulsions, there was no significant difference in fiber water content before and after lyophilization (Figure 3.8A,E). However, lyophilization was found to significantly decrease the water content of 20% aqueous phase HRP- and AP-fibers by 10% and 40%, respectively (Figure 3.8C,G). We then investigated the effect of lyophilization on protein bioactivity retention and if the decrease in water content observed upon lyophilization could prevent rapid bioactivity loss of the encapsulated proteins. After 1 day of lyophilization, all protein loaded-fibers retained significantly higher bioactivity than their non-lyophilized counterparts for all formulations (Figure 3.8B,D,F,H). Lyophilization resulted in bioactivities 1.2X, 1.5X, 1.7X, and 6.6X higher for EEHRP5, EEHRP20, EEAP5, and EEAP20 fibers, respectively. These results also indicated that our lyophilization procedure did not have a detrimental effect on protein structure, which would have resulted in a greater activity loss for lyophilized samples. After overnight lyophilization, fibers were removed from vacuum and stored at room temperature with non-lyophilized fibers. After 7 days, we also observed that lyophilization significantly increased the bioactivity recovered from the encapsulated proteins for all formulations except EEAP20. The recovered protein bioactivity after 7 days was 1.5X, 1.6X, and 3.2X higher for lyophilized EEHRP5, EEHRP20, and EEAP5 fibers, respectively, compared to their storage without one-time lyophilization. This resulted in greater than 60% recovery of initial protein bioactivity for those formulations.

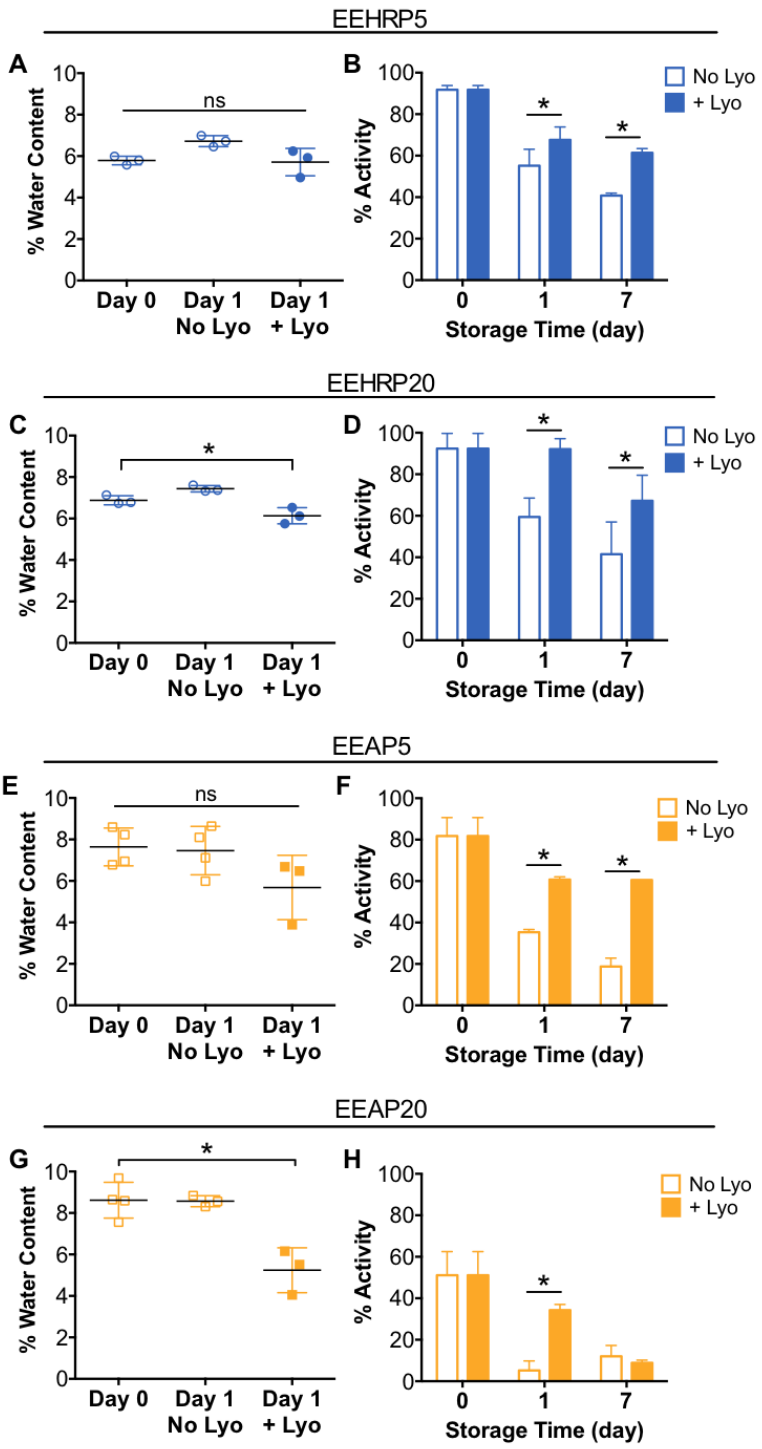

Figure 3.8. Lyophilization of protein-loaded fibers can reduce water content and significantly extend protein bioactivity retention during storage. Water content of protein-loaded fibers immediately after electrospinning, one day after electrospinning stored at room temperature, and one day after electrospinning stored under lyophilization of electrospun fibers A) EEHRP5, C)

*EEHRP20, E) EEAP5, and G) EEAP20. After lyophilization overnight, fibers were stored at room temperature for a total storage time of 7 days. Bioactivity of proteins recovered from electrospun fibers B) EEHRP5, D) EEHRP20, F) EEAP5, and H) EEAP20 with or without overnight lyophilization over 7 days. Data representative of results from n=3 fiber punches per formulation and presented as mean ± standard deviation. *p<0.05.*

Finally, we evaluated one formulation, EEHRP5 for longer term storage at room temperature following lyophilization. After four weeks of storage, enzymes in lyophilized fibers retained 35% of their activity compared to 20% non-lyophilized formulations, a statistically significance increase in the recovered bioactivity (Figure 3.9). While the proteins lost 65% of their activity when stored for 4 weeks at room temperature, the ability of electrospun fibers to stabilize proteins is promising and may further extend shelf life for formulations stored under less harsh conditions, such as at 4 °C or under desiccation.

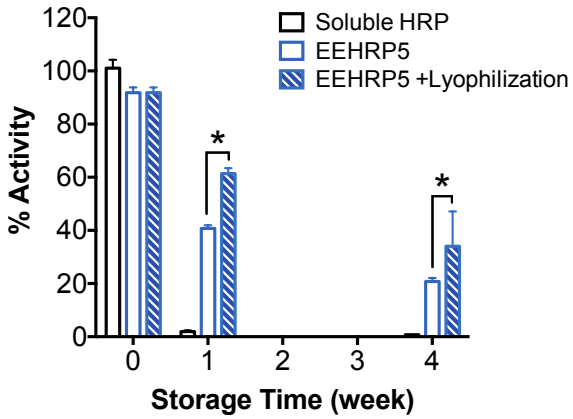

*Figure 3.9. Fiber lyophilization preserves protein bioactivity after 4 weeks of room temperature storage. After electrospinning, EEHRP5 fibers were lyophilized overnight and stored at room temperature for four weeks, testing protein bioactivity immediately after electrospinning, after overnight lyophilization, and after 4 weeks of room temperature storage. Data is representative of results from n=3 fiber punches per formulation and presented as mean ± standard deviation. *p<0.05.*

Commonly, proteins are stored in lyophilized form rather than in solution to prevent protein hydrolysis and loss of active conformation. To compare storage of proteins in electrospun fibers to this conventional storage method, we evaluated the decay in protein activity following storage at 37 °C as a lyophilized solid (as provided by the supplier). Additionally, we were interested in the potential of the electrospinning platform to store therapeutic proteins long term, both in emulsion electrospun fibers and in hydrophilic fibers. Thus, we also characterized protein shelf-life when formulated in PVA nanofibers spun from aqueous blend solutions, both with and without lyophilization. This comparison also allowed us to determine the impact of emulsion electrospinning specifically on protein stability. We found that lyophilized AP protein lost ~20% activity after 1 week and ~30% after 3 weeks of storage (Figure 3.10). Loss of bioactivity was accelerated when proteins were electrospun into PVA nanofibers, but this activity loss was completely prevented through fiber lyophilization, as was observed for proteins formulated in emulsion electrospun fibers (Figure 3.10). Lyophilization of protein-loaded PVA fibers achieved equivalent levels of protein activity as storage of protein in lyophilized form through the time points investigated in our study. These observations suggest two main sources contribute to protein deactivation when formulated in emulsion electrospun fibers. First, the emulsion electrospinning process, compared to electrospinning aqueous solutions, results in an initial loss of protein function, likely due to protein exposure to organic solvents during formulation. Second, residual water in the nanomaterials, present in fibers electrospun both from emulsions and aqueous solutions, result in a reduced protein conformational stability, causing further loss of bioactivity. In this work, we have identified methods to overcome both phases of protein activity loss through reduction of the emulsion aqueous phase percentage and use of hydrophilic polymer excipients, and removal of residual water in the material with lyophilization, respectively.

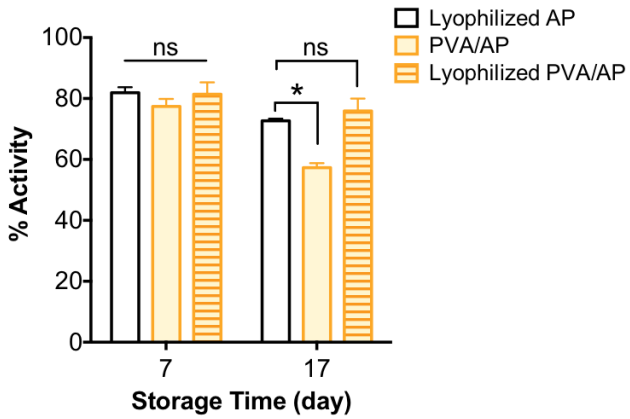

*Figure 3.10. Bioactivity of lyophilized AP, AP-loaded PVA electrospun nanofibers, and lyophilized AP-loaded PVA electrospun nanofibers stored at 40 °C. Data representative of results from n=3 fiber punches per formulation and presented as mean ± standard deviation. *p<0.05.*

While published data on the shelf life of proteins in electrospun fibers is limited, a study by Pinto *et al.* observed ~60% and ~40% bioactivity was retained by proteins released from non-lyophilized fibers after 2 and 4 weeks, respectively [23]. This activity decay profile was similar to that observed for our non-lyophilized HRP protein formulations. Despite the similarity in activity loss kinetics, it is important to note that the referenced study used a different polymer (polycaprolactone), protein (trypsin), and a 5% aqueous phase emulsion. Thus, further work is required to fully characterize the stability of additional biotherapeutics in electrospun nanomaterials. Lyophilization of proteins in paper-based networks is highly utilized in microfluidic devices, in which dry storage of proteins is advantageous to enhance stability over long-term storage of the device [66]. Results from our study support the application of this technique used in paper-based microfluidics to extend protein storage in polymeric nanofibers. Overall, we can conclude that lyophilization of protein-loaded electrospun fibers results in more shelf-stable biologic formulations, and we have shown that this technique can extend the lifetime of both HRP and AP for at least 7 days at room temperature for emulsion electrospun fibers and for at least 17 days at 40°C for hydrophilic electrospun fibers.

Importantly, we observed equivalent stability of proteins stored as lyophilized powder and in lyophilized hydrophilic nanofibers. This storage method involves only a one-time lyophilization step, reducing the need for costly equipment and power, and may eliminate the need for refrigeration to maintain protein stability over this time frame. Thus, this is an attractive strategy for protein stabilization and storage, which is a major problem for polymeric-based protein delivery systems and bioactive scaffolds for tissue engineering.

3.4.6 *Functionality of Antigens Encapsulated in Eudragit L100 Fibers*

As our platform demonstrated promise in encapsulating and releasing bioactive enzymes, we next evaluated the ability of emulsion electrospun fibers to deliver more relevant protein-based antigens. To generate cellular immunity against a certain antigen, the antigen must first be taken up and processed by dendritic cells for presentation to T cells. Depending on the pathway of internalization, the origin of the antigen, and the unique cytokine milieu the cell is exposed to during uptake, the antigen will be processed through a distinct pathway for surface presentation on either the major histocompatibility complex (MHC) class I or II protein. One major distinction of the presentation pathways depends on if the antigen is sensed from inter- or extracellular detection mechanisms. Traditionally, extracellular antigens are shuttled into the MHC-II pathway to be presented to $CD4^+$ T cells and only specific cell types have the ability to present antigen on MHC-II, such as dendritic cells and B cells. In contrast, most cells express the protein MHC-I and use it to present antigens that are derived intracellularly, as would be the case for an intracellular viral infection. Some cells also have the unique ability to process extracellular antigens and present them on MHC-I, a process called cross-presentation. While the mechanisms behind this phenomenon are still being elucidated, this process is thought to be influenced by a variety of factors such as the pathway of internalization, the phenotype of the cell at the time of antigen uptake, the source of the antigen, and the engagement of different cell surface receptors [67]. Peptides from the processed antigen

bound by an MHC protein on the surface of cells are then recognized by T-cell receptors (TCR) on naïve T cells in lymphoid organs. The pathway of antigen internalization and presentation also dictates which type of T cells the antigen presenting cell can activate, with presentation on MHC-I being recognized by $CD8^+$ T cells and presentation on MHC-II being recognized by $CD4^+$ T cells. Maintenance of antigen structure is critical to its immune function and proper epitope recognition, with naïve T cells only recognizing precise amino acid sequences between 8 – 20 in length.

We evaluated the ability of the antigen ovalbumin to be processed and presented to T cells after encapsulation into emulsion electrospun Eudragit L100 fibers with a 5% aqueous phase. The materials were verified for antigen loading (wt%) and 100% encapsulation efficiency using a micro BCA assay (data not shown). Immediately following electrospinning and solvent evaporation, fibers were dissolved in RPMI 1640 and incubated with the dendritic cell line DC2.4 for protein uptake and processing. Twenty-four hours later, the T cell line B3Z, a $CD8^+$ T cell hybridoma that recognizes the ovalbumin epitope SIINFEKL ($OVA_{257\text{-}264}$), was co-cultured with the antigen-treated DCs. Presentation of the antigen by DCs to T cells will result in TCR ligation of the B3Z cells, which induces the production of the enzyme β-galactosidase that can be quantified through the production of a colorimetric product following the addition of the substrate β-d-galactopyranoside. Ovalbumin released from emulsion electrospun fibers was processed by DCs and presented to $CD8^+$ T cells immediately following formulation (Figure 3.11A) and after 7 days of storage at room temperature (Figure 3.11B). Importantly, the encapsulated protein retained its antigenicity even after 1 week of room temperature storage, further supporting the utility of this platform for its ability to load and stabilize protein-based pharmaceutics. Interestingly, we observed presentation of antigen to T cells when the protein ovalbumin was delivered by our fibers even though there was little antigen presentation when the protein was delivered in soluble form to the dendritic cells. This inability of the protein ovalbumin to be cross-presented to $CD8^+$ T

cells has been observed previously [68,69]. The successful cross-presentation of the ovalbumin protein to T cells when delivered by electrospun fibers suggests potential interactions of the polymeric materials and the dendritic cells that may lead to differential processing of the antigen.

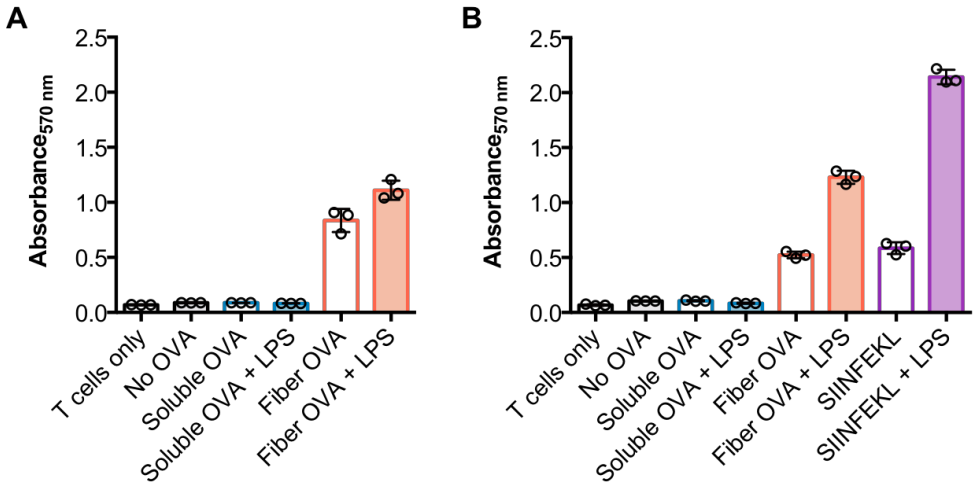

*Figure 3.11. Ovalbumin encapsulated in emulsion electrospun fibers is functional and can activate antigen-specific CD8⁺ T cells A) immediately after formulation and B) after 7 days of storage. Ovalbumin-loaded fibers were stored at room temperature following lyophilization overnight. Internal positive controls include soluble ovalbumin (100 μg mL^{-1}) and SIINFEKL peptide (synthesized in-house, 10 μM) with LPS stimulation (0.5 μg mL^{-1}). Data representative of results from n=3 fiber punches per formulation and presented as mean ± standard deviation. *p<0.05.*

Maintaining the functionality of antigens loaded into materials-based platforms is a critical parameter for the elicitation of antigen-specific immunity, both during the formulation process and upon vaccine storage. While the antigenicity of ovalbumin following electrospinning into nanofibers has not been evaluated for other polymers, the antigen protective antigen (PA), produced by the gram-positive bacteria *Bacillus anthracis* that causes the disease anthrax, has been evaluated using this platform. After the loading of the PA into poly(vinyl pyrrolidone) electrospun nanofibers fibers, the antigen was found to retain functionality through the observance of the inflammatory cytokine IL-6 following incubation with the human monocytic cell line, MM6 [70]. The

antigen used in our study, ovalbumin, has been loaded into many other nanotechnology platforms, most notably micro- and nanoparticles. Ovalbumin encapsulation into PLGA nanoparticles was achieved through a novel microfabrication method, StampEd Assembly of polymer Layers (SEAL), and stable protein conformation was demonstrated after 30 days when stored at 4 °C under desiccation [71]. It is important to note that these particles included the protein stabilizer sucrose. Moreover, the antigen hemagglutinin (HA) was shown to retain its immunogenicity after 6 months of storage at 4 °C in Eudragit/trehalose nanoparticles [72].

$CD8^+$ T cell immunity is essential in the fight against many infectious diseases as well as cancer. However, the administration of protein antigens *in vivo* generally fail to activate cross presentation and the priming of $CD8^+$ T cells [73]. To take advantage of this molecular mechanism, formulation strategies for protein-based antigens have been developed, specifically ones utilizing nanotechnology. Cross-presentation of exogenously-delivered antigen has been reported for PLGA-based particle systems, in which the particles escape the endosome and reach the cytoplasm to be presented on MHC-I [74]. Delivery of the antigen ovalbumin in these materials enhanced cross-presentation to T cells *in vitro* compared to soluble delivery of the protein. Similarly, PEI nanoparticles also demonstrated enhanced presentation of antigen on MHC-I compared to soluble antigen, which the authors believe is due to the endosomal-disruptive effect of the cationic polymer PEI, although this cross-presentation ability was only found for certain PEI-antigen weight ratios [75]. pH-responsive micellar nanoparticles composed of amphiphilic diblock copolymers of size less than 100 nm were designed with endosomolytic properties to enhance cross-presentation [76]. These materials were found to induce cross-presentation of ovalbumin *in vitro*. This effect was found to be partially dependent on endosome acidification, proteasomal processing, and transport from the ER. In addition to polymeric particles, lipid-based particulates have also been shown to enhance cross-presentation to

exogenously-delivered proteins. Multilamellar vesicles with crosslinked lipid bilayers enhanced surface presentation on MHC-I as well as activation of CD8+ T cells [77].

While the cross-presentation ability of these platforms is attributed to polymeric and particulate properties that favor internalization by phagocytosis, micropinocytosis, or receptor-mediated endocytosis, such mechanisms are not likely to be contributing to the cross-presentation of whole proteins released from our nanofibers. It may be possible that the presence of the Eudragit polymer is influencing the mechanism of protein uptake into the phagosome-to-cytosol pathway, in which proteins access the cytosol and are processed through the proteasome/TAP pathway to be loaded onto MHC-I. Additionally, our lab has found that co-delivery of antigens with the DC-stimulating adjuvant MPLA can enhance cross-presentation of exogenously-delivered proteins [78]. This phenomenon has also been observed for TLR signaling in general, in which MHC-I accumulates in phagosomes that contain TLR agonists, enhancing cross presentation [79]. Thus, it is possible that the state of the dendritic cell during antigen uptake and processing may influence its intracellular trafficking, which may be modulated by the Eudragit polymer in the formulation, although there is not significance literature on the immunogenic properties of this co-polymer.

We next tested if the presence of the electrospun fibers would impact B3Z activation by DCs by treating DCs with soluble OVA and blank electrospun fibers. As seen in Figure 3.13, the presence of the fibers with soluble OVA did not induce B3Z activation as observed with delivery of OVA-loaded fibers or the supernatant of dissolved OVA-loaded fibers. Further experiments are needed to fully elucidate the enhanced B3Z activation of DCs treated with OVA-loaded electrospun fibers.

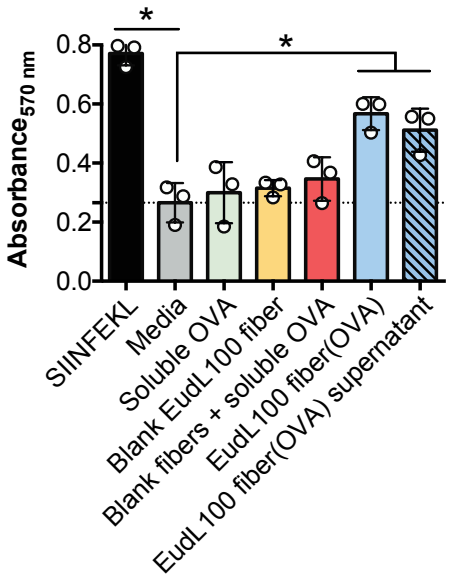

*Figure 3.12. Activation of B3Z T cell is not driven by the presence of fibers during treatment of DCs with antigen. DC2.4 cells were treated with soluble OVA, soluble OVA with blank Eudragit L100 fibers, or OVA-loaded emulsion electrospun Eudragit L100 fibers at 0.1 mg mL^{-1} OVA. Positive control of SIINFEKL peptide was used. After 24 hours, cells were washed and incubated with B3Z T cells for 24 hours. B3Z T cell activation was assayed as described. Data representative of results from n=3 per formulation and presented as mean ± standard deviation. *p<0.05.*

3.4.7 *In Vitro Mucoadhesion*

In mucosal drug delivery, extended retention time of the therapeutic is extremely advantageous in enhancing drug absorption as well as extending drug release at these surfaces. Mucosal surfaces are covered by a negatively-charged glycoprotein matrix that functions to protect the epithelial layer, bind invading pathogens, and reduce intestinal inflammation by separating commensal bacteria from epithelial cells [80]. In the gastrointestinal tract specifically, this mucus layer is turned over every ~4-5 hours, making mucosal drug delivery a challenge due to the rapid clearance of substances at these surfaces. Biomaterials engineering has taken advantage of the properties of the glycoprotein matrix to design materials that can ionically interact with the mucus layer

and prolong the residence time of drug formulations [81]. There are many theories to describe the mucoadhesion process, including wetting, electrostatics, diffusion, adsorption, and fracture [82]. Alternatively, materials can be designed with "stealth" properties that allow for free diffusion through mucus, preventing their entrapment and subsequent clearance from the body [83]. In the scope of this project, it is advantageous for our nanofibers to exhibit mild mucoadhesive properties. Since this system is designed for drug release at mucosal surface, rather than to be taken up by mucosal cells, a prolonged residence time of the materials could create a drug depot that increases the concentration of the therapeutic, potentially improving drug diffusion and absorption [84]. However, too strong of an interaction between the materials and mucus could cause premature adhesion of the fibers along the GI tract. It is not likely that our, nor other cationic mucoadhesive materials, will interact with mucins in acidic environments, such as the stomach, as the isoelectric point of porcine gastric mucin was found to be 2 – 3, giving mucin a neutral charge in acidic conditions [85,86]. This reduced interaction between mucoadhesive cationic materials and mucin in acidic environments has been demonstrated in *in vitro* turbidity experiments [61]. As the Eudragit L100 co-polymer is comprised of methyl methacrylate and methacrylic acid, it possesses a carboxylic side group that can hydrogen bond with the mucus glycoproteins under certain ionic conditions. We sought to further characterize the Eudragit L100 nanofibers for mucoadhesive properties and their interaction with mucin solutions.

First, a technique to measure the detachment force of nanofibers from a 2% mucin solution in PBS (pH ~6) using an Instron mechanical testing machine was developed. We found that there was significantly higher work of adhesion (3X increase) for Eudragit L100 fibers to be detached compared to our mount-only control, indicating interaction with the mucin solution (Figure 3.13A,B). Qualitatively, the Eudragit L100 fibers swelled and formed a hydrogel upon incubation with the mucin solution compared to non-mucoadhesive PLGA fibers, whose macroscopic structure did not change (Figure 3.13D).

This finding led us to evaluate the swelling ratios for these materials, a common metric for hydrogel characterization. Eudragit L100 fibers expanded to 60-times their original mass upon interaction with mucin glycoprotein solutions (Figure 3.13C). The interaction of mucin with Eudragit L100 in different ionic conditions was further evaluated with a turbidity experiment and compared to the cationic mucoadhesive polymer, chitosan. In both acidic and neutral pH conditions, Eudragit L100 did not significantly interact with mucin, as the optical density of mucin solutions with varying weight ratios of Eudragit L100 polymer was not higher than Eudragit L100 in the same buffer without mucin (Figure 3.13E,F). The increased optical density of Eudragit L100 solutions at pH 2 are likely due to the insolubility of the polymer in these conditions, rather than an interaction with mucin. In contrast, methylglycol chitosan did show complexation with mucin at pH 6 (Figure 3.13E) but not at pH 2 (Figure 3.13F), representing the ionic interactions of the cationic polymer with negatively charged mucin in neutral conditions but not in acidic conditions when mucin is net neutral.

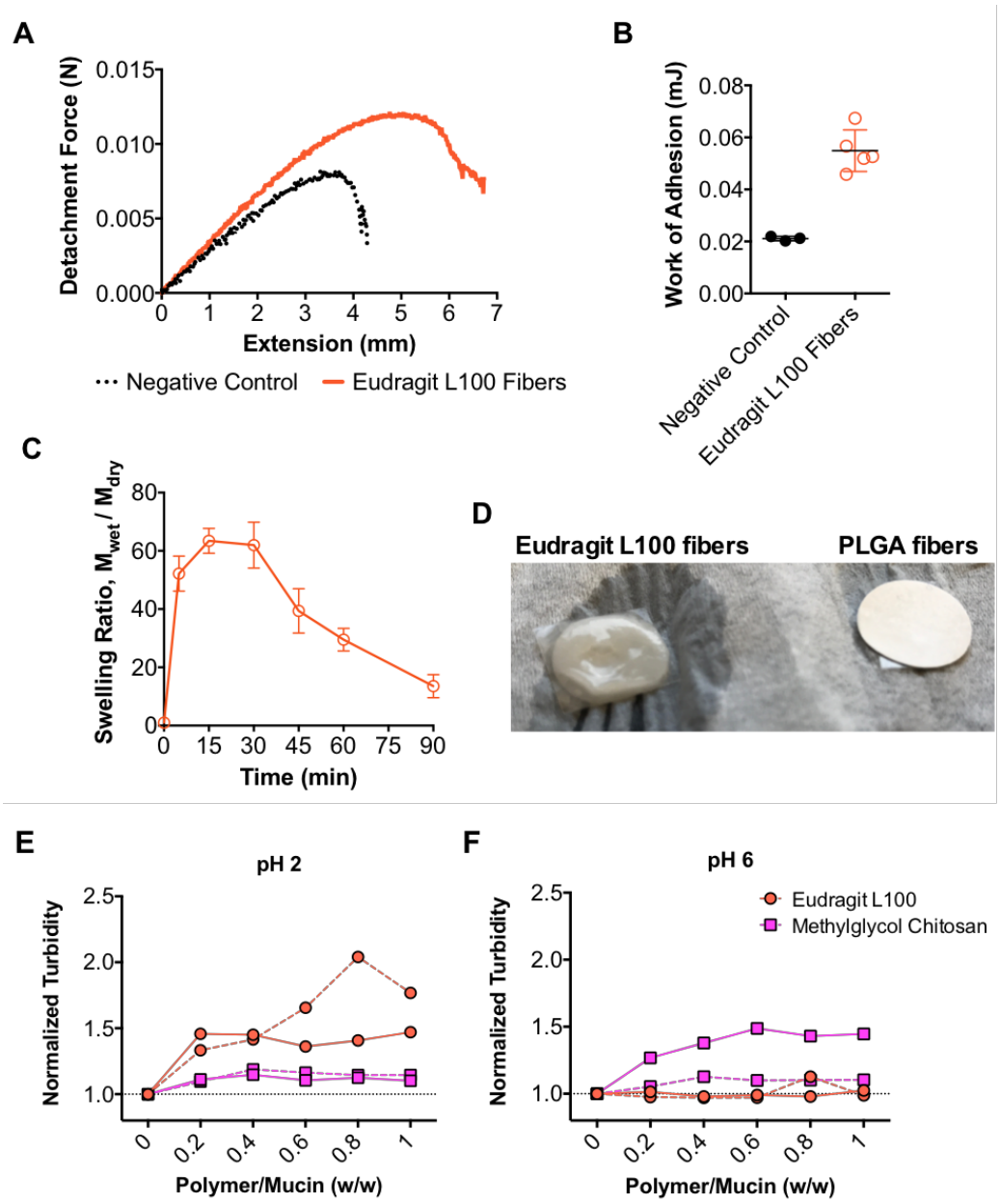

Figure 3.13. Eudragit L100 fibers exhibit mucoadhesive properties in vitro. A) Detachment force vs. extension plot and B) work of adhesion following Eudragit L100 fiber incubation in a 2% mucin/PBS solution. C) Ratio of wet/dry mass of Eudragit L100 fibers upon incubation in a 2% mucin/BSA solution at 37 °C. D) Eudragit L100 and PLGA fibers after 5-minute incubation in a 2% mucin/PBS solution. Turbidity of Eudragit L100 and methylglycol chitosan polymers with (solid lines) or without (dashed lines) mucin at E) pH 2 and F) pH 6. Data is representative of results from n=3 samples per experiment and presented as mean ± standard deviation.

These data provided mixed results on the mucoadhesive properties of EudragitL100 fibers. While solutions of the polymer did not show interactions with mucin in acidic nor neutral conditions, formation of fibers with EudragitL100 produced materials that took in water and swelled to 60X their dry mass when incubated with mucin solutions. This interaction required more work to detach the fibers from the surface of the mucin solution, indicating that the materials can interact with mucosal surfaces, albeit weakly. Other literature has indicated the probability of Eudragit polymer interactions with mucus due to its hydrophobicity, which can cause mucoadhesion in addition to electrostatic interactions [83].

3.4.8 *In Vivo Retention in Gastrointestinal Tract*

Finally, we evaluated the retention of protein in the gastrointestinal tract after oral administration either in soluble form or encapsulated in Eudragit L100 fibers. To allow for oral gavage of our materials into mice, fibers were micronized into particles $<$200 μm in size. The micronization process was verified to cause no protein leakage from the fibers and 100% protein was recovered from micronized fibers (data not shown). Protein clearance rates from the gastrointestinal were found to be similar after soluble and fiber delivery of proteins orally, with the maximum radiance of the fluorescently-labeled protein in the GI-tract occurring between $4 - 8$ hours after administration and dissipating by 24 hours (Figure 3.14). These equivalent rates of protein clearance are expected for the time points evaluated in our study, as we sought to characterize protein location from administration to clearance. Additionally, although our *in vitro* evaluation did indicate modest interaction between Eudragit fibers and mucus solutions, results from the *in vivo* retention study do not support strong mucoadhesion of the nanofibers. This conclusion is supported by a study by Eaimtrakarn *et al.*, in which Eudragit L100 films were found to move through the gastrointestinal tract without adherence to the mucus layer until dissolution in the jejunum of the small intestine [87].

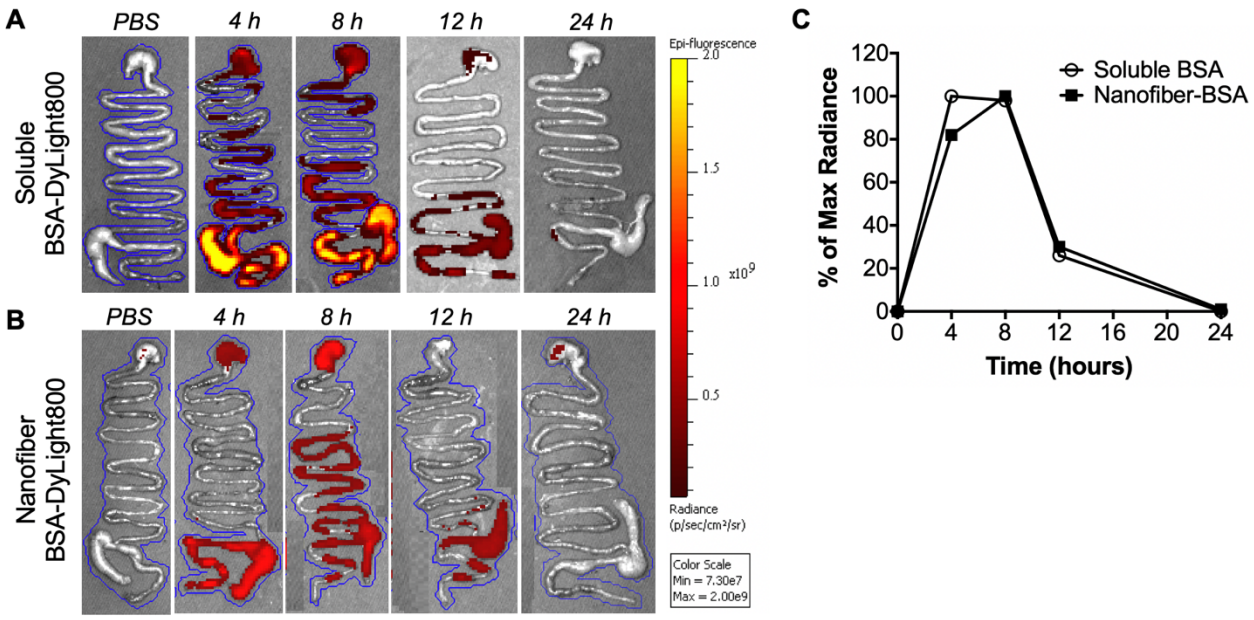

Figure 3.14. Retention of BSA delivered in A) soluble form or B) loaded in micronized Eudragit L100 fibers in the mouse gastrointestinal tract after oral administration. C) Percentage of the maximum radiance in the gastrointestinal tract over 24 hours. Data is representative of n=1 mouse per time point.

Other mucoadhesive biomaterial platforms such as films and nanoparticles have been evaluated for extended dose retention at mucosal surfaces. Thiolated Eudragit-coated chitosan microparticles were found to remain associated with the small intestine 6 hours after oral administration, while the unthiolated Eudragit-coated particles signal decreased between 4 and 6 hours [88]. In another study, thiolated Eudragit nanoparticles demonstrated enhanced association with the intestinal mucosa 2 hours after intraluminal administration compared to non-functionalized Eudragit particles [89]. Many additional studies evaluating the interaction of biomaterials with mucosal surfaces either do not measure therapeutic retention out to 24 hours or evaluate the carrier only without non-carrier controls.

Although our materials did not significantly extend protein retention in the GI tract for more than 24 hours, we expect differences in protein uptake and immune responses with our delivery system due to favorable attributes such as protection of

protein from deactivation in the gastric environment and rapid release of the protein in small intestinal conditions, leading to a higher local concentration of bioactive at the mucosal surface. However, it is also possible that there are differences in the protein retention at mucosal surfaces of the GI tract at shorter time scales than were investigated in our study. In the case that these hypotheses are not supported by further *in vivo* analysis, fibers can be modified with mucoadhesive side groups through thiolation [90] as well as including an additional mucoadhesive polymer during electrospinning [91,92]. As mentioned previously, the balance of extending dose retention at mucosal surfaces and limiting nonspecific adherence must be maintained when developing new mucosal drug delivery systems.

3.5 Conclusions

In conclusion, two model proteins, horseradish peroxidase and alkaline phosphatase, were loaded into Eudragit L100 fibers using an emulsion electrospinning technique. We investigated the emulsion parameters of aqueous phase percentage and inclusion of a hydrophilic polymer and the electrospinning parameter of flow rate to optimize protein loading and bioactivity. Using this optimized method, both proteins were loaded into fibers at high efficiencies and were released in a pH-controlled manner with minimal non-specific protein release. We identified that bioactivity retention of the proteins could be enhanced through decreasing the aqueous phase percentage in the emulsion and including a hydrophilic polymer with the protein. Flow rate during electrospinning was not observed to have an effect on protein bioactivity, demonstrating that the electrospinning process was not detrimental to protein structure and that material productivity can be increased without compromising therapeutic activity for future manufacturing scale-up. Further, encapsulation in emulsion electrospun fibers provided protection of proteins from degradation by gastric enzymes and acidic environments.

Protein stability in emulsion electrospun fibers was found to be dependent on the protein loaded both during electrospinning and upon storage. HRP stability over 4 weeks was enhanced through fiber formulation while the formulation type (in fibers vs. in solution) had no effect on AP stability. For both proteins, a one-time lyophilization of emulsion electrospun fibers significantly extended the shelf life of the product over 7 days when stored at room temperature. Eudragit fibers were also demonstrated to load and release functional antigens, leading to the cross presentation to $CD8^+$ T cells. These antigens showed full antigenicity even after one week of storage at room temperature. Thus, protein-loaded Eudragit L100 fibers are a promising new biotechnology platform for peroral protein delivery to overcome the challenge of the harsh gastric environment, which is a critical first step when developing new dosage forms for this administration route, and as a shelf-stable platform for protein-based therapeutics and vaccines.

3.6 Acknowledgements

The authors thank Kevin Liu for assistance with SEM imaging and Hangyu Zhang for assistance with TEM imaging. The authors also thank and acknowledge Tiffany Ohlsen for her senior capstone work on encapsulating proteins in PVA blend electrospun fibers and her contributions to data presented in this document, specifically Figure 3.10. Part of this work was conducted at the Molecular Analysis Facility, a National Nanotechnology Coordinated Infrastructure site at the University of Washington which is supported in part by the National Science Foundation (grant ECC-1542101), the University of Washington, the Molecular Engineering & Sciences Institute, the Clean Energy Institute, and the National Institutes of Health. This work was supported by NIH grant HD075703 and AI112002 to K.A.W. H.F. acknowledges additional financial support from the National Science Foundation Graduate Research Fellowship Program (DGE-1256082) and the Achievement Rewards for College Scientists Foundation Scholar Award.

3.7 References

[1] S. Mitragotri, P.A. Burke, R. Langer, Overcoming the challenges in administering biopharmaceuticals: formulation and delivery strategies., Nat. Rev. Drug Discov. 13 (2014) 655–72. doi:10.1038/nrd4363.

[2] M.M. Levine, G. Dougan, Optimism over vaccines administered via mucosal surfaces, Lancet. 351 (1998) 1375–1376. doi:10.1016/S0140-6736(05)79439-3.

[3] V.K. Pawar, J.G. Meher, Y. Singh, M. Chaurasia, B. Surendar Reddy, M.K. Chourasia, Targeting of gastrointestinal tract for amended delivery of protein/peptide therapeutics: Strategies and industrial perspectives, J. Control. Release. 196 (2014) 168–183. doi:10.1016/j.jconrel.2014.09.031.

[4] M. Goldberg, I. Gomez-Orellana, Challenges for the oral delivery of macromolecules., Nat. Rev. Drug Discov. 2 (2003) 289–95. doi:10.1038/nrd1067.

[5] M. Yu, J. Wu, J. Shi, O.C. Farokhzad, Nanotechnology for protein delivery: Overview and perspectives, J. Control. Release. 240 (2016) 24–37. doi:10.1016/j.jconrel.2015.10.012.

[6] S. Gupta, A. Jain, M. Chakraborty, J.K. Sahni, J. Ali, S. Dang, Oral delivery of therapeutic proteins and peptides: a review on recent developments, Drug Deliv. 20 (2013) 237–246. doi:10.3109/10717544.2013.819611.

[7] J.D. Schulz, M. Patt, S. Basler, H. Kries, D. Hilvert, M.A. Gauthier, J.C. Leroux, Site-Specific Polymer Conjugation Stabilizes Therapeutic Enzymes in the Gastrointestinal Tract, Adv. Mater. 28 (2016) 1455–1460. doi:10.1002/adma.201504797.

[8] G. Fuhrmann, J.-C. Leroux, Improving the stability and activity of oral therapeutic enzymes-recent advances and perspectives., Pharm. Res. 31 (2014) 1099–105. doi:10.1007/s11095-013-1233-y.

[9] T.J. Sill, H. a von Recum, Electrospinning: Applications in drug delivery and tissue engineering, Biomaterials. 29 (2008) 1989–2006. doi:10.1016/j.biomaterials.2008.01.011.

[10] S. Agarwal, J.H. Wendorff, A. Greiner, Use of electrospinning technique for biomedical applications, Polymer (Guildf). 49 (2008) 5603–5621. doi:10.1016/j.polymer.2008.09.014.

[11] X. Hu, S. Liu, G. Zhou, Y. Huang, Z. Xie, X. Jing, Electrospinning of polymeric nanofibers for drug delivery applications, J. Control. Release. 185 (2014) 12–21. doi:10.1016/j.jconrel.2014.04.018.

[12] W. Ji, Y. Sun, F. Yang, J.J.J.P. Van Den Beucken, M. Fan, Z. Chen, J.A. Jansen, Bioactive electrospun scaffolds delivering growth factors and genes for tissue engineering applications, Pharm. Res. 28 (2011) 1259–1272. doi:10.1007/s11095-010-0320-6.

[13] A.L. Yarin, Coaxial electrospinning and emulsion electrospinning of core-shell fibers, Polym. Adv. Technol. 22 (2011) 310–317. doi:10.1002/pat.1781.

[14] A.L. Yarin, S. Koombhongse, D.H. Reneker, Taylor cone and jetting from liquid droplets in electrospinning of nanofibers, J. Appl. Phys. 90 (2001) 4836–4846. doi:10.1063/1.1408260.

[15] D.H. Reneker, I. Chun, Nanometre diameter fibres of polymer, produced by electrospinning, Nanotechnology. 7 (1996) 216–223. doi:10.1088/0957-4484/7/3/009.

[16] V.P. Shastri, J.C. Sy, A.S. Klemm, Emulsion as a means of controlling electrospinning of polymers, Adv. Mater. 21 (2009) 1814–1819. doi:10.1002/adma.200701630.

[17] E.H. Sanders, R. Kloefkorn, G.L. Bowlin, D.G. Simpson, G.E. Wnek, Two-phase

electrospinning from a single electrified jet: Microencapsulation of aqueous reservoirs in poly(ethylene-co-vinyl acetate) fibers, Macromolecules. 36 (2003) 3803–3805. doi:10.1021/ma021771l.

[18] T. Briggs, J. Matos, G. Collins, T.L. Arinzeh, Evaluating protein incorporation and release in electrospun composite scaffolds for bone tissue engineering applications, J. Biomed. Mater. Res. - Part A. 103 (2015) 3117–3127. doi:10.1002/jbm.a.35444.

[19] Z. Wang, Y. Qian, L. Li, L. Pan, L.W. Njunge, L. Dong, L. Yang, Evaluation of emulsion electrospun polycaprolactone/hyaluronan/epidermal growth factor nanofibrous scaffolds for wound healing, J. Biomater. Appl. 30 (2015) 1–13. doi:10.1177/0885328215586907.

[20] J. Hu, L. Tian, M.P. Prabhakaran, X. Ding, S. Ramakrishna, Fabrication of nerve growth factor encapsulated aligned poly(ε-caprolactone) nanofibers and their assessment as a potential neural tissue engineering scaffold, Polymers (Basel). 8 (2016) 54. doi:10.3390/polym8020054.

[21] J.S. Choi, S.-H. Han, C. Hyun, H.S. Yoo, Buccal adhesive nanofibers containing human growth hormone for oral mucositis., J. Biomed. Mater. Res. B. Appl. Biomater. 104 (2015) 1396–1406. doi:10.1002/jbm.b.33487.

[22] X. Li, Y. Su, S. Liu, L. Tan, X. Mo, S. Ramakrishna, Encapsulation of proteins in poly(l-lactide-co-caprolactone) fibers by emulsion electrospinning, Colloids Surfaces B Biointerfaces. 75 (2010) 418–424. doi:10.1016/j.colsurfb.2009.09.014.

[23] S.C. Pinto, A.R. Rodrigues, J.A. Saraiva, J.A. Lopes-da-Silva, Catalytic activity of trypsin entrapped in electrospun poly(ϵ-caprolactone) nanofibers, Enzyme Microb. Technol. 79 (2015) 8–18. doi:10.1016/j.enzmictec.2015.07.002.

[24] T. Briggs, T.L. Arinzeh, Examining the formulation of emulsion electrospinning for improving the release of bioactive proteins from electrospun fibers, J. Biomed. Mater. Res. - Part A. 102 (2014) 674–684. doi:10.1002/jbm.a.34730.

[25] L.W. Place, M. Sekyi, J. Taussig, M.J. Kipper, Two-Phase Electrospinning to Incorporate Polyelectrolyte Complexes and Growth Factors into Electrospun Chitosan Nanofibers, Macromol. Biosci. 16 (2016) 371–380. doi:10.1002/mabi.201500288.

[26] G. Bruni, L. Maggi, L. Tammaro, A. Canobbio, R. Di Lorenzo, S. D'Aniello, C. Domenighini, V. Berbenni, C. Milanese, A. Marini, Fabrication, Physico-Chemical, and Pharmaceutical Characterization of Budesonide-Loaded Electrospun Fibers for Drug Targeting to the Colon, J. Pharm. Sci. 104 (2015) 3798–3803. doi:10.1002/jps.24587.

[27] M. Hamori, S. Yoshimatsu, Y. Hukuchi, Y. Shimizu, K. Fukushima, N. Sugioka, A. Nishimura, N. Shibata, Preparation and pharmaceutical evaluation of nano-fiber matrix supported drug delivery system using the solvent-based electrospinning method, Int. J. Pharm. 464 (2014) 243–251. doi:10.1016/j.ijpharm.2013.12.036.

[28] X. Shen, D. Yu, L. Zhu, C. Branford-White, K. White, N.P. Chatterton, Electrospun diclofenac sodium loaded Eudragit® L 100-55 nanofibers for colon-targeted drug delivery, Int. J. Pharm. 408 (2011) 200–207. doi:10.1016/j.ijpharm.2011.01.058.

[29] L.E. Aguilar, A.R. Unnithan, A. Amarjargal, A.P. Tiwari, S.T. Hong, C.H. Park, C.S. Kim, Electrospun polyurethane/Eudragit® L100-55 composite mats for the pH dependent release of paclitaxel on duodenal stent cover application, Int. J. Pharm. 478 (2015) 1–8. doi:10.1016/j.ijpharm.2014.10.057.

[30] M. Jin, D.-G. Yu, X. Wang, C.F.G.C. Geraldes, G.R. Williams, S.W.A. Bligh, Electrospun Contrast-Agent-Loaded Fibers for Colon-Targeted MRI, Adv. Healthc.

Mater. 5 (2016) 977–985. doi:10.1002/adhm.201500872.
[31] C.J.H. Davitt, E.C. Lavelle, Delivery strategies to enhance oral vaccination against enteric infections, Adv. Drug Deliv. Rev. 91 (2015) 52–69. doi:10.1016/j.addr.2015.03.007.
[32] A.A. Date, J. Hanes, L.M. Ensign, Nanoparticles for oral delivery: Design, evaluation and state-of-the-art, J. Control. Release. 240 (2016) 504–526. doi:10.1016/j.jconrel.2016.06.016.
[33] Y. Ilan, Oral immune therapy: targeting the systemic immune system via the gut immune system for the treatment of inflammatory bowel disease, Clin. Transl. Immunol. 5 (2016) e60. doi:10.1038/cti.2015.47.
[34] Y. Li, A. Hongliang, J. Ae, K. Zhu, Encapsulation and controlled release of lysozyme from electrospun poly(e-caprolactone)/poly(ethylene glycol) non-woven membranes by formation of lysozyme–oleate complexes, (2007). doi:10.1007/s10856-007-3175-6.
[35] Y. Dai, J. Niu, J. Liu, L. Yin, J. Xu, In situ encapsulation of laccase in microfibers by emulsion electrospinning: Preparation, characterization, and application, Bioresour. Technol. 101 (2010) 8942–8947. doi:10.1016/j.biortech.2010.07.027.
[36] T.G. Kim, D.S. Lee, T.G. Park, Controlled protein release from electrospun biodegradable fiber mesh composed of poly(ε-caprolactone) and poly(ethylene oxide), Int. J. Pharm. 338 (2007) 276–283. doi:10.1016/j.ijpharm.2007.01.040.
[37] W. Ji, F. Yang, J.J.J.P. Van Den Beucken, Z. Bian, M. Fan, Z. Chen, J.A. Jansen, Fibrous scaffolds loaded with protein prepared by blend or coaxial electrospinning, Acta Biomater. 6 (2010) 4199–4207. doi:10.1016/j.actbio.2010.05.025.
[38] P. Peh, N.S.J. Lim, A. Blocki, S.M.L. Chee, H.C. Park, S. Liao, C. Chan, M. Raghunath, Simultaneous Delivery of Highly Diverse Bioactive Compounds from Blend Electrospun Fibers for Skin Wound Healing, Bioconjug. Chem. 26 (2015) 1348–1358. doi:10.1021/acs.bioconjchem.5b00123.
[39] Y. Yang, X. Li, M. Qi, S. Zhou, J. Weng, Release pattern and structural integrity of lysozyme encapsulated in core-sheath structured poly(dl-lactide) ultrafine fibers prepared by emulsion electrospinning, Eur. J. Pharm. Biopharm. 69 (2008) 106–116. doi:10.1016/j.ejpb.2007.10.016.
[40] Y. Yang, X. Li, S. He, L. Cheng, F. Chen, S. Zhou, J. Weng, Biodegradable ultrafine fibers with core-sheath structures for protein delivery and its optimization, Polym. Adv. Technol. 22 (2011) 1842–1850. doi:10.1002/pat.1681.
[41] Y. Yang, X. Li, W. Cui, S. Zhou, R. Tan, C. Wang, Structural stability and release profiles of proteins from core-shell poly (DL-lactide) ultrafine fibers prepared by emulsion electrospinning, J. Biomed. Mater. Res. - Part A. 86 (2008) 374–385. doi:10.1002/jbm.a.31595.
[42] J. Karttunen, S. Sanderson, N. Shastri, Detection of rare antigen-presenting cells by the lacZ T-cell activation assay suggests an expression cloning strategy for T-cell antigens., Proc. Natl. Acad. Sci. U. S. A. 89 (1992) 6020–4. doi:10.1073/pnas.89.13.6020.
[43] A.M. Azevedo, V.C. Martins, D.M.F. Prazeres, V. Vojinović, J.M.S. Cabral, L.P. Fonseca, Horseradish peroxidase: A valuable tool in biotechnology, Biotechnol. Annu. Rev. 9 (2003) 199–247. doi:10.1016/S1387-2656(03)09003-3.
[44] J.L. Millán, Alkaline Phosphatases : Structure, substrate specificity and functional relatedness to other members of a large superfamily of enzymes., Purinergic Signal. 2 (2006) 335–41. doi:10.1007/s11302-005-5435-6.

[45] M. Di Marco, S. Shamsuddin, K.A. Razak, A.A. Aziz, C. Devaux, E. Borghi, L. Levy, C. Sadun, Overview of the main methods used to combine proteins with nanosystems: Absorption, bioconjugation, and encapsulation, Int. J. Nanomedicine. 5 (2010) 37–49. doi:10.2147/IJN.S6458.

[46] J.-P. Colletier, B. Chaize, M. Winterhalter, D. Fournier, Protein encapsulation in liposomes: efficiency depends on interactions between protein and phospholipid bilayer, BMC Biotechnol. 2 (2002) 9. doi:10.1186/1472-6750-2-9.

[47] D.A. Nguyen, H.S. Fogler, Facilitated diffusion in the dissolution of carboxylic polymers, AIChE J. 51 (2005) 415–425. doi:10.1002/aic.10329.

[48] D.F. Evans, G. Pye, R. Bramley, A.G. Clark, T.J. Dyson, J.D. Hardcastle, Measurement of gastrointestinal pH profiles in normal ambulant human subjects, Gut. 29 (1988) 1035–1041. doi:10.1136/gut.29.8.1035.

[49] M.T. Cook, G. Tzortzis, D. Charalampopoulos, V. V. Khutoryanskiy, Microencapsulation of probiotics for gastrointestinal delivery, J. Control. Release. 162 (2012) 56–67. doi:10.1016/j.jconrel.2012.06.003.

[50] E.L. McConnell, H.M. Fadda, A.W. Basit, Gut instincts: Explorations in intestinal physiology and drug delivery, Int. J. Pharm. 364 (2008) 213–226. doi:10.1016/j.ijpharm.2008.05.012.

[51] S.F. Chou, D. Carson, K.A. Woodrow, Current strategies for sustaining drug release from electrospun nanofibers, J. Control. Release. 220 (2015) 584–591. doi:10.1016/j.jconrel.2015.09.008.

[52] N. Han, P.A. Bradley, J. Johnson, K.S. Parikh, A. Hissong, M.A. Calhoun, J.J. Lannutti, J.O. Winter, Effects of hydrophobicity and mat thickness on release from hydrogel-electrospun fiber mat composites, J. Biomater. Sci. Polym. Ed. 24 (2013) 2018–2030. doi:10.1080/09205063.2013.822246.

[53] P. Tipduangta, P. Belton, L. Fábián, L.Y. Wang, H. Tang, M. Eddleston, S. Qi, Electrospun Polymer Blend Nanofibers for Tunable Drug Delivery: The Role of Transformative Phase Separation on Controlling the Release Rate, Mol. Pharm. 13 (2016) 25–39. doi:10.1021/acs.molpharmaceut.5b00359.

[54] J.M.F. Jabal, L. McGarry, A. Sobczyk, D.E. Aston, Substrate effects on the wettability of electrospun titania- poly(vinylpyrrolidone) fiber mats, Langmuir. 26 (2010) 13550–13555. doi:10.1021/la1017399.

[55] S.K. Lai, Y.Y. Wang, J. Hanes, Mucus-penetrating nanoparticles for drug and gene delivery to mucosal tissues, Adv. Drug Deliv. Rev. 61 (2009) 158–171. doi:10.1016/j.addr.2008.11.002.

[56] J.K. Tessmar, A.M. Göpferich, Matrices and scaffolds for protein delivery in tissue engineering, Adv. Drug Deliv. Rev. 59 (2007) 274–291. doi:10.1016/j.addr.2007.03.020.

[57] B. Kim, N.A. Peppas, In vitro release behavior and stability of insulin in complexation hydrogels as oral drug delivery carriers, Int. J. Pharm. 266 (2003) 29–37. doi:10.1016/S0378-5173(03)00378-8.

[58] A. Makhlof, Y. Tozuka, H. Takeuchi, Design and evaluation of novel pH-sensitive chitosan nanoparticles for oral insulin delivery, Eur. J. Pharm. Sci. 42 (2011) 445–451. doi:10.1016/j.ejps.2010.12.007.

[59] A. Kumar, C. Montemagno, H.-J. Choi, Smart Microparticles with a pH-responsive Macropore for Targeted Oral Drug Delivery, Sci. Rep. 7 (2017) 3059. doi:10.1038/s41598-

017-03259-x.
[60] Y. Zhang, W. Wei, P. Lv, L. Wang, G. Ma, Preparation and evaluation of alginate-chitosan microspheres for oral delivery of insulin, Eur. J. Pharm. Biopharm. 77 (2011) 11–19. doi:10.1016/j.ejpb.2010.09.016.
[61] G. Fuhrmann, A. Grotzky, R. Lukić, S. Matoori, P. Luciani, H. Yu, B. Zhang, P. Walde, A.D. Schlüter, M.A. Gauthier, J.-C. Leroux, Sustained gastrointestinal activity of dendronized polymer–enzyme conjugates, Nat. Chem. 5 (2013) 582–589. doi:10.1038/nchem.1675.
[62] K.M. Turner, G. Pasut, F.M. Veronese, A. Boyce, G. Walsh, Stabilization of a supplemental digestive enzyme by post-translational engineering using chemically-activated polyethylene glycol, Biotechnol. Lett. 33 (2011) 617–621. doi:10.1007/s10529-010-0474-7.
[63] S. Frokjaer, D.E. Otzen, Protein drug stability: a formulation challenge., Nat. Rev. Drug Discov. 4 (2005) 298–306. doi:10.1038/nrd1695.
[64] W.F. Weiss IV, T.M. Young, C.J. Roberts, Principles, approaches, and challenges for predicting Protein Aggregation Rates and Shelf Life, J. Pharm. Sci. 98 (2009) 1246–1277. doi:10.1002/jps.21521.
[65] E.Y. Chi, S. Krishnan, T.W. Randolph, J.F. Carpenter, Physical stability of proteins in aqueous solution: Mechanism and driving forces in nonnative protein aggregation, Pharm. Res. 20 (2003) 1325–1336. doi:10.1023/A:1025771421906.
[66] S. Ramachandran, E. Fu, B. Lutz, P. Yager, Long-term dry storage of an enzyme-based reagent system for ELISA in point-of-care devices., Analyst. 139 (2014) 1456–62. doi:10.1039/c3an02296j.
[67] F.M. Cruz, J.D. Colbert, E. Merino, B.A. Kriegsman, K.L. Rock, The Biology and Underlying Mechanisms of Cross-Presentation of Exogenous Antigens on MHC-I Molecules, Annu. Rev. Immunol. 35 (2017) 149–76. doi:10.1146/annurev-immunol.
[68] C. Zhang, J. Zhang, G. Shi, H. Song, S. Shi, X. Zhang, P. Huang, Z. Wang, W. Wang, C. Wang, D. Kong, C. Li, A Light Responsive Nanoparticle-Based Delivery System Using Pheophorbide A Graft Polyethylenimine for Dendritic Cell-Based Cancer Immunotherapy, Mol. Pharm. 14 (2017) 1760–1770. doi:10.1021/acs.molpharmaceut.7b00015.
[69] R.A. Rosalia, E.D. Quakkelaar, A. Redeker, S. Khan, M. Camps, J.W. Drijfhout, A.L. Silva, W. Jiskoot, T. van Hall, P.A. van Veelen, G. Janssen, K. Franken, L.J. Cruz, A. Tromp, J. Oostendorp, S.H. van der Burg, F. Ossendorp, C.J.M. Melief, Dendritic cells process synthetic long peptides better than whole protein, improving antigen presentation and T-cell activation, Eur. J. Immunol. 43 (2013) 2554–2565. doi:10.1002/eji.201343324.
[70] K.E. Knockenhauer, K.M. Sawicka, E.J. Roemer, S.R. Simon, Protective antigen composite nanofibers as a transdermal anthrax vaccine., in: Annu. Int. Conf. IEEE Eng. Med. Biol. Soc., 2008: pp. 1040–1043. doi:10.1109/IEMBS.2008.4649337.
[71] K.J. McHugh, T.D. Nguyen, A.R. Linehan, D. Yang, A.M. Behrens, S. Rose, Z.L. Tochka, S.Y. Tzeng, J.J. Norman, A.C. Anselmo, X. Xu, S. Tomasic, M.A. Taylor, J. Lu, R. Guarecuco, R. Langer, A. Jaklenec, Fabrication of fillable microparticles and other complex 3D microstructures, Science (80-.). 357 (2017) 1138–1142. doi:10.1126/science.aaf7447.
[72] P.N. Shastri, M.C. Kim, F.S. Quan, M.J. D'Souza, S.M. Kang, Immunogenicity and protection of oral influenza vaccines formulated into microparticles, J. Pharm. Sci. 101

(2012) 3623–3635. doi:10.1002/jps.23220.
[73] S. Raychaudhuri, K.L. Rock, Fully mobilizing host defense: building better vaccines, Nat.Biotechnol. 16 (1998) 1025–1031. doi:10.1038/3469.
[74] H. Shen, A.L. Ackerman, V. Cody, A. Giodini, E.R. Hinson, P. Cresswell, R.L. Edelson, W.M. Saltzman, D.J. Hanlon, Enhanced and prolonged cross-presentation following endosomal escape of exogenous antigens encapsulated in biodegradable nanoparticles, Immunology. 117 (2006) 78–88. doi:10.1111/j.1365-2567.2005.02268.x.
[75] J. Chen, Z. Li, H. Huang, Y. Yang, Q. Ding, J. Mai, W. Guo, Y. Xu, Improved antigen cross-presentation by polyethyleneimine-based nanoparticles, Int. J. Nanomedicine. 6 (2011) 77–84. doi:10.2147/IJN.S15457.
[76] J.T. Wilson, S. Keller, M.J. Manganiello, C. Cheng, C.C. Lee, C. Opara, A. Convertine, P.S. Stayton, PH-responsive nanoparticle vaccines for dual-delivery of antigens and immunostimulatory oligonucleotides, ACS Nano. 7 (2013) 3912–3925. doi:10.1021/nn305466z.
[77] J.J. Moon, H. Suh, A. Bershteyn, M.T. Stephan, H. Liu, B. Huang, M. Sohail, S. Luo, S.H. Um, H. Khant, J.T. Goodwin, J. Ramos, W. Chiu, D.J. Irvine, Interbilayer-crosslinked multilamellar vesicles as synthetic vaccines for potent humoral and cellular immune responses., Nat. Mater. (2011). doi:10.1038/nmat2960.
[78] H. Frizzell, J. Park, N. Comandante Lou, K.A. Woodrow, Role of heterogeneous cell population on modulation of dendritic cell phenotype and activation of CD8 T cells for use in cell-based immunotherapies, Cell. Immunol. 311 (2017) 54–62. doi:10.1016/j.cellimm.2016.10.004.
[79] P. Nair-Gupta, A. Baccarini, N. Tung, F. Seyffer, O. Florey, Y. Huang, M. Banerjee, M. Overholtzer, P.A. Roche, R. Tampé, B.D. Brown, D. Amsen, S.W. Whiteheart, J.M. Blander, TLR signals induce phagosomal MHC-I delivery from the endosomal recycling compartment to allow cross-presentation., Cell. 158 (2014) 506–21. doi:10.1016/j.cell.2014.04.054.
[80] J.R. Turner, Intestinal mucosal barrier function in health and disease, Nat. Rev. Immunol. 9 (2009) 799–809. doi:10.1038/nri2653.
[81] L.M. Ensign, R. Cone, J. Hanes, Oral drug delivery with polymeric nanoparticles: The gastrointestinal mucus barriers, Adv. Drug Deliv. Rev. 64 (2012) 557–570. doi:10.1016/j.addr.2011.12.009.
[82] J.D. Smart, The basics and underlying mechanisms of mucoadhesion, Adv. Drug Deliv. Rev. 57 (2005) 1556–1568. doi:10.1016/j.addr.2005.07.001.
[83] G. Flemström, A. Hällgren, O. Nylander, L. Engstrand, E. Wilander, A. Allen, Adherent surface mucus gel restricts diffusion of macromolecules in rat duodenum in vivo, Am. J. Physiol. Liver Physiol. 277 (1999) G375–G382. doi:10.1152/ajpgi.1999.277.2.G375.
[84] K. Khanvilkar, M.D. Donovan, D.R. Flanagan, Drug transfer through mucus, Adv. Drug Deliv. Rev. 48 (2001) 173–193. doi:10.1016/S0169-409X(01)00115-6.
[85] S. Lee, M. Müller, K. Rezwan, N.D. Spencer, Porcine gastric mucin (PGM) at the water/poly(dimethylsiloxane) (PDMS) interface: Influence of pH and ionic strength on its conformation, adsorption, and aqueous lubrication properties, Langmuir. 21 (2005) 8344–8353. doi:10.1021/la050779w.
[86] C.E. Wagner, B.S. Turner, G.H. Mckinley, K. Ribbeck, A perturbation study of the structure and association dynamics of MUC5AC gels, Biomacromolecules. (2017) 1–22.

doi:10.1021/acs.biomac.7b00809.

[87] S. Eaimtrakarn, Y. Itoh, J. ichi Kishimoto, Y. Yoshikawa, N. Shibata, K. Takada, Retention and transit of intestinal mucoadhesive films in rat small intestine, Int. J. Pharm. 224 (2001) 61–67. doi:10.1016/S0378-5173(01)00738-4.

[88] J.S. Quan, H.L. Jiang, E.M. Kim, H.J. Jeong, Y.J. Choi, D.D. Guo, M.K. Yoo, H.G. Lee, C.S. Cho, pH-sensitive and mucoadhesive thiolated Eudragit-coated chitosan microspheres, Int. J. Pharm. 359 (2008) 205–210. doi:10.1016/j.ijpharm.2008.04.003.

[89] Y.Y. Zhang, X. Wu, L. Meng, R. Ai, N. Qi, H. He, H. Xu, X. Tang, Thiolated Eudragit nanoparticles for oral insulin delivery: preparation, characterization and in vivo evaluation., Int. J. Pharm. 436 (2012) 341–50. doi:10.1016/j.ijpharm.2012.06.054.

[90] A. Bernkop-Schnürch, A. Greimel, Thiomers: The next generation of mucoadhesive polymers, Am. J. Drug Deliv. 3 (2005) 141–154. doi:10.2165/00137696-200503030-00001.

[91] F. Brako, B. Raimi-Abraham, S. Mahalingam, D.Q.M. Craig, M. Edirisinghe, Making nanofibres of mucoadhesive polymer blends for vaginal therapies, Eur. Polym. J. 70 (2015) 186–196. doi:10.1016/j.eurpolymj.2015.07.006.

[92] G. Mythri, K. Kavitha, M.R. Kumar, S.D. Jagadeesh Singh, Novel mucoadhesive polymers- A review, J. Appl. Pharm. Sci. 1 (2011) 37–42.

Chapter 4. MUCOSAL ADJUVANTS TO ENHANCE IMMUNE RESPONSES TO ORAL VACCINES

Portions adapted from: **Frizzell, H.**, Park, J., & Woodrow, K. A. Activation of intestinal $CD8^+$ T cells by an oral vaccine through nanofiber-mediated gastric protection of epitopes and the mucosal adjuvant PEI. *Manuscript in preparation.*

4.1 Abstract

The elicitation of immunity at mucosal surfaces is challenging due to low antigen absorption and the propensity for regulatory immune responses against the delivered antigen. While oral vaccination can elicit mucosal immunity, which is necessary for protection from many pathogens that infect the body at these surfaces, protein-based vaccines suffer at this anatomical site due to aforementioned challenges. The use of mucosal adjuvants can both recruit cell populations to enhance antigen internalization and activate mucosal immune cells, shifting immunity from regulatory to protective. Here, we evaluate a library of adjuvants *in vitro* and *in vivo* for their ability to stimulate intestinal immune cells, modulate vaccine uptake, and elicit adaptive immune responses when used in an oral vaccine. We observe the adjuvants CpG and PEI to activate epithelial cells to produce the chemokine, CCL20. PEI, but not CpG, increased protein uptake in dendritic cells and epithelial cells *in vitro*. While efforts to quantify antigen uptake in intestinal antigen presenting cell populations *in vivo* proved challenging, oral immunization studies reveal differential action of adjuvants in eliciting systemic and mucosal immune responses. Compared to known mucosal adjuvant cholera toxin and clinical adjuvant monophosphoryl lipid A (MPLA), CpG in the vaccine formulation enhanced systemic and mucosal antibodies as well as $CD4^+$ T cells. Cytotoxic $CD8^+$ T

cell responses were induced with PEI, while the ability to activate $CD8^+$ T cells was limited by other adjuvants. These differences may be due to the observed effects on epithelial cell activation and protein uptake. Overall, this work identifies novel mucosal adjuvants that can be used to elicit humoral or cellular immune responses to oral vaccines.

4.2 Introduction

In Chapter 3, Eudragit L100 nanofibers loaded with proteins were fabricated such that the proteins maintained their activity during the encapsulation process, were protected from deactivation in simulated gastric conditions, and were released into the small intestine in response to a change in pH. These materials allow for the vaccine antigen to overcome the first barrier, the degradative conditions in the stomach, through protection in gastric conditions followed by delivery of bioactive protein in the small intestine. This chapter reports of efforts to overcome additional barriers to oral protein delivery, namely limited protein absorption in the small intestine and the bias for tolerogenic immune responses [1].

Subunit vaccines commonly rely on the presence of adjuvants to amplify immune responses to the antigen. This is especially critical for mucosal vaccines, as activation of adaptive immunity is more difficult at these surfaces due to their constant exposure to external substances, resulting in more tolerogenic immune responses [2]. While potent adjuvants have been identified for parenteral vaccines, mucosal adjuvants have different requirements. Parenteral vaccines directly access cells in the tissue, including antigen-presenting cells (APCs). In contrast, mucosally-delivered vaccines first encounter cells of the epithelium. It is known that APCs and epithelial cells (ECs) express different pattern recognition receptors (PRRs) that adjuvants antagonize. PRR expression also depends on the anatomical location of the cells. Thus, adjuvants that function through APC-expressed PRRs may not demonstrate activity at mucosal surfaces due to this differential expression.

Here, we evaluate the ability of adjuvants to activate intestinal epithelial cells. Adjuvant-mediated activation of epithelial cells is also necessary to overcome oral tolerance. In the gut, dendritic cells (DCs) are conditioned to be tolerogenic by signals that epithelial cells secrete constitutively, such as the cytokines TGF-β and IL-10 and the metabolite retinoic acid [3]. DC secretion of these retinoic acid and TGF-β results in T_{reg} differentiation of naïve antigen-specific T cells [4]. To achieve activation of helper type-1 (T_H1) T cell responses, APCs must produce a different panel of cytokines during antigen presentation, such as IL-12 and IL-23. Signals secreted by epithelial cells, particularly IL-15, can control APCs to produce such inflammatory cytokines and activate immunity rather than tolerance to dietary antigens [5]. Thus, adjuvant selection has the potential to activate epithelial cells such that signaling is shifted from tolerogenic to inflammatory.

In addition to immune stimulation, it is also possible for adjuvants to influence vaccine uptake at the intestinal epithelium. Transport of orally delivered proteins is thought to occur primarily through the specialized intestinal M cells and Goblet cells along the epithelium. In addition to epithelial cells, antigen presenting cells can be recruited to the epithelium and extend trans-epithelial dendrites (TEDs) to sample luminal antigens [6]. Insights from the field of mucosal immunology have identified a mechanism of enhanced DC sampling of antigen from the intestinal lumen that is dependent on crosstalk between epithelial cells and DCs [7]. Increase of TED formation by DCs is enhanced through the delivery of toll-like receptor (TLR) ligands [8]. Additionally, oral delivery of the adjuvant CpG ODN induced the production of the DC-recruiting chemokine CCL20 that increased TEDs formation at these CCL20-rich regions [9]. It is of note that in this study by Yin *et al.*, the vaccine antigen utilized was a whole inactivated influenza virus that was directly administered into the ileum of the small intestine [9]. CCL20-mediated DC recruitment can also influence $CD8^+$ T cell responses [10] that differentiate into cytotoxic T lymphocytes in order to directly kill pathogen-infected cells [11].

Thus, in this chapter we characterize select adjuvants for use in oral vaccines with a focus on epithelial cell signaling. Adjuvant-induced DC recruitment is proposed as a new strategy to enhance uptake and efficacy of orally delivered vaccines. Results show that adjuvants with different mechanisms of cellular stimulation had distinct differences in activation of adaptive immune responses when used in oral protein vaccines. Preliminary experiments suggest that the ability to modulate epithelial cell signaling and antigen uptake may drive the mucosal activity of certain adjuvants. In pilot experiments, we observe the rapid expansion of $MHCII^{+}$ cells in the small intestinal epithelium and different DC populations in the lymph nodes when certain adjuvants are used, identifying a potential mechanism to enhance adaptive immune responses.

4.3 Materials and Methods

4.3.1 *Materials*

Albumin–fluorescein isothiocyanate conjugate (FITC-BSA), N,N-Dimethylformamide (DMF) (anhydrous, 99.8%), sodium bicarbonate, Tris-HCl, and branched polyethyleneimine (PEI) (25 kDa) was purchased from Sigma-Aldrich (St. Louis, MO, USA). Bovine serum albumin (BSA), trypsin-EDTA (0.25%), and HEPES sodium salt was purchased from Thermo Fisher Scientific (Waltham, MA, USA). Dulbecco's Phosphate-Buffered Saline (PBS) was purchased from Corning Inc. (Corning, NY, USA). Ovalbumin (OVA) was purchased from InvivoGen (San Diego, CA, USA). Sodium chloride (NaCl) was purchased from EMD Millipore (Gibbstown, NJ, USA). (Ethylenedinitrilo)tetraacetic acid, disodium salt, dehydrate (EDTA) was purchased from Avantor Performance Materials (Center Valley, PA, USA). Caco-2 cells were kindly provided by the lab of Suzie Pun (University of Washington) and DC2.4 cells and B3Z cells were kindly provided by the lab of James Lai (University of Washington).

4.3.2 *Adjuvant treatment of epithelial cells in vitro*

Caco-2 cells were seeded at 50,000 cells per well in 12-well plates (Corning) in DMEM (Thermo) with 20% heat-inactivated fetal bovine serum, sodium pyruvate, non-essential amino acids, penicillin/streptomycin (all from Invitrogen, Carlsbad, CA), and L-glutamine (Cellgro, Manassas, VA) and grown in a 37 °C incubator (5% CO_2, 95% relative humidity) for four days. Medium was removed and replaced with fresh medium or medium with monophosphoryl lipid A (MPLA) (1 μg mL^{-1}), CpG ODN 1826 (50 μg mL^{-1}), 5'ppp-ds RNA (1 μg mL^{-1}), peptidoglycan from *B. subtilis* (10 μg mL^{-1}), muramyl dipeptide (10 μg mL^{-1}), flagellin from *B. subtilis* (10 μg mL^{-1}), lipopolysaccharide (LPS) (10 μg mL^{-1}) (all from Invivogen), polyethyleneimine (10 μg mL^{-1}) (Sigma), cholera toxin from *Vibrio cholerae* (10 μg mL^{-1}) (Sigma), or human IL-1β (10 ng mL^{-1}) (PeproTech, Rocky Hill, NJ, USA). After 72 hours, the supernatant was removed and assayed for production of CCL20 using a sandwich ELISA developed in-house. Briefly, a flat non-tissue culture treated 96-well plate (Corning) was coated with mouse anti-human CCL20 (PeproTech) at 1 μg mL^{-1} and incubated overnight at room temperature. The plate was washed with wash buffer (PBS with 0.05% Tween 20) and blocked with 1% BSA for 1 hour at room temperature. Following plate washing, recombinant human CCL20 standards (1,500 – 2 pg mL^{-1}) (PeproTech) and conditioned medium samples were added and incubated for 2 hours at room temperature. Samples were removed, the plate was washed, and biotinylated rabbit anti-human CCL20 (PeproTech) was added to each well. After a 2-hour incubation, the plate was washed and streptavidin-HRP (R&D Systems) was added for 30 minutes. A final plate washing was performed and TMB substrate (R&D Systems) was added to each well. To stop the reaction, ELISA stop solution (R&D Systems) was added. The plate was read at 570 nm using a reference wavelength of 450 nm with a Tecan Infinite 200 PRO microplate reader (Tecan, Männedorf, Switzerland). Concentrations of CCL20 in each sample were determined from a standard curve.

4.3.3 *Antigen uptake by epithelial and dendritic cells in vitro*

DC2.4 and Caco-2 cells were seeded at 100,000 and 50,000 per well, respectively, in 24-well plates overnight. Cells were treated with FITC-BSA (10 μg mL^{-1}) only or with polyethyleneimine (10 μg mL^{-1}), CpG ODN 1826 (10 μg mL^{-1}), or IL-1β (10 μg mL^{-1}) for 4 hours. To compare the differences in uptake of BSA in soluble versus a particulate form, FITC-BSA was complexed with polyethyleneimine at PEI:BSA 1:1 (m:m) and vortexed for 30 seconds. Cells were then treated with soluble FITC-BSA, FITC-BSA/PEI complexes, or FITC-BSA+PEI for 4 hours. Cells were then washed, detached, stained with Live/Dead Fixable Violet (Thermo Fisher Scientific), fixed in 1.6% PFA, and analyzed by flow cytometry using a CantoII for FITC-BSA uptake in the live population. Flow cytometry analysis was performed using FlowJo software (Treestar).

4.3.4 *In vivo studies*

4.3.4.1 Animals

Female C57Bl/6J and OT-II mice (6-8 weeks old) were purchased from The Jackson Laboratory. Animal studies were approved by the Institutional Animal Care and Use Committee (IACUC) at the University of Washington. All animals were cared for in accordance with IACUC guidelines.

4.3.4.2 Dendritic cell migration time course

Age-matched female C56Bl/6J were immunized with OVA (1 mg) with or without an adjuvant cocktail of CT (10 μg), CpG (50 μg), and PEI (50 μg) in 200 μL by oral gavage using a 22G metal gavage needle. At indicated time points, mice were sacrificed and mesenteric lymph nodes and small intestines were collected. Organs were processed as described below and analyzed by flow cytometry.

4.3.4.3 Antigen uptake and immunohistochemistry

Age-matched female C56Bl/6J were immunized with BSA-FITC (1 - 10 mg) with or without CT (10 µg) in 200 µL by oral gavage using a 22G metal gavage needle. At indicated time points, mice were sacrificed and mesenteric lymph nodes and small intestines were collected. Organs were processed as described below and analyzed by flow cytometry. In some experiments, small intestines were collected for analysis by immunohistochemistry. Small intestines were flushed with PBS, cut open longitudinally, and incubated with paraformaldehyde (4%) for 20 minutes at room temperature. Small intestines were washed and incubated in sucrose (30%) for 1.5 hours at room temperature. Small intestines were rolled and snap-frozen in OCT compound (Thermo). Cross sections (20 µm thick) were prepared by the Histology and Imaging Core at the University of Washington. Sections were dried then cold acetone (-20°C) was added and allowed to evaporate. Sections were washed in Tris-buffered saline (50 mM Tris-Cl, 150 mM NaCl, pH 7.5), blocked with 1% BSA for 30 minutes at room temperature, and incubated with hamster anti-mouse CD11c-N418 (20 µg mL^{-1}) (eBioscience) overnight at 4°C. After washing, sections were incubated with rabbit anti-hamster IgG-TRITC (5 µg mL^{-1}) (Thermo) for 1 hour at room temperature followed by mounting in Fluoromount-G with DAPI (Thermo). Tissue sections were imaged using a Nikon Eclipse Ti microscope (Nikon, Melville, NY, USA) equipped with an Andor (model number DR-328G-C01-SIL) fluorescence camera (Andor, Belfast, UK).

4.3.4.4 Activation of $CD4^+$ T cells by DCs isolated from orally immunized mice

Age-matched female C56Bl/6J were immunized with OVA (1 mg) with CT (20 µg) in 200 µL by oral gavage using a 22G metal gavage needle. Twenty-four hours later, mice were sacrificed and mesenteric lymph nodes and small intestines were collected. Organs

were processed into single cell suspensions as described below and enriched for $CD11c^+$ cells by positive selection using CD11c microbeads (Miltenyi Biotec, Auburn, CA, USA). $CD11c^+$ cells were seeded in U-bottom 96-well plates at 20,000 cells per well. As a positive control, exogenous OVA (20 µg) with LPS (2 µg mL^{-1}) were individually added to some wells. After 24 hours, $CD11c^+$ DCs were washed and co-cultured with CFSE-stained $CD4^+$ T cells from OT-II spleens. Briefly, spleens were collected and digested in Collagenase D (1 mg mL^{-1}) with DNaseI (40 µg mL^{-1}) at 37 °C for 30 min. Spleens were passed through a 70 µm cell strainer, washed with PBS, and red blood cells were lysed. $CD4^+$ T cells were isolated by negative selection using a $CD4^+$ T cell isolation kit (Miltenyi). $CD4^+$ T cells were stained with CFSE (10 µM) in 1% BSA/PBS at 37 °C for 10 min followed by quenching on ice. CFSE-stained $CD4^+$ T cells were added to DCs at DC:T 1:1 and 1:10. Three days later, plates were centrifuged and supernatant was collected for analysis of cytokine production by ELISA (PeproTech IFN-γ ELISA kit following manufacturer's instructions). Cells were incubated with Fc block (anti-mouse CD16/CD32) for 5 min at 4 °C followed by surface staining for 40 min at 4 °C. Cells were washed and stained with LIVE/DEAD Fixable Violet Dead Cell Stain (Thermo) on ice for 20 min. Cells were washed, resuspended in FACS buffer, fixed in 2% PFA/PBS, and analyzed by flow cytometry on a LSRII. Flow cytometry analysis was performed using FlowJo software.

4.3.4.5 Oral immunizations to evaluate adaptive immune responses

Age-matched female C56Bl/6J were immunized with OVA (1 mg) with or without CT (10 µg), MPLA (20 µg), branched PEI (200 µg), or CpG ODN 1826 (100 µg) in 200 µL by oral gavage using a 22G metal gavage needle. These doses were chosen based on demonstrated efficacy when used orally (CT, CpG, MPLA) or at another mucosal surface (PEI). Animals were not fasted prior to immunization nor were anesthetized during the procedure. The immunization schedule consisted of immunizations every 4 weeks for a total of 3-4 doses.

4.3.4.6 Fluid collection and enzyme-linked immunosorbent assays (ELISAs)

Blood was collected biweekly from the submental vein and serum was isolated by centrifugation and stored at -20°C until analysis. The small intestine was washed with 5 mL PBS with 0.1 mg mL^{-1} trypsin inhibitor (Sigma) and 50 mM EDTA. Intestinal lavage fluid was vortexed and centrifuged at 2,000 x g for 30 min at 4°C. Supernatant was collected and stored at -20°C until analysis. Antigen-specific IgG and IgA antibodies were assayed from serum and intestinal lavage by ELISA. OVA in 10 mM sodium bicarbonate (2 µg mL^{-1}) was used to coat well of immunoassay ELISA plates (Costar) at 4°C overnight. Plates were washed with PBS with 1% Tween-20 (PBS-T) and blocked with 2% bovine serum albumin (BSA) in PBS-T for 2 hours at room temperature. Plates were washed with PBS-T and incubated with samples starting at 1:100 dilution for serum and 1:10 dilution for intestinal lavage and incubated at 37°C for 2 hours. Samples were also added at equivalent dilutions to wells without OVA to identify background signal for each sample. Plates were washed and incubated with HRP-conjugated goat anti-mouse IgG (Thermo) or goat anti-mouse IgA (Thermo) (1:2000 dilution) for 2 hours at 37°C. Plates were washed and incubated with TMB substrate (BioLegend) for 1 hour at room temperature. Plates were read at 605 nm. Titers were determined as the inverse dilution that was 2-fold higher than blank absorbance value.

4.3.4.7 Organ processing and flow cytometry analysis

Organs were harvested 14 days after the last immunization and processed to generate single cell suspensions as follows. Spleens were collected and processed through a 40 µm cell strainer followed by red blood cell lysis. Mesenteric lymph nodes were collected and processed through a 40 µm cell strainer. The small intestine was collected and flushed as described above to collect the luminal contents. Peyer's patches and remaining mucus was subsequently removed followed by opening of the intestine longitudinally and processing into 1 cm fragments. Small intestinal fragments were

incubated in 0.15 mg mL^{-1} 1,4-dithioerythritol (DTE) (Sigma) in complete HBSS (10 mM HEPES, 25 mM Na bicarbonate, 20% FBS) for 30 minutes at 37°C with lateral shaking (230 rpm) followed by collection of intraepithelial lymphocytes (SI-IEL) through a 100 µm cell strainer. SI-IELs were washed with HBSS and further purified by density gradient centrifugation with a 44%/77% Percoll (GE Healthcare) gradient. Small intestinal tissue fragments were recollected following SI-IEL release, washed to remove remaining DTE, and digested with 1 mg mL^{-1} Collagenase VIII in RPMI 1640 with 40 µg mL^{-1} DNase I (Sigma) for 45 minutes at 37°C with lateral shaking (230 rpm). Small intestinal lamina propria (SI-LP) cells were collected through a through a 100 µm cell strainer and purified by density gradient centrifugation as described for SI-IELs. Single cells suspensions were incubated with Fc block and LIVE/DEAD Fixable Near-IR Dead Cell Stain (Thermo) for 15 min at room temperature. Cells were washed and stained with surface antibodies for 30 min at 4°C. The following surface antibodies were used in these studies: anti-mouse CD45-FITC (30-F11), CD45-Alexa700 (30-F11), CD11c-APC (N418), CD11c-PerCP/Cy5.5 (N418), I-A/I-E-PerCP/Cy5.5 (M5/114.15.2), CD86-BV510 (GL-1), CD86-BV605 (GL-1), H-2Kb bound to SIINFEKL Antibody-PE/Cy7 (25-D1.16), CD11b-BV711 (M1/70), CD103-PE (2E7), CCR7-PE/Cy7 (4B12), CD3-Alexa700 (17A2), CD4-BV605 (RM4-5), CD4-APC (GK1.5), CD8α-BV510 (53-6.7), CD8α-FITC (KT-15), CD44-PerCP/Cy5.5 (IM7), CD44-PE (IM7), CD62L-APC-eFluor780 (MEL-14). In oral immunization studies, after surface staining, cells were washed and stained with the following tetramers for 15 min at room temperature: H-2K(b) $OVA_{257-264}$ PE-labeled tetramer and I-A(b) $OVA_{325-335}$ APC-labeled tetramer (NIH Core Tetramer Facility) followed by intracellular staining with the Foxp3 Transcription Factor Staining Buffer Set (eBioscience) per manufacturer's instructions. Cells were stained with the following intracellular antibodies: anti-mouse T-bet-PE/Cy7 (4B10) and Foxp3-BV421 (MF-14). Cells were washed and resuspended in FACS buffer for analysis on an Attune NxT flow cytometer (Thermo). Flow cytometry analysis was performed using FlowJo software.

4.3.5 *Statistics*

Results are expressed as the mean ± standard deviation. When comparing outcomes between groups, statistical analysis was performed by one-way analysis of variance (ANOVA) using Tukey's multiple comparison post-test. When comparing outcomes between the same group of different conditions (for example, no treatment *vs.* treated), multiple t-tests were used with multiple comparison correction using the Holm-Sidak method. Statistical analyses were performed using GraphPad Prism 6 software. Statistical significance was defined as $p < 0.05$ (*, $p < 0.05$).

4.4 Results and Discussion

4.4.1 *Adjuvants induce epithelial cells to secrete DC-recruiting chemokines*

The most common mucosal adjuvants, cholera toxin (CT) and *E. coli* heat labile enterotoxin (LT), are not suitable for clinical use due to their high toxicity [13]. Novel adjuvants that can elicit immune responses at mucosal surfaces without compromising the tissue integrity nor causing severe inflammation and cell death are needed. Many adjuvants that agonize PRRs on cells are being evaluated in pre-clinical studies. In particular, TLR and NOD-like receptor agonists have shown much promise in their ability to activate innate immune cells and generate protective responses [14]. In addition to stimulating immune cells to process and present antigen, it has been shown that certain adjuvants and other immune cytokines can induce the production of chemokines [15]. Of interest to oral vaccination is the chemokine CCL20, which recruits immature DCs that express the chemokine receptor CCR6 [16]. These DCs can be recruited from the surrounding tissue as well as from circulating monocytes [10]. Upon DC maturation, cells downregulate the expression of this receptor and upregulate CCR7, which responds to the

chemokine CCL21 produced in lymph nodes [17,18]. In this way, DCs migrate to lymph nodes and secondary lymphoid organs once they have processed antigen and have a mature phenotype required for effective antigen presentation to naïve T cells. In the intestine, epithelial cells primarily produce the chemokine CCL20, which can recruit DCs to the epithelial layer [19]. Importantly, it has been demonstrated that these recruited DCs can extend dendrites between epithelial cells and access antigens in the intestinal lumen [8]. Through these transepithelial extensions, DCs can both uptake antigens as well as be activated by the adjuvant.

Thus, we first evaluate a library of adjuvants for their ability to induce small intestinal epithelial cells to produce CCL20 *in vitro*. Adjuvants included MPLA (TLR-4), CpG ODN (TLR-9), dsRNA (TLR-3, RIG-I), peptidoglycan (TLR-2), muramyl dipeptide (NOD2), and flagellin (TLR-5). We also included the cationic polymer-based adjuvant PEI, as it has been shown to potentiate immune responses [20], as well as the positive controls LPS (TLR-4), CT, and IL-1β. We chose these adjuvants based on their demonstrated immunogenicity in the literature, their ability to stimulate epithelial cells, and due to the diversity of immune activation mechanisms [9,14,20]. For example, TLR-4 is a cell-surface receptor that recognizes Gram-negative bacteria while TLR-9 is an intracellular receptor that recognizes unmethylated CpG sequences in single-stranded DNA. Of the 10 adjuvants tested, only 3, the TLR-9 agonist CpG ODN, the cationic polymer polyethyleneimine (PEI), and the cytokine IL-1β, induced significantly more CCL20 to be secreted by epithelial cells than was produced at steady state (Figure 4.1).

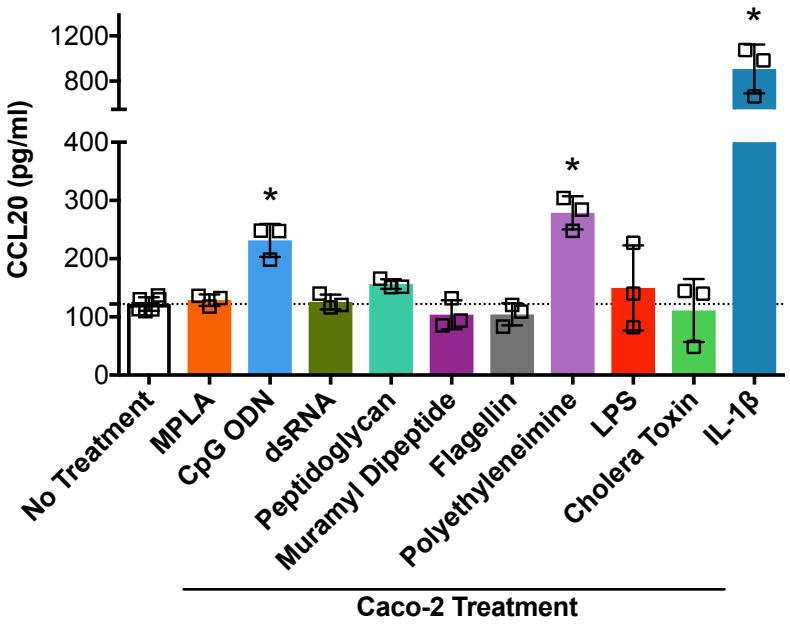

*Figure 4.1. Production of the chemokine CCL20 by Caco-2 cells after 72-hour treatment with different adjuvants in vitro. All adjuvants were dosed at 10 μg mL^{-1}. Data representative of n=3 per experimental group and presented as mean ± standard deviation. All groups were compared against the no treatment control, with *p<0.05.*

The TLR-9 adjuvant CpG has been shown to stimulate CCL20 production by intestinal epithelial cells [9,21]. The increased CCL20 concentration in the small intestine resulted in the capture of antigen by DCs as well as an overall increase in the frequency of dendrite extension into the lumen [9]. The cationic polymer PEI has been shown to have immunogenic activity both after systemic and nasal mucosal delivery [20,22]. However, PEI has not, to the best of our knowledge, been implicated in the activation of epithelial cells nor in inducing CCL20 production. Our data also emphasize the importance of mucosal adjuvant choice, as all adjuvants do not have the same effect on intestinal epithelial cells, which likely will impact downstream immunological processes and immunization efficacy.

4.4.2 *DC migration towards chemokines and epithelial cell supernatants*

Upon identification of promising epithelial cell-activating adjuvants, we evaluated the migration of immature DCs towards epithelial cell conditioned medium *in vitro* using both the DC line DC2.4 and bone marrow-derived DCs. In initial experiments, we observed a low migratory capacity of DC2.4s and mature BMDCs towards CCL20 (Figure S4.1). In contrast, mature BMDCs (pre-activated with an adjuvant cocktail of LPS, poly[I:C], and CpG) were incredibly responsive to the chemokine CCL21, whose receptor CCR7 is known to be upregulated upon DC stimulation (Figure S4.1). As BMDCs demonstrated an increased migratory capacity compared to the DC2.4 cell line, immature BMDCs without adjuvant stimulation were then assessed for migration towards epithelial cell supernatants. However, BMDC migration was found to be equivalent for all conditioned medium groups and there was no migration observed for the positive control of CCL20 in serum-free medium (Figure S4.2A). Thus, it is likely that the BMDCs, which were used on day 8 of derivation, had already begun to differentiate into a mature phenotype and were not responsive to CCL20. This hypothesis is supported by a study by Wang *et al.*, in which they observed upregulation of costimulatory receptors on BMDCs starting at day 6 of culture [23]. We then utilized the DC line DC2.4 to determine the migration of immature DCs towards the conditioned medium. Similar to the results observed for BMDC migration, there was no difference in the percentage of migrated DCs between the conditioned medium groups and no migration in response to CCL20 (Figure S4.1B), further validating low migratory capacity of DC2.4 cells.

Such transwell migration assays have been used to investigate the appropriate chemokines to induce DC migration into implants *in vivo* as well as in immunology studies. A study by Sierro *et al.* observed migration towards Caco-2 conditioned supernatants as well as recombinant CCL20 by $CD34^{+}$-derived DCs from cord blood (~4% migration of total cells) [24]. Similarly, Thorley et al. derived DCs from blood monocytes and detected DC migration towards the chemokine CCL20 [25]. DCs derived from peripheral blood

mononuclear cells were also shown to be responsive to CCL20, with 6% of the DCs migrating towards Caco-2 supernatants that were found to contain CCL20 [26]. Finally, intestinal lymph DCs have been shown to migrate in response to CCL20, although at higher chemokine concentrations than used in our study [27]. Due to the existing literature on DC responsiveness to the chemokine CCL20, we expect our migration results thus far are due to the low migratory capacity of the DC2.4 cell line and a semi-mature phenotype of the BMDCs, in which the CCL20 receptor CCR6 has been downregulated.

4.4.3 *Oral delivery of adjuvants expands intestinal antigen presenting cell population*

After identification of adjuvants that could induce the production of CCL20 *in vitro*, we then quantified the expansion of immune cell populations in both the small intestine and mesenteric lymph nodes after oral administration of adjuvants. As a proof-of-concept, we first administered the known mucosal adjuvant CT and analyzed cell populations in the small intestine and mesenteric lymph nodes. Two hours after administration, cell population percentages in the small intestine were similar between untreated and CT-treated mice (Figure 4.2A). However, we did observe an expansion of $CD45^{+}MHCII^{+}$ antigen presenting cells in the mesenteric lymph nodes (Figure 4.2B). These cells were predominately $CD11c^{-}$, indicating that this expanded population is not DCs but likely macrophages or monocytes, although such markers for specific identification were not included in this study. This is in contrast to other studies, in which an increase in the number of DCs in the small intestine and in the follicle-associated epithelium of Peyer's patches was increased 2 hours after CT administration [28,29]. In the mesenteric lymph nodes, the maximum number of DCs was observed 24 hours after oral adjuvant delivery [28,29].

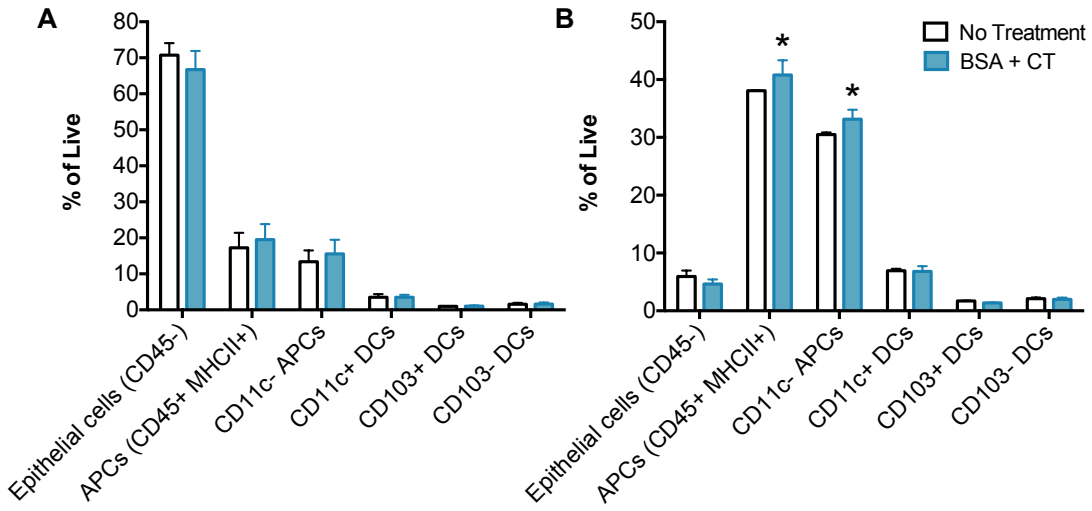

*Figure 4.2. The effect of the mucosal adjuvant CT on the antigen presenting cell population in the A) small intestine and B) mesenteric lymph nodes 2 hours after oral administration. CT was orally delivered at a dose of 20 μg/mouse. Data representative of n=3 mice per group and presented as mean ± standard deviation. Statistical analysis was performed between no treatment and CT-treated groups for each cell type. *$p<0.05$.*

Recruitment of DCs at mucosal surfaces and in draining lymph node occurs during infection as well as after the delivery of pattern recognition receptor agonists. As mentioned previously, the adjuvant CT has shown to expand the DC population in the small intestine [29]. The adjuvant CpG has shown to recruit DCs to the intestinal lamina propria and induce the formation of transepithelial dendrites, although it is important to note that CpG was directly injected into ligated intestinal loops in this study [9]. The ability to recruit DCs by chemokines, cytokines, and adjuvants has been reported for the nasal and vaginal mucosa. DCs numbers were expanded in the nasal epithelium after the nasal delivery of dead bacteria (peak at day 1), live bacteria (peak at day 1), live virus (peak at day 5), and soluble protein antigen (peak at day 1) [30]. In another study, polyethyleneimine increased the percentage of DCs in the draining lymph nodes 24 hours after intranasal administration [20]. In studies that aimed to recruit DCs in the vaginal tract, a study by Ramanathan *et al.* looked at recruitment of DCs through topical

administration of various compounds and found that GM-CSF, but not CCL20, enriched the vaginal mucosa with $CD11b^+$ DCs [31]. The adjuvant CpG has also been used in the vaginal mucosa, expanding the $MHCII^+CD11c^+$ DC population 48 hours after administration [32].

While some of adjuvants evaluated in our study, such as CT and CpG, have been orally administered in previous literature, it may be needed to increase sampling time points to capture the kinetics of cell migration in response to oral adjuvant administration. Thus, we next conducted a pilot experiment to identify the time-course of this observed APC migration. We also included analysis of the small intestine lamina propria and intraepithelial cells separately. Mice were orally dosed with OVA in an adjuvant cocktail (CT/CpG/PEI) as a positive control (designated as OVA+adjuvant). Small intestines and mesenteric lymph nodes were analyzed by flow cytometry at 1, 2, and 4 hours after administration. A control mouse receiving OVA only without adjuvants was included for the 4-hour time point. In the intraepithelial compartment of the small intestine, we observed a dramatic increase in $MHCII^+$ $CD11c^-$ cells at all time points compared to OVA without adjuvant (4h) (Figure 4.3A,B). Similar percentages of DCs ($MHCII^+$ $CD11c^+$) and their phenotype (CD86 and MHCII-SIINFEKL expression) were observed in both groups at all time points (Figure 4.3A,B). In the small intestinal lamina propria, we observed a decrease in $CD11c^-$ $MHCII^+$ cells in response to OVA with the adjuvant cocktail over time (Figure 4.3A,C). In contrast, the DC population in the lamina propria was found to increase over time after adjuvant delivery (Figure 4.3A,C). It is possible that $CD11c^-$ $MHCII^+$ cells in the LP differentiate into DCs or migrate into the IEL compartment, resulting in a reduction in percentage. However, the percentage at the 4-hour time point was similar between OVA only and OVA+adjuvant groups. Thus, it is unknown if OVA without adjuvant also results in a change in this population over time. DCs in the LP had similar expression of CD86 and MHCII-SIINFEKL over all time points

and groups (Figure 4.3C). LP DCs had much higher expression of CD86 and MHCII-SIINFEKL compared to IEL DCs.

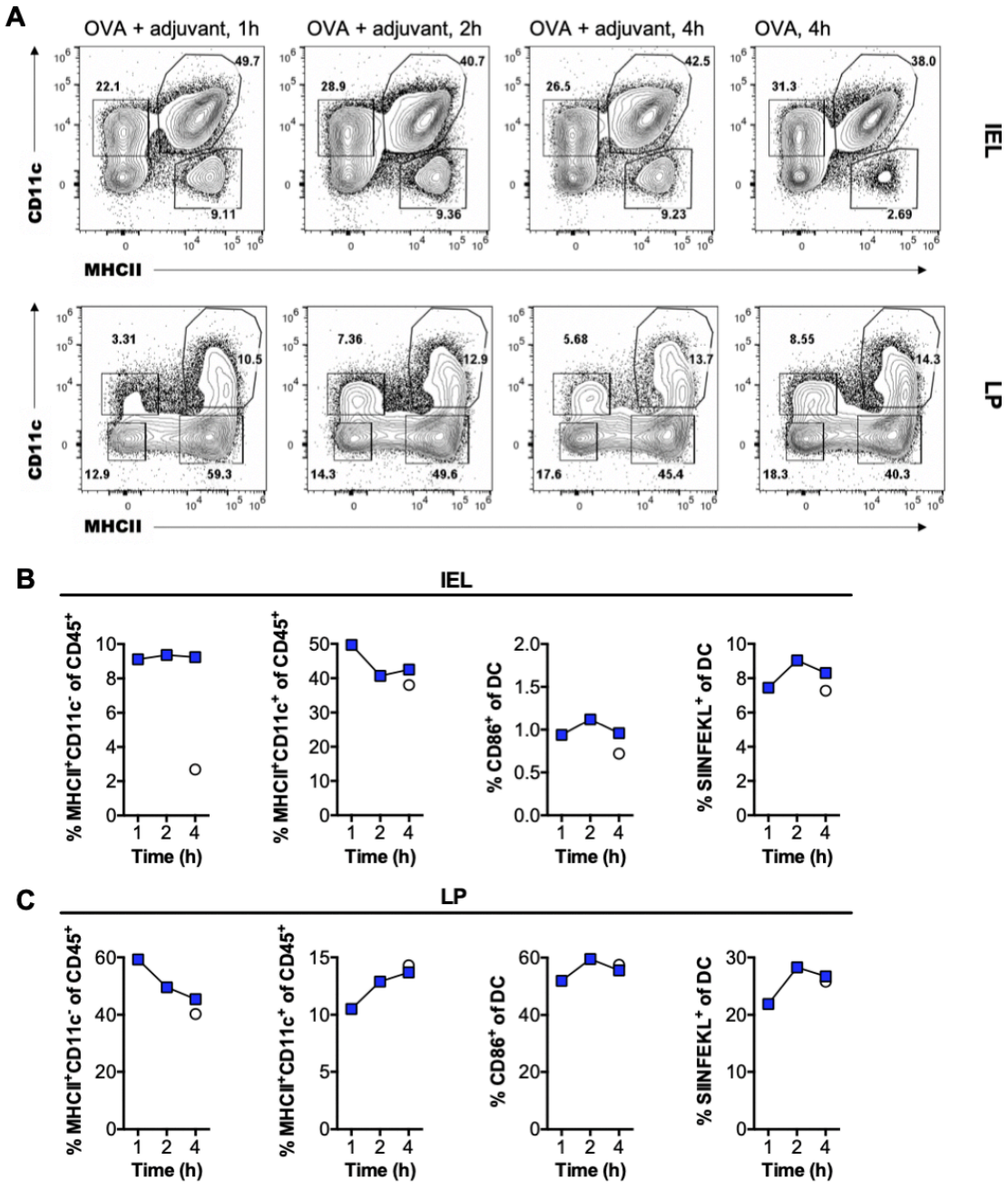

Figure 4.3. Kinetics of antigen presenting cell recruitment in the small intestinal intraepithelial layer and lamina propria after oral adjuvant administration. Mice were orally immunized with OVA (1 mg) with or without an adjuvant cocktail of CT (10 μg), CpG (50 μg), and PEI (50 μg). Immune cell populations were evaluated from the small intestine by flow cytometry. A)

Representative plots and quantification of CD11c and MHCII populations among CD45$^+$ cells in the B) intraepithelial compartment or C) lamina propria. Data representative of n=1 mouse per group and presented as mean.

In the mLNs, we observed the presence of a CD8α^{int}CD11b$^+$ DC population at the 4-hour time point with OVA+adjuvant compared to earlier time points and to OVA alone at 4h (Figure 4.4A). Myeloid CD11b$^+$ DCs are known to respond to the chemokines CCL20 and CCL9 in gut-associated lymphoid tissue and thought to be a migratory population [33]. CD8α^+CD11b$^+$ DCs have been shown to produce inflammatory, rather than tolerogenic, cytokines upon TLR activation and were not involved in Foxp3$^+$ T cell induction [34]. Thus, it is possible that with the use of this adjuvant cocktail a more inflammatory DC population migrates to or expands in the lymph nodes to initiate effector T cell responses compared to antigen alone. We also looked at T cell phenotypes in the mLNs at the 4-hour time point. With OVA alone, we observed both effector (CD62L$^-$) and central (CD62L$^+$) memory CD8$^+$ T cells among the CD44$^+$ antigen-experienced population (Figure 4.4B). In contrast, when adjuvant was co-delivered with OVA the T cell response was primarily effector-memory (CD62L$^-$) (Figure 4.4B). Effector T cells downregulate CD62L and are able to exit lymph nodes and enter circulation [35,36]. These results may indicate an increase in effector T cells with adjuvant-containing oral vaccines, although this hypothesis is yet to be tested in a properly powered study.

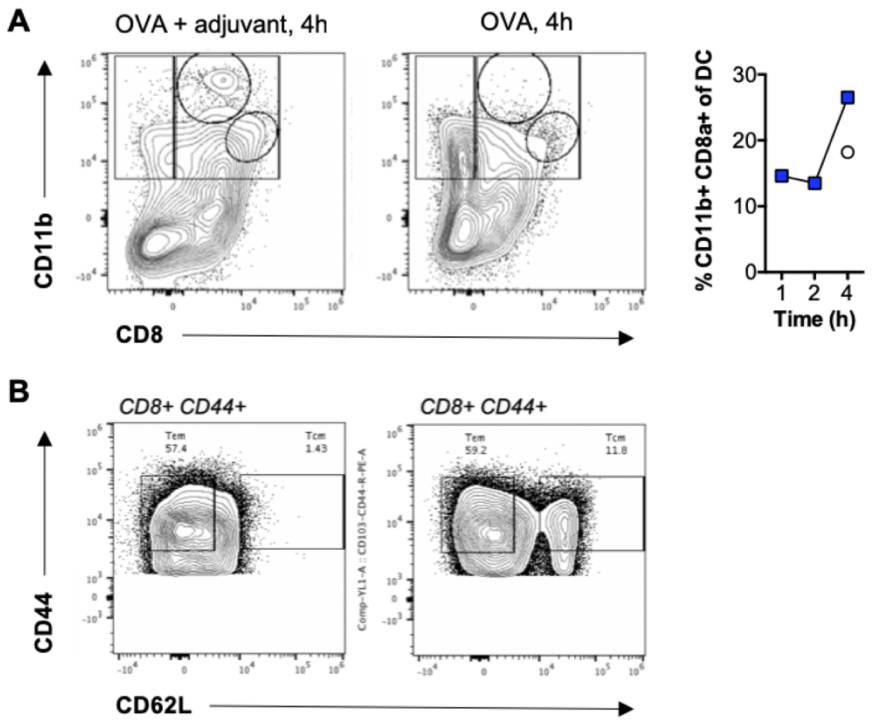

Figure 4.4. Effect of oral adjuvant administration on immune cell populations in the mesenteric lymph nodes. Mice were orally immunized with OVA (1 mg) with or without an adjuvant cocktail of CT (10 μg), CpG (50 μg), and PEI (50 μg). Four hours later, immune cell populations were evaluated from the mesenteric lymph nodes by flow cytometry. A) CD8 and CD11b expression among $CD11c^+$ cells, B) CD62L expression among $CD8^+CD44^+$ cells. Data representative of n=1 mouse per group and presented as mean.

Overall, this pilot study gives insight into the time course of DC migration in response to orally administered vaccines, where as early as 1h $MHCII^+$ cells expand in the IEL and by 4h migratory DCs can be found in the mLNs in response to adjuvant. It also gives insights into antigen presenting cell populations that may be involved in the induction of adaptive immunity after oral immunization with the use of adjuvants for future studies to evaluate in depth.

4.4.4 *Adjuvants modulate antigen uptake by DCs and epithelial cells in vitro*

In addition to the ability of adjuvants to stimulate cells to secrete immune signals such as cytokines and chemokines to condition and recruit DCs, adjuvants can also influence the uptake of extracellular antigens by cells. To determine if CCL20-inducing adjuvants could enhance antigen uptake, we co-delivered the fluorescently labeled protein bovine serum albumin (BSA-FITC) and adjuvants to dendritic and epithelial cell lines *in vitro.* Adjuvant delivery did not cause cell toxicity (Figure 4.5A,B), with over 90% cell viability for all treatment groups, but did impact cellular uptake of the protein. In DCs, delivery of the adjuvant PEI significantly increased the amount of protein that the DCs internalized, with a mean fluorescence intensity (MFI) significantly higher than cells treated with protein only or protein plus CpG or IL-1β (Figure 4.5C). This metric represents the amount of protein associated with each DC. Similar to the trend observed in DCs, delivery of PEI with the protein also increased uptake in epithelial cells, increasing the percentage of the total epithelial cells that internalized the protein (Figure 4.5D). Differences in MFI were insignificant between groups. This enhancement of antigen uptake by epithelial cells is particularly important for oral vaccine delivery, in which antigens have been shown to be shuttled from the intestinal lumen to DCs in the lamina propria by epithelial goblet cells [37]. This could serve as a mechanism to achieve protein uptake following oral delivery in addition to the acquisition of protein antigens by DC transepithelial dendrites.

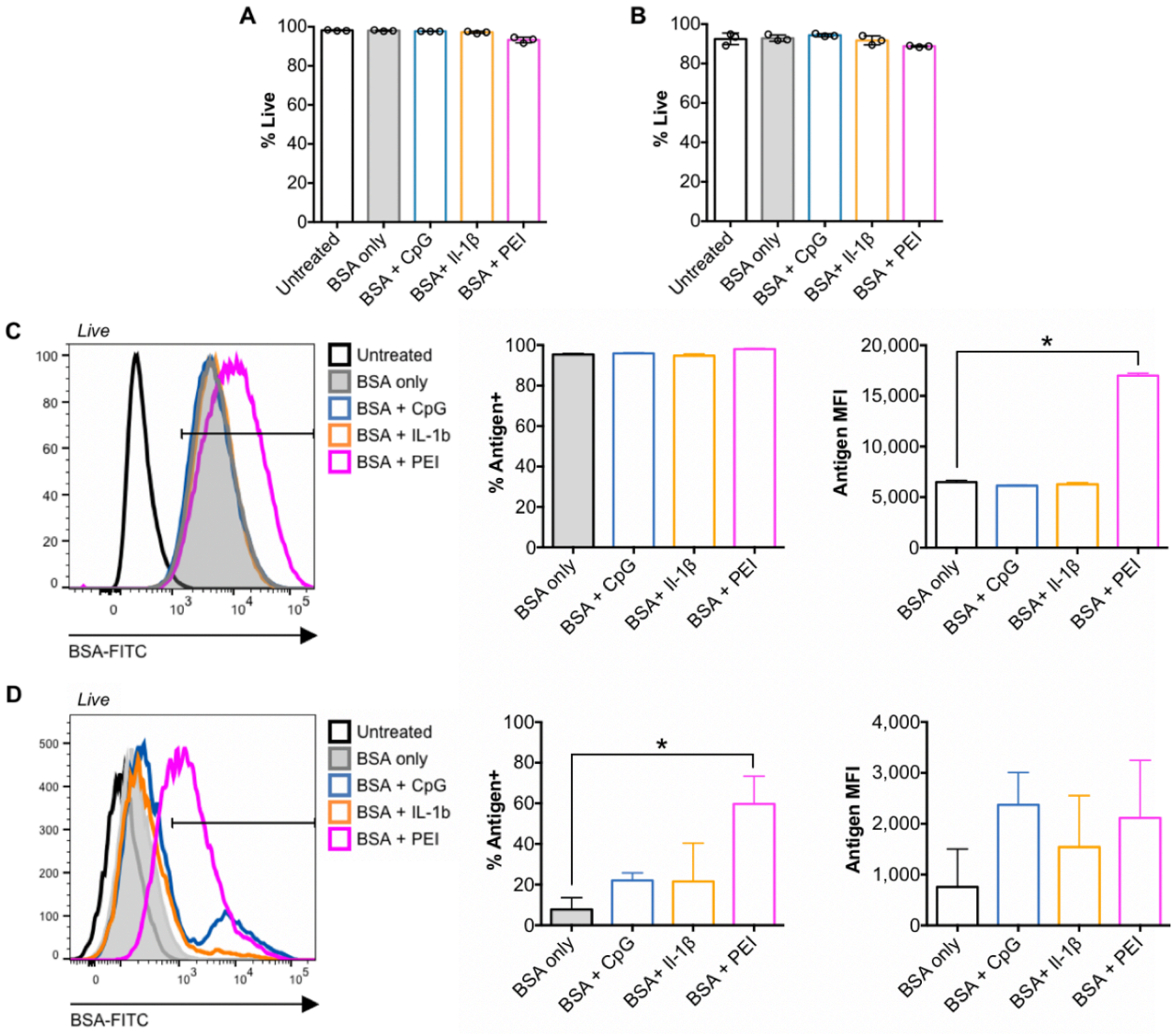

*Figure 4.5. Co-delivery of PEI with protein antigen enhances uptake in DCs and epithelial cells in vitro. Viability and protein uptake of A,C) DC2.4 and B,D) Caco-2 cells following 4-hour incubation with BSA-FITC (10 μg mL^{-1}) ± adjuvants (all 10 μg mL^{-1}). Data representative of n=3 per experimental group and presented as mean ± standard deviation. Experimental groups were compared to the BSA only group using one-way ANOVA with multiple comparisons, followed by Dunnett's multiple comparison post-test. *p<0.05.*

Since the delivery of proteins in particulate form has been shown to increase cellular uptake, we also formed immune complexes composed of protein and the cationic polymer

PEI. Complexation of the protein with the cationic polymer significantly increased protein uptake in DC2.4 cells compared to the same dose of PEI without complexation (Figure 4.6A). In contrast, PEI complexation was found to reduce uptake of protein in Caco-2 intestinal epithelial cells compared to polymer and protein co-delivery (Figure 4.6B). These results may point to the differences in protein internalization between dendritic and epithelial cells, with the former having preference for the uptake of particulates. One study investigating the internalization of PLGA nanoparticles in different epithelial cell lines observed low particle uptake in Caco-2 cells [38]. Previous literature has observed a size-dependence of Caco-2 particle uptake, with higher internalization of 0.1 μm particles compared to those larger than 1 μm [39]. Overall, these results support the claim that protein-polymer complexes can modulate protein uptake and demonstrate that protein internalization can be targeted to either DCs or epithelial cells through such complexation.

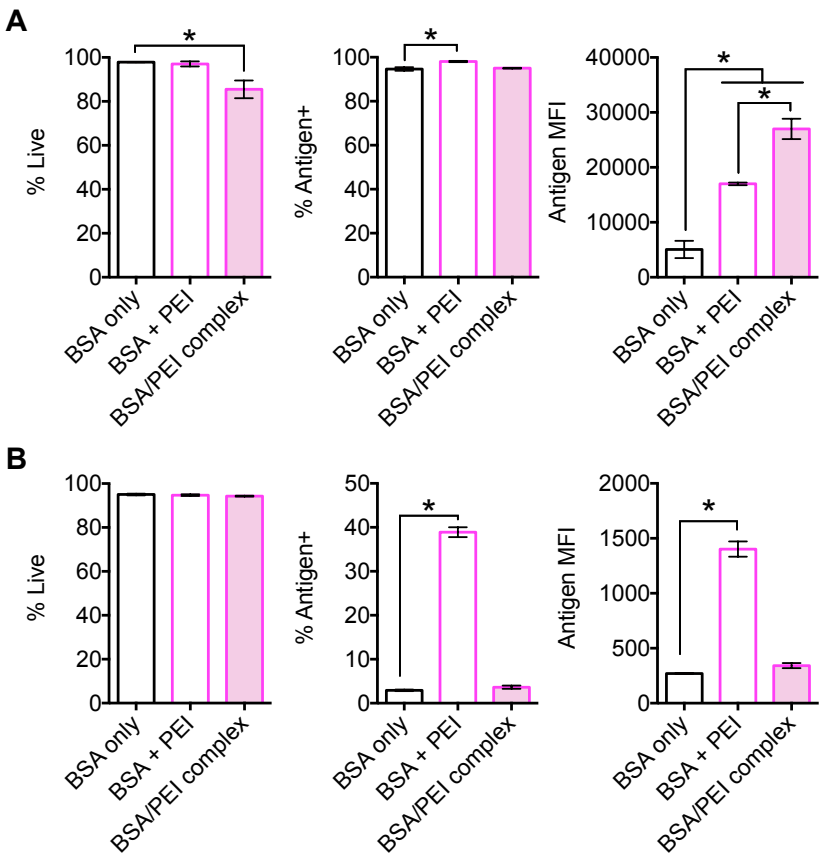

Figure 4.6. PEI complexation with protein antigens can enhance uptake in A) DC2.4 cells but not B) Caco-2 intestinal epithelial cells. Cells were treated with BSA-FITC (10 μg mL^{-1}), BSA-FITC (10 μg mL^{-1}) and PEI (10 μg mL^{-1}), or BSA-FITC/PEI complexes (each 10 μg mL^{-1}). BSA-FITC/PEI complexes were produced by mixing BSA and PEI at a 1:1 mass ratio and vortexing for 30 seconds. Data representative of n=3 per group and presented as mean ± standard deviation.

4.4.5 *Protein localization and uptake*

We next quantified if adjuvant-mediated DC recruitment could enhance protein uptake in the small intestine following oral administration *in vivo*. First, we delivered soluble protein and visualized its location in the small intestine 2 hours later. We observed the fluorescent protein signal predominately in the ileum of the small intestine (Figure 4.7), but also in the duodenum and jejunum. Protein was localized at the intestinal villi

epithelial lining rather than in the underlying tissue. These data support evaluating protein location within the small intestinal tissue using immunohistochemistry (IHC) techniques for future studies with various adjuvants and delivery systems.

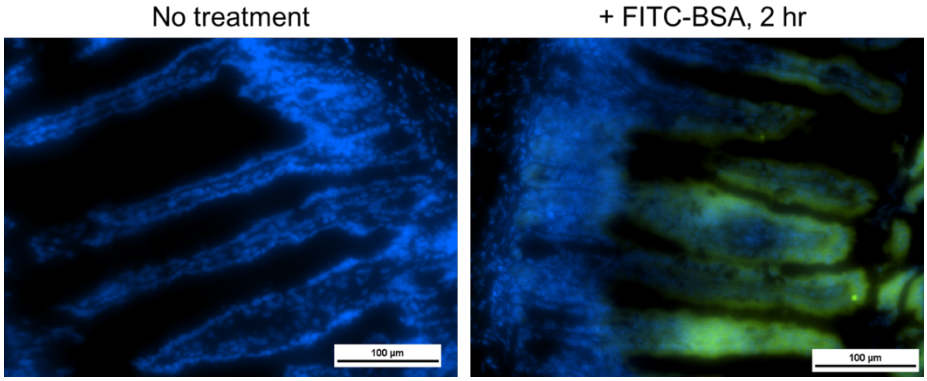

Figure 4.7. Protein localization in small intestine epithelial villi following oral delivery. Mice were treated with 500 µg BSA-FITC by oral gavage and sacrificed 2 hours later. Small intestines were prepared for microscopy and imaged using a Nikon Eclipse Ti microscope equipped with an Andor fluorescence camera. Data representative of n=1 mouse per experimental group.

Additionally, the localization of protein in small intestinal and mesenteric lymph node cell populations was evaluated using flow cytometry after oral protein administration. Modest protein uptake was observed in $CD103^-$ and $CD103^+$ DCs 4 hours after oral administration (Figure 4.8). However, upon further increase of the protein dose and co-delivery with CT, protein uptake was not observed in any cell populations (data not shown). These data support the characterization of antigen uptake in different cell populations and the magnitude of antigen internalization for evaluation of a variety of adjuvants and delivery systems after further characterization and optimization of experimental methods. Low levels of protein uptake have been quantified using flow cytometry following oral delivery with polymeric nanoparticles. In one study, two days after the oral administration of FITC-BSA-loaded PLGA nanoparticles 0.01% of total small intestinal cells were fluorescence-positive [40]. Commonly, protein absorption is demonstrated through microscopy of intestinal cross sections [41–43]. Unfortunately, the

ideal dose and sampling time to detect protein uptake in small intestinal cells, and specifically DCs, has not been established.

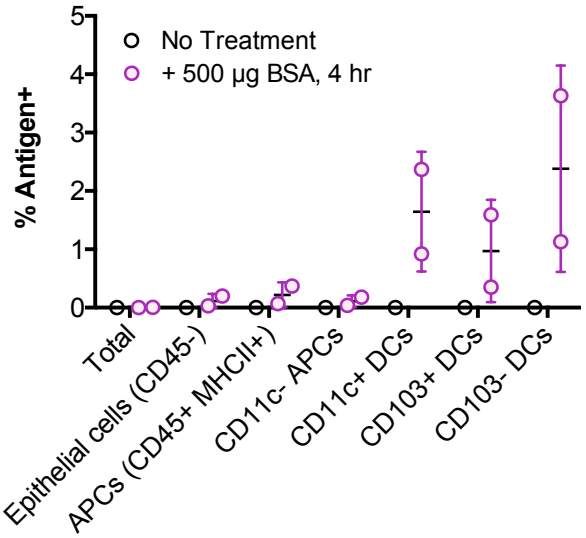

Figure 4.8. Percentage of FITC⁺ cells in the small intestine 4 hours after oral administration of 500 µg BSA-FITC. Data representative of up to of n=2 mice per group and presented as mean ± standard deviation.

Finally, we aimed to verify antigen uptake by intestinal DCs by evaluating the ability of DCs from orally immunized mice to activate antigen-specific T cells. Ovalbumin co-formulated with CT adjuvant was orally delivered to mice and 24 hours later CD11c$^+$ DCs were isolated from the small intestine lamina propria and the mesenteric lymph nodes. DCs were cultured overnight either with or without further stimulation by LPS *ex vivo*. Ovalbumin-specific CFSE$^+$ CD4$^+$ T cells from the spleen of OT-II transgenic mice were co-cultured with DCs for 72 hours. Positive controls of isolated DCs from untreated mice incubated with ovalbumin protein *ex vivo* were included for both organs. After 3 days, no proliferation of CD4$^+$ T cells was observed following co-culture with small intestinal DCs, including the positive control, indicating the inability of isolated DCs to present antigen to naïve T cells (Figure 4.9A,C). This may be due to the low viability of the isolated cells, the low efficiency of the CD11c$^+$ selection process, or the lack of antigen presentation capacity of the cells, although the latter is unlikely due to existing literature

demonstrating antigen presentation by isolated gut DCs [44]. In contrast, DCs isolated from the mesenteric lymph nodes retained their ability to present antigen, as was verified by the positive control (Figure 4.9B,D). Modest T cell proliferation (~10%) was observed by MLN DCs from mice treated with ovalbumin and CT, although this proliferation was not statistically significant compared to proliferation elicited by MLN DCs from untreated mice (Figure 4.9D). The production of the cytokine IFN-γ by T cells when they become activated by antigen presenting cells can also be used as to evaluate the acquisition of antigen by mucosal DCs and their ability to present to antigen-specific T cells. Thus, we measured the production of IFN-γ in the supernatant of mucosal DC-T cell co-cultures after 72 hours. We did not detect any IFN-γ produced in cultures with DCs isolated from the small intestine, except for from one mouse treated with ovalbumin and CT with LPS stimulation *ex vivo* (Figure 4.9E). This is in line with the lack of proliferation observed for samples with intestinal DCs. We detected higher levels of IFN-γ in co-cultures of T cells with DCs isolated from the mesenteric lymph nodes, although differences in cytokine production between the untreated and treated groups was not statistically significant (Figure 4.9F).

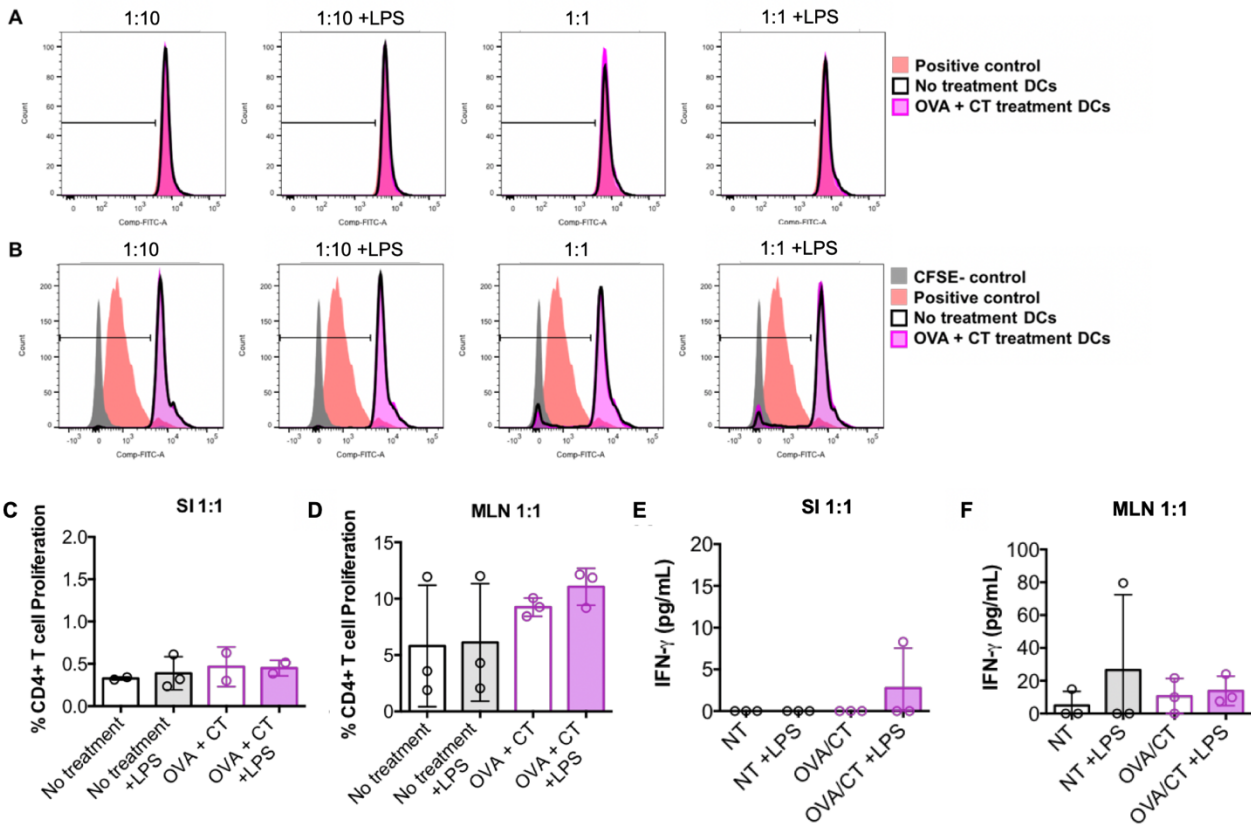

Figure 4.9. Activation of antigen-specific $CD4^+$ T cells ex vivo by mucosal DCs from untreated or ovalbumin and CT-orally treated mice from the A) small intestine and B) mesenteric lymph nodes as determined by CFSE dilution. Percentage of total $CD4^+$ T cells that proliferated after co-culture with C) small intestine DCs and D) mesenteric lymph node DCs (1:1) was quantified. IFN-γ production by $CD4^+$ T cells after co-culture with mucosal DCs (1:1) from untreated or ovalbumin and CT-orally treated mice from the E) small intestine and F) mesenteric lymph nodes. Data representative of n=3 mice per experimental group per organ and data is presented as mean ± standard deviation.

Thus far, experiments to evaluate antigen uptake and processing in intestinal DCs have produced underwhelming results. The inability to robustly and confidently determine the degree of DC antigen uptake following oral protein delivery may be due to a few reasons. One, it may be possible that unformulated oral protein delivery is leading to complete or extensive protein degradation. Quantification of antigen uptake by intestinal

DCs was achieved in a study by Zhu *et al.*, but antigen was delivered encapsulated in nanoparticles, which may have protected the protein antigen during GI tract transit as well as facilitated uptake due to its particulate form. Two, the time points investigated in our studies may not be capturing the exact moment during which DCs are loaded with antigen in the small intestinal lamina propria, the mesenteric lymph nodes, or during their migration.

In a final effort to quantify uptake of orally administered proteins, we investigated if nanoparticle formulation could be used to visualize antigen uptake in the small intestine after oral delivery as a positive control. In this pilot study, BSA-FITC was formulated in PLGA nanoparticles and administered to mice by oral gavage. Two hours after oral administration, both lymphoid ($CD45^+$) and epithelial ($EpCAM^+$) cells were analyzed for BSA-FITC uptake. We also segmented the small intestine into the duodenum, jejunum, and ileum to determine if signal dilution was occurring from bulk processing of the small intestine, in which absorption occurred only in certain anatomical segments of the intestine. In mice (n=2) that received BSA-FITC in PLGA NPs, 1% and 22% of epithelial cells were found to be $FITC^+$ (Figure S4.3A). In mice that received soluble BSA-FITC (n=2), <1% of epithelial cells were $FITC^+$ (Figure S4.3A). However, this difference was not statistically significant due to the high variability observed in the PLGA NP group. Uptake among intraepithelial $CD45^+$ cells was also equivalent between soluble and PLGA NP groups (Figure S4.3A). In the lamina propria, increased uptake in ileal epithelial cells was observed in one mouse in the PLGA NP group but there was no significant difference between groups (Figure S4.3B). Similarly, no differences in uptake were observed in $CD45^+$ and DC populations (Figure S4.3B). While this was a pilot study and not appropriately powered, these results suggest that nanoparticle uptake occurs in more distal regions of the intestinal tract such as the ileum. The data also suggest that PLGA NP formulation could increase uptake in epithelial cells. However, we still observed low

and inconsistent results in quantifying protein uptake in different cell populations in the small intestine similar to our previous experiments.

4.4.6 *Induction of adaptive immune responses by oral adjuvants*

As approaches to evaluate potent mucosal adjuvants *in vitro* for DC recruitment and antigen uptake thus far proved less than optimal, we moved to screening adjuvants *in vivo* to verify differences in activity and potency before evaluation of mechanism. As CpG and PEI demonstrated adjuvant activity *in vitro*, these adjuvants were considered for *in vivo* testing. Additionally, we included the mucosal adjuvant CT as a positive control and the adjuvant MPLA as an adjuvant that was not observed to induce CCL20 expression by epithelial cells but is used in vaccine formulations clinically [45]. Naïve mice were orally vaccinated with OVA with or without CT, CpG, PEI, or MPLA for a total of 3 immunizations with a 4-week interval between doses. Low serum anti-OVA IgG responses were observed after the second immunization for all groups excluding CpG, which led us to immunize mice with an additional dose (Figure 4.10). One week after the third immunization, we observed robust production of serum anti-OVA IgG in the CpG adjuvant group followed by MPLA and CT (Figure 4.10). One mouse from the PEI group mounted a strong antibody response similar to that observed for CpG (Figure 4.10).

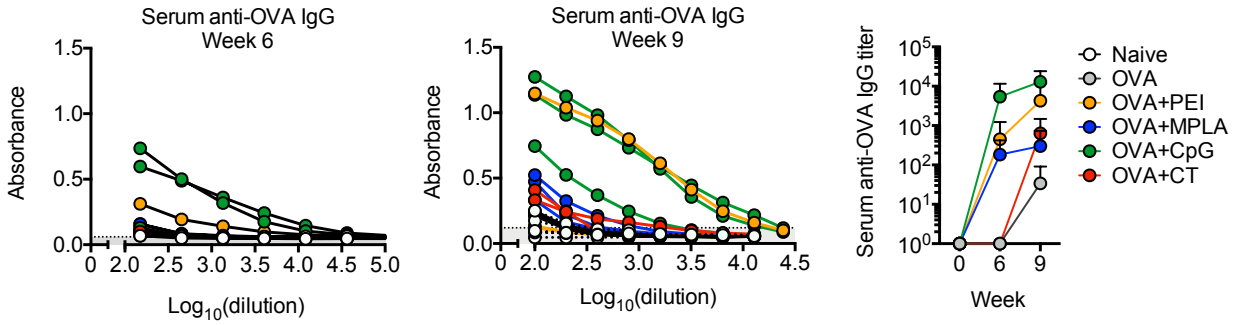

Figure 4.10. Systemic antibody responses to oral vaccines with different adjuvants. Mice were immunized with OVA (1 mg) with or without the adjuvants CT (10 μg), MPLA (20 μg), branched PEI (200 μg), or CpG ODN 1826 (100 μg). Mice were boosted with the same vaccine formulation

every 4 weeks. Serum was collected and assayed for the presence of OVA-specific IgG two weeks after the second immunization and one week after the third immunization. Data representative of n=3 mice per group and presented as mean ± standard deviation.

Two weeks after the last immunization, small intestinal lavage fluid was collected and assayed for antigen specific production of IgA to evaluate local mucosal immune responses. As expected, CT increased IgA in the small intestinal lumen (Figure 4.11). CpG was the only other adjuvant observed to induce IgA secretion upon oral administration (Figure 4.11). Overall, intestinal IgA responses were low. Further studies may optimize the assay protocol or analyze IgA from fecal samples rather than intestinal wash, which may dilute the antibody below limits of detection.

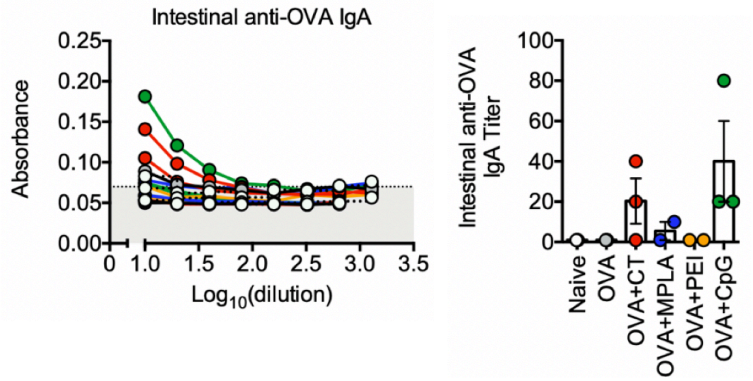

Figure 4.11. Intestinal antibody responses to oral vaccines with different adjuvants. Mice were immunized with OVA (1 mg) with or without the adjuvants CT (10 μg), MPLA (20 μg), branched PEI (200 μg), or CpG ODN 1826 (100 μg). Mice were boosted with the same vaccine formulation every 4 weeks. Small intestinal lavage fluid was collected and assayed for the presence of OVA-specific IgA two weeks after the fourth immunization. Data representative of n=3 mice per group and presented as mean ± standard deviation.

We also evaluated the cellular response to different mucosal adjuvants. Two weeks after the last immunization, mesenteric lymph nodes (mLNs) and small intestinal intraepithelial lymphocytes (SI IEL) and lamina propria cells (SI LP) were analyzed. In

the gut-draining mLNs, similar percentages of $CD44^+$ $CD4^+$ were observed between groups (Figure 4.12A). Antigen-specific (I-A(b) $OVA_{325\text{-}335}$ $tetramer^+$) $CD4^+$ T cells were increased in all vaccinated groups but this increase was not statistically significant compared to naïve (Figure 4.12B). As OVA-specific T cell numbers were low, we were not able to analyze polarization of T cells activated in response to the vaccine. Among the CD8 population in the mLNs, the percentages of $CD44^+$ cells were also similar between groups (Figure 4.12C). We unexpectedly observed the highest antigen-specific (H-2K(b) $OVA_{257\text{-}264}$ tetramer+) $CD8^+$ T cell percentage in the OVA only group; however, this was not statistically significant compared to naïve (Figure 4.12D). Upon activation in lymphoid organs, T cells re-enter circulation and can home to mucosal sites to enact effector function. Thus, we looked in two compartments of the small intestine, the intraepithelial cells and the lamina propria, for the presence of antigen-specific T cells in response to vaccination. The intraepithelial layer houses memory $CD8^+$ T cells while $CD4^+$ T cells predominately reside in the underlying lamina propria. In the lamina propria, we observed an increase in $CD44^+$ $CD4^+$ T cells when PEI was used as an adjuvant (Figure 4.12E). CT also expanded this population but was not statistically different than naïve. Among this population, we observed that CpG increased the percentage of OVA-specific T cells at this site (Figure 4.12F). In the IEL, OVA and OVA+CT groups were unfortunately excluded from analysis due to ineffective processing, in which $<50\%$ of the cells were $CD8^+$. In other groups, this population makes up $>80\%$ of the total cells. The percentage of $CD44^+$ $CD8^+$ T cells was similar between all groups (Figure 4.12G). However, we observed that PEI significantly increased the OVA-specific $CD8^+$ T cell population compared to naïve (Figure 4.12H). In the nasal mucosa, the polymeric adjuvant polyethyleneimine (PEI) was shown to expand immune cell populations and enhance uptake of protein antigens in the nasal-associated lymphoid tissue and draining lymph nodes. However, the role of epithelial cell-DC crosstalk in this process was not investigated nor has this polymer been investigated as an adjuvant at

other mucosal surfaces [20]. PEI has been used as a transfection agent to increase intracellular delivery of nucleic acids. Taking advantage of this feature, nanoparticles composed of PEI and OVA demonstrated enhanced MHCI presentation by DCs [46]. These findings may explain the enhanced $CD8^+$ T cell activation we achieved through use of PEI as an adjuvant.

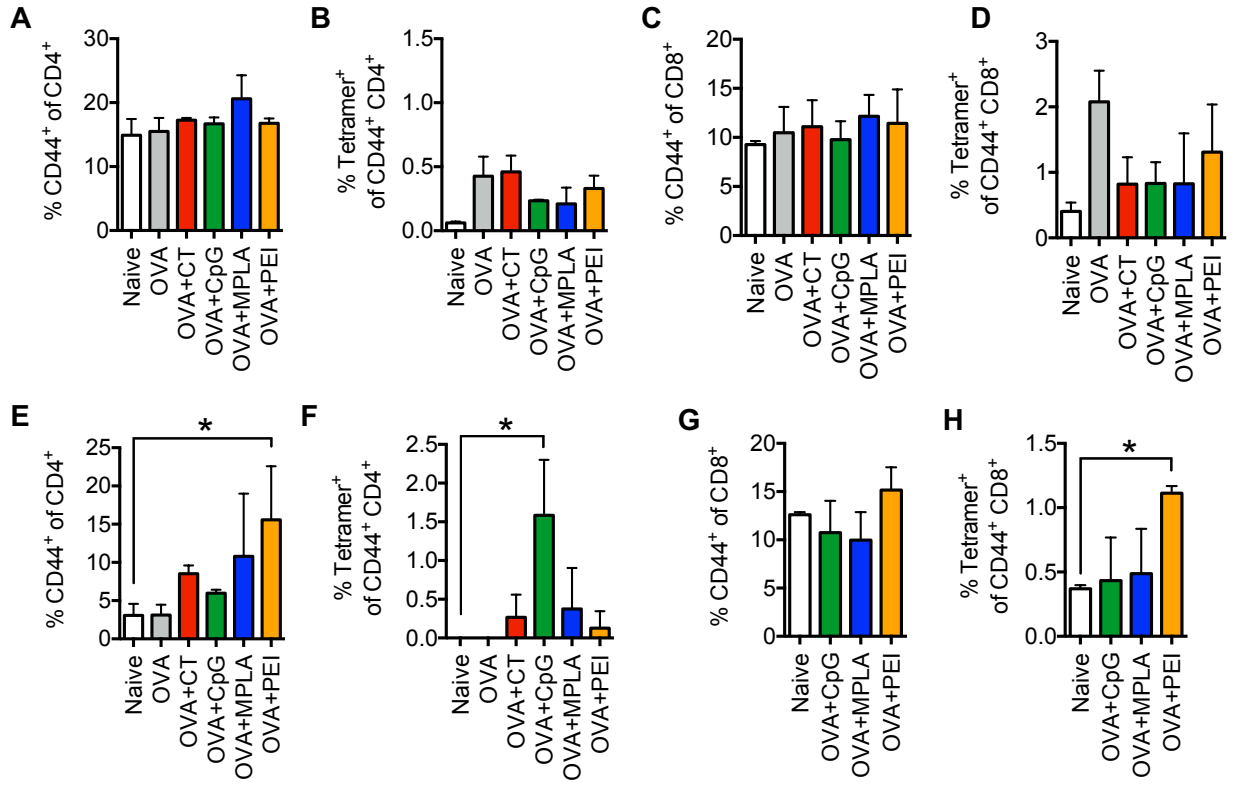

Figure 4.12. Cellular immune responses to oral vaccines with different adjuvants. Mice were immunized with OVA (1 mg) with or without the adjuvants CT (10 μg), MPLA (20 μg), branched PEI (200 μg), or CpG ODN 1826 (100 μg). Mice were boosted with the same vaccine formulation every 4 weeks. Mesenteric lymph nodes (A-D) and small intestinal lamina propria (E, F) and intraepithelial cells (G, H) were collected two weeks after the fourth immunization and analyzed by flow cytometry for $CD4^+$ and $CD8^+$ T cell CD44 expression and antigen-specific ($tetramer^+$) expansion. Data representative of n=2-3 mice per group and presented as mean ± standard deviation.

Overall, we observed that CpG delivered orally can drive systemic and mucosal humoral immune responses as well as activate antigen-specific $CD4^+$ T cells in the small intestine. PEI also demonstrated cellular activity through increased T_H1 $CD4^+$ T cells in the mLNs and increasing the antigen-specific $CD8^+$ population in the small intestine. However, PEI was not observed to activate humoral immunity in the intestine and was inconsistent in eliciting systemic antibodies. In terms of cellular immune responses, CpG and PEI were the most potent adjuvants, where CpG established CD4 responses and PEI established CD8 responses (Table 4.1). Future work may focus on the scale-up of these experiments and the use of more robust methods to track antigen-specific cells, such as the use of pentamers or adoptive transfer of transgenic antigen-specific T cells prior to immunization. These methods would enhance the characterization of the antigen-specific cellular immune response in terms of polarization in response to different mucosal adjuvants delivered orally.

Table 4.1. Summary of adaptive immune responses elicited from orally delivered adjuvants.

Adjuvant	Serum IgG	Intestinal IgA	CD4	CD8
CT	+	+		
CpG	+++	+	++	
MPLA	+	-		
PEI	+/-	-	+	++

4.5 Conclusions

In conclusion, this work has investigated adjuvants for use in oral vaccines and establish the adaptive immune profiles of four adjuvants when used orally. We find that in addition to CT, the TLR-9 agonist CpG ODN and the cationic polymer PEI can be used as adjuvants to amplify adaptive immune responses to oral subunit vaccines. In contrast to the clinically relevant TLR-4 agonist MPLA, which was not as robust of a

mucosal adjuvant, CpG and PEI modulated epithelial cell signaling *in vitro*. As signals secreted by epithelial cells can control DC function, this feature may contribute to the mucosal adjuvant activity observed. In pilot studies, the application of these mucosal adjuvants in combination results in a dramatic expansion in small intestinal intraepithelial $MHCII^+$ cells that may be better poised to internalize antigen and initiate immune responses. We also observed different DC populations in the draining lymph nodes with the use of adjuvants, which may modulate the polarization and magnitude of the adaptive immune responses. CpG elicited robust humoral responses both systemically and mucosally while antibody production in response to PEI was inconsistent. However, PEI activated $CD8^+$ T cell responses in the small intestine. This may be due to the ability of PEI to increase antigen uptake in both epithelial and DCs observed *in vitro*. This study was the first evaluation of PEI as an oral adjuvant and shows much potential by this route. Ultimately, these data suggest the use of different adjuvants to generate specific immune responses depending on the desired immunological outcome. This is an important consideration for the development of immunity in the intestine to either combat infection, cancer, or autoimmunity. Future work may quantify in depth the adjuvant mechanism of action, specifically into modulation of signaling cytokines in the intestine and its effect on DC migration, phenotype, and antigen uptake *in vivo*. In the context of this thesis, future work will incorporate the identified adjuvants CpG and PEI in an oral vaccine platform for further evaluation of immune responses.

4.6 Acknowledgements

The authors thank Jaehyung Park, Rachel Creighton, and Alton Cao for assistance with *in vivo* studies. The authors also thank the labs of Suzie Pun at the University of Washington for Caco-2 cells and James Lai at the University of Washington for DC2.4 and B3Z cells. This work was supported by NIH grant HD075703 and AI112002 to

K.A.W. H.F. acknowledges additional financial support from the National Science Foundation Graduate Research Fellowship Program (DGE-1256082) and the Achievement Rewards for College Scientists Foundation Scholar Award.

4.7 References

[1] S. Gupta, A. Jain, M. Chakraborty, J.K. Sahni, J. Ali, S. Dang, Oral delivery of therapeutic proteins and peptides: a review on recent developments, Drug Deliv. 20 (2013) 237–246. doi:10.3109/10717544.2013.819611.

[2] N. Lycke, Recent progress in mucosal vaccine development: potential and limitations, Nat. Rev. Immunol. 12 (2012) 592–605. doi:10.1038/nri3251.

[3] D. Artis, Epithelial-cell recognition of commensal bacteria and maintenance of immune homeostasis in the gut., Nat. Rev. Immunol. 8 (2008) 411–20. doi:10.1038/nri2316.

[4] C.-M. Sun, J.A. Hall, R.B. Blank, N. Bouladoux, M. Oukka, J.R. Mora, Y. Belkaid, Small intestine lamina propria dendritic cells promote de novo generation of Foxp3 T reg cells via retinoic acid, J. Exp. Med. 204 (2007) 1775–1785. doi:10.1084/jem.20070602.

[5] R.W. Depaolo, V. Abadie, F. Tang, H. Fehlner-Peach, J.A. Hall, W. Wang, E. V Marietta, D.D. Kasarda, T.A. Waldmann, J.A. Murray, C. Semrad, S.S. Kupfer, Y. Belkaid, S. Guandalini, B. Jabri, Co-adjuvant effects of retinoic acid and IL-15 induce inflammatory immunity to dietary antigens, Nature. 471 (2011) 220–225. doi:10.1038/nature09849.

[6] M. Rescigno, M. Urbano, B. Valzasina, M. Francolini, G. Rotta, R. Bonasio, F. Granucci, J.P. Kraehenbuhl, P. Ricciardi-Castagnoli, Dendritic cells express tight junction proteins and penetrate gut epithelial monolayers to sample bacteria., Nat. Immunol. 2 (2001) 361–367. doi:10.1038/86373.

[7] M. Rimoldi, M. Chieppa, M. Vulcano, P. Allavena, M. Rescigno, Intestinal epithelial cells control dendritic cell function, in: Ann. N. Y. Acad. Sci., 2004: pp. 66–74. doi:10.1196/annals.1309.009.

[8] M. Chieppa, M. Rescigno, A.Y.C. Huang, R.N. Germain, Dynamic imaging of dendritic cell extension into the small bowel lumen in response to epithelial cell TLR engagement., J. Exp. Med. 203 (2006) 2841–52. doi:10.1084/jem.20061884.

[9] Y. Yin, T. Qin, X. Wang, J. Lin, Q. Yu, Q. Yang, CpG DNA assists the whole inactivated H9N2 influenza virus in crossing the intestinal epithelial barriers via transepithelial uptake of dendritic cell dendrites., Mucosal Immunol. 9 (2014) 1–16. doi:10.1038/mi.2014.110.

[10] M. Le Borgne, N. Etchart, A. Goubier, S. a. Lira, J.C. Sirard, N. Van Rooijen, C. Caux, S. Aït-Yahia, A. Vicari, D. Kaiserlian, B. Dubois, Dendritic cells rapidly recruited into epithelial tissues via CCR6/CCL20 are responsible for CD8+ T cell crosspriming in vivo, Immunity. 24 (2006) 191–201. doi:10.1016/j.immuni.2006.01.005.

[11] S.P. Sittig, G. Bakdash, J. Weiden, A.E. Sköld, J. Tel, C.G. Figdor, I.J.M. De Vries, G.

Schreibelt, A Comparative Study of the T Cell Stimulatory and Polarizing Capacity of Human Primary Blood Dendritic Cell Subsets, Mediators Inflamm. 2016 (2016). doi:10.1155/2016/3605643.

[12] M.B. Lutz, N. Kukutsch, a L. Ogilvie, S. Rössner, F. Koch, N. Romani, G. Schuler, An advanced culture method for generating large quantities of highly pure dendritic cells from mouse bone marrow., J. Immunol. Methods. 223 (1999) 77–92. doi:10.1016/S0022-1759(98)00204-X.

[13] J. Holmgren, C. Czerkinsky, K. Eriksson, A. Mharandi, Mucosal immunisation and adjuvants: A brief overview of recent advances and challenges, Vaccine. 21 (2003). doi:10.1016/S0264-410X(03)00206-8.

[14] F. Steinhagen, T. Kinjo, C. Bode, D.M. Klinman, TLR-based immune adjuvants, Vaccine. 29 (2011) 3341–3355. doi:10.1016/j.vaccine.2010.08.002.

[15] S. Awate, L.A. Babiuk, G. Mutwiri, Mechanisms of action of adjuvants, Front. Immunol. 4 (2013) 114. doi:10.3389/fimmu.2013.00114.

[16] E. Schutyser, S. Struyf, J. Van Damme, The CC chemokine CCL20 and its receptor CCR6, Cytokine Growth Factor Rev. 14 (2003) 409–426. doi:10.1016/S1359-6101(03)00049-2.

[17] S. Sozzani, P. Allavena, G. D'Amico, W. Luini, G. Bianchi, M. Kataura, T. Imai, O. Yoshie, R. Bonecchi, A. Mantovani, Differential regulation of chemokine receptors during dendritic cell maturation: a model for their trafficking properties., J. Immunol. 161 (1998) 1083–1086. http://www.jimmunol.org/content/161/3/1083 (accessed October 5, 2017).

[18] M.-C. Dieu-Nosjean, A. Vicari, S. Lebecque, C. Caux, Regulation of dendritic cell trafficking: a process that involves the participation of selective chemokines, J. Leukoc. Biol. 66 (1999) 252–262. doi:10.1002/jlb.66.2.252.

[19] S. Fujiie, K. Hieshima, D. Izawa, T. Nakayama, R. Fujisawa, H. Ohyanagi, O. Yoshie, Proinflammatory cytokines induce liver and activation-regulated chemokine/macrophage inflammatory protein-3alpha/CCL20 in mucosal epithelial cells through NF-kappaB., Int. Immunol. 13 (2001) 1255–1263. doi:10.1093/intimm/13.10.1255.

[20] F. Wegmann, K.H. Gartlan, a M. Harandi, S. a Brinckmann, M. Coccia, W.R. Hillson, W.L. Kok, S. Cole, L.P. Ho, T. Lambe, M. Puthia, C. Svanborg, E.M. Scherer, G. Krashias, a Williams, J.N. Blattman, P.D. Greenberg, R. a Flavell, a E. Moghaddam, N.C. Sheppard, Q.J. Sattentau, Polyethyleneimine is a potent mucosal adjuvant for viral glycoprotein antigens, Nat Biotechnol. 30 (2012) 883–888. doi:10.1038/nbt.2344.

[21] M.J. McCluskie, R.D. Weeratna, A.M. Krieg, H.L. Davis, CpG DNA is an effective oral adjuvant to protein antigens in mice, Vaccine. 19 (2000) 950–957. doi:10.1016/S0264-410X(00)00215-2.

[22] N.C. Sheppard, S.A. Brinckmann, K.H. Gartlan, M. Puthia, C. Svanborg, G. Krashias, S.C. Eisenbarth, R.A. Flavell, Q.J. Sattentau, F. Wegmann, Polyethyleneimine is a potent systemic adjuvant for glycoprotein antigens, Int. Immunol. 26 (2014) 531–538. doi:10.1093/intimm/dxu055.

[23] W. Wang, J. Li, K. Wu, B. Azhati, M. Rexiati, Culture and Identification of Mouse Bone Marrow-Derived Dendritic Cells and Their Capability to Induce T Lymphocyte Proliferation., Med. Sci. Monit. 22 (2016) 244–50. doi:10.12659/MSM.896951.

[24] F. Sierro, B. Dubois, A. Coste, D. Kaiserlian, J.P. Kraehenbuhl, J.C. Sirard, Flagellin stimulation of intestinal epithelial cells triggers CCL20-mediated migration of dendritic

cells., Proc. Natl. Acad. Sci. U. S. A. 98 (2001) 13722–7. doi:10.1073/pnas.241308598.
[25] A.J. Thorley, P. Goldstraw, A. Young, T.D. Tetley, Primary Human Alveolar Type II Epithelial Cell CCL20 (Macrophage Inflammatory Protein-3α)–Induced Dendritic Cell Migration, Am. J. Respir. Cell Mol. Biol. 32 (2005) 262–267. doi:10.1165/rcmb.2004-0196OC.
[26] H. Li, M. Chehade, W. Liu, H. Xiong, L. Mayer, M.C. Berin, Allergen-IgE Complexes Trigger CD23-Dependent CCL20 Release From Human Intestinal Epithelial Cells, Gastroenterology. 133 (2007) 1905–1915. doi:10.1053/j.gastro.2007.09.024.
[27] H. Kobayashi, S. Miura, H. Nagata, Y. Tsuzuki, R. Hokari, T. Ogino, C. Watanabe, T. Azuma, H. Ishii, In situ demonstration of dendritic cell migration from rat intestine to mesenteric lymph nodes: relationships to maturation and role of chemokines., J. Leukoc. Biol. 75 (2004) 434–442. doi:10.1189/jlb.0603250.
[28] N.G. Anosova, S. Chabot, V. Shreedhar, J. a Borawski, B.L. Dickinson, M.R. Neutra, Cholera toxin, E. coli heat-labile toxin, and non-toxic derivatives induce dendritic cell migration into the follicle-associated epithelium of Peyer's patches., Mucosal Immunol. 1 (2008) 59–67. doi:10.1038/mi.2007.7.
[29] F. Anjuère, C. Luci, M. Lebens, D. Rousseau, C. Hervouet, G. Milon, J. Holmgren, C. Ardavin, C. Czerkinsky, In vivo adjuvant-induced mobilization and maturation of gut dendritic cells after oral administration of cholera toxin., J. Immunol. 173 (2004) 5103–5111. doi:10.4049/jimmunol.173.8.5103.
[30] A.S. McWilliam, S. Napoli, A.M. Marsh, F.L. Pemper, D.J. Nelson, C.L. Pimm, P.A. Stumbles, T.N. Wells, P.G. Holt, Dendritic cells are recruited into the airway epithelium during the inflammatory response to a broad spectrum of stimuli., J. Exp. Med. 184 (1996) 2429–32. doi:10.1084/jem.184.6.2429.
[31] R. Ramanathan, J. Park, S.M. Hughes, W.R. Lykins, H.R. Bennett, F. Hladik, K. a. Woodrow, Effect of Mucosal Cytokine Administration on Selective Expansion of Vaginal Dendritic Cells to Support Nanoparticle Transport, Am. J. Reprod. Immunol. 74 (2015) 333–344. doi:10.1111/aji.12409.
[32] D. Sajic, A.J. Patrick, K.L. Rosenthal, Mucosal delivery of CpG oligodeoxynucleotides expands functional dendritic cells and macrophages in the vagina, Immunology. 114 (2005) 213–224. doi:10.1111/j.1365-2567.2004.02081.x.
[33] A. Iwasaki, B.L. Kelsall, Localization of distinct Peyer's patch dendritic cell subsets and their recruitment by chemokines macrophage inflammatory protein (MIP)-3α, MIP-3β, and secondary lymphoid organ chemokine, J. Exp. Med. 191 (2000) 1381–1393. doi:10.1084/jem.191.8.1381.
[34] K. Fujimoto, T. Karuppuchamy, N. Takemura, M. Shimohigoshi, T. Machida, Y. Haseda, T. Aoshi, K.J. Ishii, S. Akira, S. Uematsu, A New Subset of CD103 + CD8α + Dendritic Cells in the Small Intestine Expresses TLR3, TLR7, and TLR9 and Induces Th1 Response and CTL Activity, J. Immunol. 186 (2011) 6287–6295. doi:10.4049/jimmunol.1004036.
[35] F. Sallusto, D. Lenlg, R. Förster, M. Lipp, A. Lanzavecchia, Two subsets of memory T lymphocytes with distinct homing potentials and effector functions, J. Immunol. (2014). doi:10.1126/science.1058867.
[36] F. Sallusto, J. Geginat, A. Lanzavecchia, Central memory and effector memory T cell subsets: function, generation, and maintenance., Annu. Rev. Immunol. 22 (2004) 745–63.

doi:10.1146/annurev.immunol.22.012703.104702.
[37] J.R. McDole, L.W. Wheeler, K.G. McDonald, B. Wang, V. Konjufca, K.A. Knoop, R.D. Newberry, M.J. Miller, Goblet cells deliver luminal antigen to CD103+ dendritic cells in the small intestine, Nature. 483 (2012) 345–349. doi:10.1038/nature10863.
[38] M.S. Cartiera, K.M. Johnson, V. Rajendran, M.J. Caplan, W.M. Saltzman, The uptake and intracellular fate of PLGA nanoparticles in epithelial cells, Biomaterials. 30 (2009) 2790–2798. doi:10.1016/j.biomaterials.2009.01.057.
[39] M.P. Desai, V. Labhasetwar, E. Walter, R.J. Levy, G.L. Amidon, The mechanism of uptake of biodegradable microparticles in Caco-2 cells is size dependent, Pharm. Res. 14 (1997) 1568–1573. doi:10.1023/A:1012126301290.
[40] Q. Zhu, J. Talton, G. Zhang, T. Cunningham, Z. Wang, R.C. Waters, J. Kirk, B. Eppler, D.M. Klinman, Y. Sui, S. Gagnon, I.M. Belyakov, R.J. Mumper, J.A. Berzofsky, Large intestine-targeted, nanoparticle-releasing oral vaccine to control genitorectal viral infection, Nat. Med. 18 (2012) 1291–1296. doi:10.1038/nm.2866.
[41] M. Garinot, V. Fiévez, V. Pourcelle, F. Stoffelbach, A. des Rieux, L. Plapied, I. Theate, H. Freichels, C. Jérôme, J. Marchand-Brynaert, Y.J. Schneider, V. Préat, PEGylated PLGA-based nanoparticles targeting M cells for oral vaccination, J. Control. Release. 120 (2007) 195–204. doi:10.1016/j.jconrel.2007.04.021.
[42] S.E. Howe, D.J. Lickteig, K.N. Plunkett, J.S. Ryerse, V. Konjufca, The uptake of soluble and particulate antigens by epithelial cells in the mouse small intestine, PLoS One. 9 (2014) e86656. doi:10.1371/journal.pone.0086656.
[43] B. Singh, S. Maharjan, T. Jiang, S.K. Kang, Y.J. Choi, C.S. Cho, Attuning hydroxypropyl methylcellulose phthalate to oral delivery vehicle for effective and selective delivery of protein vaccine in ileum, Biomaterials. 59 (2015) 144–159. doi:10.1016/j.biomaterials.2015.04.017.
[44] I.M. Belyakov, S.A. Hammond, J.D. Ahlers, G.M. Glenn, J.A. Berzofsky, Transcutaneous immunization induces mucosal CTLs and protective immunity by migration of primed skin dendritic cells, J. Clin. Invest. 113 (2004) 998–1007. doi:10.1172/JCI200420261.
[45] C.R. Casella, T.C. Mitchell, Putting endotoxin to work for us: Monophosphoryl lipid a as a safe and effective vaccine adjuvant, Cell. Mol. Life Sci. 65 (2008) 3231–3240. doi:10.1007/s00018-008-8228-6.
[46] J. Chen, Z. Li, H. Huang, Y. Yang, Q. Ding, J. Mai, W. Guo, Y. Xu, Improved antigen cross-presentation by polyethyleneimine-based nanoparticles, Int. J. Nanomedicine. 6 (2011) 77–84. doi:10.2147/IJN.S15457.

Chapter 5. BIOMATERIAL FORMULATION OF ANTIGENS TO STUDY THE EFFECT OF GASTROINTESTINAL DIGESTION ON IMMUNE RESPONSES

Portions adapted from: **Frizzell, H.**, Park, J., & Woodrow, K. A. Activation of intestinal $CD8^+$ T cells by an oral vaccine through nanofiber-mediated gastric protection of epitopes and the mucosal adjuvant PEI. *Manuscript in preparation.*

5.1 Abstract

Orally administered vaccines are exposed to digestive environments in the gastrointestinal tract, which can result in antigen cleavage depending on amino acid sequence. Studies have shown that gastric digestion of proteins leads to tolerogenic responses, while digestion-resistant proteins induce inflammation and allergy. Here, we investigate how gastrointestinal digestion affects the immunogenic potential of a model protein antigen, ovalbumin (OVA), in terms of innate and T cell activation, which have been less studied. We find that OVA pre-exposed to simulated digestion conditions is unable to induce dendritic cell maturation compared to native OVA. Activation of antigen-specific $CD4^+$ and $CD8^+$ T cells by dendritic cells treated with digested OVA was predicted based on susceptibility of the epitope sequences to cleavage by gastrointestinal enzymes. Resistance of the CD4 epitope to gastrointestinal enzyme cleavage resulted in equivalent levels of $CD4^+$ T cell proliferation. However, IFN-γ production was reduced with gastrointestinal-digested OVA, potentially due to the less mature dendritic cell phenotype observed. As the CD8 epitope contains gastric enzyme cleavage sites, $CD8^+$ T cell activation was reduced when dendritic cells were treated with gastric-digested OVA.

We next developed and evaluated polymeric delivery platforms to provide protection from gastric digestion, in which emulsion electrospun fibers demonstrated enhanced ability to prevent antigen release in gastric conditions compared to nanoparticles. While gastric protection on its own was not sufficient to induce $CD8^+$ T cell responses in mice after oral administration, protection in combination with the use of the mucosal adjuvant polyethyleneimine resulted in significantly increased $CD8^+$ T cells in lymphoid organs and the small intestine epithelium. Thus, we evaluated the immunological consequences of gastrointestinal digestion of antigens and highlight the need to protect susceptible immunogenic epitopes to activate adaptive immunity. We also identify biomaterial delivery systems capable of providing protection in the gastric environment. A robust oral vaccination strategy for the activation of $CD8^+$ T cells is established through epitope protection and adjuvant selection.

5.2 Introduction

Immunization through the oral route provides many immunological and practical advantages in terms of the development of mucosal immunity and ease of administration [1]. However, protein-based subunit vaccines are sensitive to the protease-rich environment in the gastrointestinal tract as are other biotherapeutics that are administered by this route [2]. In the context of oral vaccines, retention of antigen structure and immunogenic epitope sequences are critical for mounting an antigen-specific immune response. How the digestive gastrointestinal environment affects the development of an immune response against orally-delivered vaccines is not fully understood.

Seminal studies established that proteins administered directly into the intestinal tract, bypassing the gastric environment, were able to elicit a systemic immune response while the same protein administered orally led to the development of oral tolerance [3]. Gastric-digested fragments of protein antigens have also been shown to suppress delayed-

type hypersensitivity responses when administered parenterally [4]. Findings in the allergy field have reported that proteins resistant to gastrointestinal enzymatic degradation are more likely to induce allergic responses [5]. A recent study also found an increased risk for the development of allergic symptoms in patients on gastric acid-inhibiting drugs, which raise the gastric pH and inactivate degradative enzymes [6]. These results support the notion that protein antigens administered orally are manipulated by the gastrointestinal environment in such a way that reduces immunogenicity, resulting in an inability to activate protective immune responses. The mechanisms governing this reduction in immunogenicity, however, is not yet known. Additionally, the effect of digestion on cellular immunity and the relative contributions of gastric and intestinal digestion have not been widely studied. Further investigation may reveal immunological mechanisms involved in the induction of tolerance or immunity and identify requirements for oral vaccines to ensure a robust immune response is established.

To prevent gastrointestinal digestion of antigens, strategies including the use of protease inhibitors, use of protease-resistant shielding proteins, and biomaterial delivery carriers have been investigated. The delivery of protease inhibitors can prevent digestion of delivered antigens through enzyme inhibition [7,8]. However, there are limitations to their clinical application, including the reduced digestion and absorption of dietary proteins, potential overproduction of proteases, and toxicity [9]. Recently, expression of protease-resistant proteins on the surface of virus-like particles provided antigen protection, were highly immunogenic, and significantly enhanced protective immune responses [10]. Material-based carriers are also commonly employed to overcome physiochemical challenges associated with different administration routes [11–13]. Such systems can sequester therapeutics from external environments and selectively mediate their release upon exposure to environmental triggers [14]. In addition to improving the bioavailability, pharmacokinetics, and targeting of therapeutics, these formulations can also be used to study immunological mechanisms [15]. Encapsulation of a protein antigen

in a gastric-resistant polymeric microparticle increased the systemic antibody response compared to oral delivery without protection [16]. Other biomaterial delivery platforms also demonstrate enhanced immune responses compared to soluble vaccine delivery [17]; however, how well these delivery systems protect vaccines from gastrointestinal digestion and how this feature affects both innate and adaptive immunity is not clear. Overall, studies investigating the role of digestion on innate immune cell functions and on T cell responses, which are required to effectively combat infection, are lacking. We hypothesize that controlled delivery systems can be used to increase our understanding of gastrointestinal digestion of vaccines and the protection requirements to elicit immune responses.

Here, we first investigate the individual effects of gastric and intestinal digestion on the immunogenicity of a model antigen ovalbumin (OVA) in terms of its ability to activate dendritic cells and be presented to antigen-specific T cells. We focus on known gastrointestinal enzyme cleavage sites within immunologically-relevant epitope sequences of OVA. The results of these experiments then motivated the design and evaluation of polymeric vaccine delivery systems to provide protection of the vaccine in specific gastrointestinal environments that cleave within these epitopes. Finally, we determine how protection of vaccines from digestion affects the elicited cellular and humoral immune response after oral administration, both systemically and mucosally. We find that protection of the $OVA_{257\text{-}264}$ CD8 epitope from gastrointestinal digestion, which was found to contain cleavage sites in contrast to the $OVA_{325\text{-}335}$ CD4 epitope, preserves the activation of epitope-specific $CD8^+$ T cells by dendritic cells *in vitro*. *In vivo*, induction of local antigen-specific $CD8^+$ T cell responses required epitope preservation in combination with specific adjuvant stimulation.

5.3 Materials and Methods

5.3.1 *Animals*

Female C57Bl/6J and OT-II mice (6-8 weeks old) were purchased from The Jackson Laboratory. All procedures were approved by and followed protocols approved by the IACUC. Mice in experimental oral vaccination studies were age-matched between groups.

5.3.2 *Cell lines and bone marrow-derived dendritic cell derivation*

The immortalized dendritic cell line DC2.4 and the $CD8^+$ T cell hybridoma cell line B3Z were provided by the Stayton lab at the University of Washington. Bone marrow-derived dendritic cells (BMDCs) were derived from the bone marrow of tibias and femurs collected from naïve female C57Bl6J mice. Bone marrow was cultured at 37°C, 5% CO_2 in complete medium (RPMI-1640 supplemented with 2 mM L-glutamine and 10% heat-inactivated fetal bovine serum [FBS, Thermo], 100 U mL^{-1} penicillin and streptomycin [Invitrogen], 1X non-essential amino acids [Gibco], 1X HEPES [Gibco]) with 20 µg mL^{-1} granulocyte-macrophage colony stimulating factor (GM-CSF) (PeproTech). On day 3 fresh medium with GM-CSF was added and on days 5 and 7 non-adherent cells were collected, spun down at 1500 rpm for 5 min, and resuspended in fresh medium with GM-CSF. BMDCs were collected by cell dissociation buffer (Gibco) and used for experiments on day 8 of culture.

5.3.3 *In vitro antigen digestion*

Chicken egg albumin (OVA, Invivogen) was added to simulated gastric (2 g L^{-1} NaCl, pH 1.2) or intestinal (6.8 g L^{-1} KH_2PO_4, pH 6.8) fluid containing pepsin (Sigma) or pancreatin from porcine pancreas (Sigma), respectively, at an OVA:enzyme mass ratio of

20:1. Samples were placed in a rotating incubator (150 rpm) at 37°C for 1 hour (gastric conditions) or 2 hours (intestinal conditions). For gastrointestinal conditions, gastric and intestinal digestion was performed in series. Following gastric digestion, samples were pH-adjusted to 7, diluted in simulated intestinal fluid, and incubated at 150 rpm and 37°C for 2 hours.

5.3.4 *Polyacrylamide gel electrophoresis*

Native and digested OVA samples added to lanes of a 4-20% Mini-PROTEAN TGX Precast Protein Gel (Bio-Rad) at 1 µg OVA. Samples were prepared in NuPAGE LDS Sample Buffer (Invitrogen) with β-mercaptoethanol (β-ME) as a reducing agent. Novex Sharp Unstained Protein Standard (Invitrogen) was used. Gels were run in a 0.1% sodium dodecyl sulfate (SDS) running buffer (25 mM Tris, 192 mM glycine) at 110 V for 1 hour. Gels were washed 3 times with DI water for 5 minutes followed by staining in 20 mL SimplyBlue SafeStain (Thermo) covered for 1 hour at room temperature with gentle shaking. Gels were washed with 100 mL DI water overnight followed by 100 mL fresh DI water for 1 hour before imaging with a Gel Doc EZ System (Bio-Rad).

5.3.5 *Dendritic cell maturation*

BMDCs were plated overnight in 48-well tissue culture-treated plates at 2.5 x 10^5 per well in complete medium with GM-CSF (20 µg mL^{-1}). The next day, medium was collected and BMDCs were treated with native OVA or OVA digests (0.1 mg mL^{-1}) for 24 hours. BMDCs were detached and cells were incubated with Fc block (anti-mouse CD16/CD32) (BDBiosciences) and LIVE/DEAD Fixable Blue Dead Cell Stain (Thermo) in PBS for 15 min at room temperature. Cells were washed, resuspended in FACS buffer (1% BSA, 1 mM [Ethylenedinitrilo]tetraacetic acid, disodium salt, dehydrate [EDTA, Avantor Performance] in PBS), and stained with the following antibodies for 30 min at 4°C: anti-mouse CD45-FITC (30-F11), CD11c-APC (N418), I-A/I-E-PerCP/Cy5.5

(M5/114.15.2), CD86-BV605 (GL-1). All antibodies were purchased from BioLegend. Supernatants were assayed for IL-12 using a standard enzyme-linked immunosorbent assay (ELISA) kit (PeproTech) following manufacturer's instructions.

5.3.6 *$CD8^+$ T cell activation*

BMDCs or DC2.4s were plated overnight in 96-well U-bottom tissue culture-treated plates at 5 x 10^4 per well in complete medium. For BMDCs, media included GM-CSF (20 µg mL^{-1}). The next day, medium was removed and DCs were treated with native OVA or digested OVA (0.1 mg mL^{-1}) for 24 hours. DCs were co-treated with lipopolysaccharide (LPS, 0.5 µg mL^{-1}) at the time of OVA addition. Cells were washed and 5 x 10^4 OVA-specific B3Z $CD8^+$ T cells were added per well. After 24 hours, plates were spun at 500 x g for 5 minutes and supernatant was removed. Cells were resuspended in lysis medium (0.15 mM chlorophenol red-β-D-galactopyranoside, 9 mM $MgCl_2$, 0.125% Nonidet P-40, and 100 µM 2-mercaptoethanol) and incubated at 37°C for 2-72 hours. The plate was read at 595 nm on an Infinite 200 PRO microplate reader (Tecan).

5.3.7 *$CD4^+$ T cell activation*

BMDCs were plated overnight in 96-well U-bottom tissue culture-treated plates at 5 x 10^4 per well in complete medium with GM-CSF (20 µg mL^{-1}). The next day, medium was removed and BMDCs were treated with native OVA or OVA digests (0.1 mg mL^{-1}) for 24 hours. Spleens from OT-II mice were chopped and digested in 1 mg mL^{-1} Collagenase D (Sigma) digestion medium (complete medium with 40 µg mL^{-1} DNase I [Sigma]) for 20 min at 37°C. Digested spleens were resuspended, passed through a 70 µm cell strainer, and red blood cells were lysed. Cells were washed and resuspended in MACS buffer followed by passage through a 70 µm cell strainer. $CD4^+$ T cells were isolated by negative selection using a $CD4^+$ T cell isolation kit (Miltenyi Biotec) following

manufacturer's instructions. Isolated $CD4^+$ T cells were stained with 10 μM CFSE in 0.1% BSA/PBS (CellTrace CFSE Cell Proliferation Kit, Thermo) for 10 min at 37°C. CFSE staining was stopped by adding ice-cold complete medium then incubating cells for 5 min on ice. $CD4^+$ T cells were added to washed BMDCs at 5 x 10^4 per well in complete medium with GM-CSF (20 μg mL^{-1}). After 72 hours, the plate was centrifuged, and supernatants were collected and stored at -20°C. Cells were resuspended in FACS buffer and incubated with Fc block and LIVE/DEAD Fixable Near-IR Dead Cell Stain (Thermo) for 15 min at room temperature. Cells were washed and stained with the following antibodies for 30 min at 4°C: anti-mouse CD3-PerCP/Cy5.5 (17A2), CD4-APC (GK1.5). After surface staining, cells were washed and prepared for intracellular staining with the Foxp3 Fix/Perm Buffer Set (BioLegend) per manufacturer's instructions. Cells were stained with the following intracellular antibodies: anti-mouse T-bet-PE/Cy7 (4B10) and Foxp3-BV421 (MF-14). All antibodies were purchased from BioLegend. Cells were washed and resuspended in FACS buffer for analysis on an Attune NxT flow cytometer (Thermo). Flow cytometry analysis was performed using FlowJo software (Treestar). Supernatants were assayed for IFN-γ using a standard enzyme-linked immunosorbent assay (ELISA) kit (PeproTech) following manufacturer's instructions.

5.3.8 *Nanoparticle synthesis*

Poly(lactic-co-glycolic acid) (PLGA) (50:50, acid-terminated, 0.55 – 0.75 dL g^{-1}) (Lactel) was dissolved in dichloromethane (Sigma) at 50 mg mL^{-1}. Ovalbumin in solution was added dropwise into the PLGA solution at 10% volume while vortexing. The primary emulsion was probe-sonicated (500 W Ultrasonic Processor GEX500) at 38% amplitude for 30 seconds followed by placement on ice, repeated for a total of 3 times. The primary emulsion was added drop-wise into an equivalent volume of 5% polyvinyl alcohol (PVA, 30 – 70 kDa, 87-90% hydrolyzed) (Sigma) while vortexing. The secondary emulsion was

sonicated as described above and transferred into 0.3% PVA and stirred overnight to allow for solvent evaporation.

Eudragit L100 was dissolved in methanol at 12.5 mg mL^{-1} and ovalbumin in solution was added dropwise into the PLGA solution at 10% volume while vortexing. The primary emulsion was sonicated at 38% amplitude for 30 seconds followed by placement on ice for a total of 3 times. The primary emulsion was added drop-wise into 100 mL citrate buffer (46.67 mM sodium citrate, 59.02 mM citric acid, pH-adjusted to 5) with 1% PVA (30 – 70 kDa, 87-90% hydrolyzed) while stirring and allowed to evaporate overnight. Nanoparticle suspensions were centrifuged at 10,000 x g for 20 min at 4°C and particles were resuspended in DI water for a total of 3 washes. After the last wash, particles were resuspended in DI water, transferred to vials and frozen at -80°C, and lyophilized.

5.3.9 *Electrospinning, nanofiber characterization, and nanofiber micronization*

Eudragit L100 nanofibers containing OVA were electrospun from an emulsion as described [18]. Eudragit L100 (kindly provided by Evonik Health Care) was dissolved in EtOH:DMF (4:1 v:v) at 15 wt%. To form an emulsion, Tween-20 was added at 0.4% volume and OVA in solution was added dropwise to the Eudragit L100/Tween-20 solution while vortexing at a 5-20% aqueous phase. This emulsion was then electrospun onto waxed paper on a metal collector using a needle-rig electrospinning set up (12.5 kV, 25 µL min^{-1} flow rate, 12 cm distance) in a fume hood. OVA-loaded Eudragit L100 nanofibers were processed into micron-sized fiber pieces (micronization) that could be passed through a 22G gavage needle by wet blending (BlendTec) in DI water pH 2. Blended fibers were passed through a 250 µm metal sieve followed by collection using vacuum filtration. Collected fibers were resuspended in DI water pH 2, frozen, and lyophilized. OVA loading in Eudragit L100 nanofibers was quantified using a MicroBCA Protein Assay Kit (Thermo) before and after micronization to confirm no loss of cargo upon the micronization process (data not shown).

5.3.10 *HRP activity assay*

HRP was electrospun in Eudragit L100 nanofibers using emulsion electrospinning as described above. Bioactivity retention of encapsulated HRP was determined by kinetic colorimetric substrate assays of the proteins after incubation in simulated gastric fluid with pepsin (1 mg mL^{-1}) for 1 hour at 37 °C. Samples or freshly prepared HRP controls were added to a 96-well flat bottom plate (5 ng mL^{-1} HRP) and TMB substrate solution (1:1 Substrate A:Substrate B, vol:vol) (BioLegend) was added to start the assay. Change in absorbance at 652 nm was monitored every 15 seconds using a Tecan Infinite 200 PRO microplate reader (Männedorf, Switzerland) over 10 minutes. The maximum increase in absorbance per minute (max slope) from the initial linear portion was determined and the retained protein bioactivity was calculated compared to fresh HRP.

5.3.11 *Release studies in simulated gastrointestinal fluids*

OVA-loaded nanoparticle and nanofiber formulations were incubated in simulated gastric fluid with or without pepsin (OVA:enzyme 20:1, m:m) for 1 hour at 37°C. For nanoparticle samples, samples were spun down at 14,000 rpm for 15 minutes and supernatant was collected. Nanoparticles were resuspended in 0.1M NaOH to dissolve remaining nanoparticles. For nanofiber samples, fiber-free supernatant was collected, and fiber mats were removed and dissolved in PBS. Protein released into the supernatant and remaining in the carrier after incubation in simulated gastric fluid was quantified by MicroBCA Assay controlling for supernatant pepsin concentration.

5.3.12 *Oral immunization*

Age-matched female C56Bl/6J were immunized with OVA in solution or in micronized Eudragit L100 emulsion electrospun fibers in 200 µL by oral gavage using a 22G metal gavage needle. Animals were not fasted prior to immunization nor were

anesthetized during the procedure. Mice were vaccinated every 4 weeks for a total of 4 immunizations. In some studies, branched PEI (100 µg) (Sigma) was included in the dose.

5.3.13 *Organ processing and staining for flow cytometry*

Organs were harvested 14 days after the last immunization and processed into single cell suspensions as follows. Spleens were collected and processed through a 40 µm cell strainer followed by red blood cell lysis. Mesenteric lymph nodes were collected and processed through a 40 µm cell strainer. The small intestine was collected and flushed with 5 mL PBS with 0.1 mg mL^{-1} trypsin inhibitor (Sigma) and 50 mM EDTA to collect the luminal contents. Peyer's patches and remaining mucus were removed followed by opening of the intestine longitudinally and processing into 1 cm fragments. Small intestinal fragments were incubated in 0.15 mg mL^{-1} 1,4-dithioerythritol (DTE) (Sigma) in complete HBSS (10 mM HEPES, 25 mM sodium bicarbonate, 20% FBS) for 30 minutes at 37°C with lateral shaking (230 rpm) followed by collection of intraepithelial lymphocytes (SI IEL) through a 100 µm cell strainer. SI IELs were washed with HBSS and further purified by density gradient centrifugation with a 44%/77% Percoll (GE Healthcare) gradient. Small intestinal tissue fragments were recollected following SI IEL release, washed to remove remaining DTE, and digested with 1 mg mL^{-1} Collagenase VIII in RPMI 1640 with 40 µg mL^{-1} DNase I for 45 minutes at 37°C with lateral shaking (230 rpm). Small intestinal lamina propria (SI LP) cells were collected through a 100 µm cell strainer and purified by density gradient centrifugation as described for SI IELs. Single cells suspensions were incubated with Fc block and LIVE/DEAD Fixable Near-IR Dead Cell Stain (Thermo) for 15 min at room temperature. Cells were washed and stained with the following tetramers for 15 min at room temperature: H-2K(b) $OVA_{257-264}$ PE-labeled tetramer and I-A(b) $OVA_{325-335}$ APC-labeled tetramer (NIH Core Tetramer Facility). Cells were washed and stained with the following antibodies for 30 min at 4°C: anti-mouse CD3-Alexa700 (17A2), CD4-BV605 (RM4-5), CD8-FITC (KT-15), CD44-PerCP/Cy5.5

(IM7). After surface staining, cells were washed and prepared for intracellular staining with the Foxp3 Transcription Factor Staining Buffer Set (eBioscience) per manufacturer's instructions. Cells were stained with the following intracellular antibodies: anti-mouse T-bet-PE/Cy7 (4B10) and Foxp3-BV421 (MF-14). Cells were washed and resuspended in FACS buffer for analysis on an Attune NxT flow cytometer (Thermo). Flow cytometry analysis was performed using FlowJo software (Treestar). Tetramer gates were set based on unstained controls from each experiment.

5.3.14 *Statistical analysis*

Data presented as mean ± standard deviation and analyzed by one-way ANOVA with Tukey's or Dunnett's multiple comparisons test using Prism (GraphPad). Statistically significant differences are indicated as $*p<0.05$, $**p<0.01$, and $***p<0.001$.

5.4 Results and Discussion

5.4.1 *Gastrointestinal digestion of OVA reduces DC maturation*

Dendritic cells have a central role in the elicitation of adaptive immune responses as well as in the induction of oral tolerance [19–21]. Thus, we first evaluated the effect of antigen digestion on dendritic cell phenotype. The model protein antigen ovalbumin (OVA) was digested in simulated gastric conditions with pepsin for 1 hour followed by intestinal digestion for 2 hours through pH adjustment and the addition of pancreatin. This protocol simulating gastrointestinal digestion induced the partial digestion of OVA through observance of low molecular weight protein fragments by SDS-PAGE gel electrophoresis (Figure 5.1A). Exposure of OVA to simulated gastric digestion alone was sufficient to generate protein fragments (Figure 5.1A). These results are in accordance with other studies that observed partial resistance of OVA to digestion in simulated

gastrointestinal conditions compared to other proteins [5,22]. Pepsin cleaves preferentially at the C-terminal side of aromatic amino acids while trypsin cleaves on the C-terminal side of positively-charged lysine and arginine residues, unless proline is on the carboxylic side of the cleavage site. As gastrointestinal enzymes are known to cleave at specific amino acid sites, we investigated commonly studied OVA CD4 ($OVA_{323-339}$) and CD8 ($OVA_{257-264}$) epitopes for their susceptibility to gastric and intestinal digestion using the ExPASy PeptideCutter tool (Figure 5.1B) [23]. Based on cleavage predictions, the $OVA_{323-339}$ epitope sequence was not vulnerable to pepsin or trypsin activity. The first identification of this antigenic fragment was from trypsin-processed OVA protein, supporting the prediction that trypsin cleaves around the epitope [24]. In contrast, both pepsin and trypsin cleavage sites are found within the $OVA_{257-264}$ epitope region, suggesting this epitope would be compromised in the gastrointestinal tract prior to cell processing and presentation. These results highlight the importance of antigen sequence in the preservation of immunogenic epitopes of orally administered vaccines.

We next determined if digested OVA would have a differential effect on the maturation of dendritic cells, which require expression of costimulatory surface molecules and secretion of inflammatory cytokines in addition to antigen presentation to activate antigen-specific T cells [25]. Bone marrow-derived $CD11c^+$ dendritic cells (BMDCs) increased expression of the costimulatory marker CD86 after incubation with native, undigested OVA (Figure 5.1C,D). Inclusion of the immunostimulant LPS was used as a positive control to identify the mature dendritic cell population, which dramatically increased CD86 expression (data not shown). In contrast, BMDCs did not mature when incubated with gastrointestinal-digested OVA (Figure 5.1C,E), indicating a loss of DC-stimulating potential of OVA upon digestion. Exposure of BMDCs to OVA exposed to only gastric digestion conditions also resulted in a lack of maturation (Figure 5.1C,E) suggesting that gastric digestion is sufficient to result in a loss of DC-stimulating potential prior to intestinal digestion. Similar trends were observed with respect to secretion of the

inflammatory cytokine IL-12 by BMDCs treated with native or digested OVA (Figure 5.1D), demonstrating that antigen digestion can result in a loss of function in addition to a less mature phenotype. This inflammatory cytokine is a necessary signal for the activation and differentiation of T_H1 $CD4^+$ T cells and their production of IFN-γ [26–28].

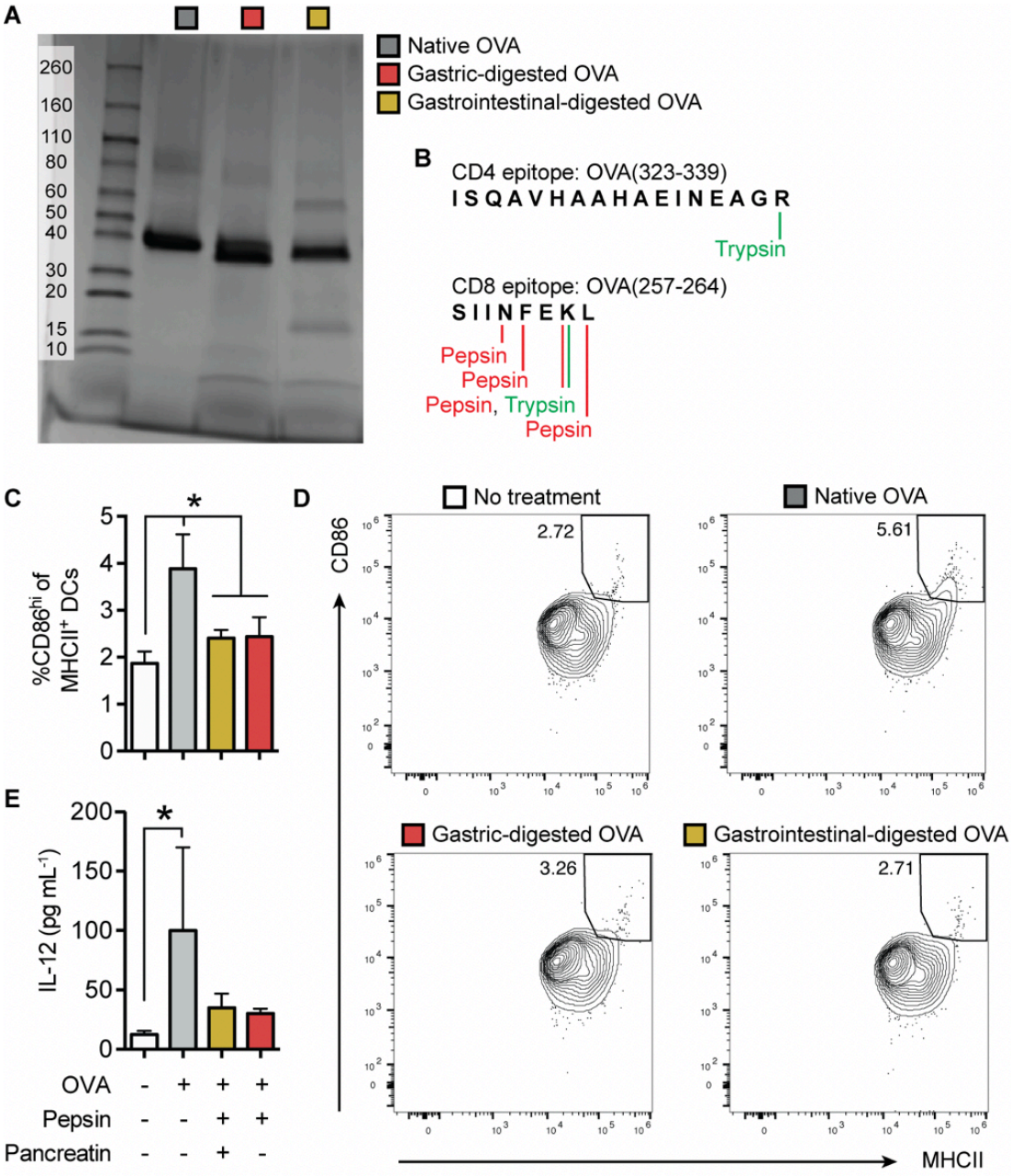

Figure 5.1. Gastric-digested OVA loses ability to mature dendritic cells. ***A)*** *OVA was incubated in simulated gastrointestinal conditions and analyzed by SDS-PAGE. Lane 1, ladder; Lane 2, native OVA; Lane 3, gastric-digested OVA; Lane 4, gastrointestinal-digested OVA.* ***B)*** *Predicted*

cleavage sites of pepsin and trypsin on most common CD4 and CD8 immunogenic epitopes of OVA generated using the ExPASy PeptideCutter tool. ***C, D)*** *BMDCs were treated with OVA digested in simulated gastrointestinal conditions for 24 hours and dendritic cell phenotype was analyzed by flow cytometry.* ***E)*** *After OVA treatment of BMDCs, supernatant was collected and assayed for IL-12 by ELISA. Data representative of n=3 per group from two independent experiments and presented as mean ± standard deviation and analyzed by one-way ANOVA (*p<0.05).*

5.4.2 *Ability of dendritic cells to activate T cells is influenced by antigen digestion in vitro*

As we observed a reduced ability of gastrointestinal OVA to activate dendritic cells, we next investigated enzymatically-modified antigen would affect dendritic cell presentation to and activation of antigen-specific $CD4^+$ and $CD8^+$ T cells. BMDCs treated with native or gastrointestinal-digested OVA were cultured with CFSE-labeled $OVA_{323-339}$-specific $CD4^+$ T cells purified from the spleens of OT-II mice. OVA exposed to gastric or intestinal digestion conditions separately were also included to evaluate the relative contribution of each digestive environment. BMDCs treated with undigested and digested OVA induced $CD4^+$ T cells to proliferate to the same degree (Figure 5.2A). This is likely due to the predicted resistance of $OVA_{323-339}$ to pepsin digestion. When assayed for the production of IFN-γ by activated CD4 T cells, representing function, reduced cytokine concentration was observed when OVA underwent simulated gastrointestinal digestion (Figure 5.2B). These results may be due to the less mature state and lack of IL-12 secretion of DCs treated with pre-digested antigen, which influences CD4 T cell activation and polarization [26,29]. $CD4^+$ T cells that underwent antigen-specific proliferation were analyzed for polarization towards T_{reg} or T_H1 through expression of the nuclear transcription factors Foxp3 and T-bet, respectively. In contrast to proliferation patterns, gastrointestinal digestion of OVA significantly increased the expression of Foxp3 and

decreased the expression of T-bet in primed $CD4^+$ T cells (Figure 5.2C). Neither gastric nor intestinal digestion of OVA on their own was sufficient to increase Foxp3 expression in $CD4^+$ T cells that had proliferated in response to antigen-presentation by BMDCs (Figure 5.2C). In contrast, we did observe a significant reduction of T-bet^+ $CD4^+$ T cells when OVA was subjected to intestinal digestion only (Figure 5.2C). These transcription factor expression results are in accordance with the decreased IFN-γ produced with gastrointestinal-digested antigens, as T-bet^+ T_H1 cells are characterized by their production of this inflammatory cytokine while $Foxp3^+$ T_{reg} cells predominately secrete IL-10 [30]. The presence of IFN-γ itself can also drive T-bet induction [31]. These results indicate that exposure to different gastrointestinal conditions can influence the polarization of $CD4^+$ T cells by BMDCs, with polarization towards the T_{reg} lineage being favored over T_H1 in response to gastrointestinal-digested antigens *in vitro*.

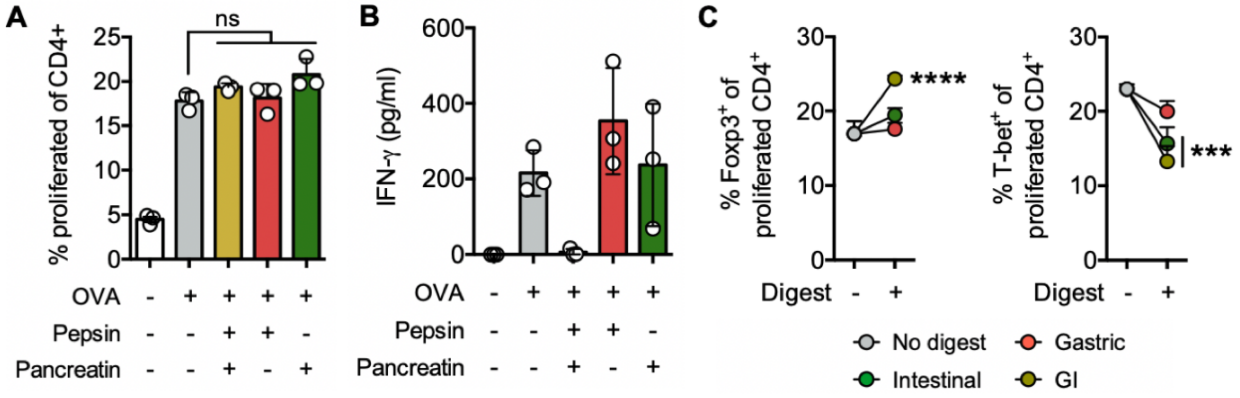

Figure 5.2. Gastrointestinal digestion of OVA affects $CD4^+$ T cell polarization but not proliferation. BMDCs were treated with native or digested OVA for 24 hours followed by co-culture with CFSE-stained $CD4^+$ OT-II T cells for 3 days. ***A)*** *Proliferation,* ***B)*** *IFN-γ secretion, and* ***C)*** *polarization of OT-II $CD4^+$ T cells 3 days after culture with BMDCs treated with OVA digested in gastrointestinal conditions. Data representative of n=3 per group from one independent experiment and presented as mean ± standard deviation and analyzed by one-way ANOVA (**p<0.01, ****p<0.0001).*

Dendritic cells are also able to present antigen on MHC class I to $CD8^+$ T cells. Activation of $CD8^+$ T cells is critical to develop cytotoxic immunity in which $CD8^+$ T cells themselves can combat infection and cancer directly [32]. To evaluate how gastrointestinal antigen digestion affects dendritic cell cross-presentation of antigens to $CD8^+$ T cells, we utilized the B3Z CTL hybridoma that is specific to $OVA_{257-264}$. Without additional stimulation of dendritic cells, cross-presentation of OVA did not occur (data not shown), but $CD8^+$ B3Z cells were able to be activated by LPS-stimulated BMDCs (Figure 5.3A) and DC2.4s (Figure 5.3B) pre-incubated with native OVA. When dendritic cells were treated with gastrointestinal-digested OVA, $CD8^+$ B3Z activation was not observed (Figure 5.3A,B). In both dendritic cell sources, only digestion of OVA in intestinal conditions resulted in $CD8^+$ B3Z activation (Figure 5.3A,B). These results indicate that the loss of cross-presentation of OVA to SIINFEKL-specific $CD8^+$ T cells is driven by gastric digestion, likely due to the susceptibility of the epitope recognized by the B3Z T cell receptor to gastric enzyme cleavage.

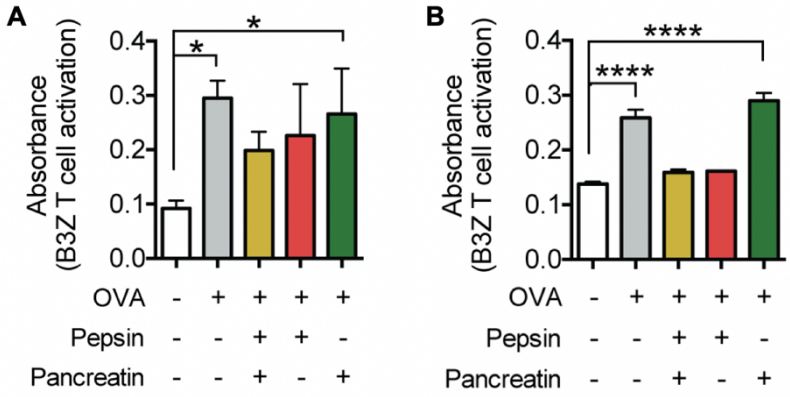

Figure 5.3. Gastrointestinal-digested OVA loses ability to be cross-presented to $CD8^+$ T cells in vitro. ***A)*** *BMDCs and* ***B)*** *DC2.4s were treated with native or digested OVA for 24 hours followed by co-culture with B3Z $CD8^+$ T cells for 24 hours. Cells were lysed and CPRG substrate was added. B3Z activation was evaluated by monitoring absorbance, indicative of* β-galactosidase-*mediated substrate conversion. Data representative of n=3 per group from 1-3 independent experiment and presented as mean ± standard deviation and analyzed by one-way ANOVA (*p<0.05, ****p<0.0001).*

5.4.3 *Differential ability of polymeric delivery platforms to protect OVA from gastrointestinal digestion*

Since gastrointestinal digestion influenced dendritic cell maturation and the ability to activate $CD4^+$ and $CD8^+$ T cell responses, we next developed vaccine delivery systems to provide protection of antigens from digestion. Commonly, nanoparticles (NPs) are used to encapsulate therapeutics and modulate their physical structure to influence trafficking and uptake [33]. Thus, we first synthesized NPs composed of the biocompatible polymer poly(lactic-co-glycolic acid) (PLGA) to provide protection of OVA from enzymatic cleavage in both gastric and intestinal conditions. We hypothesized these polymeric NPs could protect OVA due to the long-term degradation profiles of PLGA-based delivery platforms *in vivo* [34]. A double emulsion method was used to produce OVA-loaded PLGA NPs (~450–600 nm diameter) (Figure S5.1). OVA-loaded PLGA NPs were incubated with BMDCs followed by co-culture with $CD8^+$ B3Z T cells. Formulation of native OVA in PLGA NPs significantly increased B3Z T cell activation compared to soluble OVA (Figure 5.4A). This is likely due to the enhanced protein uptake in DCs observed with PLGA NP-formulation (Figure S5.2). Concurrently, we produced PLGA NPs loaded with pre-digested OVA to separate the effect of digestion from NP formulation, as the latter was observed to affect immune responses compared to soluble antigen. Interestingly, gastric-digested OVA encapsulated in PLGA NPs led to significant activation of $CD8^+$ B3Z cells in contrast to the loss of antigenicity observed when soluble OVA was digested in gastric conditions (Figure 5.4B). These data demonstrate that particulate formulation of digested antigens may recover their potential to induce antigen-specific $CD8^+$ T cell responses. We hypothesize that formulation of digested OVA in NPs may modulate uptake of antigens or access more immunogenic intracellular trafficking pathways, leading to enhanced cross-presentation compared to digested antigen in soluble form.

To evaluate the function of OVA-loaded PLGA NPs to protect antigens from gastrointestinal digestion, we next exposed NPs to simulated conditions prior to incubation with DCs. Although NP formulation of OVA enhanced B3Z T cell activation, this capability was completely abrogated when NPs were pre-exposed to simulated gastrointestinal conditions (Figure 5.4A). Incubation of OVA-loaded PLGA NPs in gastric or intestinal conditions separately revealed that the loss of function occurred in the gastric environment, as NPs exposed to intestinal conditions retained their ability to activate B3Z cells (Figure 5.4A). Evaluation of PLGA NP physical properties after incubation in simulated gastrointestinal fluids revealed no change in particle diameter nor polydispersity index (PDI) that may have contributed to the observed loss of function (Figure S5.1). These data led us to hypothesize that OVA encapsulation in PLGA NPs may be compromised upon exposure to simulated gastric conditions leading to loss of function, as it is known that NP delivery systems suffer from an initial burst release of their loaded cargo [35]. To test this, we quantified the release of OVA from PLGA NPs in simulated gastric conditions with and without the gastric protease pepsin. After 1 hour in simulated gastric conditions without pepsin, PLGA NPs released ~20% of the total encapsulated OVA (Figure 5.4C). Inclusion of pepsin in the medium accelerated release of OVA from the NPs, with ~60% of OVA released from the NPs after 1 hour (Figure 5.4C). Based on these results, protein-loaded NPs released a majority of encapsulated protein in the gastric environment where we aimed to protect antigen from digestion. Thus, we explored additional biomaterial-based formulation strategies to limit antigen release in gastric conditions and provide protection from digestion.

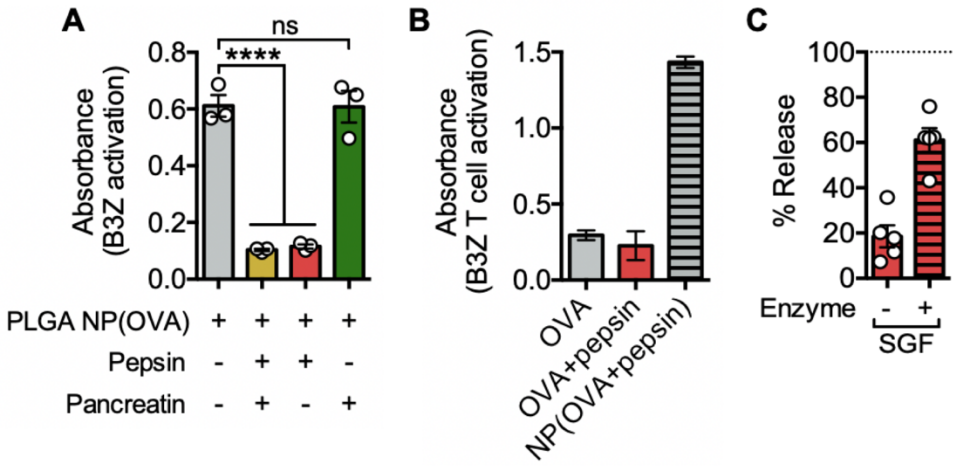

Figure 5.4. OVA-loaded PLGA NPs lose ability to activate CD8⁺ T cells after exposure to simulated gastric conditions. OVA-loaded PLGA NPs were incubated in simulated gastrointestinal conditions and added to BMDCs for 24 hours. Cells were washed and co-cultured with B3Z CD8⁺ T cells for 24 hours. Cells were lysed and CPRG substrate was added. B3Z activation was evaluated by monitoring absorbance, indicative of β-galactosidase-*mediated substrate conversion into a colorimetric product.* ***B)*** *OVA was digested in simulated gastric conditions and formulated in PLGA NPs. Gastric-digested OVA-loaded PLGA NPs were used in BMDC-B3Z CD8⁺ T cell activation assays as described above.* ***C)*** *OVA-loaded PLGA NPs were incubated in simulated gastric conditions with or without pepsin for 1 hour. OVA release was quantified by MicroBCA. Data representative of n=3 per group from 1-2 independent experiment and is presented as mean ± standard deviation and analyzed by one-way ANOVA (ns, not significant; ****p<0.0001).*

In Chapter 3, we identified emulsion electrospinning as a technique to encapsulate proteins in polymeric nanofibers, in which the protein is located in an aqueous core surrounded by a polymeric shell [18]. We hypothesized that this formulation strategy could provide better protection of encapsulated proteins in digestive conditions compared to NPs as synthesized by double emulsion. Orally delivered vaccines need to be absorbed at the intestinal epithelium to access immune cells and inductive sites. However, the use of hydrophobic polymers, such as PLGA, in nanofiber formulation results in slow, sustained release of the encapsulated protein. Even after 24 hours, at which point orally administered substances are cleared from the body, less than 20% of the total protein is

released (Figure S5.3). Thus, we chose to use a pH-responsive polymer Eudragit L100, which is soluble in pH conditions above 6, to encapsulate antigens in the gastric environment while facilitating release in the intestine for absorption and initiation of immune responses. We have demonstrated that 100% of the loaded cargo is released within 1 hour after exposure of fibers to simulated intestinal pH conditions [18]. While we cannot determine the effect of complete protection from both gastric and intestinal digestion conditions on immune responses to oral vaccines, this strategy elucidates how effective gastric protection alone is at improving responses to antigens administered orally and provides insight to the formulation requirements of oral vaccines. As we observed that gastric digestion drove the loss of $CD8^+$ T cell activation capacity of OVA, preventing this activity loss may be desirable to generate multifunction immune responses *in vivo*.

To validate that OVA-loaded Eudragit L100 emulsion electrospun fibers could protect antigens in gastric conditions, we first quantified OVA release in simulated gastric conditions with or without pepsin as evaluated for OVA-loaded PLGA NPs. Additionally, we compared the release profiles of Eudragit L100 electrospun nanofibers with Eudragit L100 NPs to identify the most relevant delivery platform. As observed with PLGA NPs, Eudragit L100 NPs released a majority of their protein cargo in pepsin-containing simulated gastric conditions (Figure 5.5A). In contrast, Eudragit L100 nanofibers limited the release of OVA in gastric conditions to $<10\%$ (Figure 5.5B). Additionally, we verified that the electrospinning process did not compromise the antigenic function of OVA. Dendritic cells (DC2.4s) treated with OVA-loaded Eudragit L100 fibers were able to activate $CD8^+$ B3Z cells (Figure 5.5C). DCs treated with blank Eudragit L100 fibers did not induce B3Z activation (Figure 5.5C). As these experiments only revealed the ability of Eudragit L100 nanofibers to control the release of functional OVA in different pH conditions, we next evaluated the platform for protection of proteins from pepsin-mediated activity loss. Here, we encapsulated the enzyme horseradish peroxidase (HRP) in Eudragit L100 nanofibers followed by exposure of fibers to simulated gastric conditions with pepsin.

After 1-hour, unprotected HRP lost ~90% of its initial activity after exposure to digestive conditions while Eudragit L100 nanofiber formulation retained ~75% enzyme activity (Figure 5.5D).

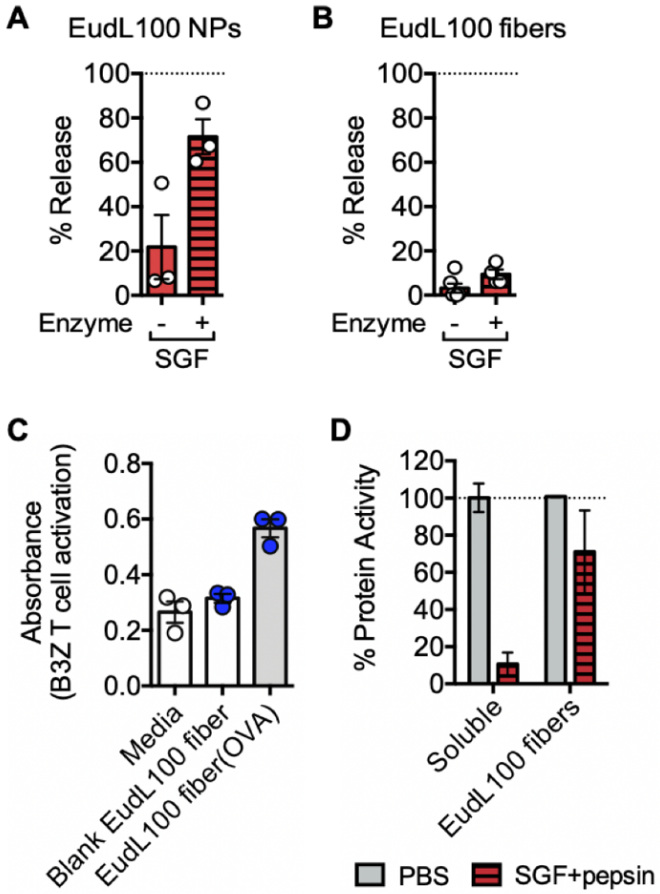

Figure 5.5. Emulsion electrospun Eudragit L100 nanofibers limit protein release in simulated gastric fluid and protect proteins from pepsin-mediated activity loss. OVA-loaded Eudragit L100 ***A)*** *NPs and* ***B)*** *nanofibers were incubated in simulated gastric conditions with or without pepsin for 1 hour. OVA release was quantified by MicroBCA.* ***C)*** *OVA-loaded EudragitL100 nanofibers were dissolved in PBS and added to DC2.4s at 0.1 mg mL^{-1} OVA for 24 hours. Cells were washed and co-cultured with B3Z CD8^{+} T cells for 24 hours. Cells were lysed and CPRG substrate was added. B3Z activation was evaluated by absorbance.* ***D)*** *Soluble HRP or HRP encapsulated in Eudragit L100 nanofibers was incubated in simulated gastric fluid with pepsin for 1 hour. Rate of substrate conversion by HRP was compared to freshly prepared enzyme to determine activity retention. Data representative of n=3 per group from 1-2 independent experiments and presented as mean ± standard.*

5.4.4 *Formulation of OVA in nanofibers preserves ability to activate T cells after gastric digestion*

Since emulsion electrospun Eudragit L100 nanofibers demonstrated gastric protection of encapsulated antigen, we next used these materials to evaluate how protection from digestion would influence the activation of T cell responses *in vitro*. OVA encapsulated in Eudragit L100 nanofibers was exposed to simulated gastrointestinal digestion conditions prior to incubation with dendritic cells. These primed dendritic cells were then cultured with OVA-specific $CD4^+$ OT-II T cells or $CD8^+$ B3Z T cells. As $CD8^+$ T cell activation was diminished upon exposure of soluble OVA to gastric digestion conditions, we hypothesized that protection from digestion through encapsulation in Eudragit L100 nanofibers may prevent this activity loss. DCs treated with OVA-loaded Eudragit L100 nanofibers cells exposed to all gastrointestinal digestion conditions were able to activate $CD8^+$ B3Z T cells, both by BMDCs (Figure 5.6A) and DC2.4s (Figure 5.6B). Compared to soluble OVA exposed to gastrointestinal digestion conditions, Eudragit L100 nanofiber formulation of OVA resulted in $CD8^+$ B3Z T cell activation (Figure 5.6C). These results demonstrate that Eudragit L100 nanofiber formulation can prevent pepsin-mediated loss of CD8 epitope immunogenicity through protection of the antigen from digestion by gastric enzymes.

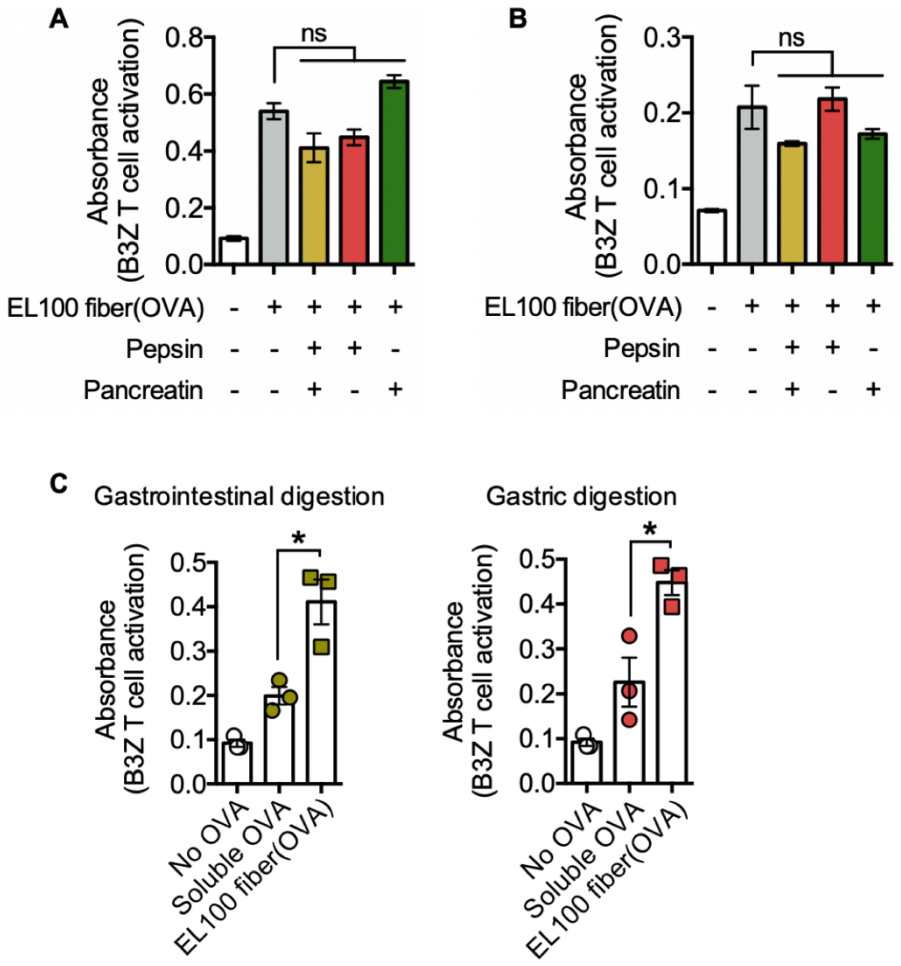

Figure 5.6. Encapsulation of OVA in Eudragit L100 nanofibers prevents loss of CD8⁺ activation ability upon exposure to simulated gastrointestinal digestion. ***A, C)*** *BMDCs and* ***B)*** *DC2.4s were treated with native or digested OVA-loaded Eudragit L100 nanofibers for 24 hours followed by co-culture with B3Z CD8⁺ T cells. After 24 hours, cells were lysed and CPRG substrate was added. B3Z activation was evaluated by monitoring absorbance, indicative of* β-galactosidase-*mediated substrate conversion into a colorimetric product. Data representative of n=3 per group from 1-3 independent experiments and presented as mean ± standard deviation and analyzed by one-way ANOVA (*p<0.05; ns, not significant).*

As observed with soluble OVA, similar levels of $CD4^+$ T cell proliferation was induced by OVA-containing Eudragit L100 nanofibers regardless of exposure to gastrointestinal conditions (Figure 5.7A). OVA encapsulation in Eudragit L100 nanofibers

induced IFN-γ production by CD4 T cells for all digestion conditions, in contrast to reduced IFN-γ observed when soluble OVA was exposed to gastrointestinal digestion (Figure 5.7B). Overall, delivery of OVA in Eudragit L100 nanofibers increased IFN-γ secretion compared to soluble OVA. As Foxp3 expression was increased only after total gastrointestinal digestion, we hypothesized gastric protection of OVA would result in Foxp3 induction similar to that observed for intestinal digestion only. However, exposure of OVA-loaded Eudragit L100 nanofibers to gastrointestinal digestion also increased the percentage of $Foxp3^+$ $CD4^+$ T cells compared to undigested OVA (Figure 5.7C). Decreased expression of the transcription factor T-bet was found to be driven by intestinal digestion of soluble OVA. Even though EudragitL100 nanofibers provide protection in gastric but not intestinal conditions, we did not observe a decrease in T-bet expression when OVA was delivered in Eudragit L100 nanofibers for all digestion conditions (Figure 5.7C). Similar to the trend observed with IFN-γ production, there was an overall increase in the percentage of proliferating $CD4^+$ T cells that were T-bet^+ in the Eudragit L100 nanofiber groups compared to soluble OVA delivery (23% vs. 30% for undigested soluble OVA and undigested EudragitL100 nanofiber-delivered OVA, respectively). As T_H1 cells are known to secrete IFN-γ, the increased T-bet expression correlates with the increase in IFN-γ observed when OVA is delivered in EudragitL100 nanofibers.

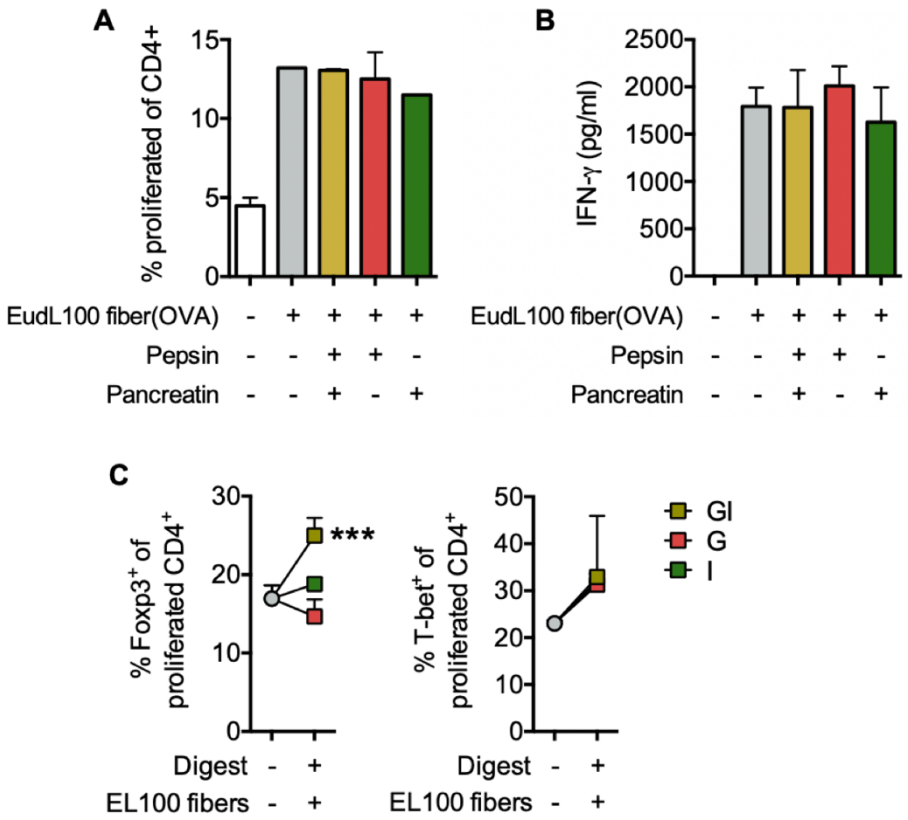

Figure 5.7. Effect of gastric protection of OVA in Eudragit L100 nanofibers on proliferation and polarization of $CD4^+$ T cells. OVA-loaded Eudragit L100 nanofibers were incubated in simulated gastrointestinal conditions and added to BMDCs for 24 hours. OVA-treated BMDCs were co-cultured with CFSE-labeled $CD4^+$ OTII T cells for 3 days. ***A)*** *Proliferation,* ***B)*** *IFN-γ secretion, and* ***C)*** *polarization of $CD4^+$ T cells 3 days after culture with BMDCs treated with Eudragit L100 nanofiber-encapsulated OVA digested in gastrointestinal conditions. Data representative of n=3 per group from one independent experiment, presented as mean ± standard deviation, and analyzed by one-way ANOVA.*

5.4.5 *Enhanced activation of intestinal $CD8^+$ T cell responses by an oral vaccine through epitope protection in nanofibers in combination with the mucosal adjuvant PEI*

We next investigated how antigen digestion would influence the activation of adaptive immune responses *in vivo*. Naïve mice were immunized with OVA by oral gavage

and boosted every 4 weeks. Based on our *in vitro* studies, we observed that gastric digestion had the most significant impact on the CD8 T cell response, likely due to the susceptibility of the SIINFEKL epitope to pepsin-mediated cleavage. Our data also suggested that gastric protection through formulation in Eudragit L100 nanofibers may recover the ability to activate cytotoxic T lymphocytes that is lost upon antigen digestion in the gastric environment. Thus, we chose to focus on how protection from gastric digestion through formulation in emulsion electrospun Eudragit L100 nanofibers would impact the SIINFEKL-specific $CD8^+$ T cell response and evaluated the expansion of these $CD8^+$ T cells after oral immunization with or without gastric protection. After oral immunization with soluble OVA or OVA in Eudragit L100 nanofibers, the percentage of antigen-experienced ($CD44^+$) $CD8^+$ T cells was similar in the spleen, mesenteric lymph nodes, and small intestinal intraepithelial compartment (IEL) between the two groups (Figure 5.8A). Additionally, the percentage of SIINFEKL-tetramer$^+$ $CD8^+$ T cells in these organs was also similar (Figure 5.8B).

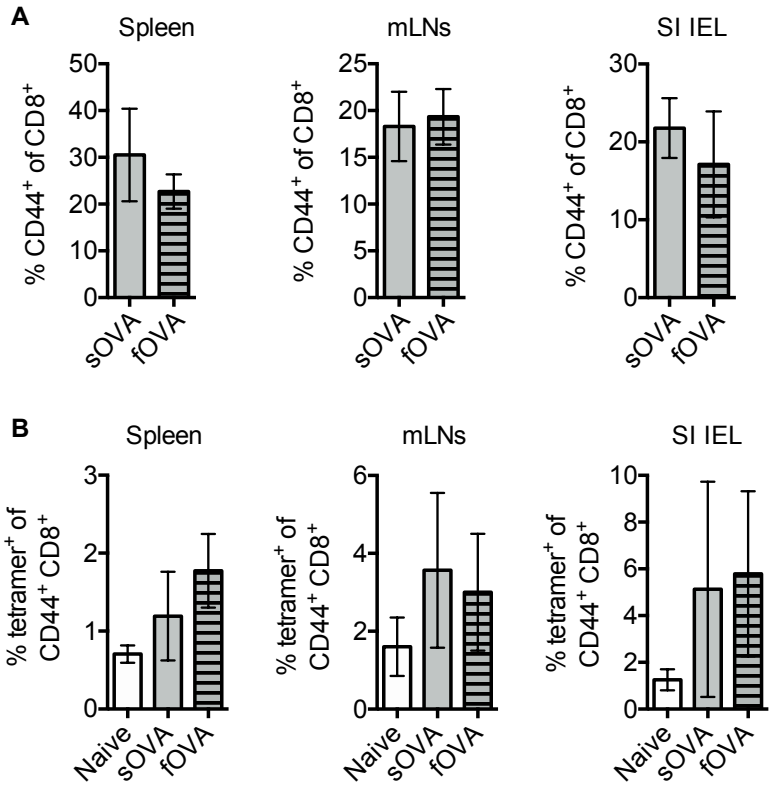

Figure 5.8. CD8⁺ T cell responses to oral immunization with unprotected or gastric-protected antigen. Female C56Bl/6J mice were treated with soluble (sOVA) or Eudragit L100 nanofiber-encapsulated OVA (fOVA) (0.2 mg OVA) by oral gavage and adaptive immune responses were evaluated 14 days after the last dose. Spleens, mesenteric lymph nodes (mLNs), and small intestinal intraepithelial cells (SI IEL) were processed into single cell suspensions and analyzed by flow cytometry. ***C)*** *Percentage of CD44⁺ of CD8⁺ T cells and* ***D)*** *H-2K(b) $OVA_{257-264}$ tetramer positive CD8⁺ CD44⁺ T cells in various organs. Data representative of n=2-6 mice per group and presented as mean ± standard deviation and analyzed by one-way ANOVA.*

As the inclusion of an adjuvant was necessary to induce cross-presentation of exogenous protein to activate CD8⁺ T cells in our *in vitro* studies, protection from gastric digestion may not be sufficient on its own to induce a CD8⁺ T cell response *in vivo*. In other studies, the use of certain adjuvants has been shown to modulate the cross-presentation of protein antigens [36]. First observed to be a potent mucosal adjuvant when used at the nasal mucosa [37], in Chapter 4 we identified the adjuvant polyethyleneimine

(PEI) to also be a robust adjuvant for CD8 responses when delivered orally. Thus, we incorporated this adjuvant in the vaccine formulation in which OVA was either delivered in soluble form or protected in Eudragit L100 nanofibers. PEI was not observed to cause histological changes to the small intestinal tissue after oral administration (Figure S5.4). We observed a significant increase in antigen-specific (tetramer$^+$) CD8$^+$ T cells in the spleens and mesenteric lymph nodes when OVA was co-delivered with PEI compared to unimmunized mice for both soluble and Eudragit L100 fiber oral delivery (Figure 5.9A,B). However, we only observed an increase in antigen-specific CD8$^+$ T cells in the small intestine when OVA was protected from gastric digestion through delivery in Eudragit L100 nanofibers and co-delivered with PEI (Figure 5.9C). These results suggest for oral vaccines to generate robust T cell responses in both lymphoid and mucosal tissues, protection of immunogenic epitopes from digestion in combination with a potent mucosal adjuvant is advantageous.

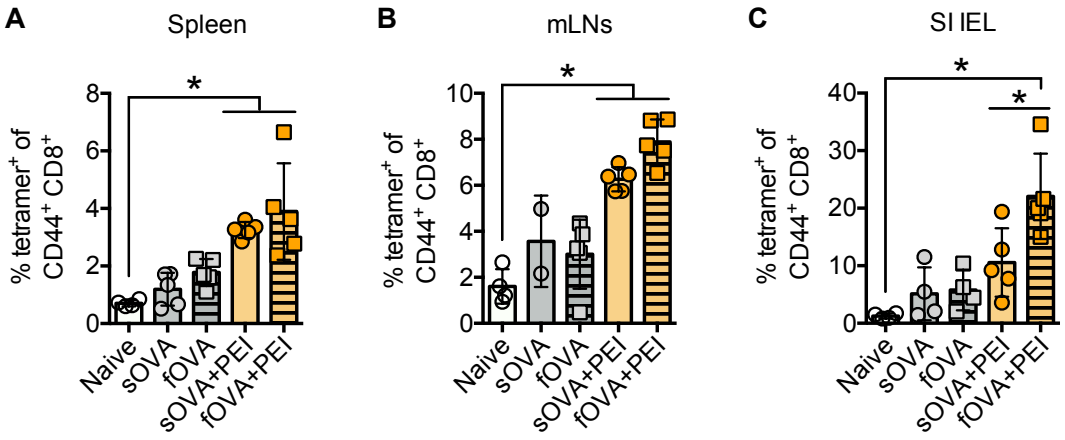

Figure 5.9. *Gastric protection of oral antigen enhances CD8$^+$ T cell responses when co-delivered with mucosal adjuvant. Female C56Bl/6J mice were treated with soluble (sOVA) or Eudragit L100 nanofiber-encapsulated OVA (fOVA) (0.2 mg OVA) with PEI (100 μg) by oral gavage and adaptive immune responses were evaluated 14 days after the last dose. A) Spleens, B) mesenteric lymph nodes (mLNs) and C) small intestinal intraepithelial cells (SI IEL) were processed into single cell suspensions and stained for analysis by flow cytometry for the percentage of H-2K(b) OVA$_{257-264}$ tetramer positive CD8$^+$ CD44$^+$ T cells. Data representative of n=2-5 mice per group and is presented as mean ± standard deviation and analyzed by one-way ANOVA.*

At the same time, we evaluated the humoral and $CD4^+$ T cell responses to unprotected or gastric-protected OVA. Similar to other studies [16], we did not observe a significant increase in antigen-specific IgG in the serum after oral OVA administration, either in soluble form or encapsulated in Eudragit L100 nanofibers (Figure S5.5A). Intestinal IgA responses were also low in both groups (Figure S5.5B). Based on our *in vitro* data, we would not expect to observe significant differences in antigen-specific $CD4^+$ T cell expansion between oral immunization with gastric-protected or unprotected OVA due to the ability of DCs to induce CD4 proliferation when treated with digested OVA. Indeed, percentages of $CD44^+$ antigen-experienced $CD4^+$ T cells in the mLNs and SI LP were similar between soluble and Eudragit L100-delivered OVA (Figure S5.5C,D). Percentages of OVA-specific $CD44^+$ $CD4^+$ T cells were also similar between groups in these organs. Overall, elicitation of antigen-specific $CD4^+$ T cells was low ($<5\%$ of the $CD44^+$ $CD4^+$ population). Thus, evaluation of the polarization of antigen-specific $CD4^+$ T cells activated in response to oral vaccination was unable to be evaluated, which is where we observed effects of gastrointestinal digestion on $CD4^+$ T cells *in vitro*. Among the general antigen-experienced population, the percentage of $Foxp3^+$ and T-bet^+ among $CD44^+$ cells was similar between both groups, although this population does not exclusively represent OVA-specific cells primed upon immunization (Figure S5.5C,D). Future studies may investigate the production of cytokines by lymphocytes re-stimulated with antigen *ex vivo* or track adoptively transferred OVA-specific T cells to determine CD4 T cell polarization.

Cytotoxic T lymphocytes in response to OVA delivered orally encapsulated in Eudragit microbeads without the use of an adjuvant [38]. In their study, splenocytes from orally immunized mice were enriched for T cells three weeks after immunization and incubated with antigen and antigen presenting cells. Antigen-specific proliferation was evaluated by [^{3}H]thymidine incorporation, which was heightened with Eudragit-coated OVA compared to mice receiving blank microbeads. However, proliferation was not

compared to OVA delivered in soluble form. Their results suggest that *in vitro* restimulation may reveal differences in T cell activation after oral immunization without the use of an adjuvant, although the impact of protection in gastric conditions was not directly evaluated in their study. As we observed increases in antigen-specific $CD8^+$ T cells in lymphoid organs of mice immunized with both soluble and gastric-protected OVA, it may be that similar levels of proliferation in response to *in vitro* stimulation would be observed. Another study encapsulating OVA in EudragitL100 microbeads observed systemic antibody responses after oral immunization compared to soluble OVA delivery [16]. This study used an OVA dose of 5 mg, 25-fold higher than the dose used in our study, which may explain the lack of antibodies observed here. Other studies that provide both antigen digestion protection and immune stimulation have observed increased systemic antibody responses at lower antigen doses [10,17,39]. However, these studies used different antigens, vaccination schedules, vaccine doses, and different immunostimulatory components and thus it is difficult to compare to our results. Antigen and adjuvant doses as well as immunization schedule may need to be optimized to effectively activate humoral responses. In contrast to antibodies, $CD4^+$ T cell responses are not widely evaluated. One study found increased levels of IL-4 from re-stimulated splenocytes with oral administration of OVA encapsulated in EudragitL100 compared to soluble OVA, but detected low levels of IFN-γ from both groups [40]. Overall, our data are in accordance with most studies to date evaluating adaptive immune responses to orally delivered protein antigens.

5.5 Conclusions

The susceptibility or resistance of proteins to gastrointestinal digestion has been implicated in the induction of oral tolerance as well as allergy. Here, we show that digestion of the protein antigen OVA results in reduced maturation of DCs and leads to

differences in both CD4 and CD8 proliferation and polarization. Consideration of the presence of gastrointestinal enzyme cleavage sites within immunogenic epitopes is of critical importance for oral vaccines, as we found an inability to activate T cells that recognized epitopes that contained such cleavage sites. Formulation of OVA in pH-responsive nanofibers sequestered OVA from the gastric environment, provided protection from digestion, and prevented loss of CD8 T cell-activating capacity. This translated to the activation of $CD8^+$ T cells when used as an oral vaccine *in vivo*, but only when the adjuvant PEI was co-delivered. We also demonstrate the broader activity of PEI as a mucosal adjuvant, particularly in the elicitation of CD8 responses. These results provide additional evidence and mechanistic insights on the requirement of oral vaccines to be resistant to enzymatic degradation. However, digestion resistance on its own was insufficient to activate CD8 immunity and required the use of specific mucosal adjuvants for immune stimulation.

5.6 References

[1] M.R. Neutra, P.A. Kozlowski, Mucosal vaccines: the promise and the challenge, Nat. Rev. Immunol. 6 (2006) 148–158. doi:10.1038/nri1777.

[2] E. Moroz, S. Matoori, J.-C. Leroux, Oral delivery of macromolecular drugs: Where we are after almost 100years of attempts., Adv. Drug Deliv. Rev. 101 (2016) 108–121. doi:10.1016/j.addr.2016.01.010.

[3] J.G. Michael, The Role of Digestive Enzymes in Orally Induced Immune Tolerance, Immunol. Invest. 18 (1989) 1049–1054. doi:10.3109/08820138909030606.

[4] S. Strobel, A.M. Mowat, H.E. Drummond, M.G. Pickering, A. Ferguson, Immunological responses to fed protein antigens in mice. II. Oral tolerance for CMI is due to activation of cyclophosphamide-sensitive cells by gut-processed antigen., Immunology. 49 (1983) 451–6. https://www.ncbi.nlm.nih.gov/pmc/articles/PMC1454306/pdf/immunology00216-0038.pdf (accessed July 30, 2019).

[5] J.D. Astwood, J.N. Leach, R.L. Fuchs, Stability of food allergens to digestion in vitro, Nat. Biotechnol. 14 (1996) 1269–1273. doi:10.1038/nbt1096-1269.

[6] G. Jordakieva, M. Kundi, E. Untersmayr, I. Pali-Schöll, B. Reichardt, E. Jensen-Jarolim, Country-wide medical records infer increased allergy risk of gastric acid inhibition, Nat. Commun. 10 (2019) 3298. doi:10.1038/s41467-019-10914-6.

[7] A. Bernkop-Schnürch, The use of inhibitory agents to overcome the enzymatic barrier to perorally administered therapeutic peptides and proteins, 1998. doi:10.1016/S0168-3659(97)00204-6.

[8] A.E. Ibañez, L.M. Coria, M.V. Carabajal, M.V. Delpino, G.S. Risso, P.G. Cobiello, J. Rinaldi, P. Barrionuevo, L. Bruno, F. Frank, S. Klinke, F.A. Goldbaum, G. Briones, G.H. Giambartolomei, K.A. Pasquevich, J. Cassataro, A bacterial protease inhibitor protects antigens delivered in oral vaccines from digestion while triggering specific mucosal immune responses, J. Control. Release. 220 (2015) 18–28. doi:10.1016/j.jconrel.2015.10.011.

[9] B.J. Bruno, G.D. Miller, C.S. Lim, Basics and recent advances in peptide and protein drug delivery, Ther. Deliv. 4 (2013) 1443–1467. doi:10.4155/tde.13.104.

[10] B. Bellier, A.H. Tenaglia, C.G. Prucca, T. Sparwasser, M.C. Serradell, P.R. Gargantini, A. Saura, L.L. Rupil, D. Klatzmann, J. Echenique, P.G. Carranza, N. Reinoso-Vizcaino, E.A. Fernández, L. Berod, R.R. Tonelli, J.P. Petiti, R.A. Martino, E. Piaggio, H.D. Luján, Efficient oral vaccination by bioengineering virus-like particles with protozoan surface proteins, Nat. Commun. 10 (2019) 361. doi:10.1038/s41467-018-08265-9.

[11] J.-W. Yoo, D.J. Irvine, D.E. Discher, S. Mitragotri, Bio-inspired, bioengineered and biomimetic drug delivery carriers, Nat. Rev. Drug Discov. 10 (2011) 521–535. doi:10.1038/nrd3499.

[12] S. Chadwick, C. Kriegel, M. Amiji, Nanotechnology solutions for mucosal immunization, Adv. Drug Deliv. Rev. 62 (2010) 394–407. doi:10.1016/j.addr.2009.11.012.

[13] S. Mitragotri, P.A. Burke, R. Langer, Overcoming the challenges in administering biopharmaceuticals: formulation and delivery strategies, Nat. Rev. Drug Discov. 13 (2014) 655–672. doi:10.1038/nrd4363.

[14] S. Mura, J. Nicolas, P. Couvreur, Stimuli-responsive nanocarriers for drug delivery, Nat. Mater. 12 (2013) 991–1003. doi:10.1038/nmat3776.

[15] D.J. Irvine, M.A. Swartz, G.L. Szeto, Engineering synthetic vaccines using cues from natural immunity, Nat. Mater. 12 (2013) 978–990. doi:10.1038/nmat3775.

[16] S.L. Jain, K.S. Barone, M.P. Flanagan, J.G. Michael, Activation patterns of murine B cells after oral administration of an encapsulated soluble antigen, Vaccine. 14 (1996) 42–48. doi:10.1016/0264-410X(95)00158-W.

[17] Q. Zhu, J. Talton, G. Zhang, T. Cunningham, Z. Wang, R.C. Waters, J. Kirk, B. Eppler, D.M. Klinman, Y. Sui, S. Gagnon, I.M. Belyakov, R.J. Mumper, J.A. Berzofsky, Large intestine-targeted, nanoparticle-releasing oral vaccine to control genitorectal viral infection, Nat. Med. 18 (2012) 1291–1296. doi:10.1038/nm.2866.

[18] H. Frizzell, T.J. Ohlsen, K.A. Woodrow, Protein-loaded emulsion electrospun fibers optimized for bioactivity retention and pH-controlled release for peroral delivery of biologic therapeutics, Int. J. Pharm. 533 (2017) 99–110. doi:10.1016/j.ijpharm.2017.09.043.

[19] S.-Y. Chang, H.-J. Ko, M.-N. Kweon, Mucosal dendritic cells shape mucosal immunity., Exp. Mol. Med. 46 (2014) e84. doi:10.1038/emm.2014.16.

[20] T. Worbs, U. Bode, S. Yan, M.W. Hoffmann, G. Hintzen, G. Bernhardt, R. Förster, O. Pabst, Oral tolerance originates in the intestinal immune system and relies on antigen carriage by dendritic cells, J. Exp. Med. 203 (2006) 519–527. doi:10.1084/jem.20052016.

[21] D. Esterházy, J. Loschko, M. London, V. Jove, T.Y. Oliveira, D. Mucida, Classical

dendritic cells are required for dietary antigen-mediated induction of peripheral T reg cells and tolerance, Nat. Immunol. 17 (2016) 545–555. doi:10.1038/ni.3408.

[22] R. López-Fandiño, G. Martos, P. Contreras, E. Molina, Egg white ovalbumin digestion mimicking physiological conditions, J. Agric. Food Chem. 58 (2010) 5640–5648. doi:10.1021/jf904538w.

[23] E. Gasteiger, C. Hoogland, A. Gattiker, S. Duvaud, M.R. Wilkins, R.D. Appel, A. Bairoch, Protein Identification and Analysis Tools on the ExPASy Server, in: Proteomics Protoc. Handb., Humana Press, Totowa, NJ, 2005: pp. 571–607. doi:10.1385/1-59259-890-0:571.

[24] R. Shimonkevitz, S. Colon, J.W. Kappler, P. Marrack, H.M. Grey, Antigen recognition by H-2-restricted T cells. II. A tryptic ovalbumin peptide that substitutes for processed antigen., J. Immunol. 133 (1984) 2067–74. http://www.ncbi.nlm.nih.gov/pubmed/6332146.

[25] A. Iwasaki, R. Medzhitov, Control of adaptive immunity by the innate immune system, Nat. Immunol. 16 (2015) 343–353. doi:10.1038/ni.3123.

[26] M. Moser, K.M. Murphy, Dendritic cell regulation of TH1-TH2 development, Nat. Immunol. 1 (2000) 199–205. doi:10.1038/79734.

[27] I. Mellman, R.M. Steinman, Dendritic cells: specialized and regulated antigen processing machines., Cell. 106 (2001) 255–8. doi:10.1016/s0092-8674(01)00449-4.

[28] G. Trinchieri, Interleukin-12: A Proinflammatory Cytokine with Immunoregulatory Functions that Bridge Innate Resistance and Antigen-Specific Adaptive Immunity, Annu. Rev. Immunol. 13 (1995) 251–276. doi:10.1146/annurev.iy.13.040195.001343.

[29] F.S. Lichtenegger, K. Mueller, B. Otte, B. Beck, W. Hiddemann, D.J. Schendel, M. Subklewe, CD86 and IL-12p70 Are Key Players for T Helper 1 Polarization and Natural Killer Cell Activation by Toll-Like Receptor-Induced Dendritic Cells, PLoS One. 7 (2012) e44266. doi:10.1371/journal.pone.0044266.

[30] J. Zhu, W.E. Paul, CD4 T cells: fates, functions, and faults, Blood. 112 (2008) 1557–1569. doi:10.1182/blood-2008-05-078154.

[31] A.A. Lighvani, D.M. Frucht, D. Jankovic, H. Yamane, J. Aliberti, B.D. Hissong, B. V. Nguyen, M. Gadina, A. Sher, W.E. Paul, J.J. O'Shea, T-bet is rapidly induced by interferon- in lymphoid and myeloid cells, Proc. Natl. Acad. Sci. 98 (2001) 15137–15142. doi:10.1073/pnas.261570598.

[32] N. Zhang, M.J. Bevan, CD8+ T Cells: Foot Soldiers of the Immune System, Immunity. 35 (2011) 161–168. doi:10.1016/j.immuni.2011.07.010.

[33] D.J. Irvine, M.C. Hanson, K. Rakhra, T. Tokatlian, Synthetic Nanoparticles for Vaccines and Immunotherapy, Chem. Rev. 115 (2015) 11109–11146. doi:10.1021/acs.chemrev.5b00109.

[34] H.K. Makadia, S.J. Siegel, Poly Lactic-co-Glycolic Acid (PLGA) as biodegradable controlled drug delivery carrier, Polymers (Basel). 3 (2011) 1377–1397. doi:10.3390/polym3031377.

[35] X. Huang, C.S. Brazel, On the importance and mechanisms of burst release in matrix-controlled drug delivery systems, J. Control. Release. 73 (2001) 121–136. doi:10.1016/S0168-3659(01)00248-6.

[36] N.I. Ho, L.G.M. Huis in 't Veld, T.K. Raaijmakers, G.J. Adema, Adjuvants Enhancing Cross-Presentation by Dendritic Cells: The Key to More Effective Vaccines?, Front.

Immunol. 9 (2018) 2874. doi:10.3389/fimmu.2018.02874.

[37] F. Wegmann, K.H. Gartlan, a M. Harandi, S. a Brinckmann, M. Coccia, W.R. Hillson, W.L. Kok, S. Cole, L.P. Ho, T. Lambe, M. Puthia, C. Svanborg, E.M. Scherer, G. Krashias, a Williams, J.N. Blattman, P.D. Greenberg, R. a Flavell, a E. Moghaddam, N.C. Sheppard, Q.J. Sattentau, Polyethyleneimine is a potent mucosal adjuvant for viral glycoprotein antigens, Nat Biotechnol. 30 (2012) 883–888. doi:10.1038/nbt.2344.

[38] K. Vogel, J. Kantor, L. Wood, R. Rivera, J. Schlom, Oral immunization with enterocoated microbeads induces antigen-specific cytolytic T-cell responses., Cell. Immunol. 190 (1998) 61–7. doi:10.1006/cimm.1998.1384.

[39] F. Sarti, G. Perera, F. Hintzen, K. Kotti, V. Karageorgiou, O. Kammona, C. Kiparissides, A. Bernkop-Schnürch, In vivo evidence of oral vaccination with PLGA nanoparticles containing the immunostimulant monophosphoryl lipid A, Biomaterials. 32 (2011) 4052–4057. doi:10.1016/j.biomaterials.2011.02.011.

[40] S.L. Jain, K.S. Barone, J.G. Michael, Activation patterns of murine T cells after oral administration of an enterocoated soluble antigen, Cell. Immunol. 167 (1996) 170–175. doi:DOI 10.1006/cimm.1996.0024.

Chapter 6. CONCLUSIONS

6.1 Summary and Future Directions

The global impact of immunization has been demonstrated since the widespread uptake of this clinical intervention, dramatically reducing the incidence and spread of infectious disease. While most vaccines are administered by injection, this administration method has drawbacks that limits immunization accessibility due to resource requirements as well as in the development of mucosal immunity. Oral immunization is one such alternative administration route that has the potential to improve vaccine access in low resource settings and establish immune responses at mucosal surfaces. However, effective oral immunization is difficult due to the myriad of physiological and immunological challenges, including the digestive gastrointestinal environment, low bioavailability, and oral tolerance. In this thesis, we focused on understanding and overcoming these barriers to oral vaccination through the use of biomaterial-based delivery platforms and applied immunology.

Upon ingestion, oral vaccines are subject to the harsh acidic and protease-rich environment in the stomach. For protein-based vaccines, macromolecular structure as well as the immunogenic epitopes necessary to simulate an adaptive immune response can be compromised. Previous work has established that antigen digestion in the gastric tract contributes to oral tolerance. Thus, we first developed a biomaterial delivery for oral vaccines focused on gastric protection and explored electrospun nanofibers for this application. This fabrication method is relevant for large-scale translation, produces a solid dosage form, and can be used with a variety of polymers. In the first specific aim, protein formulation in pH-responsive nanofibers was developed using emulsion electrospinning. We found that varying emulsion parameters impacted protein bioactivity and were able to achieve 100% bioactivity retention through reduction of the aqueous

phase percentage in the emulsion. These materials were observed to have a core/shell architecture, which limited protein release in acidic environments and provided partial protection from pepsin-mediated activity loss. Shelf life of these protein-loaded materials could be extended through lyophilization to reduce residual water content of the fibers.

While the first aim developed an electrospinning platform to protect vaccines in the gastric environment and facilitate their release in the intestine for uptake, aim 2 focused on the use of adjuvants to stimulate intestinal epithelial cells to overcome subsequent barriers to oral vaccination. Epithelial cells are known to regulate immunity in the intestine, as they communicate to underlying immune cells and condition them to be immunotolerant. Through stimulation of epithelial cells, the signaling profile can be changed such that immune cells are activated and recruited for antigen internalization to mediate adaptive immune responses. We aimed to develop a new strategy to increase immune responses to oral vaccines through targeting these important immune cells. The TLR agonist CpG and cationic polymer PEI were found to increase adaptive immune responses to orally delivered protein vaccine antigens, with CpG increasing antibody and $CD4^+$ T cell responses and PEI expanding $CD8^+$ T cell responses *in vivo*. *In vitro*, these two adjuvants induced intestinal epithelial cells to secrete DC-recruiting cytokines, which may contribute to their activity observed *in vivo*. PEI was also found to modulate antigen uptake in both epithelial and dendritic cells. However, at this time we cannot definitively say that the enhanced adaptive immunity observed by certain adjuvants is due to this differential action. Future work may more robustly evaluate the immune signatures of each adjuvant over the course of the immune response, potentially through transcriptional analysis.

Finally, we applied the pH-responsive nanofiber delivery platform to further study the role of gastrointestinal digestion on the immunogenicity of protein-based vaccines. While multiple studies have supported the notion that the gastric environment leads to tolerogenic rather than immunogenic responses, the mechanisms behind this effect are not

known. Additionally, if protection in the intestinal environment is also necessary has not been evaluated. We hypothesized that cleavage of protein antigens by gastrointestinal enzymes would reduce their potential to activate immune responses. We find that both gastric and intestinal digestion reduce the ability of a model antigen to induce dendritic cell maturation and secretion of the inflammatory cytokine IL-12. However, the induction of T cell proliferation depends on if relevant immune epitopes contain gastrointestinal enzyme cleavage sites. Using the nanofiber platform developed, we demonstrate that antigen formulation in nanofibers can protect susceptible epitopes from enzymes and induce T cell proliferation after exposure to simulated gastrointestinal conditions. In contrast to nanofibers, nanoparticles did not effectively protect antigens from gastric conditions and lost function similar to unprotected antigens. When administered orally to mice *in vivo*, soluble and fiber-encapsulated antigens both demonstrated low induction of immune responses. However, when combined with adjuvants identified in the second aim, $CD8^+$ T cell responses, which recognized antigen epitopes that were susceptible to gastric enzyme cleavage, were enhanced. Overall, this work demonstrates how gastrointestinal digestion influences innate immune cell activation and antigen processing, leading to differences in T cell activation potential. For vaccines with immunogenic epitopes that contain cleavage sites for gastrointestinal enzymes, prevention of such digestion through protective biomaterial formulation is a strategy to increase epitope-specific immune responses. While in this work we predominately focused on the antigen-specific $CD8^+$ T cell response, as we found this epitope to contain multiple cleavage sites, future work may focus on the difference in functional responses of antigen-specific $CD4^+$ T cells. While the epitopes recognized by the T cell receptors for these cells did not contain cleavage sites within the epitope, we did observe differences in polarization and cytokine secretion. Finally, how protection of antigen epitopes from gastrointestinal digestion through biomaterial formulation as well as the use of different adjuvants impacts the development

of immune memory will be critical to evaluate for the translation of such vaccine technologies.

During the course of this dissertation, additional work was completed investigating dendritic cell priming *ex vivo* to develop cells with higher antigen loading and an enhanced ability to activate $CD8^+$ T cells for use in cell-based vaccines and immunotherapies (Appendix C). Through an NSF GROW pre-doctoral fellowship, the expression and regulation of fatty acid binding proteins, which are known to be involved in cellular metabolism, in tissue-resident memory T cells was studied. This work was completed in the laboratory of Dr. Laura Mackay at the University of Melbourne and Doherty Institute for Infection and Immunity.

6.2 List of Publications and Presentations

Peer-reviewed publications

1. **Frizzell, H.**, & Woodrow, K. A. Biomaterial approaches for understanding and overcoming immunological barriers to effective oral vaccination. *Manuscript in review.*
    - Chapter 2
2. **Frizzell, H.**, Ohlsen, T. J., & Woodrow, K. A. (2017). Protein-loaded emulsion electrospun fibers optimized for bioactivity retention and pH-controlled release for peroral delivery of biologic therapeutics. I*nternational Journal of Pharmaceutics*, *533*(1), 99-110.
    - Chapter 3
3. **Frizzell, H.**, Park, J., & Woodrow, K. A. Activation of intestinal $CD8^+$ T cells by an oral vaccine through nanofiber-mediated gastric protection of epitopes and the mucosal adjuvant PEI. *Manuscript in preparation.*
    - Chapters 4 & 5
4. **Frizzell, H.**, Park, J., Lou, N. C., & Woodrow, K. A. (2017). Role of heterogeneous cell population on modulation of dendritic cell phenotype and activation of CD8 T cells for use in cell-based immunotherapies. *Cellular Immunology*, *311*, 54-62.
    - Appendix C

5. **Frizzell, H.***, Fonseca, R.*, Christo, S. N., Evrard, M., Freestone, D., Park, S. L., & Mackay, L. K. Organ-specific expression of fatty acid binding proteins in tissue-resident lymphocytes. *Manuscript in review. (*equally contributed to this work).*
    - Work conducted in the lab of Laura Mackay at the Doherty Institute for Infection and Immunity and the University of Melbourne through an NSF GROW Fellowship
6. Golan-Paz, S., **Frizzell, H.**, & Woodrow, K. A. (2019). Cross-Platform Comparison of Therapeutic Delivery from Multilamellar Lipid-Coated Polymer Nanoparticles. *Macromolecular Bioscience*, *19*(4), 1800362.
7. Park, J., **Frizzell, H.**, Zhang, H., Woodrow, K. A. Flt3-L enhances trans-epithelial migration and immune functions of intravaginally administered dendritic cells. *Manuscript in preparation.*
8. Ramanathan, R., Park, J., Read, B., **Frizzell, H.**, Krogstad, E. A., Woodrow, K. A. Antibody nanoparticle immune complexes for vaginal OVA delivery and cross presentation to $CD8^+$ T cells. *Manuscript in preparation.*

Presentations at national conferences

1. **Frizzell, H.**, & Woodrow, K. A. "Selective Protection of Proteins in Polymeric Biomaterials to Understand the Effect of Gastrointestinal Digestion on Immunogenicity," Society for Biomaterials Annual Meeting & Exposition. April 3 – 6, 2019, Seattle, Washington, Poster Presentation.
2. **Frizzell, H.**, & Woodrow, K. A. "Optimization Of Protein-Loaded Electrospun Fibers For Targeted Intestinal Delivery," Biomedical Engineering Society Annual Meeting. October 11 – 14, 2017, Phoenix, Arizona. Oral Presentation.
3. **Frizzell, H.**, Park, J., Lou Comandante, N., & Woodrow, K. A. "Dendritic Cell Priming In Heterogeneous Cultures Modulates Phenotype And Function For Immunotherapy," Biomedical Engineering Society Annual Meeting. October 11 – 14, 2017, Phoenix, Arizona. Oral Presentation.

APPENDIX A: CHAPTER 4 SUPPLEMENTARY INFORMATION

Supplementary Methods

Bone marrow dendritic cell derivation

Bone marrow-DCs (BMDCs) were derived as previously described [12]. Briefly, tibias and femurs were collected from the hind limbs of 8-12-week-old female C57BL/6J mice (Jackson Laboratory, Bar Harbor, ME, USA) and the bone marrow was flushed out. Red blood cells were lysed and the remaining cells were cultured on petri dishes in complete cell culture medium: RPMI-1640 (Cellgro), 2 mM L-glutamine (Cellgro), 10 mM HEPES, 1x non-essential amino acids, 1 mM Na Pyruvate, 55 μM 2-mercapthoethanol, 1% penicillin/streptomycin, and 10% heat-inactivated fetal bovine serum (all from Invitrogen) with 20 ng mL^{-1} GM-CSF (PeproTech). After 3, 5, and 7 days of culture the cells were supplemented with new medium and GM-CSF at 20 ng mL^{-1}. BMDCs were used for experimentation between day 7 and 9.

Dendritic cell migration in vitro

BMDCs or DC2.4s were seeded on the apical side of a 5 μm transwell membrane filter in 24-well plates (Corning) at 100,000 cells per membrane and allowed to attach for 30 minutes. Serum-free medium, CCL20 (250 ng mL^{-1}) in serum-free medium, or supernatants from Caco-2 cells treated with adjuvant were added into the lower chamber of the wells. After 2 hours, the membranes were processed for quantification of the number of migrated DCs by removing the non-migrated cells from the apical side of the membrane using cotton swabs and adding 0.25% trypsin in the lower well in contact with the basolateral side of the membrane. Detached cells were collected, washed in FACS buffer (1% BSA in PBS), fixed in 1.6% PFA, and quantified using a CantoII flow cytometer.

Nanoparticle synthesis, characterization, and in vivo uptake study

Poly(lactic-co-glycolic acid) (PLGA) (50:50, acid-terminated, 0.55 – 0.75 dL g^{-1}) (Lactel, Birmingham, AL, USA) was dissolved in dichloromethane (Sigma) at 50 mg mL^{-1}. BSA-FITC in solution was added dropwise into the PLGA solution at 10% volume while vortexing. The primary emulsion was probe-sonicated (500 W Ultrasonic Processor GEX500) at 38% amplitude for 30 seconds followed by placement on ice, repeated for a total of 3 times. The primary emulsion was added drop-wise into an equivalent volume of 5% polyvinyl alcohol (PVA, 30 – 70 kDa, 87-90% hydrolyzed) (Sigma) while vortexing. The secondary emulsion was sonicated as described above and transferred into 0.3% PVA and stirred overnight to allow for solvent evaporation.

Age-matched female C56Bl/6J were immunized with BSA-FITC in PLGA nanoparticles (5 mg) in 200 µL by oral gavage using a 22G metal gavage needle. Two hours later, mice were sacrificed and small intestines were collected. Small intestines were flushed with PBS and processed into three sections of equal length. Single cell suspensions of small intestinal IEL and LP cells were generated and stained for flow cytometry analysis following methods as described in the main text (Section 4.3.4.7). Cells were analyzed for BSA-FITC uptake on an Attune NxT flow cytometer (Thermo) and analyzed using FlowJo software.

Supplementary Figures

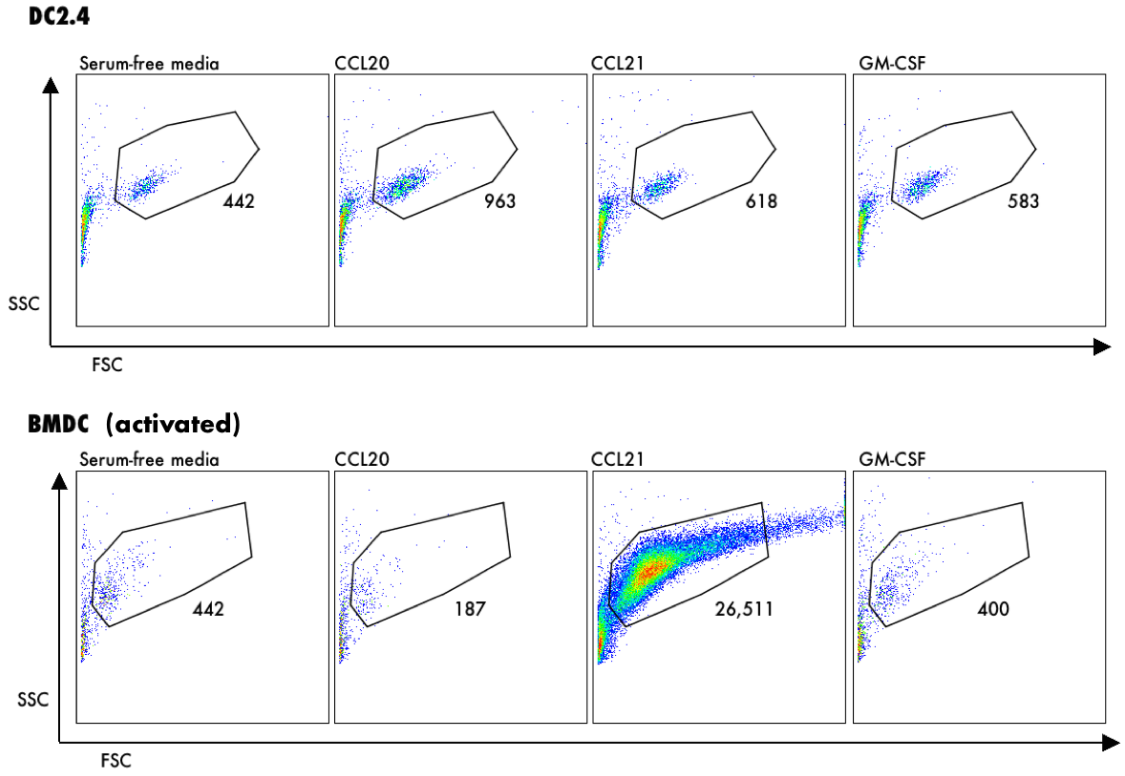

Figure S4.1. Maturation status of DCs influences responsiveness to chemokines. DC2.4 cells and mature BMDCs were seeded on the apical side of a transwell membrane with 5 μm pores and the degree of migration towards serum-free RMPI, CCL20, CCL21, or GM-CSF (all 250 ng mL^{-1}) in the lower chamber was evaluated after 2 hours. Data representative of n=1 per group.

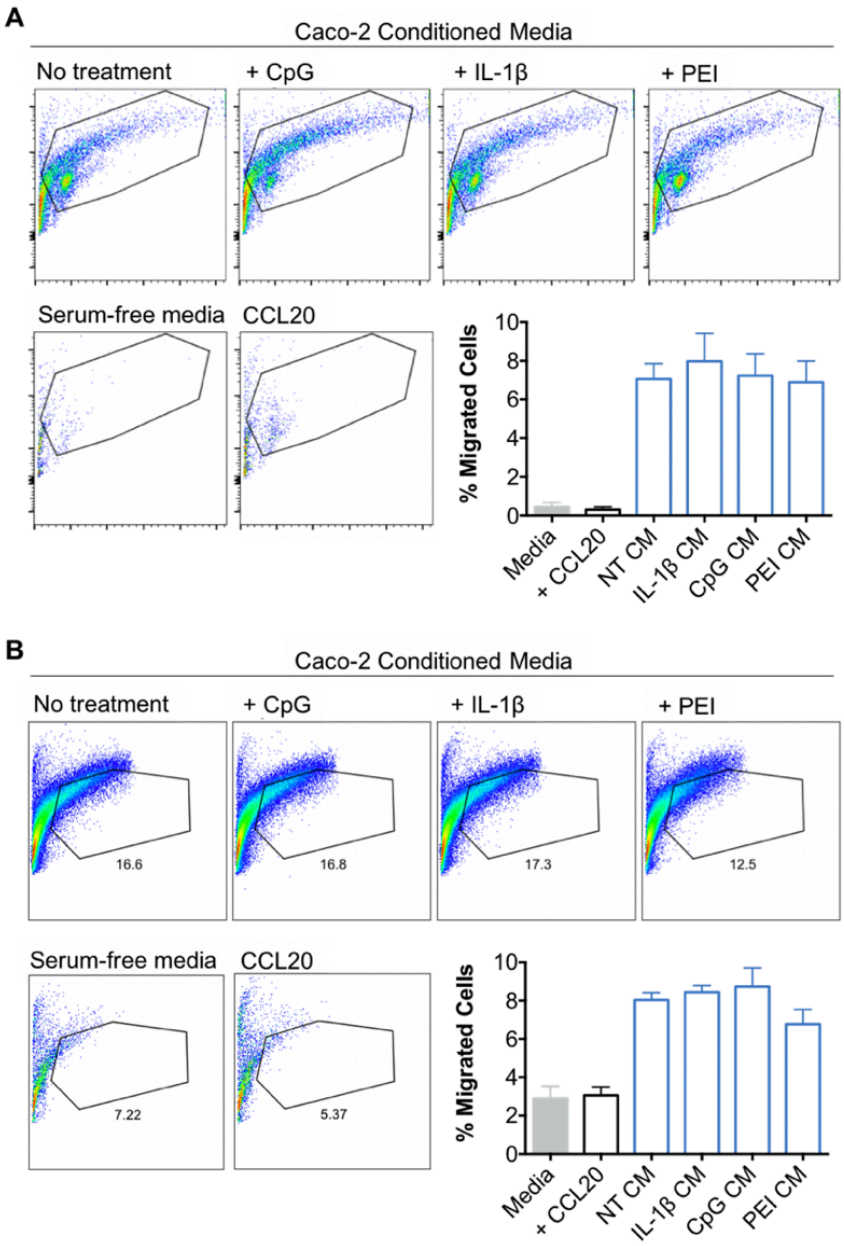

Figure S4.2. Migration of A) semi-mature BMDCs and B) DC2.4 cells towards Caco-2 conditioned media (CM) through a 5 μm transwell membrane after 2 hours. Data representative of n=3 per experimental group and presented as mean ± standard deviation.

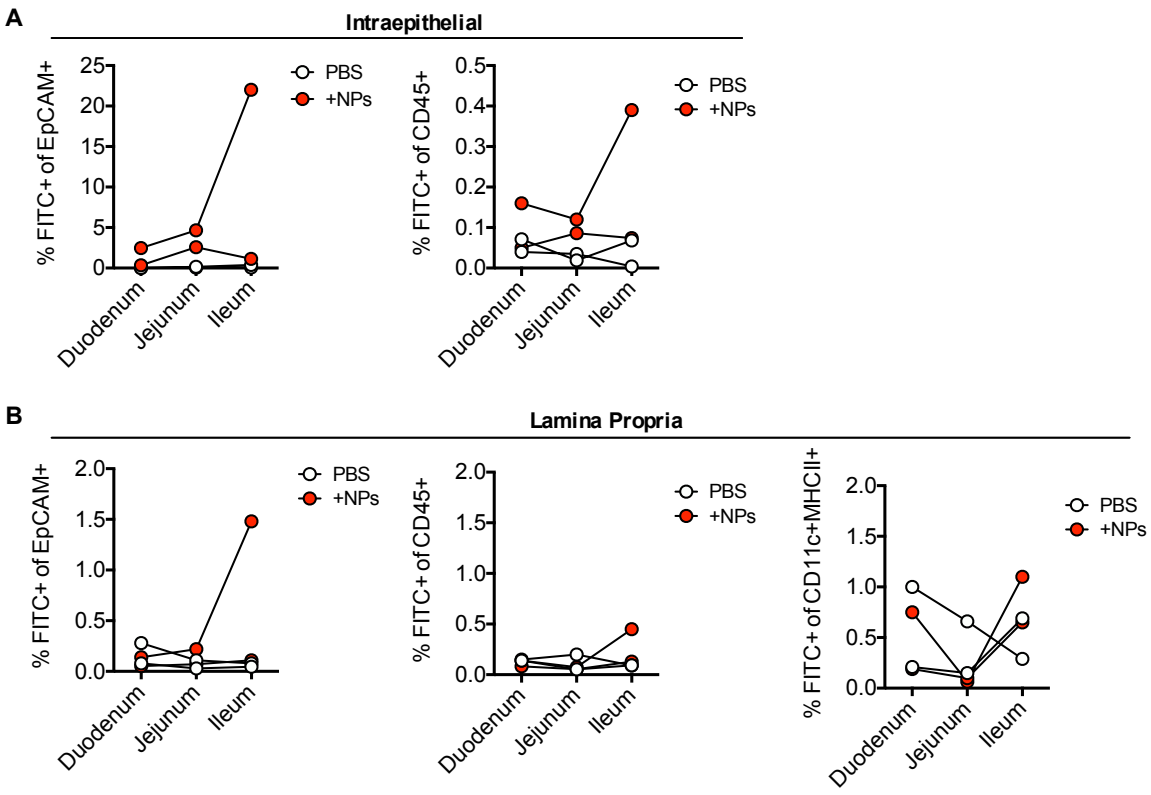

Figure S4.3. Protein uptake after oral delivery in PLGA nanoparticles. Mice were orally administered PBS or PLGA nanoparticles (5 mg) encapsulating BSA-FITC. Two hours after administration, mice were sacrificed, small intestines were collected, and separated in into three sections. Small intestinal sections were processed into single cell suspensions of A) intraepithelial cells and B) lamina propria cells. Cells were stained and analyzed for uptake of BSA by flow cytometry. Data representative of n=2 mice per group and presented as mean ± standard deviation.

APPENDIX B: CHAPTER 5 SUPPLEMENTARY INFORMATION

Supplementary Methods

Dendritic cell protein uptake

BSA was fluorescently labeled using DyLight 800 NHS Ester (Thermo) following manufacturer's instructions and encapsulated in PLGA NPs. DC2.4 cells were seeded at 100,000 per well in 24-well plates overnight in complete medium (RPMI 1640 supplemented with 2 mM L-glutamine, 10% FBS, and 100 U mL^{-1} penicillin and streptomycin). Cells were treated with BSA-Dylight800 (10 μg mL^{-1}) in soluble form or encapsulated in PLGA NPs for 4 hours. Cells were then washed, detached, stained with Live/Dead Fixable Violet (Thermo Fisher Scientific), fixed in 1.6% PFA, and analyzed by flow cytometry using a CantoII for BSA uptake in the live population. Flow cytometry analysis was performed using FlowJo software (Treestar).

Nanoparticle characterization

Nanoparticle size was determined by dynamic light scattering (Zetasizer, Malvern) in PBS or simulated gastrointestinal fluids with or without enzymes (pepsin and pancreatin for gastric and intestinal fluids, respectively).

PLGA emulsion electrospun nanofiber synthesis and release studies

In some studies, BSA was loaded in emulsion electrospun PLGA nanofibers. PLGA was dissolved in HFIP at 15 wt%. To form an emulsion, Tween-20 was added at 1% volume and BSA in solution was added dropwise to the PLGA/Tween-20 solution while vortexing at a 10% aqueous phase. The emulsion was then electrospun onto waxed paper on a metal collector using a needle-rig electrospinning set up (12 kV, 40 μL min^{-1} flow rate, 12 cm distance) in a fume hood. BSA-loaded PLGA nanofibers were massed and

placed in PBS at 37°C under lateral shaking (150 rpm). At the designated time points, sample was removed for analysis followed by volume replacement. Samples were analyzed by MicroBCA Protein Assay Kit (Thermo) to quantify protein release following manufacturer's instructions.

Fluid collection and enzyme-linked immunosorbent assay (ELISA)

Blood was collected biweekly and serum was separated by centrifugation and stored at -20°C until analysis. The small intestine was washed with 5 mL PBS with 0.1 mg mL^{-1} trypsin inhibitor (Sigma) and 50 mM EDTA. Intestinal lavage fluid was vortexed and centrifuged at 2,000 x g for 30 min at 4°C. Supernatant was collected and stored at -20°C until analysis. Antigen-specific IgG and IgA antibodies were assayed from serum and intestinal lavage fluid by ELISA. OVA (2 - 5 µg mL^{-1}) in 10 mM sodium bicarbonate was adsorbed to 96-well high-binding ELISA plates (Costar) at 4°C overnight. Plates were washed with PBS with 1% Tween-20 (PBS-T) and blocked with 2% bovine serum albumin (BSA) in PBS-T for 2 hours at room temperature. Plates were washed with PBS-T and incubated with pre-diluted samples and incubated at 37°C for 2 hours, starting at 1:100 sample dilution for serum and 1:10 sample dilution for intestinal lavage fluid. Samples were also added at equivalent dilutions to wells without pre-adsorbed OVA to identify background signal for each sample. Plates were washed and incubated with HRP-conjugated goat anti-mouse IgG (Thermo) or goat anti-mouse IgA (Thermo) (1:1000 - 1:2000 dilution) for 2 hours at 37°C. Plates were washed and incubated with TMB substrate (BioLegend) for 1 hour at room temperature. Absorbance was read at 605nm.

Immunohistochemistry

Female C56Bl/6J were administered BSA-FITC (10 mg) and PEI (50 µg) by oral gavage. Four hours later, mice were sacrificed, and small intestines were flushed with PBS, cut open longitudinally, and incubated with paraformaldehyde (4%) for 20 minutes at

room temperature. Small intestines were washed and incubated in sucrose (30%) for 1.5 hours at room temperature. Small intestines were rolled and snap-frozen in OCT compound (Thermo). Cross sections (20 μm thick) were prepared by the Histology and Imaging Core at the University of Washington. Sections were dried and cold acetone (-20°C) was added to sections and allowed to evaporate. Sections were washed in Tris-buffered saline (50 mM Tris-HCl, 150 mM NaCl, pH 7.5), blocked with 1% BSA for 30 minutes at room temperature, and incubated with hamster anti-mouse CD11c-N418 (20 μg mL^{-1}) (eBioscience) overnight at 4°C. After washing, sections were incubated with rabbit anti-hamster IgG-TRITC (5 μg mL^{-1}) for 1 hour at room temperature followed by mounting in Fluoromount-G with DAPI (Thermo). Sections were imaged using a Nikon Eclipse Ti microscope (Nikon, Melville, NY, USA) equipped with an Andor (model number DR-328G-C01-SIL) fluorescence camera (Andor, Belfast, UK).

Supplementary Figures

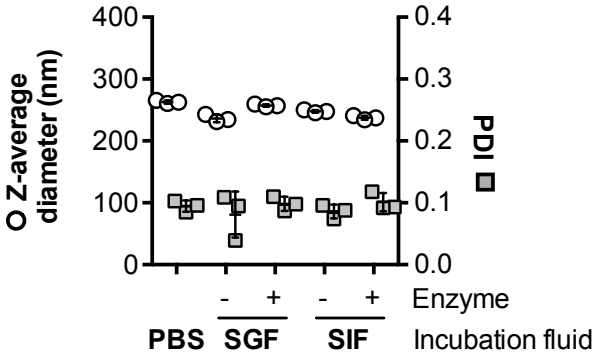

Figure S5.1. Simulated gastrointestinal fluids do not affect PLGA NP diameter or polydispersity index. PLGA NPs were incubated in PBS or simulated gastric (SGF) or intestinal (SIF) fluids with or without pepsin or pancreatin, respectively. NP diameter (left axis) and PDI (right axis) were determined by dynamic light scattering. Data representative of n=3 per group.

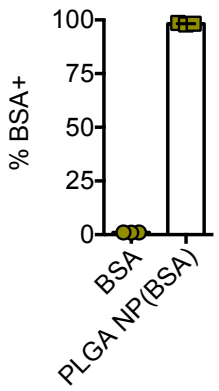

Figure S5.2. Enhanced dendritic cell uptake of proteins when formulated in PLGA NPs. DC2.4 cells were treated with soluble BSA-DyLight800 or PLGA NP-encapsulated BSA-DyLight800 at 10 ug mL^{-1} BSA. Uptake of BSA was evaluated after 4 hours by flow cytometry. Data representative of n=3 per group.

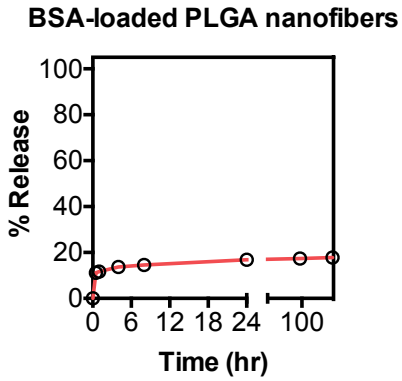

Figure S5.3. BSA release from PLGA nanofibers formed by emulsion electrospinning.

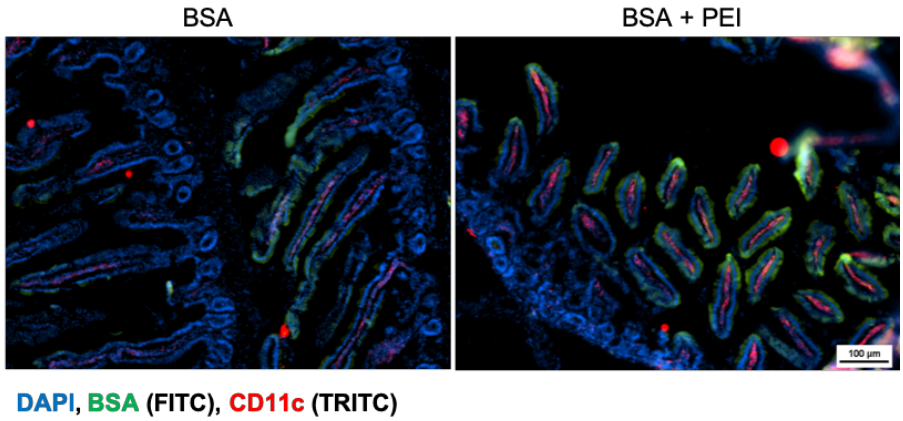

*Figure S5.4. Histology of small intestine after oral administration of PEI. Fluorescent microscopy images of small intestinal cross sections of mice treated with BSA-FITC (10 mg) and **A)** no*

*adjuvant or **B)** PEI (50 μg) 4 hours after oral gavage. Blue, DAPI; Green, BSA-FITC; Red, CD11c.*

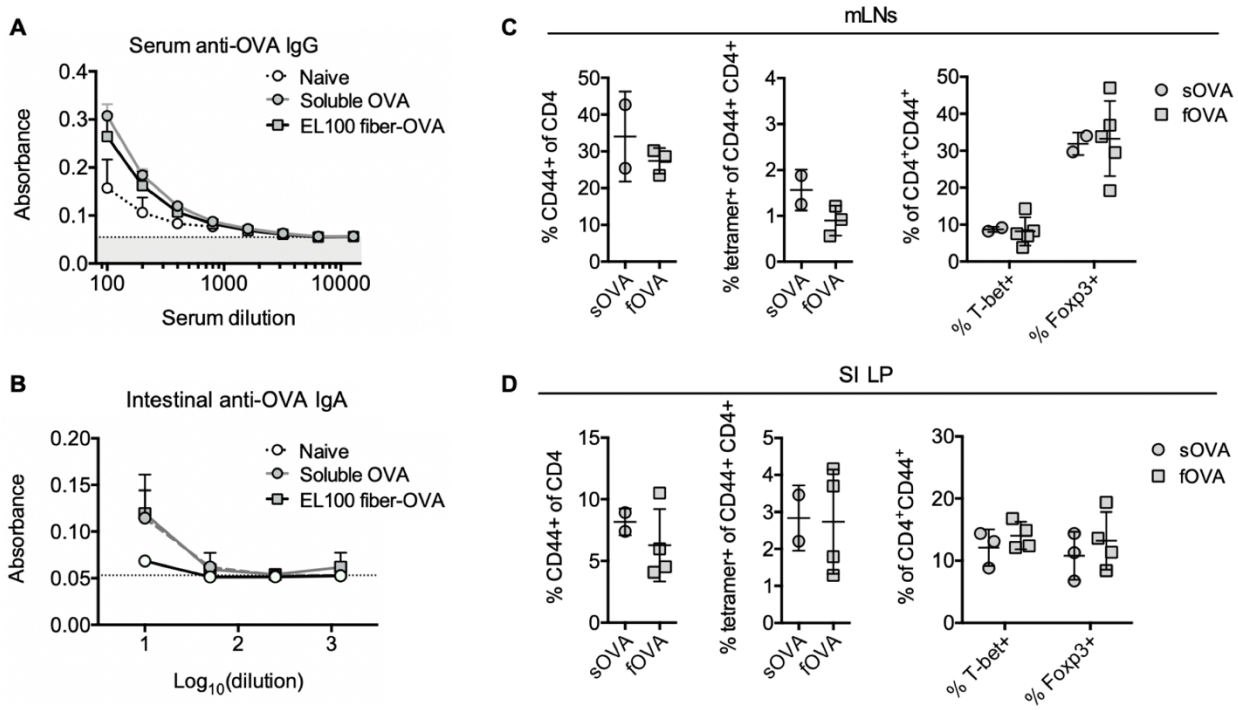

*Figure S5.5. Antibody and $CD4^+$ T cell responses to oral immunization with unprotected or gastric-protected antigen. Female C56Bl/6J mice were treated with soluble or Eudragit L100 nanofiber-encapsulated OVA (0.2 mg) by oral gavage and adaptive immune responses were evaluated 14 days after the last dose. Antigen-specific **A)** serum IgG and **B)** small intestinal IgA were quantified by ELISA. Mesenteric lymph nodes (mLNs) and small intestinal lamina propria (SI LP) were processed into single cell suspensions and stained for analysis by flow cytometry. Percentage of $CD44^+$ $CD4^+$ T cells, I-A(b) $OVA_{325\text{-}335}$ tetramer positive $CD44^+$ $CD4^+$ T cells, and T-bet$^+$ or Foxp3$^+$ $CD44^+$ $CD4^+$ T cells in **C)** mLNs and **D)** SI LP. Data representative of n=2-6 mice per group and is presented as mean ± standard deviation and analyzed by one-way ANOVA.*

APPENDIX C: DENDRITIC CELL-BASED VACCINE PROGRAMMING

Publication: **Frizzell, H.**, Park, J., Lou, N. C., & Woodrow, K. A. (2017). Role of heterogeneous cell population on modulation of dendritic cell phenotype and activation of CD8 T cells for use in cell-based immunotherapies. *Cellular Immunology*, *311*, 54-62.

Abstract

Dendritic cell (DC)-based immunotherapies have much utility in their ability to prime antigen-specific adaptive immune responses. However, there does not yet exist a consensus standard to how DCs should be primed. In this study, we aimed to determine the role of heterogeneous co-cultures, composed of both CD11c+ (DCs) and CD11c- cells, in combination with monophosphoryl lipid A (MPLA) stimulation on DC phenotype and function. Upon DC priming in different co-culture ratios, we observed reduced expression of MHCII and CD86 and increased antigen uptake among CD11c+ cells in a CD11c-dependent manner. DCs from all culture conditions were induced to mature by MPLA treatment, as determined by secretion of pro-inflammatory cytokines IL-12 and TNF-α. Antigen-specific stimulation of CD4+ T cells was not modulated by co-culture composition, in terms of proliferation nor levels of IFN-γ. However, the presence of CD11c- cells enhanced cross-presentation to CD8+ T cells compared to purified CD11c+ cells, resulting in increased cell proliferation along with higher IFN-γ production. These findings demonstrate the impact of cell populations present during DC priming, and point to the use of heterogeneous cultures of DCs and innate immune cells to enhance cell-mediated immunity.

Introduction

Dendritic cells (DCs) are unique immune cells that bridge the innate and adaptive immune systems through their ability to effectively present antigen to T cells [1]. DC-based immunotherapies prime DCs *ex vivo* with a specific antigen, induce their maturation, and then re-administer them back into the body where they will home to the lymph nodes and activate the adaptive immune system [2]. Many DC-based therapies have moved into clinical trials and demonstrated safety and the ability to elicit antigen-specific immune responses. However, these studies have shown only modest performance in objective clinical outcomes such as tumor response rates [3,4]. While the exact mechanism for these observed outcomes has not been fully elucidated, using DC-vaccines in combination with other immuno-regulatory therapies as well as generating DCs that are more immunogenic and functional for administration are active areas of investigation [5]. The efficacy of DC-vaccines to generate desired immune responses has been probed with respect to parameters such as type of antigen loaded, maturation stimuli used, route of administration, and the subsets of DCs utilized [4,6,7]. Overall, generation of these DC-therapies has not been optimized and its achievement is critical to understand how to generate more effective immunotherapies.

One strategy to improve DC-therapies involves the use adjuvants, such as toll-like receptor (TLR) agonists, to activate DCs and induce their maturation and migration to lymph nodes where they can interact with T cells [8–10]. This stimulation renders DCs with the ability to effectively activate encountered T cells and induce lineage commitment and effector responses. Specifically, the TLR4-agonist monophosphoryl lipid A (MPLA) has been shown to increase the function of antigen presenting cells (DCs and macrophages) to induce T cell proliferation and polarization into T-helper 1 cells (T_H1), which are important in fighting intracellular pathogens and tumors [11,12]. Many DC-therapy clinical trials have shown a superiority of mature over immature DCs in terms of clinical outcomes [13,14]. Thus, in adoptive cell transfers, DCs are commonly pulsed with

stimulating factors, such as TLR ligands, to induce their maturation and enhance their effectiveness [15].

In the generation of these therapies for pre-clinical studies, DCs are frequently derived from monocyte precursors in the bone marrow using granulocyte macrophage-colony stimulating factor (GM-CSF), which is a growth factor that generates a heterogeneous population of both CD11c+ (DCs) and CD11c- cells (non-DC monocytes and granulocytes) [16–18]. For application in human clinical trials, DCs are commonly derived from blood monocytes [19]. Crosstalk between cell populations, particularly between immune cell populations, has been shown to exist dynamically. Such communication can control immune responses and influence the balance between inflammation and tolerance [20–23]. For instance, paracrine signaling of cytokines and other soluble factors can activate nearby cells and propagate the immune response [24,25]. Additionally, direct cell-cell contact via receptor binding can also induce intracellular signaling that leads to activation and suppression of cellular programs or the production of immunological factors in a variety of immune settings [25–27]. The effect of such cell crosstalk can be observed in the context of DC-based therapies, in which the use of the bone marrow-derived heterogeneous CD11c+ and CD11c- population significantly increased the percentage of tumor-free mice after melanoma challenge compared to the purified DC population. This study demonstrated the importance of the presence of CD11c- cells in achieving the desired immune response of restricting tumor growth [17]. Extensive crosstalk and cell-cell communication could occur in this heterogeneous environment to modulate DC maturation, antigen uptake, processing, and presentation, which are critical for the success of DC-based therapies. Although this parameter has shown to be necessary to induce antitumor protection in mice *in vivo*, the role of cell populations present during *ex-vivo* priming is still significantly understudied. Moreover, how DC phenotype and immunogenicity is affected by TLR activation when DCs are cultured in a heterogeneous cell population has not been investigated.

We aim to further exploit the use of heterogeneous co-cultures to strengthen DC-therapies. Here, we explore how different percentages of CD11c- cells present during DC priming and stimulation influence DC phenotype and capability of activating adaptive immune responses. Such findings can impact priming protocols for cell-based therapies to produce superior DCs, thereby potentially leading to improved clinical outcomes. In this study, we hypothesized that DC phenotype, antigen uptake, and functional ability to stimulate T cells are controlled by MPLA stimulation in combination with the composition of the CD11c+/- population in culture. Interestingly, the heterogeneous population of MPLA-treated CD11c+/- cells at specific ratios negatively affected DC maturation and preferentially induced CD8+ T cell proliferation via cross-priming. Hence, we demonstrate that an *ex vivo* DC preparation protocol based on a combination of heterogeneous cells and TLR stimulation can possibly be a potent strategy to enhance cellular immunity against tumors or infections.

Materials and Methods

Derivation of bone marrow DCs and CD11c+ isolation

Bone marrow-DCs were derived as previously described [29]. Briefly, tibias and femurs were collected from the hind limbs of 8-12-week-old female C57BL/6 mice (Jackson Laboratory, Bar Harbor, ME) and the bone marrow was flushed out. Red blood cells were lysed and the remaining cells were cultured on petri dishes in complete cell culture media: RPMI-1640 (Cellgro, Manassas, VA), 2 mM L-glutamine (Cellgro), 10 mM HEPES, 1x non-essential amino acids, 1 mM Na Pyruvate, 55 μM 2-mercapthoethanol, 1% penicillin/streptomycin, and 10% heat-inactivated fetal bovine serum (all from Invitrogen, Carlsbad, CA) with 20 ng mL^{-1} GM-CSF (PeproTech, Rocky Hill, NJ). After 3, 5, and 7 days of culture the cells were supplemented with new media and GM-CSF (20 ng mL^{-1}). On day 8, all cells were detached, collected, and magnetically labeled with anti-CD11c microbeads (Miltenyi Biotec, Auburn CA). Labeled cells were flowed through a magnetic

column and CD11c+ cells were isolated by positive selection. The retained fraction (CD11c enriched) was separated from the eluted fraction (CD11c reduced) and used for further experimentation. Immediately after separation, the CD11c enriched isolate was found to be 70.98% CD11c+ ± 20.22 and the CD11c reduced isolate was found to be 26.36% CD11c+ ± 7.90 as identified by flow cytometry (FACS Canto II). Data were analyzed using FlowJo software (Tree Star).

CD11c+ DC phenotype analysis with and without TLR stimulus

After CD11c+ cell isolation, cells were seeded in 24-well plates at varying ratios of cells from the CD11c enriched isolate to cells from the CD11c reduced isolate. Ratios of 8:1, 1:1, and 1:8 were investigated. Wells with only CD11c enriched and reduced isolate cells were included as controls. Total cell number was kept constant for all ratios at 250,000 cells per well. After seeding, cells received either media only or stimulation with MPLA (10 μg mL^{-1}) (InvivoGen, San Diego, CA). Lipopolysaccharide (LPS) stimulation (1 μg mL^{-1}) of CD11c enriched cells was included in the first experiment as a positive control. Twenty-four hours later, all cells were collected using Cell Dissociation Buffer (Thermo Fisher Scientific, Waltham, MA), blocked with anti-Fc antibody, and stained with APC anti-mouse CD11c, PerCP/Cy5.5 anti-mouse MHC Class II (MHCII), Brilliant Violet (BV) 605 anti-mouse CD86 (antibodies purchased from BD Biosciences, Franklin Lakes, NJ), and LIVE/DEAD® Fixable Violet Dead Cell Stain (Thermo Fisher Scientific). After fixation with 1.6% paraformaldehyde, cells were analyzed by flow cytometry (FACS Canto II). Flow cytometry data were analyzed by FlowJo software for surface marker expression of the live, CD11c+ gated population.

Antigen uptake

Cells were seeded at varying CD11c enriched to CD11c reduced isolate ratios in 24-well plates as described above and fluorescently labeled ovalbumin (OVA-Alexa Fluor 647) (Thermo Fisher Scientific) was added to cultures at a concentration of 10 μg mL^{-1}

simultaneously with MPLA stimulus (10 μg mL^{-1}). Twenty-four hours later, all cells were collected, washed extensively, stained with PerCP anti-mouse CD11c and LIVE/DEAD® Fixable Violet, fixed with 1.6% paraformaldehyde, and analyzed by flow cytometry (LSRII). Flow cytometry data were analyzed by FlowJo software for OVA-Alexa Fluor 647 signal of live cells.

Antigen-specific CD4+ and CD8+ T cell proliferation assay

Following CD11c isolation of bone marrow cells, cells were seeded at CD11c enriched to CD11c reduced isolate ratios of 8:1, 1:1, and 1:8 in 96-well plates at 10,000 total cells per well. Controls of CD11c enriched and reduced cells only were included. Cells were incubated with MPLA stimulus (2 μg) and EndoFit ovalbumin (20 μg) (InvivoGen) for 24 hours before co-culture with T cells. CD11c enriched cells without treatment with ovalbumin were included as a negative control and CD11c enriched cells treated with LPS (0.2 μg) were included as a positive control. CD4+ and CD8+ T cells were collected from the spleens of OTII and OTI transgenic mice (Jackson Laboratory, New Harbor, ME), respectively. Briefly, spleens were collected and placed in 4 mL digestion media at 1.5 mg mL^{-1} Collagenase D and 40 μg mL^{-1} DNase I (Sigma-Aldrich, St. Louis, MO) in RPMI-1640. Spleens were then incubated at 37 °C for 30 minutes. Connective tissue was filtered out by a 70 μm cell strainer, and red blood cells were lysed. To select for CD4+ or CD8+ T cells, remaining splenocytes were incubated with magnetically-labeled antibodies and isolated by negative selection through a magnetic column (Miltenyi). Purified T cells were then labeled with carboxyfluorescein succinimidyl ester (CFSE) (10 μM) (Thermo Fisher Scientific) for proliferation tracking. T cells were co-cultured with OVA- and MPLA-treated CD11c+/- cells at CD11c+/- cells:T cells 1:10 for CD4+ and 1:30 for CD8+ T cell proliferation analysis. After 72 hours, cells were collected, stained with APC anti-mouse CD4 or APC anti-mouse CD8 (BD Biosciences) and LIVE/DEAD® Fixable Violet, fixed with 1.6% paraformaldehyde, and analyzed by flow cytometry (LSRII). Fraction

diluted was quantified by the CFSE signal dilution of the live, CD4+ or CD8+ population. Proliferation index was calculated using FlowJo v9 Proliferation Platform.

Analysis of cytokine production

Concentration of cytokines IL-12, IL-10, IL-1β, TNF-α in the cell culture supernatant of CD11c+/- co-cultures after 24 hour MPLA treatment and of cytokines IL-4 and IFN-γ accumulated in the cell culture supernatant from CD11c+/- and T cell cultures after 72 hours were analyzed by enzyme-linked immunosorbent assay (ELISA) according to the manufacturer's instructions (PeproTech).

Statistical analysis

Results are expressed as the mean ± standard deviation. When comparing outcomes between groups, statistical analysis was performed by one-way analysis of variance (ANOVA) using Tukey's multiple comparison post-test. When comparing outcomes between the same group of different conditions (no stimulus vs MPLA-treated), multiple t-tests were used with multiple comparison correction using the Holm-Sidak method. Statistical analyses were performed using GraphPad Prism 6 software. Statistical significance was defined as $p<0.05$ (*$p<0.05$; **$p<0.01$; ***$p<0.005$; ****$p<0.001$).

Results

Co-cultures of CD11c+ and CD11c- cells modulate adjuvant-induced DC maturation

We examined DC maturation marker expression from co-cultures of varying ratios of CD11c+ and CD11c- cells to understand how these heterogeneous cell populations respond to TLR stimulation. The co-culture groups investigated were CD11c enriched, CD11c reduced, and combinations of 8:1, 1:1, and 1:8, respectively. MPLA-stimulation induced the upregulation of the maturation markers CD86 and MHCII among the CD11c+ DC population for all co-culture conditions as quantified by mean fluorescence intensity (MFI). Compared to non-stimulated cells of the same culture condition, stimulation by

MPLA resulted in an MFI increase of up to 14- and 3-fold for CD86 and MHCII respectively, demonstrating the ability of DCs to strongly respond to maturation stimuli (Figure 1a). However, although all cultures were exposed to the same amount of adjuvant, DCs in the presence of CD11c- cells did not upregulate surface markers CD86 and MHCII to the same extent as when cultured as a CD11c+ enriched population (Figure 1b,c, respectively). Surface upregulation was further dampened with increased fraction of CD11c- cells in the culture.

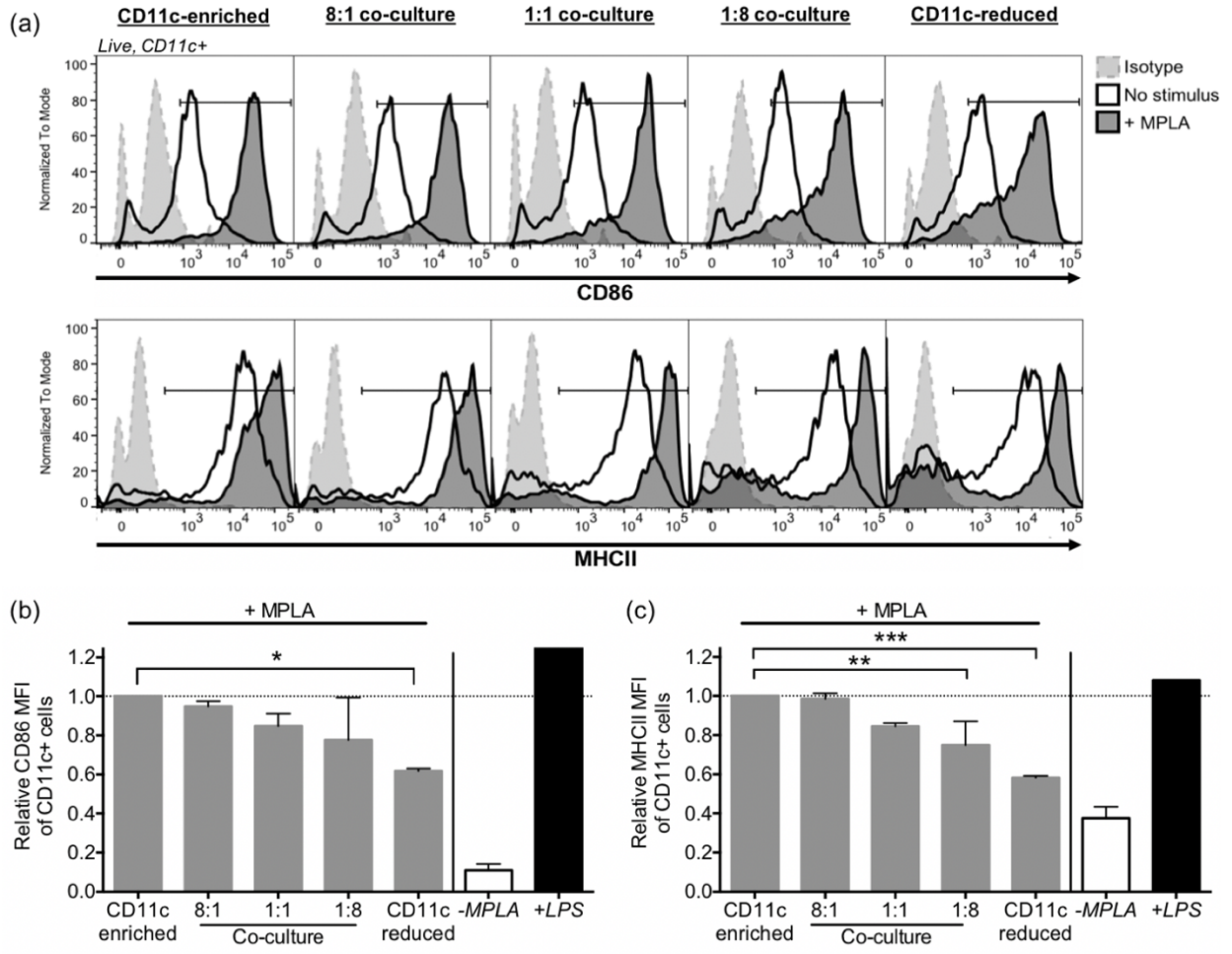

Figure 1. Presence of bone marrow-derived CD11c cells reduces extent of inflammatory surface marker expression by CD11c+ DCs upon MPLA stimulation. Bone marrow- derived cells were separated into CD11c enriched and CD11c reduced isolates, co-cultured at varying ratios, and treated with or without MPLA (10 μg mL^{-1}). (a) The CD11c+ population was analyzed for expression of CD86 and MHCII. Relative mean fluorescence intensity (MFI) of (b) CD86 and (c)

*MHCII of CD11c+ cells after MPLA stimulation for 24 h under different co-culture conditions. Untreated and LPS-treated (1 $\mu g\ mL^{-1}$) CD11c enriched cells were included as negative and positive controls, respectively. Data is representative of the mean of three independent experiments ± standard deviation. Statistical analysis was performed by one-way analysis of variance using Tukey's multiple comparison post-test comparing groups against the CD11c enriched culture condition. ***$p < 0.005$; **$p < 0.01$; *$p < 0.05$.*

In the absence of MPLA stimulation, the majority of CD11c+ cells did not co-express the maturation markers MHCII and CD86 for all co-cultures (Figure 2a,b). We observed a slight decrease in the percentage of CD11c+ cells that were double positive for both markers as the percentage of CD11c- cells in the culture increased, although this trend was not significant. Upon MPLA stimulation, we observed a significantly lower percentage of CD86 and MHCII double positive CD11c+ cells in co-cultures containing a higher fraction of CD11c- cells (Figure 2a,c). Low expression of these activation markers was observed on the CD11c- population for all culture ratios after MPLA stimulation, in which MFI values of CD86 and MHCII were up to ~12- and 9-fold less than that of the CD11c+ population, respectively (data not shown). From these data, we can conclude that the presence of CD11c- cells during DC priming with a TLR adjuvant impede MPLA-driven DC maturation and result in DCs with a less mature phenotype.

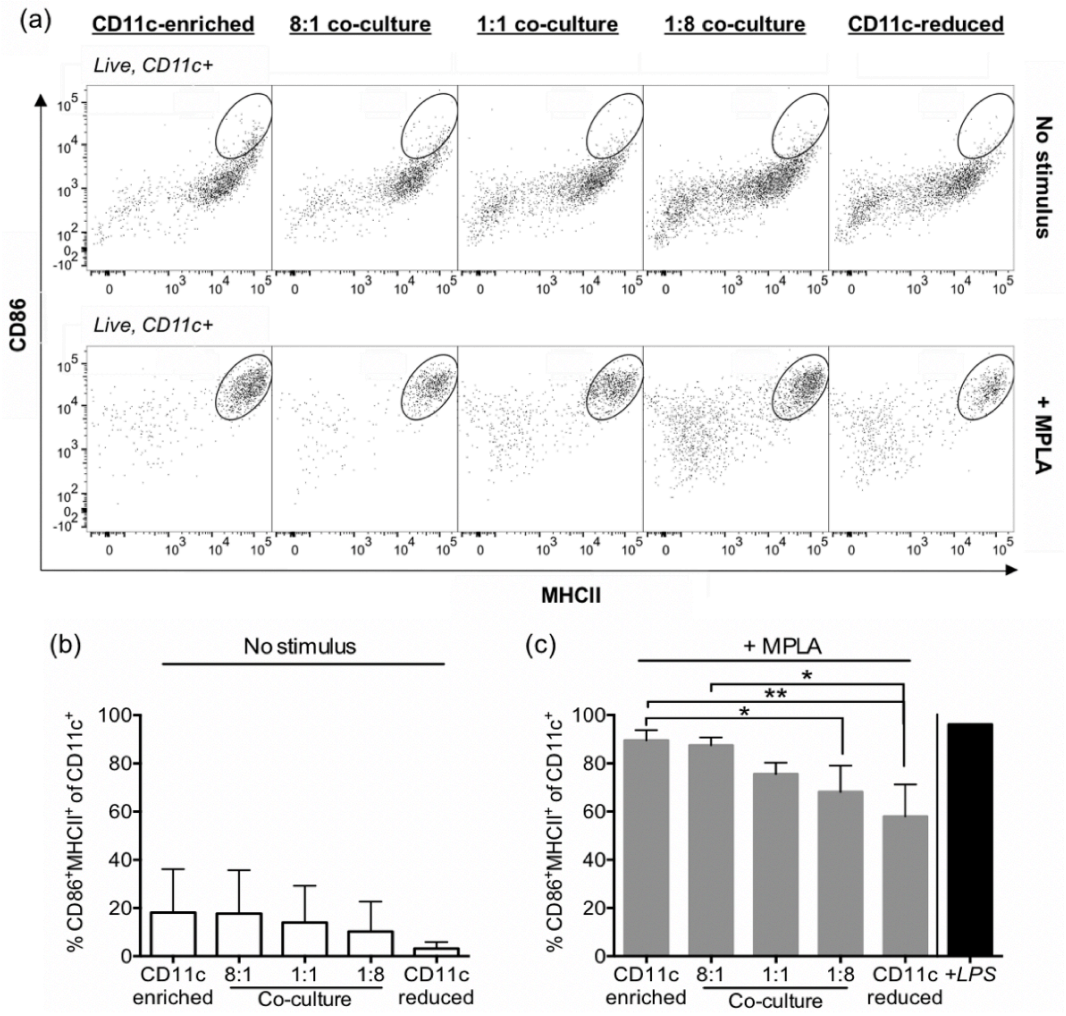

*Figure 2. Presence of bone marrow-derived CD11c cells reduces CD11c+ DC maturation by MPLA adjuvant. Bone marrow-derived cells were separated into CD11c enriched and CD11c reduced isolates, co-cultured at varying ratios, and treated with or without MPLA (10 μg mL^{-1}). (a) Representative flow plots showing CD86 and MHCII co-expression on CD11c+ cells both with and without MPLA stimulation. Percentage of live, CD11c+ cells that were CD86+ MHCII+ double positive 24 h after co-culture at varying ratios (b) without MPLA stimulation and (c) with MPLA stimulation. LPS-treated (1 μg mL^{-1}) CD11c enriched cells were included as a positive control. Data representative of the mean of three independent experiments ± standard deviation. Statistical analysis was performed by one-way analysis of variance using Tukey's multiple comparison post- test comparing groups against the CD11c enriched culture condition. **p < 0.01; *p < 0.05.*

To investigate how the co-culture conditions modulate cytokine secretion from cells, we analyzed co-culture supernatants both with and without MPLA treatment for

the presence of common inflammatory cytokines. Without adjuvant stimulation, all culture conditions secreted low levels of the cytokines IL-12 and TNF-α (Figure 3a,b), whereas no secretion of IL-10 or IL-1β was detected. After addition of MPLA, we observed a dramatic increase up to 400- and 56-fold in the concentration of IL-12 and TNF-α, respectively, compared to non-stimulated cells of the same culture condition (Figure 3a,b). Similar concentrations of TNF-α was detected from all cultures and although not statistically significant, we observed a trend for increased IL-12 secretion with increased percentage of CD11c+ cells present. Thus, for the common cytokines investigated, co-culture ratio does not play a role in modulating cytokine secretion.

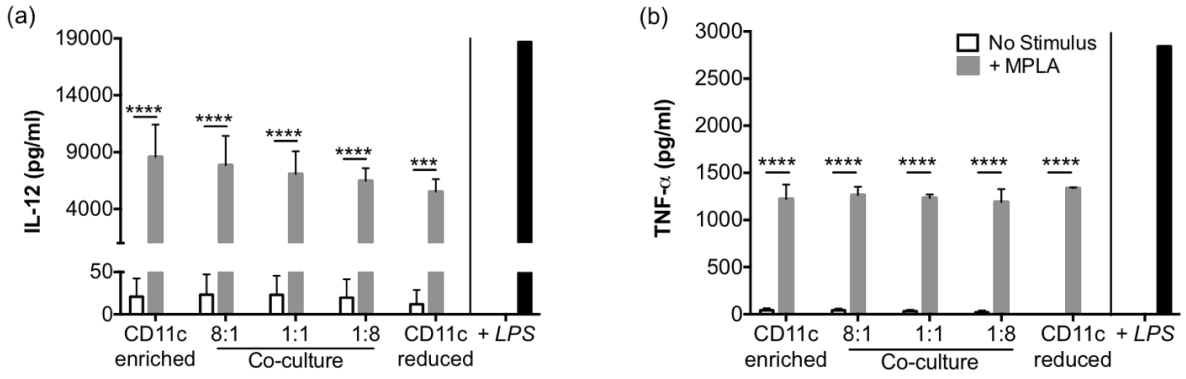

*Figure 3. MPLA adjuvant stimulation induces enhanced inflammatory cytokine expression by all CD11c± co-culture ratios. Bone marrow-derived cells were separated into CD11c enriched and CD11c reduced isolates, co-cultured at varying ratios, and received either no stimulus or MPLA treatment (10 $\mu g\ mL^{-1}$). Supernatants were assessed by ELISA for the presence of (a) interleukin-12 (IL-12) and (b) tumor necrosis factor alpha (TNF-α) after 24h. Data is representative of the mean of three independent experiments ± standard deviation. Statistical analysis was performed by comparing no stimulus and MPLA treatment values for each co-culture condition using multiple t-tests. ****$p < 0.001$; ***$p < 0.005$.*

Combination of both CD11c+ and CD11c- cells enhances antigen uptake by DCs

Given that DC maturation status was observed to be dependent on CD11c+/- co-culture ratio, we hypothesized that antigen uptake by MPLA-stimulated CD11c+ cells would also be influenced by the presence of CD11c- cells in culture since antigen uptake capacity is downregulated upon DC maturation. The elucidation of this parameter is

critical in order to achieve high DC loading of antigen during ex vivo priming. Using an OVA-Alexa Fluor 647 antigen, we treated CD11c+/- cultures with both MPLA and OVA simultaneously and observed that almost all of the CD11c+ population in co-culture with CD11c- cells was OVA+. Degree of antigen uptake was found to be dependent on the CD11c- fraction in the culture, as OVA MFI of CD11c+ cells increased as the percentage of CD11c- cells in the culture increased (Figure 4a). In particular, we observed a significant increase in uptake of OVA by almost two-fold in the 1:8 co-culture compared to the CD11c+ enriched population. In contrast, a low percentage of the CD11c- population was OVA+ and displayed lower OVA signal per cell (Figure 4b). In summary, the presence of CD11c- cells during DC maturation and antigen loading enhance uptake of antigen in CD11c+ DCs.

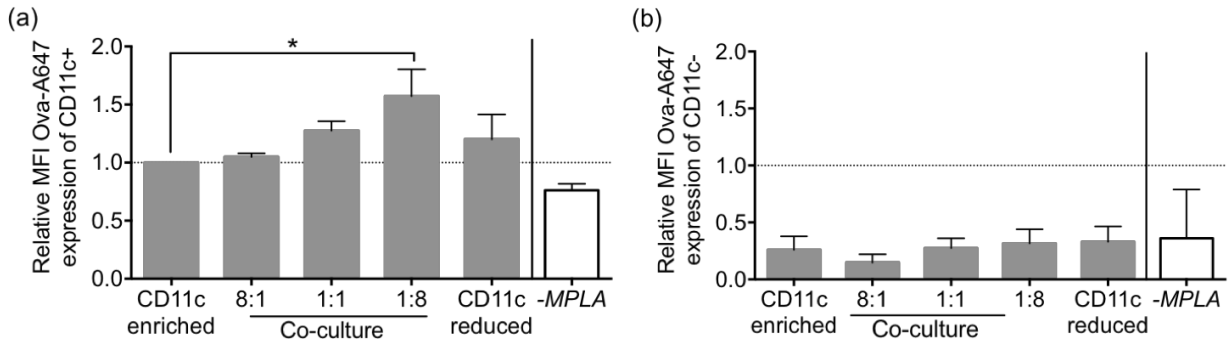

*Figure 4. Presence of CD11c- cells enhances antigen uptake in CD11c+ DCs. Bone marrow-derived cells were separated into CD11c enriched and CD11c reduced isolates, co- cultured at varying ratios, and were incubated with ovalbumin-Alexa Fluor 647 (OVA) (10 μg) in combination with MPLA treatment (10 μg mL^{-1}). The presence of OVA was analyzed by flow cytometry for both the (a) CD11c+ population and (b) CD11c- population. CD11c enriched cells not treated with adjuvant were included as a negative control. To reduce mouse-to-mouse variability, OVA MFI was normalized to the CD11c+ population from the CD11c enriched culture condition from each experimental replicate. Data is representative of the mean of three independent experiments ± standard deviation. Statistical analysis was performed by one-way analysis of variance using Tukey's multiple comparison post-test comparing groups against the CD11c enriched culture condition. *$p < 0.05$.*

Presence of CD11c- cells enhance CD8+ T cell proliferation and activation

We next sought to understand the functional differences of DCs when cultured in the presence of CD11c- cells at varying ratios through investigation of CD4+ and CD8+ T cell proliferation. Through the utilization of T cells bearing transgenic receptors specific for OVA epitopes, we elucidated DC antigen presentation and capacity to stimulate antigen-specific T cells. Upon culture of CD4+ T cells with OVA-pulsed, MPLA-stimulated CD11c+/- cell ratios, we observed a similar percentage of CD4+ T cells that underwent at least one round of proliferation (fraction diluted) from all co-culture conditions, with around 80% of all T cells undergoing at least one round of proliferation (Figure 5a,b). We also investigated the secretion of T cell cytokines IFN-γ and IL-4 after 72 hours to identify T cell polarization into a T_H1 or T_H2 phenotype, respectively. No IL-4 was detected in any cultures and IFN-γ was detected in all cultures at similar levels (Figure 5c). These data indicate that the presence of CD11c- cells do not prevent or reduce MHCII presentation to CD4+ T cells nor their polarization toward the T_H1 lineage.

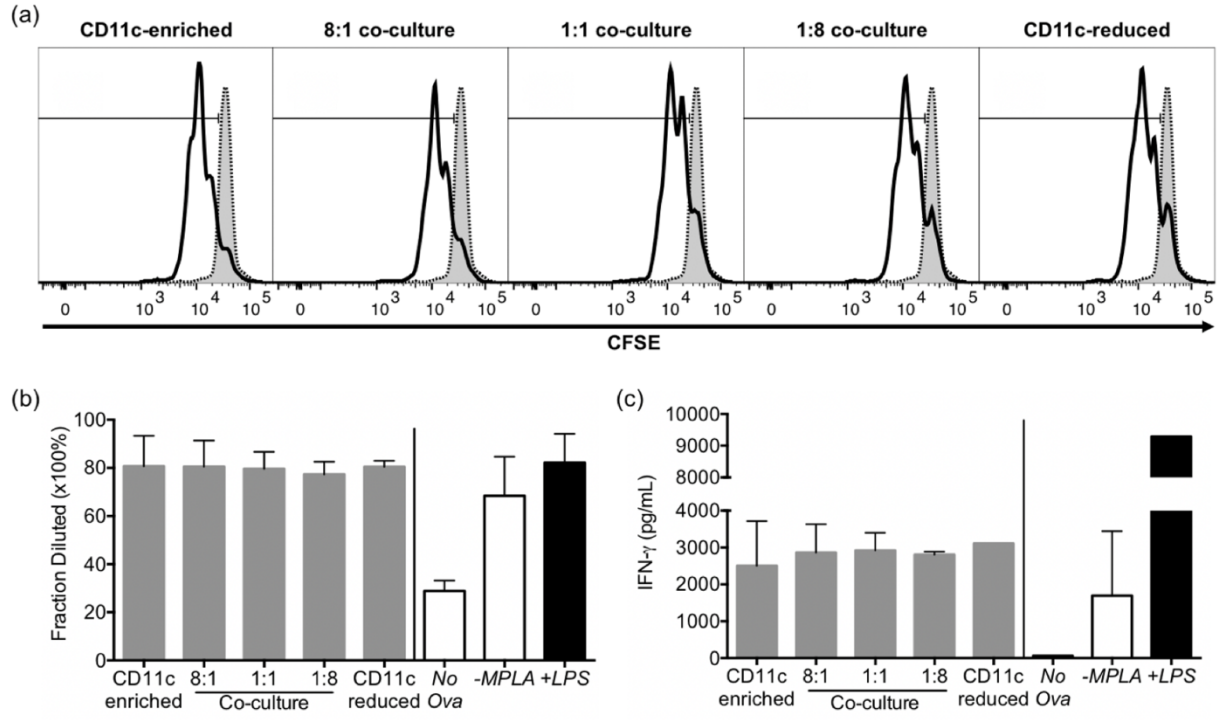

Figure 5. Equivalent activation of antigen-specific CD4+ T cells by all CD11c± co-culture ratios. Bone marrow-derived cells were separated into CD11c enriched and CD11c reduced isolates, co-

cultured at varying ratios, incubated with ovalbumin (OVA) (10 μg) in combination with MPLA treatment (10 μg mL^{-1}) for 24 h, and then cultured with OVA-specific CFSE+ CD4+ T cells at CD11c±:T cell 1:10 for 72 h. (a) Dilution of CFSE+ signal among CD4+ T cells after culture with CD11c± cells was observed by flow cytometry. (b) Fraction of CD4+ T cells diluted with respect to CD11c± ratio. (c) Supernatants were assessed by ELISA for the presence of interferon gamma (IFN-γ). CD11c enriched cells that were not incubated with ovalbumin antigen before co-culture with T cells were included as a negative control for the assay. Untreated and LPS-treated (0.2 μg) CD11c enriched cells were included as negative and positive controls, respectively. Data is representative of the mean of three independent experiments ± standard deviation.

Upon co-culture of OVA-pulsed, MPLA-stimulated CD11c+/- cells with CD8+ T cells, we observed a trend in the percentage of CD8+ T cells that underwent at least one round of division and percentage of CD11c- cells in the co-culture (Figure 6a,b). Strikingly, as the percentage of CD11c- fraction increased in the culture, more rounds of division by CD8+ T cells were induced, resulting in an increased proliferation index (i.e. the average number of cell divisions that the responding T cells underwent) of up to 127% (Figure 6c). The average percentage of CD8+ T cells that underwent more than 1 round of proliferation was 15% when cultured with CD11c enriched cells and increased to 38% when cultured with CD11c reduced cells. This same trend was observed for the secretion of IFN-γ, in which higher production of the anti-viral cytokine was achieved through co-culture of CD8+ T cells with both CD11c+ and CD11c- cells (Figure 6d). These results demonstrate that the presence of CD11c- cells enhance MHCI cross-presentation by antigen-presenting cells and the activation of CD8+ T cells compared to cultures of CD11c+ only.

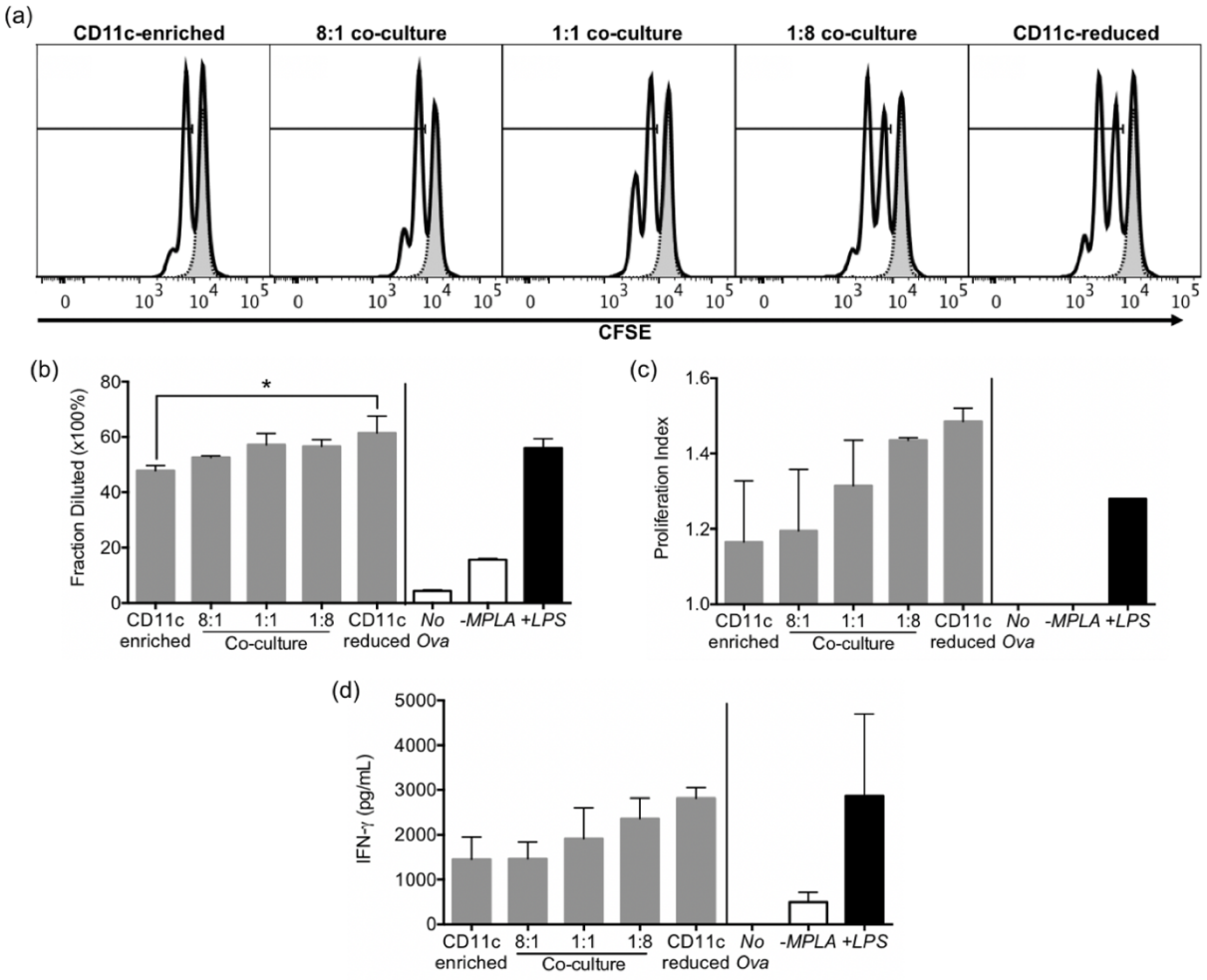

*Figure 6. Presence of CD11c cells enhances antigen-specific CD8+ T cell priming. Bone marrow-derived cells were separated into CD11c enriched and CD11c reduced isolates, co-cultured at varying ratios, incubated with ovalbumin (OVA) (10 μg) in combination with MPLA treatment (10 μg mL^{-1}) for 24 h, and then cultured with OVA-specific CFSE+ CD8+ T cells at CD11c±:T cell 1:30 for 72 h. (a) Dilution of CFSE+ signal among CD8+ T cells after culture with CD11c± cells was observed by flow cytometry. (b) Fraction of CD8+ T cells diluted and (c) proliferation index of CD8+ T cells with respect to CD11c± ratio. (d) Supernatants were assessed by ELISA for the presence of interferon gamma (IFN-γ). CD11c enriched cells that were not incubated with ovalbumin antigen before co-culture with T cells were included as a negative control for the assay. Untreated and LPS-treated (0.2 μg) CD11c enriched cells were included as negative and positive controls, respectively. Data is representative of the mean of two independent experiments ± standard deviation. Statistical analysis was performed by one-way analysis of variance using Tukey's multiple comparison post-test comparing groups against the CD11c enriched culture condition. *$p < 0.05$.*

Discussion

Dendritic cell based immunotherapies have promise in vaccination and therapeutic interventions through the role of DCs to induce antigen-specific adaptive immune responses [30–32]. The importance of the maturation state of the adoptively transferred DC and the types of immune cells present during *ex vivo* priming is known to influence immune responses *in vivo*. For example, the use of the CD11c- immune cell population along with DCs as well as the use of different DC subsets in combination has shown to be beneficial in pre-clinical studies of DC-therapies [17,22,33,34]. Clearly, understanding the *ex vivo* preparation of DCs for immunotherapies can have large impacts on the quality of effector adaptive immunity and the clinical efficacy of such interventions [5,35]. Here, we show for the first time the influence of CD11c- cells at varying percentages in culture upon TLR stimulation on CD11c+ DC maturation status, antigen uptake, and ability to activate effector T cells.

In our study, we produced a cell co-culture environment wherein crosstalk can occur among bone marrow-derived CD11c+ and CD11c- cells either directly (via cell-cell interaction) or indirectly (via signaling proteins). We found that the presence of CD11c- cells in culture during adjuvant stimulation resulted in significantly reduced expression of the surface markers CD86 and MHCII of CD11c+ cells in a CD11c- dose-dependent manner. According to a previous study, DC derivation from bone marrow results in a population comprised of DCs, macrophages, monocytes, and granulocytes such as neutrophils. These innate immune cells have been shown to communicate with each other both directly and indirectly, ultimately modulating the resulting immune response of the host [28]. Neutrophils can directly communicate with DCs, such as through the binding of DC-SIGN surface receptor, which can induce DC activation. However, ligation of DC-SIGN by neutrophils has also been shown to interrupt TLR 4-mediated signaling of DCs [36–38]. Macrophages also contribute to immune signaling and respond to various stimuli by secreting factors that balance pro-inflammatory (IL-1, IL-6, IL-23) and anti-

inflammatory/wound healing (IL-10, TGF-β, IL-4) responses [39,40]. Additionally, regulatory macrophages can inhibit inflammatory functions in response to stress [39]. In these ways, DC phenotype can be modulated by the response of CD11c- cells that are in close proximity, such as in our co-culture system in the present study. Though we investigated DC maturation using cultures of cells derived from monocyte precursors in the bone marrow, for practical clinical application DCs are commonly derived from blood monocytes. While similar cell types may be generated through both methods, the specific effect of non-DCs from protocols using blood monocytes will need to be investigated.

Robust uptake of antigen by DCs is critical in *ex vivo* DC preparation for enhancing *in vivo* stimulation of T cells [41,42]. In accordance with down-regulation of antigen endocytosis of DCs upon maturation [43–45], we found that OVA uptake positively correlated with immature status of CD11c+ cells in the co-culture. However, due to the nature of our experimental set-up, the amount of OVA increased per CD11c+ cell in co-cultures with increased CD11c- cells. Thus, we do not know how the combination of the more immature status of CD11c+ cells and the increased ratio of OVA to CD11c+ cell contributed to OVA uptake in the CD11c+ population. Interestingly, we also found that OVA was taken up primarily by CD11c+ cells in the co-culture system. This uptake peaked at the co-culture ratio of 1:8 but not the CD11c reduced control, which included CD11c+ cells that exhibited the lowest levels of maturation phenotype. Therefore, it is conceivable that the immature status of CD11c+ DCs still positively controls antigen uptake but there is specific ratio of antigen concentration to a single CD11c+ cell for a maximum antigen uptake. These indicate that we can possibly generate DCs using the co-culture system with both desired qualities of maximum antigen loading and mature phenotype [35,46,47].

Ability of DCs to stimulate CD4+ and CD8+ T cells ultimately controls the effector functionality of the therapy. For applications in DC-based cancer immunotherapy, the elicitation of both CD8+ cytotoxic T lymphocytes (CTLs) and T_H1 CD4+ T cells is

critical for tumor eradication [34]. The generation of CTLs requires the presentation of exogenous antigens or proteins onto MHC Class I. DCs possess this function through adapting their endocytic and phagocytic pathways [48]. Cross-presentation of extracellular peptide onto MHCI molecules have been shown to be favored for high density antigens [49]. Thus, if more OVA is being taken up by CD11c+ cells when co-cultured with CD11c- cells during MPLA stimulation and antigen priming, it is possible that there is higher frequency of OVA-MHCI complexes that are able to activate CD8+ T cells. Additionally, depending on the maturation state of the DC, encountered antigens can be favored to be processed in distinct endocytic compartments, which can influence the fate of the antigen for MHCI or MHCII presentation [50]. Thus, OVA presentation on MHCI may be favored when cells are cultured with both CD11c+ and CD11c- cells, which is supported by our data. These finding may contribute to the results of a previous study, in which there was a significant increase in the percentage of tumor-free animals when vaccinated with both CD11c+ and CD11c- cells but not with CD11c+ cells alone [51].

In our study, we expected highest CD4+ T cell proliferation from the CD11c+ isolate only culture, in which we observed a CD11c+ cell phenotype of higher frequencies and densities of the costimulatory molecules MHCII and CD86. However, as we observed similar abilities of all co-cultures to activate CD4+ T cells and induce IFN-γ secretion (T_H1 polarization), our results may indicate that the maturation level of the DCs, the number of mature DCs, or both was sufficient to activate CD4+ T cells from all culture ratios. Importantly, the presence of CD11c- cells did not hinder the ability of DCs to present to and activate CD4+ T cells. Results from both CD8+ and CD4+ T cell proliferation studies highlight the phenotypic differences in cells derived using different culture methods that are important to keep in mind for future studies, in which certain types of immune responses are desired for therapeutic efficacy.

Conclusions

In conclusion, we have shown that by varying the cellular composition in culture during DC priming and maturation, adaptive immune responses can be modulated, most notably amplifying CD8+ T cell stimulation and the production of type II interferons. Our data thus support the use of CD11c+ DCs and other immune cell populations, such as monocytes and granulocytes, as an *ex vivo* DC culture strategy for DC-therapies to activate CD4+ T cells while enhancing the expansion of CD8+ T cells, which are critical for the success of immunotherapies. Future work should focus on mechanisms of communication between heterogeneous CD11c+ and CD11c- populations and on recapitulation of this observed increase in cross-priming of CD8+ T cells in *in vivo* experiments.

Acknowledgements

The authors thank D.M. Koelle and F. Hladik for thoughtful feedback on the studies. This work was supported by the National Institutes of Health HD075703 to K.A.W. H.F. acknowledges additional financial support from the National Science Foundation Graduate Research Fellowship Program (DGE-1256082) and the Achievement Rewards for College Scientists Foundation Scholar Award.

References

[1] P. Guermonprez, J. Valladeau, L. Zitvogel, C. Théry, S. Amigorena, Antigen Presentation and T Cell Stimulation by Dendritic Cells, Annu. Rev. Immunol. 20 (2002) 621–667. doi:10.1146/annurev.immunol.20.100301.064828.

[2] C.G. Figdor, I.J.M. de Vries, W.J. Lesterhuis, C.J.M. Melief, Dendritic cell immunotherapy: mapping the way., Nat. Med. 10 (2004) 475–80. doi:10.1038/nm1039.

[3] K. Palucka, J. Banchereau, Dendritic-Cell-Based Therapeutic Cancer Vaccines, Immunity. (2013). doi:10.1016/j.immuni.2013.07.004.

[4] T. Kazemi, V. Younesi, F. Jadidi-Niaragh, M. Yousefi, Immunotherapeutic approaches for cancer therapy: An updated review Tumor escape from immune system, Artif. Cells, Nanomedicine, Biotechnol. (2015) 1–11. doi:10.3109/21691401.2015.1019669.

[5] C.L.-L. Chiang, K. Balint, G. Coukos, L.E. Kandalaft, Potential approaches for more

successful dendritic cell-based immunotherapy., Expert Opin. Biol. Ther. 15 (2015) 569–582. doi:10.1517/14712598.2015.1000298.

[6] I. Bonaccorsi, G. Pezzino, B. Morandi, G. Ferlazzo, Novel perspectives on dendritic cell-based immunotherapy of cancer, Immunol. Lett. 155 (2013) 6–10. doi:10.1016/j.imlet.2013.09.021.

[7] D.W.O. Neill, S. Adams, N. Bhardwaj, Review in translational hematology Manipulating dendritic cell biology for the active immunotherapy of cancer, Blood J. 104 (2015) 2235–2247. doi:10.1182/blood-2003-12-4392.Supported.

[8] M. Schnare, G.M. Barton, A.C. Holt, K. Takeda, S. Akira, R. Medzhitov, Toll-like receptors control activation of adaptive immune responses., Nat. Immunol. (2001). doi:10.1038/ni712.

[9] F. Steinhagen, T. Kinjo, C. Bode, D.M. Klinman, TLR-based immune adjuvants, Vaccine. 29 (2011) 3341–3355. doi:10.1016/j.vaccine.2010.08.002.

[10] C. Pasare, R. Medzhitov, N. Haven, Toll-Dependent Control Mechanisms of CD4 T Cell Activation, 21 (2004) 733–741.

[11] G. De Becker, The adjuvant monophosphoryl lipid A increases the function of antigen-presenting cells, Int. Immunol. 12 (2000) 807–815. doi:10.1093/intimm/12.6.807.

[12] J. Ismaili, J. Rennesson, E. Aksoy, J. Vekemans, B. Vincart, Z. Amraoui, F. Van Laethem, M. Goldman, P.M. Dubois, Monophosphoryl lipid A activates both human dendritic cells and T cells., J. Immunol. 168 (2002) 926–932. doi:10.4049/jimmunol.168.2.926.

[13] A. Draube, N. Klein-González, S. Mattheus, C. Brillant, M. Hellmich, A. Engert, M. von Bergwelt-Baildon, Dendritic cell based tumor vaccination in prostate and renal cell cancer: A systematic review and meta-analysis, PLoS One. 6 (2011). doi:10.1371/journal.pone.0018801.

[14] H. Jonuleit, A. Giesecke-Tuettenberg, T. Tüting, B. Thurner-Schuler, T.B. Stuge, L. Paragnik, A. Kandemir, P.P. Lee, G. Schuler, J. Knop, A.H. Enk, A comparison of two types of dendritic cell as adjuvants for the induction of melanoma-specific T-cell responses in humans following intranodal injection, Int. J. Cancer. 93 (2001) 243–251. doi:10.1002/ijc.1323.

[15] M.S. Labeur, B. Roters, B. Pers, A. Mehling, T.A. Luger, T. Schwarz, S. Grabbe, Generation of tumor immunity by bone marrow-derived dendritic cells correlates with dendritic cell maturation stage., J. Immunol. 162 (1999) 168–75. http://www.jimmunol.org/content/162/1/168.full (accessed January 5, 2016).

[16] J.I. Mayordomo, T. Zorina, W.J. Storkus, L. Zitvogel, C. Celluzzi, L.D. Falo, C.J. Melief, S.T. Ildstad, W. Martin Kast, A.B. Deleo, M.T. Lotze, Bone marrow-derived dendritic cells pulsed with synthetic tumour peptides elicit protective and therapeutic antitumour immunity, Nat. Med. 1 (1995) 1297–1302. doi:10.1038/nm1295-1297.

[17] S. Campisano, S. Mac Keon, S. Gazzaniga, M.S. Ruiz, M.D. Traian, J. Mordoh, R. Wainstok, Anti-melanoma vaccinal capacity of CD11c-positive and -negative cell populations present in GM-CSF cultures derived from murine bone marrow precursors, Vaccine. (2013). doi:10.1016/j.vaccine.2012.10.114.

[18] L. Mendoza, J. Bubeník, J. Símová, T. Jandlová, V. Vonka, R. Mikysková, Prophylactic, therapeutic and anti-metastatic effects of BMDC and DC lines in mice carrying HPV 16-associated tumours., Int. J. Oncol. 23 (2003) 243–7. doi:10.3892/ijo.23.1.243.

[19] L.H. Butterfield, Dendritic cells in cancer immunotherapy clinical trials: Are we making progress?, Front. Immunol. 4 (2013) 3–9. doi:10.3389/fimmu.2013.00454.

[20] M. Rescigno, U. Lopatin, M. Chieppa, Interactions among dendritic cells, macrophages, and epithelial cells in the gut: implications for immune tolerance, Curr. Opin. Immunol. 20 (2008) 669–675. doi:10.1016/j.coi.2008.09.007.

[21] J. Diana, Y. Simoni, L. Furio, L. Beaudoin, B. Agerberth, F. Barrat, A. Lehuen, Crosstalk between neutrophils, B-1a cells and plasmacytoid dendritic cells initiates autoimmune diabetes., Nat. Med. (2013). doi:10.1038/nm.3042.

[22] G. Bakdash, I. Schreurs, G. Schreibelt, J. Tel, Crosstalk between dendritic cell subsets and implications for dendritic cell-based anticancer immunotherapy., Expert Rev. Clin. Immunol. 10 (2014) 915–26. doi:10.1586/1744666X.2014.912561.

[23] H. Shen, A. Iwasaki, A crucial role for plasmacytoid dendritic cells in antiviral protection by CpG ODN-based vaginal microbicide, J. Clin. Invest. (2006). doi:10.1172/JCI28681.

[24] A. Kelso, Cytokines: Principles and prospects, Immunol. Cell Biol. 76 (1998) 300–317. doi:10.1046/j.1440-1711.1998.00757.x.

[25] M.L. Schmitz, A. Weber, T. Roxlau, M. Gaestel, M. Kracht, Signal integration, crosstalk mechanisms and networks in the function of inflammatory cytokines, Biochim. Biophys. Acta - Mol. Cell Res. 1813 (2011) 2165–2175. doi:10.1016/j.bbamcr.2011.06.019.

[26] A. Carroll-Portillo, J.L. Cannon, J. Te Riet, A. Holmes, Y. Kawakami, T. Kawakami, A. Cambi, D.S. Lidke, Mast cells and dendritic cells form synapses that facilitate antigen transfer for T cell activation., J. Cell Biol. 210 (2015) 851–864. doi:10.1083/jcb.201412074.

[27] I. Striz, A. Slavcev, J. Kalanin, M. Jaresová, S.I. Rennard, Cell-cell contacts with epithelial cells modulate the phenotype of human macrophages., Inflammation. 25 (2001) 241–6. doi:10.1023/A:1010975804179.

[28] A. Rivera, M.C. Siracusa, G.S. Yap, W.C. Gause, Innate cell communication kick-starts pathogen-specific immunity, Nat. Immunol. 17 (2016) 356–363. doi:10.1038/ni.3375.

[29] M.B. Lutz, N. Kukutsch, a L. Ogilvie, S. Rössner, F. Koch, N. Romani, G. Schuler, An advanced culture method for generating large quantities of highly pure dendritic cells from mouse bone marrow., J. Immunol. Methods. 223 (1999) 77–92. doi:10.1016/s0022-1759(98)00204-x.

[30] S. Anguille, E.L. Smits, E. Lion, V.F. Van Tendeloo, Z.N. Berneman, Clinical use of dendritic cells for cancer therapy, Lancet Oncol. 15 (2014) 257–267. doi:10.1016/S1470-2045(13)70585-0.

[31] J. Datta, J.H. Terhune, L. Lowenfeld, J. a Cintolo, S. Xu, R.E. Roses, B.J. Czerniecki, Optimizing dendritic cell-based approaches for cancer immunotherapy., Yale J. Biol. Med. 87 (2014) 491–518. doi:10.1586/14760584.6.3.333.

[32] K.F. Bol, G. Schreibelt, W.R. Gerritsen, I.J.M. de Vries, C.G. Figdor, Dendritic Cell-Based Immunotherapy: State of the Art and Beyond, Clin. Cancer Res. 22 (2016) 1897–1906. doi:10.1158/1078-0432.CCR-15-1399.

[33] F. Wimmers, G. Schreibelt, A.E. Sköld, C.G. Figdor, I.J.M. De Vries, Paradigm Shift in Dendritic Cell-Based Immunotherapy: From in vitro Generated Monocyte-Derived DCs to Naturally Circulating DC Subsets., Front. Immunol. 5 (2014) 165. doi:10.3389/fimmu.2014.00165.

[34] S.P. Sittig, G. Bakdash, J. Weiden, A.E. Sköld, J. Tel, C.G. Figdor, I.J.M. De Vries, G.

Schreibelt, A Comparative Study of the T Cell Stimulatory and Polarizing Capacity of Human Primary Blood Dendritic Cell Subsets, Mediators Inflamm. 2016 (2016). doi:10.1155/2016/3605643.

[35] H. Dewitte, R. Verbeke, K. Breckpot, R.E. Vandenbroucke, C. Libert, S.C. De Smedt, I. Lentacker, Choose your models wisely: how different murine bone marrow-derived dendritic cell protocols influence the success of nanoparticulate vaccines in vitro., J. Control. Release. 195 (2014) 138–46. doi:10.1016/j.jconrel.2014.06.024.

[36] K.P.J.M. van Gisbergen, Neutrophils mediate immune modulation of dendritic cells through glycosylation-dependent interactions between Mac-1 and DC-SIGN, J. Exp. Med. 201 (2005) 1281–1292. doi:10.1084/jem.20041276.

[37] I.S. Ludwig, T.B.H. Geijtenbeek, Y. van Kooyk, Two way communication between neutrophils and dendritic cells., Curr. Opin. Pharmacol. 6 (2006) 408–13. doi:10.1016/j.coph.2006.03.009.

[38] T.B.H. Geijtenbeek, S.J. van Vliet, E.A. Koppel, M. Sanchez-Hernandez, C.M.J.E. Vandenbroucke-Grauls, B. Appelmelk, Y. van Kooyk, Mycobacteria Target DC-SIGN to Suppress Dendritic Cell Function, J. Exp. Med. 197 (2002) 7–17. doi:10.1084/jem.20021229.

[39] D.M. Mosser, J.P. Edwards, Exploring the full spectrum of macrophage activation., Nat. Rev. Immunol. 8 (2008) 958–69. doi:10.1038/nri2448.

[40] F.O. Martinez, S. Gordon, The M1 and M2 paradigm of macrophage activation: time for reassessment, F1000Prime Rep. 6 (2014) 1–13. doi:10.12703/P6-13.

[41] L.C. Bonifaz, D.P. Bonnyay, A. Charalambous, D.I. Darguste, S.-I. Fujii, H. Soares, M.K. Brimnes, B. Moltedo, T.M. Moran, R.M. Steinman, In Vivo Targeting of Antigens to Maturing Dendritic Cells via the DEC-205 Receptor Improves T Cell Vaccination, J. Exp. Med. J. Exp. Med. 038151000 (2004) 815–824. doi:10.1084/jem.20032220.

[42] S.E. Strome, S. Voss, R. Wilcox, T.L. Wakefield, K. Tamada, D. Flies, A. Chapoval, J. Lu, J.L. Kasperbauer, D. Padley, R. Vile, D. Gastineau, P. Wettstein, L. Chen, Strategies for antigen loading of dendritic cells to enhance the antitumor immune response., Cancer Res. 62 (2002) 1884–9. http://www.ncbi.nlm.nih.gov/pubmed/11912169.

[43] R.M. Steinman, J. Swanson, The endocytic activity of dendritic cells., J. Exp. Med. 182 (1995) 283–8. doi:10.1084/jem.182.2.283.

[44] I. Mellman, R.M. Steinman, Dendritic Cells: Specialized and Regulated Antigen Processing Machines, Cell. 106 (2001) 255–258. doi:http://dx.doi.org/10.1016/S0092-8674(01)00449-4.

[45] J.M. Blander, Phagocytosis and antigen presentation: a partnership initiated by Toll-like receptors., Ann. Rheum. Dis. 67 Suppl 3 (2008) iii44-i49. doi:10.1136/ard.2008.097964.

[46] A. Lanzavecchia, F. Sallusto, Regulation of T cell immunity by dendritic cells., Cell. 106 (2001) 263–266. doi:10.1016/S0092-8674(01)00455-X.

[47] A. Reschner, P. Hubert, P. Delvenne, J. Boniver, N. Jacobs, Innate lymphocyte and dendritic cell cross-talk: A key factor in the regulation of the immune response, Clin. Exp. Immunol. 152 (2008) 219–226. doi:10.1111/j.1365-2249.2008.03624.x.

[48] O.P. Joffre, E. Segura, A. Savina, S. Amigorena, Cross-presentation by dendritic cells, Nat. Rev. Immunol. 12 (2012) 557–569. doi:10.1038/nri3254.

[49] C. Kurts, J.F. Miller, R.M. Subramaniam, F.R. Carbone, W.R. Heath, Major histocompatibility complex class I-restricted cross-presentation is biased towards high

dose antigens and those released during cellular destruction., J. Exp. Med. 188 (1998) 409–414. doi:10.1084/jem.188.2.409.

[50] B. Chatterjee, A. Smed-Sörensen, L. Cohn, C. Chalouni, R. Vandlen, B.C. Lee, J. Widger, T. Keler, L. Delamarre, I. Mellman, Internalization and endosomal degradation of receptor-bound antigens regulate the efficiency of cross presentation by human dendritic cells, Blood. 120 (2012) 2011–2020. doi:10.1182/blood-2012-01-402370.

[51] S. Campisano, S. Mac Keon, S. Gazzaniga, M.S. Ruiz, M.D. Traian, J. Mordoh, R. Wainstok, Anti-melanoma vaccinal capacity of CD11c-positive and -negative cell populations present in GM-CSF cultures derived from murine bone marrow precursors., Vaccine. 31 (2013) 354–61. doi:10.1016/j.vaccine.2012.10.114.

VITA

Hannah E. Frizzell was born in Nacogdoches, Texas and graduated from Nacogdoches High School in 2009. Hannah received her B.S. in Biomedical Engineering from The University of Texas at Austin in 2014, where she worked in the laboratory of Dr. Nicholas Peppas on oral siRNA delivery using hydrogel nanoparticles for the treatment of inflammatory bowel diseases. During her undergraduate education, Hannah also received training in the laboratory of Dr. Melody Swartz at the École polytechnique fédérale de Lausanne (EPFL) in Lausanne, Switzerland targeting nanoparticles to lymphatic endothelial cells for drug delivery. Hannah began her doctoral work at the University of Washington in 2014 as an NSF GRFP fellow in the laboratory of Dr. Kim Woodrow in the Department of Bioengineering focused on mucosal drug and vaccine delivery and immunoengineering. She completed her PhD in 2019. Hannah was also awarded a pre-doctoral NSF GROW fellowship to conduct research in the laboratory of Dr. Laura Mackay at the University of Melbourne/The Peter Doherty Institute for Infection and Immunity studying tissue-resident memory T cell metabolism. In her free time, Hannah enjoys hiking, tennis, live music, knitting, traveling, and biking.